SELF-ASSEMBLING POLYMERIC NANOPARTICLES FOR ENHANCED INTRA-ARTICULAR ANTI-INFLAMMATORY PROTEIN DELIVERY

A Dissertation
Presented to
The Academic Faculty

by

Rachel Elisabeth Whitmire

In Partial Fulfillment
of the Requirements for the Degree
Doctor of Philosophy in
Bioengineering

George W. Woodruff School of Mechanical Engineering
Georgia Institute of Technology
May 2012

SELF-ASSEMBLING POLYMERIC NANOPARTICLES FOR ENHANCED INTRA-ARTICULAR ANTI-INFLAMMATORY PROTEIN DELIVERY

Approved by:

Dr. Andrés J. García, Advisor
Department of Mechanical Engineering
Georgia Institute of Technology

Dr. Julia Babensee
Department of Biomedical Engineering
Georgia Institute of Technology

Dr. Marc Levenston
Department of Mechanical Engineering
Stanford University

Dr. L. Andrew Lyon
Department of Chemistry
Georgia Institute of Technology

Dr. Nael McCarty
Department of Pediatrics
Emory University

Dr. Niren Murthy
Department of Biomedical Engineering
Georgia Institute of Technology

Date Approved: 13 January 2012

To my parents, who instilled in me the joy of knowledge
and the uncontrollable desire to share it.

ACKNOWLEDGEMENTS

To my advisor, Andrés J. García, thank you for providing an open and nurturing lab community for me to grow up in. In the final stage of this thesis, I have started to fully appreciate your guidance and insight, as well as your underlying desire for each of us to be completely prepared for anything that might come our way. Thank you for being my biggest skeptic and biggest advocate, and for allowing me to do stupid things and still having faith that I could move past those mistakes. I will be a proud representative of your training as I transition to the real world.

To my first research mentor, Dr. Jennifer West, who took a chance on me as a fledgling bioengineer. The opportunity she gave me was much more than washing glassware and restocking pipettes. Thank you for giving me real, exciting research to do and for sparking my passion for this field.

To my immunology teacher, Dr. Alma Moon Novotny, who probably still does not know just how much her class changed my life. She not only taught me how cool the immune system is, but showed me day in and day out how to be an inspiring, engaging teacher. I aspire to be as cool as her when I grow up.

My thesis was funded in part by the National Science Foundation's Graduate Fellowship Program, for which I am extremely grateful because it made my poor graduate existence a little bit easier and also provided the freedom for me to explore this thesis project. Thank you also to the reviewers who chose my application. I do not know who you are, but you have my eternal gratitude as well.

To my committee, who provided me with constructive criticism and support through this process. Thank you for challenging me. To Dr. L. Andrew Lyon who made sure that I knew the chemistry of my project like a chemist and to Dr. Niren Murthy who allowed me to pretend I was a polymer chemist in his lab. Dr. Babensee kept me on my toes about the inner workings of the IL-1 pathway. Dr. McCarty graciously agreed to serve

on my committee, even though he had to commute from Emory. I appreciated his input and questioning during this thesis process. Dr. Levenston was an integral late-comer to my thesis committee. His expertise and advice on the in vivo portion of this thesis were invaluable.

Dr. D. Scott Wilson was crucial to this project. Scott was always a great ideas guy, and when I came to him with the concept that became this thesis project, he sketched out at least five different options off the top of his head, one of which led to the material in this thesis project. Scott's enthusiasm and passion for his work and his never-ending optimism helped me to keep my spirits up during all the times when things went belly-up in lab (which were sometimes, ok - most times, my fault). Thank you for being an awesome mentor, friend, and late-night lab buddy. Making particles at 10pm doesn't seem so bad when I'm not the only one in lab.

Dr. Neetu Singh was my first collaborator in the Lyon lab. She introduced me to microgels and let me play in the ancient halls of Boggs building so I could make samples for my experiments. To Dr. Antoinette "Toni" Bonhivert South, who continued the microgel synthesis project and patiently helped me through much of the optimization steps for making multi-layered microgel coatings. And to Michael Smith, who spent a semester collaborating with me on hollow microgel particles for protein delivery. I really appreciate all of the time and energy that went into that side project.

To The Lab:

First and foremost, to Kellie (Burns) Templeman, who was so patient with me while I learned my way around lab and somehow turned into a responsible lab member. I will miss your hilarious sense of humor, your love of Georgia Tech, and your wry commentary on lab politics. You are also one of the hardest working people I know. I am still in awe of you keeping the lab running while also being in school part-time AND being pregnant with your second child. You truly amaze me. Thanks for dragging me to Starbucks so many times during the most trying part of my thesis. Your friendship means the world to me.

Ed Phelps, for your help, companionship, and listening ear. We came into the lab

together and we get to leave the lab at the same time too. Thanks for helping me trouble-shoot my project and for acting as an awesome tech support guy. Good luck with your next adventure! Asha, my little lab friend, thank you for making me laugh, first and foremost. Your awesome quirky sense of humor and positive outlook on life are a joy to be around! Thank you for being my dutiful rat leg holder for my animal work. Thanks for all the fun times, including our escapades at SFB. :-) Stacie, thank you for letting me constantly interrupt you with random thoughts and crazy things. You were an awesome deskmate, bake-mate, and lab mate. You will get through this thesis adventure too, my friend! Ted "Tedulous" Lee, thanks for bringing the preppy back to our lab. Your ability to simultaneously chill out and still pull off really cool work inspires me. Some day I'll come visit you in your corner office at J&J! To my new girls, Amy and Apoorva, thank you for putting up with my "jaded old grad student" rants and being awesome lair-mates. Amy, your cheesecake is going to be the stuff of legends in the García lab. Thanks for making my birthday celebration so special! Apoorva, congratulations on your upcoming marriage! It makes a huge difference during this thesis process to have someone to keep you well-balanced. :-) Chi-Chi, thanks for all your advice on living in Boston. I can't wait to explore some of the places you suggested! Imen, thank you for being so supportive while I finished up my thesis. Susan, you have given me such an interesting perspective on science and life. Ram, best of luck in the job search. Ankur, you have really established yourself in the lab. Congratulations on some fantastic work, and thanks for the tandoori chicken! Nduka, best wishes on finishing your thesis and your upcoming marriage!

One of my predecessors, Dr. Tim Petrie, taught me everything he knew about molecular cloning. He also provided endless entertainment and humor. Tim, thanks for the great stories, lab insight, and for reminding me that the gym is always essential to grad student life. Dr. Abbey Wojtowicz, I am so glad we were desk mates, and I look forward to being neighbors in Cambridge soon! Thank you for being a truly stellar example of a hard working, balanced grad student. Dr. Amanda (Walls) Bridges, for being the first guinea pig on the microgels project and for allowing me to pepper you with questions during your time here. To Dr. Sean and Dr. Dave, you two were the double trouble of the lab. Thank

you for being the anchors of the lab and making sure the rigors of cell adhesion were drilled into our heads.

To all of my Tech friends, this thesis journey is a marathon. Although you are too many to name here, your support as a grad student community is a rare and wonderful thing. Thank you for providing a nurturing environment to me as a baby grad student, and for allowing me to pass on some of that spirit as I prepare to move on to the next phase of my life.

To my sweet friend, Julia Henkels. You let me talk you into joining BGSAC and somehow I roped you into being my prodigy. Thank you for being an awesome friend, first and foremost, and for taking my pet project and running with it. In that same vein, I have to give Ashley Allen a big thank-you for carrying on BGSAC as my grand-president. I'm so proud of my girls for getting the BioEs organized and social! You go, girls!

To "The Crew" of 2006: Gina Cremona, Andres Bratt-Leal and Erin Spinner, Ashley Carson Brown (and her other half, Chris Brown), Ivan Caceres, Melissa Li, Vivek Kumar, Casey Holliday Ankeny (and Randy Ankeny) and Nnenna Adimora Finn. You guys have become some of my best friends. I will dearly miss our times together, but we will just have to plan fun reunions around the country!

Andrea Para, you are my partner in crime, my 2nd floor bathroom buddy, and my cinnamon pancake friend! Thank you for laughing till we cry, bitching till we feel better, and all around just being awesome. I adore you, girlfriend!

Brock Wester provided a shining example of Georgia Tech-ness and grad student life. Thank you for creating a social hub at your house for so many years. I have fond memories of parties on your back deck!

To Gina, Ashley, Erin, and Andrea for getting me into spin and yoga. Although 8am Friday was not the easiest time to be at the gym, y'all made it worth it! Thanks for inspiring me and pushing me. Ashley and Gina, especially to you, because you have both been great inspirations to me to keep up my yoga practice. Thank you.

To my first year roomies of 1128 McMillan St. - Ryan "Ryn" Maladen, Mel(issa) Li, and Stephen "Schneeve" Brink. Thank you for putting up with my quirks and for keeping

me sane in that first year. Mel, I have to thank you especially, since you were the one who introduced Jay and me. At the gym. When we were all nasty and sweaty. It started what I consider to be the best thing to ever happen to me, and you started it. :-) Ryan, the man who thought he would never meet any girl at Tech who was Indian, and pretty, and smart, and could put up with you. Seeing you find love with Laveeta makes me very happy for you. I wish you both the best in your life together! To Steve, you taught me the value of authentic Hatch green chiles and Honey Bunches of Oats. Thanks for bringing a whole lot of awesome nerd conversation and basketball to our house's evenings.

To my dog park friends as an ever-rotating group. You listened to me jabber on about my nerdy obsessions and made sure that I had a semblance of balance outside of the lab. Thank you for giving Emma such a warm welcome and for making us feel at home in our neighborhood!

To Susanne, my best friend in Atlanta, I feel like we were separated at birth. I am so grateful that we met and have found each other to be friends, confidants and canine mommies together. You have kept me so grounded (and well-dressed :-)), especially during my time as a bachelorette here. Without your offers to get out and hike, or to just have coffee and girl time, I would be a complete stress ball right now. I can't tell you how much I value our friendship. I will miss having you around the corner when we move to Boston. It just means an excuse to go travel the country together! South Beach, here we come!

Moria, I have loved getting to know you and your precious family in the past two years. You have an amazing gift for words, and your wit and humor have made me laugh so much! Thank you for sharing your sweet daughter Uma with us, too. She helped me feel more connected to the "real world" and reminded me to delight in the small things in life. From being a tiny pea in the pod to being a vivacious toddler who knows my name (and my dog's :-)), it has been so cool to be a part of her young life. You and Neil have done an amazing job raising her thus far, and I cannot wait to see what a stellar woman she will grow into under your influence.

To my neighbors Carl, Sharon, and Stella, I am so blessed to have such sweet people just around the corner. I know Carl can't resist Emma's puppy eyes and he is always willing to

share treats with her. Emma and I will miss your company at the dog park!

Dave and Wister, you two are the grandparents I never had here in Atlanta. Dave, your stories of travels and adventures always made me want to rush out and see more of the world. Your sense of adventure and constant interest in current events (and even my science stuff!) kept me on my toes during our conversations at the park. Thank you for coming to my proposal, too. It meant a lot to have you there!

Stephanie Taylor, my dear, sweet friend, I cannot tell you how much your friendship means to me, especially as I have been on this rollercoaster called a PhD. Your steady faith in me and your listening ear helped me get through many a frustrating moment in this journey. I know you probably thought I was crazy when I switched from Civil Engineering into this thing called Bioengineering, but you have been so supportive of me through it all, so thank you for being the best friend a girl could ask for. :-)

Raechelle May, you have been such a support for me. Thanks for many nights of girl talk and margaritas (up and dooowwwwnnn :-)). You kept me sane and listened to my rollercoaster of emotions going through this thesis. Thanks for just being you. Sure you don't want to move to Boston? I'm going to miss you!

To my family, especially my parents, who both are wonderfully nerdy in their own right. Thank you for giving me the opportunity to spread my wings, letting me go thousands of miles away but always keeping me grounded. Even though my official school days are over, you have instilled in me a never-ending desire to know more. Thank you for the legacy of learning that you have given me. Thanks, Nana, for being the artistic foil to my analytical self. I am so grateful for the times that you came to Atlanta to hang out with me, and for reminding me to not take myself so seriously all the time! Mancub, when I left for graduate school, you were still a little kid. I can't believe you are now taller than me (!!!) and are starting to think about college yourself. You have come so far, and I am so proud of you. I wish that Atlanta and Houston weren't so far apart because I have missed seeing you grow up day to day. Now that I am no longer a poor graduate student, we've got to spend more time hanging out!

And saving the best for last, to the love of my life, Jay. Darling, you are the best thing

that has happened to me. I knew when I chose Tech, that it was the right place to be, but in my wildest dreams, I couldn't have imagined that the most right thing about it would be you. I am ridiculously fortunate to have found you and to be blessed with the awesome thing we have together. Thank you for being my rock in times of crisis (of which there were many), letting me cry on your shoulder at sappy movies (yes, lots of those, too), and for challenging me and making me stronger. Thank you for driving all the way to Birmingham in the snow to pick up our sweet puppy, Emma, and for being the best wuppy daddy to her. Watching you with her has taught me a whole new way of loving. You have made this experience so incredibly rich for me, and I can't wait to continue our adventure together.

"Being deeply loved by someone gives you strength,
while loving someone deeply gives you courage."
Lao Tzu

TABLE OF CONTENTS

LIST OF TABLES

LIST OF FIGURES

List of symbols and abbreviations

AA	Amino acid
ACL	Anterior cruciate ligament
AIBN	Asobisisobutyronitrile
BME	β-mercaptoethanol
BSA	Bovine serum albumin
CHM	Cyclohexyl methacrylate
CIA	Collagen-induced arthritis
DMF	Dimethyl formamide
ECM	Extracellular matrix
EDTA	Ethylene diamine tetraacetic acid
FBS	Fetal bovine serum
HIG-82	Female rabbit synoviocyte cell line
IFN-γ	Interferon gamma
IGF-1	Insulin-like growth factor I
IL-1	Interleukin-1
IL-1ra	Interleukin-1 receptor antagonist
IL-1rI	Interleukin-1 receptor, type I
IL-1rII	Interleukin-1 receptor, type II
K.O.	Knock-out
MIA	Monosodium iodoacetate
MMP	Matrix metalloproteinase
MMT	Medial meniscal transection
MTT	(3-(4,5-Dimethylthiazol-2-yl)-2,5-diphenyltetrazolium bromide, a colorimetric assay for measuring cell proliferation
MW	Molecular weight
NaOH	Sodium hydroxide
NCS	Neonatal calf serum
NO	Nitric oxide
NSAIDs	Non-steroidal anti-inflammatory drugs
OA	Osteoarthritis
PBS	Phosphate-buffered saline
PDI	Polydispersity index
PG	Proteoglycans
PS	Penicillin streptomycin
RAFT	Reverse addition-fragmentation chain transfer
RPMI-1640	Bicarbonate buffered growth medium, developed at Roswell Park Memorial Institute
TEGM	Tetraethylene glycol methacrylate
TGF-β	Transforming growth factor beta
THF	Tetrahydrofuran
TNF-α	Tumor necrosis factor alpha

SUMMARY

Osteoarthritis (OA) affects 26 million Americans, or approximately 14% of the adult population. The incidence of OA is predicted to dramatically increase in the next 20 years as the US grows older and the rate of obesity continues to increase. There are currently no clinical interventions that cure OA. Current biomaterial delivery systems exhibit several limitations. First, most drug-delivery particles are hydrophobic, which is not optimal for hydrophilic protein encapsulation. Second, hydrophobic particles, such as PLGA, could cause wear damage to the already-fragile OA cartilage structure. Additionally, these particles usually suffer from non-specific protein adsorption, which causes increased phagocytosis and can lead to increased inflammation. New therapies that increase the effectiveness of OA treatments or reverse OA disease progression will greatly decrease the economic costs and individual pain associated with this disease.

The goal of this thesis was to develop a new drug-delivering material to deliver anti-inflammatory protein for treating OA. Our central hypothesis for this work is that a controlled release/presentation system will more effectively deliver anti-inflammatory protein therapies to the OA joint.

The primary goal of this work was to synthesize a block copolymer that could self-assemble into injectable, sub-micron-scale particles and would allow an anti-inflammatory protein, IL-1ra, to be tethered to its surface for efficient protein delivery. The block copolymer incorporated an oligo-ethylene monomer for tissue compatibility and non-fouling behavior, a 4-nitrophenol group for efficient protein tethering, and cyclohexyl methacrylate, a hydrophobic monomer, for particle stability. We engineered the copolymer and tested it in both in vitro culture experiments and an in vivo model to evaluate protein retention in the knee joint. The rationale for this project was that the rational design and synthesis of a new drug- and protein-delivering material can create a modular polymer particle that can

deliver multi-faceted therapies to treat OA.

This work characterizes the in vitro and in vivo behavior of our polymer particle system. The protein tethering strategy allows IL-1ra protein to be tethered to the surface of these particles. Once tethered, IL-1ra maintains its bioactivity and actively targets synoviocytes, cells crucial to the OA pathology. This binding happens in an IL-1-dependent manner. Furthermore, IL-1ra-tethered particles are able to inhibit IL-1β-induced NF-κB activation. These studies show that this particle system has the potential to deliver IL-1ra to arthritic joints and that it has potential for localizing/targeting drugs to inflammatory cells of interest as a new way to target OA drug treatments.

CHAPTER I

SPECIFIC AIMS

1.1 Outline

1.1.1 Problem Statement

Osteoarthritis (OA) affects 26 million Americans, or approximately 14% of the adult population[68]. The incidence of OA is expected to dramatically increase in the next 20 years as the US grows older and the rate of obesity continues to increase. By 2030, 25% of adults in the US, or about 67 million people, will be affected by OA[202], with the obesity pandemic disproportionately adding to that population. According to the well-respected Framingham study on osteoarthritis, obesity and old age both increase the risk of developing OA, as do previous joint trauma and occupational physical loading[172]. The US economy will also spend a lot of money treating both the symptoms and the resulting quality-of-life losses from this disease. One estimate puts the current total economic cost of OA at $185.5 billion: $149.4 billion of that is paid by insurance companies, and $36.1 billion comes from out-of-pocket expenses.

There are currently no clinical interventions that cure OA. Patients can only treat the disease symptoms with palliative measures, such as non-steroidal anti-inflammatory drugs (NSAIDs), steroid injections, and administration of drugs or proteins directly to the joint. These measures are chronic treatments that require ongoing visits to the doctor, which can reduce patient compliance. The eventual outcome of this disease is total joint replacement, which is major surgery and significantly affects quality of life[61]. New therapies that increase the effectiveness of OA treatments or reverse OA disease progression will greatly decrease the economic costs and individual pain associated with this disease.

Osteoarthritis is a complex pathology that involves the immune/inflammatory system. There is mounting evidence that the cytokine interleukin-1 (IL-1) plays a prominent role in

OA. This pro-inflammatory cytokine stimulates the expression and upregulation of a myriad of destructive immune molecules, including IL-6, IL-8 and MMP-13[169][13][44][278]. Researchers have examined the role of IL-1 in OA disease progression by creating IL-1 knock-out mice and by using interleukin-1 receptor antagonist (IL-1ra), the natural protein inhibitor of IL-1, either through gene therapy or bolus protein injections[191][74][118][139]. In general, modulating IL-1levels or activity has improved OA progression in the short term[350][124]. These results are promising, but a more robust therapeutic strategy is needed to deliver therapeutically relevant IL-1ra to treat OA because the current treatments either have serious safety concerns (gene therapy), require repeated dosing (protein injections), and/or suffer from high cost, systemic side effects, and low patient compliance.

Retaining and controlling the delivery of small molecule drugs and anti-inflammatory proteins in the joint has proved very difficult. By using a carrier, such as polymer particles or PEGylation, researchers have increased the residence time of drug-eluting particles from a few hours to a few days. The size and material of the carrier vehicle influence how long the material resides in the joint. Adhesive moieties, such as RGD and phage-panned peptides, have been used to increase the particle retention rate as well. In animal studies, only a few adhesive particle types had improved retention over non-adhesive particles[112][292]. Additionally, combining targeting moieties with immunomodulatory molecules like drugs or proteins has not been explored in a particle system in OA, although there has been significant interest in these combination therapies for cancer treatment[112][226].

1.1.2 Project Significance

This project is significant because it develops a modular material that self-assembles into nanoparticles of the appropriate size for controlled IL-1ra protein delivery to treat OA-related inflammation.

1.1.3 Objective

This thesis seeks to create a novel polymer drug delivery platform for sustained delivery of anti-inflammatory proteins to the joint.

1.1.4 Central Hypothesis

Our central hypothesis is that a controlled release/presentation system will more effectively deliver anti-inflammatory protein therapies to the joint.

1.1.5 Rationale

The rational design and synthesis of a new drug- and protein-delivering material can create a modular polymer particle that can deliver multi-faceted therapies to the joint to treat OA.

1.1.6 Specific Aim 1

The goal of this aim is to engineer a new block copolymer via RAFT polymerization methods from tetraethylene glycol methacrylate and cyclohexyl methacrylate monomers to create a particle system that presents moieties on its surface for covalent protein tethering.

The hypothesis for this aim is that we can design a reverse addition-fragmentation chain transfer (RAFT)-based amphiphilic block copolymer that incorporates the 4-nitro-phenol (pNP) leaving group. This copolymer will form particles that covalently tether IL-1ra to the particle surface in mild aqueous conditions while maintaining the protein bioactivity. We will first verify that all components of this new polymer can be synthesized and show that our synthetic strategy is able to form a block copolymer. We will then determine the conditions necessary to yield particles in our desired size range. Finally, we will optimize conditions for tethering IL-1ra to the particles.

The expected outcomes for this aim are the creation of a block copolymer by RAFT polymerization that will self-assemble under aqueous conditions to form particles in our desired size range. Additionally, we expect that this polymer particle will allow protein to be tethered to its surface in controlled densities.

1.1.7 Specific Aim 2

The goal of this aim is to evaluate our RAFT-based amphiphilic copolymer for IL-1ra protein presentation in vitro.

We will tether our particles with IL-1ra, show that the protein maintains its bioactivity, and then test the specificity, cytocompatibility, and bioactivity of our protein-decorated particles in a cell culture model.

The expected outcomes of this aim are that our block copolymer particles will allow protein tethering and will maintain the proteins bioactivity. We also expect that our protein-tethered particles will target our cells of interest and will modulate the IL-1β-induced inflammatory cascade in vitro.

1.1.8 Specific Aim 3

The goal of this aim is to evaluate the effect of surface-bound IL-1ra on particle retention and cellular targeting in the healthy rat knee joint.

The working hypothesis for this aim is that our IL-1ra-tethered polymer particles will have longer residence time in the rat knee joint compared to a single bolus dose of IL-1ra protein. We will inject IL-1ra tethered particles and soluble IL-1ra into the knee joints of rats. We will use a near-infrared dye to to track the residence time of our IL-1ra-tethered particles and soluble protein in vivo. We will look for particle localization in the knee joints post-mortem by histological sectioning. We will also evaluate whether the particles have any negative effect on the cartilage morphology using EPIC-μCT imaging.

The expected outcomes for this aim are that our IL-1ra-tethered particles will be retained for a longer time than bolus protein and will also localize to inflammatory cells within the synovial joint space in a healthy rat knee.

1.1.9 Broader Impacts

This work provides a new, modular polymer particle system for drug delivery for intra-articular delivery to treat OA. Our use of IL-1ra for targeting particles to inflammatory cells is unique and shows promise for use in osteoarthritis treatments. The polymer itself adds to an expanding library of RAFT polymerization-based polymers. The polymer particles are appropriately sized for retention in the articular joint space and show no adverse effects on the native joint tissue. The modular nature of our protein tethering moiety will allow for stoichiometric variation of tethered proteins of both targeting and therapeutic benefit.

A host of disease states that show upregulated IL-1 could benefit from this therapeutic strategy. Because the particle core can encapsulate hydrophobic drugs for a multi-therapy treatment, IL-1ra-targeted particles could be loaded with a broad range of drugs for treating diseases from cancer to arthritis.

CHAPTER II

LITERATURE REVIEW

2.1 Significance and Prevalence of Osteoarthritis

Osteoarthritis (OA) affects 26 million Americans, or approximately 14% of the adult population[68]. The incidence of OA is predicted to dramatically increase in the next 20 years as the US grows older and the rate of obesity continues to increase. By 2030, OA will affect 25% of adults in the US, or about 67 million people[202][42], with the obesity pandemic disproportionately adding to that population. According to the well-respected Framingham study on osteoarthritis, obesity and old age both increase the risk of developing OA, as do previous joint trauma and occupational physical loading[172]. The US economy will also spend a lot of money treating both the symptoms and the resulting quality-of-life and productivity losses from this disease[203]. One estimate puts the current total economic cost of OA at $185.5 billion: $149.4 billion of that is paid by insurance companies, and $36.1 billion comes from out of pocket expenses[202].

There are currently no clinical interventions that cure OA. Patients can only treat the disease symptoms with palliative measures such as non-steroidal anti-inflammatory drugs (NSAIDs), steroid injections, and administration of drugs or proteins directly to the joint[361]. These measures are chronic treatments that require ongoing visits to the doctor, which can reduce patient compliance. The eventual outcome of this disease is total joint replacement, which is major surgery and significantly affects quality of life[61]. New therapies that treat OA symptoms or reverse OA disease progression will greatly decrease the economic costs and individual pain associated with this disease[34][361].

2.2 Pathology of OA

Osteoarthritis is a disease that involves the breakdown of cartilage tissue and the underlying bone structure in a joint. It also involves other joint tissues and the synovial membrane around the joint[68]. For example, a normal knee joint is comprised of the interface between

the femoral head and the tibial plateau. This joint is classified as a synovial joint because the bony surfaces are covered in articular cartilage and are surrounded by a fibrous capsule and a synovial membrane[129].

In the healthy knee, each bony surface is covered by a stratified layer of articular cartilage to allow easy articulating movement. Wedges of fibrocartilage called menisci on either side of the femoral heads help protect the joint further during mechanical loading. Synovial fluid, a filtered version of blood plasma, lubricates and feeds the joint tissue. Chondrocytes resist compressive forces by secreting extracellular biomolecules like aggrecan, collagen II, and hyaluronic acid, creating a complex hydrophilic extracellular environment[152]. OA causes drastic changes to all of these joint components and involves the cartilage, synovium, and the bone[296].

During OA, cytokines, aggrecanases and matrix metalloproteinases (MMPs) secreted by disregulated chondrocytes and synovial fibroblasts degrade the cartilage tissues extracellular matrix (ECM), damaging the cartilage mechanical properties and function by reducing the tissue hydration and structural integrity[276][289]. Synovial fluid (SF) constituents also get degraded by these inflammatory enzymes, reducing its lubricating action. These enzymatic changes, paired with changes in the mechanical loading environment, cause the articular cartilage to differentiate into a more bone-like state and also to damage the supporting menisci. Scientists still debate what initially causes OA, but ultimately, the mechanical changes, inflammatory cells, and their associated cytokines all contribute to the progression of this disease.

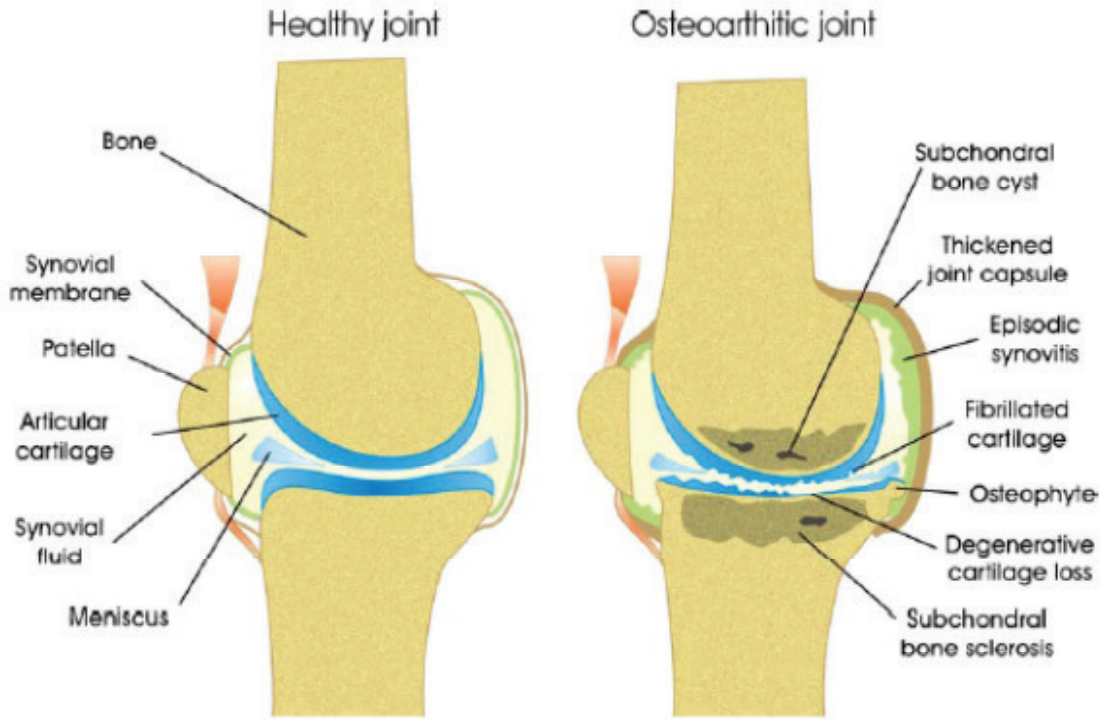

Figure 2.1: Diagram of healthy and osteoarthritic (OA) knees (Gerwin+ 2006). OA causes fibrillation and loss of cartilage, inflammation of the synovial membrane, and changes to subchondral bone.

Osteoarthritis is a disease that causes cartilage thinning and fibrillation, subchondral bone hardening and bone spurs, known as osteophytes, within a joint (Fig. 2.1)[169][146][208]. The literature still debates whether cartilage damage initiates these changes, or whether the initial inflammation from an injury or tissue damage propagates the disease[289][290][228]. However, what is known is that a set of diverse initiating events all result in the same clinical symptoms[169] that doctors diagnose as either primary or secondary OA, based on the cause of arthritis. Primary OA degenerates the joint tissue over time without an acute cause, although there are several well-known risk factors, such as age, obesity and hereditary predisposition[154]. Secondary OA stems from an initiating event, usually joint trauma, that creates a cartilage defect, inflammatory environment and structural abnormalities in the joint loading[218][154].

2.3 Inflammation in the OA joint

Osteoarthritis is characterized by localized inflammation in one or a few joints and does not cause systemic joint inflammation the way rheumatoid arthritis does. However, during OA, large quantities of immune cells infiltrate into the affected joint space, thus localizing large quantities of inflammatory cytokines to the area[33][278][290][316]. Researchers have sought to identify soluble markers of OA to allow for minimally invasive, early diagnosis of this disease to facilitate preventative treatment rather than end-stage palliative measures[243]. However, early diagnosis of OA is extremely difficult because early-stage OA is usually asymptomatic and people are unaware they are developing the disease.

Inflammatory cells play a large role in OA progression. Joints affected by primary OA have pervasive inflammatory cell infiltration that includes T helper cells, T suppressor cells, B lymphocytes, macrophages, and granulocytes[287][306]. Ishii and colleagues have shown that both Th1 and Th2 cells are present in OA infiltrates[186]. T lymphocytes are detectable in OA synovial cultures and comprise about 22% of total cells. Macrophage levels in OA and RA cultures were similar[58]. CD14+ synovial macrophages have been implicated in osteoclast formation and bone resorption[2][51]. Selectedly removing these synovial macrophages from human OA-derived cultures using CD14+ beads reduced the levels of pro-inflammatory cytokines such as IL-6, IL-8, and proteinases such as MMP-1 and MMP-3[51].

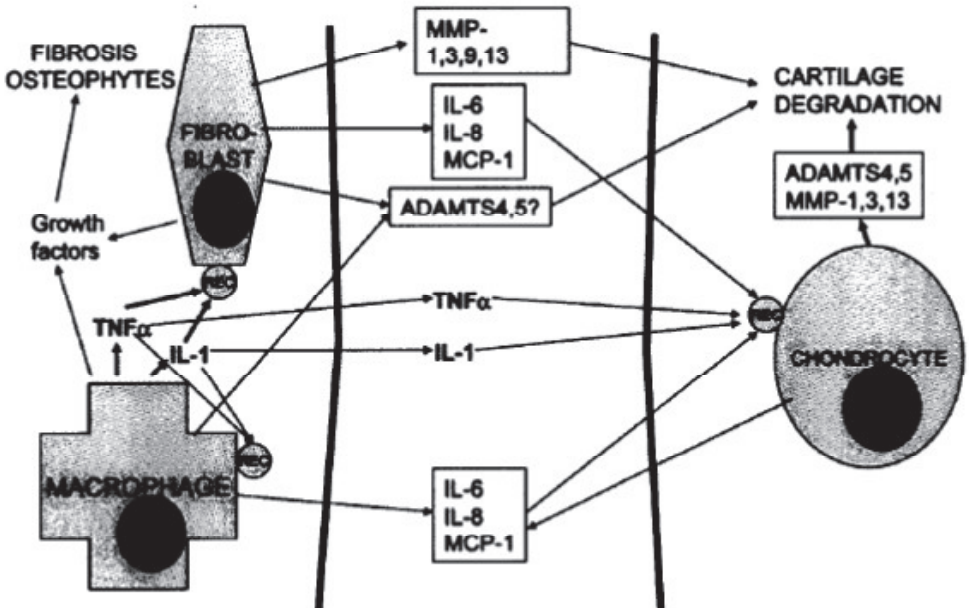

Figure 2.2: Interconnection of cell types and cytokines in OA signaling (Bondeson+ 2010).

The joint synovium, specifically synovial macrophages, are directly implicated in OA disease pathology, rather than acting as a bystander (Fig. 2.2)[43][289][50][49][341]. In the synovial joint there are two distinct cell types within the synovial lining: type A macrophage-derived synoviocytes, and type B fibroblast-like synoviocytes (FLS). Type A cells are defined by the following surface molecules: CD11b, CD68, CD14, CD163, and Fcγ RIIIa. The FLS, or type B, cells differ from type A by expressing prolyl hydroxylase and synthesizing fibronectin, fibrillin-1, and tenascin. The common markers for both types of synoviocytes are CD44 (HA receptor), VCAM-1 and ICAM-1. Disregulated Type B synoviocytes have been specifically linked to the OA pathology because they are the primary source of HA, an important lubricating component of synovial fluid[146].

2.3.1 Cytokines in OA

The two main cytokines in OA are IL-1 and TNF-alpha[50][4][14][35][64][51][151][299][155][153][231][266][265][125][122][234][232][233][359][72][199][347][322]. IL-1 upregulates a host of pro-inflammatory cytokines, like IL-6, and matrix metalloproteinases, such as MMP-3,

which indicate joint inflammation[169][13]; however, IL-1 also controls cartilage homeostasis[77][121][340]. TNF-α acts synergistically with IL-1 during OA to incite inflammation and tissue destruction. However, while TNF-α is the dominant cytokine in RA and directly drives IL-1 production, IL-1 and TNF-α share responsibility for the destructive environment as independently functioning members of the OA cytokine team[64][50][88][87][267][352]. TGF-β also plays a complicated homeostatic role in OA. On the one hand, it maintains the chondrocytic anabolic pathway by driving the repair response through Smads[18], but TGF-β gene therapy in mice resulted in osteophyte formation and joint fibrosis[18][342]. Interestingly, loss of the TGF-β receptor caused chondrocyte differentiation and an OA-like phenotype in a mouse model[303][225]. IL-1 downregulates expression of the TGF-β Receptor II, which reduces cell responsiveness to TGF-β and disrupts cartilage homeostasis[280]. The exact regulation of these cytokines plays a crucial role in OA disease progression and provides powerful targets for future OA therapies. In addition to higher expression of these cytokines, synovial joint cells upregulate the associated cytokine receptors and become highly sensitive to changes in protein levels[184]. Arthritic chondrocytes express twice as many IL-1 receptors (IL-1RI) as normal, healthy chondrocytes and act as the dominant cell type in OA[235][309]. This upregulation, together with lower expression levels of the non-signaling receptor (IL-1RII)[12], increases the probability that IL-1β binds to a signaling IL-1R on OA chondrocytes and transduces inflammatory signals than if it were exposed to healthy chondrocytes. OA cells only need 1% of IL-1Rs to be occupied in order to stimulate MMP production, whereas healthy cells require 4% receptor occupancy to produce the same MMP levels[235].

2.3.2 MMPs in OA

In addition to cytokines, matrix metalloproteinases (MMPs) also participate in OA joint destruction. MMPs play a destructive role in OA by cleaving structural ECM proteins. Current literature has shown that OA synovial fluid contains aggrecan fragments generated by MMP and aggrecanase cleavage[328]. High levels of MMP-1, -3, -8, -9 and -13 are found in OA SF, while they are not detectable in healthy SF[44][278][333]. MMP-13 specifically

is expressed in OA joints but not adult healthy joints[239][40][285][357][138].

By administering MMP inhibitors (both specific and non-specific) to IL-1-stimulated bovine cartilage explants, Wilson et al. were able to delay the IL-1-induced loss of compression modulus but did not reduce its magnitude, which suggests that non-MMP-dependent mechanisms also play a role in matrix degradation[365].

A family of "a disintegrin and metalloproteinase with thrombospondin motifs", or ADAMTS, are also involved in OA. ADAMTS-4 and -5 have been shown to play a role in destruction in the OA joint. In fact, IL-1 upregulates ADAMTS-4 expression in bovine cartilage and chondrocytes[278]. However, in mice, ADAMTS-5 is the controlling ADAMTS detected in OA studies, whereas ADAMTS-4 is implicated as the major factor in humans[150][149][133][134][181][230][318][323][345].

2.4 Osteoarthritis and IL-1

IL-1 has been used to induce an osteoarthritic phenotype in animal models. When IL-1 is injected into the knee joint of rabbits, infiltrating cells invade the tissue and cause a significant loss of proteoglycans in the cartilage tissue. After 24 h, IL-1 causes cartilage destruction that looks like 7-14 days of arthritis progression in other arthritis animal models[272][6]. In culture models of OA, the removal of exogenous IL-1 allows cartilage explants to recover their expression of glycosaminoglycans (GAGs) and to reestablish normal mechanical properties[262]. Additionally, IL-1 inhibits the synthesis of collagen II, the main structural ECM molecule in cartilage, which contributes to the decline of the cartilage tissue structure during OA[194]. Hyaluronic acid, a normal component of the joint SF, can modulate this IL-1-induced collagen inhibition to maintain tissue homeostasis, but because HA production is also significantly reduced during OA, HA cannot exert as much influence over the cartilage environment.

IL-1 directly causes the osteoarthritic phenotype by upregulating itself and other pro-inflammatory cytokines, such as IL-6, IL-8, and other proteins that destroy matrix, such as matrix metalloproteinases and ADAMTS proteins. These proteins in turn cleave crucial

ECM components, such as collagen II and aggrecan, and inhibit the production of lubricating synovial fluid components like hyaluronic acid. Collagen cleavage, for example, affects the integrity of the cartilage tissue and thus also affects its macro ability to resist compressive loads and cyclical stress and eventually exposing the underlying bone to more severe forces.

During osteoarthritis, IL-1 expression increases in the synovial fluid, the superficial synovial lining cells, as well as in the superficial and middle layers of the cartilage[25][266]. MMP-3 also localizes to the same tissues during OA, which is expected because IL-1 upregulates MMP-3, as well as nitric oxide (NO), MMP-1, and MMP-13[373]. Both prostaglandin D2 and IFN-γ can reverse this IL-1-mediated cartilage destruction, in part by stimulating IL-1ra production[263]. However, OA chondrocytes coordinate inflammatory cytokine and NO expression[238]. They also have lower levels of IFN-γ receptors which makes them less responsive to any increase in IFN-γ and interferes with IFN-γ's ability to offset the destructive forces of IL-1[3].

One of the consequences of increased NO levels in arthritic tissue is a NO-dependent downregulation of IL-1ra expression[269]. Conversely, higher levels of the IL-1 decoy receptor (sIL-1RII) inhibit IL-1-induced NO synthesis in multiple cell types, such as chondrocytes, synovial cells, and epithelial cells[14]. The presence of sIL-1RII benefits the joint environment by reducing the amount of IL-1 mRNA that accumulates in cells while also stimulating PG synthesis. The relationship between NO and IL-1ra synthesis in OA is specifically IL-1-mediated. Reduced TNF-R levels did not affect NO production in OA tissue[14].

The severity and progression of osteoarthritis can be attenuated by modulating different parts of the IL-1 pathway, specifically by affecting the levels of IL-1, IL-1ra, or the IL-1 receptors present in the joint[82][64][72][91][125][156][293][298].

The IL-1 pathway can be modulated by directly affecting the levels of IL-1β or IL-1ra in the affected joint space. For example, pro-IL-1β must be cleaved by caspase-1 (aka ICE) in order to form mature, active IL-1β. Inhibiting caspase-1 could reduce the amount of active IL-1 present and could attenuate IL-1-induced destruction[82]. Adding more IL-1ra

can shift the balance between inflammatory and anti-inflammatory pathways during OA as well[128][6][66][177]. Exogenous protein, gene therapy and stimulation of IL-1ra production by native cells can all contribute to modulating the IL-1 signal cascade[1][21][135][354].

Another way to interfere with the IL-1 pathway is to shift the type of IL-1 receptors and/or the amount of receptors present. There are only about 200 IL-1R in primary cells, but a cell only needs about 10 occupied receptors to transduce a signal[308][329][92]. Reducing the number of IL-1 receptors on OA inflammatory cells could modulate the severity of cartilage destruction and joint damage. IFN-γ, IL-10, IL-13, IGF-1, and TGF-β all modulate the levels of IL-1R. IL-1 receptors can be used to modulate the IL-1 cascade either by increasing the levels of soluble and/or non-signaling receptors present or by reducing the amount of membrane-bound signaling IL-1RI. TGF-β reduces overall IL-1R expression[103], IL-10 and IFN-γ reduce both IL-1RI and IL-1RII[90], and IL-13 and IGF-1 increase the amount of IL-1RII present in the OA joint[80][168][351]. Each of these proteins has functions beyond merely regulating IL-1 expression, and those alternate actions have to be taken into account when deciding how to employ them for OA treatment. For example, TGF-β reduces IL-1R levels, but when delivered to the joint by gene therapy, it also induces osteophyte formation and joint fibrosis[18][342].

Exogenous IL-1R can also have positive effects on OA disease progression[108][85]. A small molecule NSAID drug, Tenidap, reduced the levels of IL-1R in a time-dependent fashion, while other common OA drugs like naproxen and dexamethasone did not produce as great an effect[268]. Tenidap also reduced the amount of collagenase and MMP-3 produced by IL-1-stimulated osteoarthritic chondrocytes. However, clinical trials of this drug were halted after the FDA blocked its full commercialization due to unacceptable benefit/risk ratios. Some patients in this trial experienced loss of bone mineralization and increased protein in their urine[123][335].

2.5 IL-1/IL-1ra

The interleukin-1 signaling pathway plays an important role in processes ranging from inflammatory events to angiogenesis. IL-1 is involved in pro-inflammatory events, but also

acts in cell homeostasis, angiogenesis, and other processes. The IL-1 family includes 3 major IL-1 proteins (IL-1α, IL-1β, IL-1ra), as well as two receptors that are differentially expressed throughout the body. IL-1β, IL-1α, and IL-1ra are all 17 kDa proteins expressed throughout development. IL-1ra was originally characterized and sequenced in seminal Nature papers in 1990[67][111][166][301][348][325][167][245][216][110]. IL-1ra shares 26% homology with IL-1β, while IL-1α and IL-1β share 22% homology, and IL-1ra and IL-1α share 18% homology. Human IL-1ra shares 76% homology with the murine and rat forms of the molecule, IL-1β is 78% homologous, and IL-1α only shares 55% similarity between human and murine/rat genes[94][187].

There are two receptors that bind all three of these IL-1 family proteins[100][99][95][102][47][237][312][136][291]. These receptors are structurally related to the TLR family of innate receptors[257][310]. The first one is the active, or signaling, IL-1R, called IL-1RI. It was originally discovered on T cells as an 80 kDa, membrane-bound receptor[100]. After IL-1 binding, the receptor can signal in two ways: one, the cytoplasmic tail undergoes serine-threonine phosphorylation and induces downstream signaling, and two, the receptor-protein complex gets internalized and translocates to the nucleus to affect signal cascades and gene expression. These two pathways activate at least 4 different downstream pathways: p38 MAPK, ERK 1/2, JNK 1/2/3, and NF-κB (Fig. 2.3)[204].

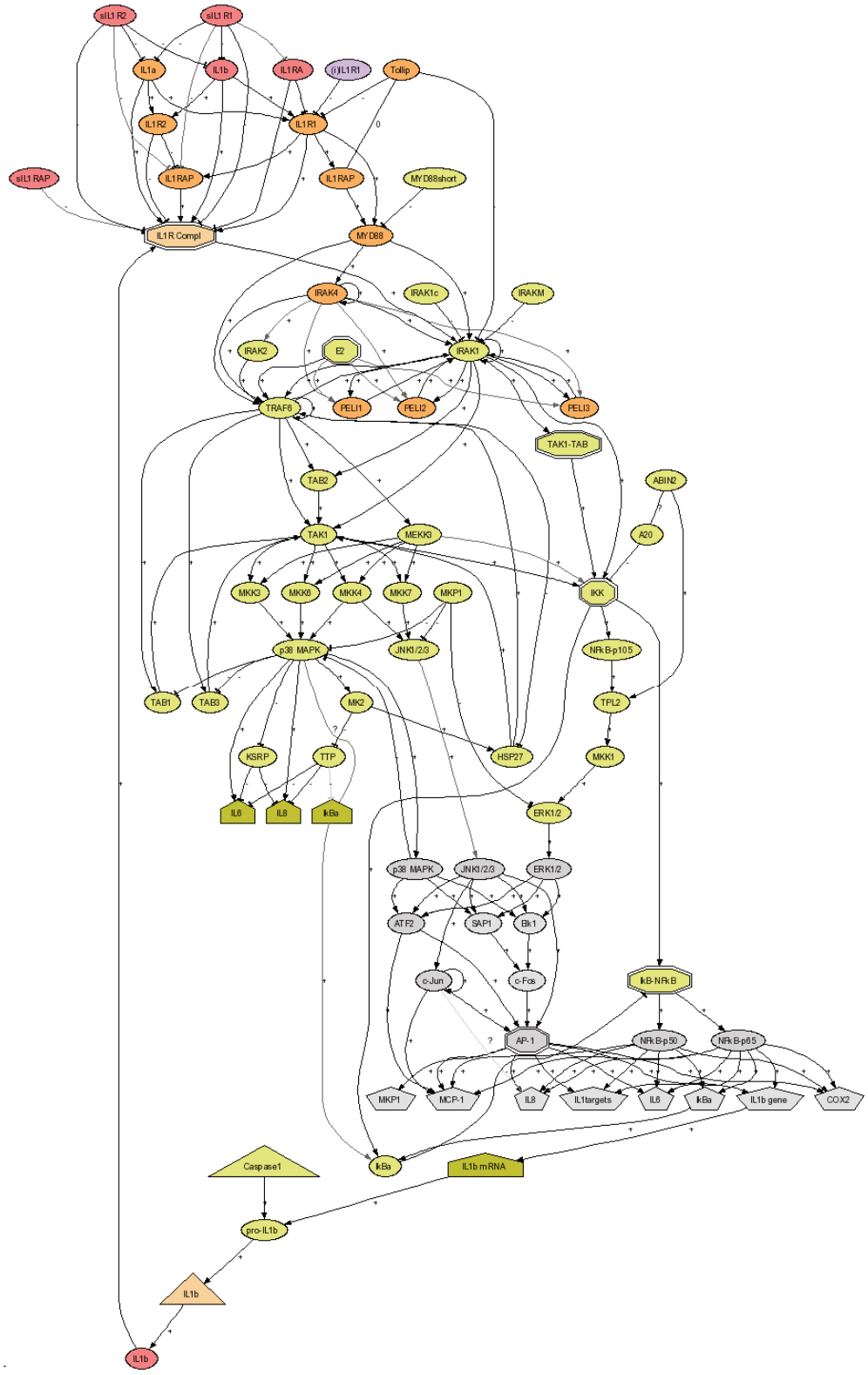

Figure 2.3: The IL-1 signalling cascade (Science Signalling Database, Kracht+ 2010).

Signaling by IL-1β and IL-1α only occurs through this IL-1RI receptor[206][84][311]. A second IL-1-binding receptor was found on macrophages and was designated IL-1RII [237][320][321]. This second receptor is only 63 kDa and is unique because it does not transduce signal, due to its short, 29-AA-long cytoplasmic tail. IL-1RI, on the other hand, has a 213-AA-long cytoplasmic domain, which allows for easy cytoplasmic phosphorylation and downstream signaling[79][101][258][284][314][320]. This pair of receptors thus acts to regulate the cellular response to IL-1β and IL-1α by providing decoy and active binding molecules[89][331]. Both of these receptors also exist in soluble form, adding to the regulation of IL-1β signaling. The relative levels of each of the four receptors (soluble IL-1RI, membrane-bound IL-1RI, soluble IL-1RII, and membrane-bound IL-1RII) determine the amount of active IL-1β that will reach a membrane-bound, signaling IL-1RI to activate the downstream signaling pathways.

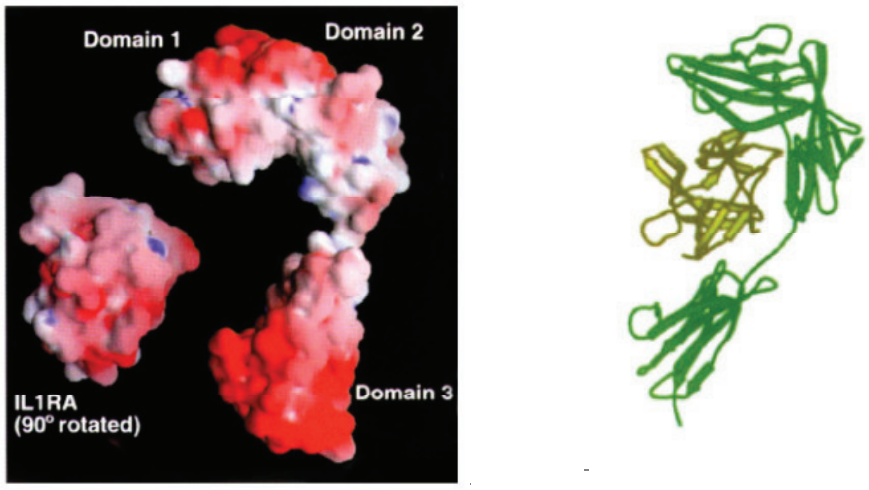

Figure 2.4: Representations of the IL-1R binding IL-1β (Schreuder+ 1997). A: Ribbon diagram of the IL-1R with IL-1β bound; B: Space-filling model of the IL-1R with IL-1β bound

All three proteins occur naturally in both secreted and intracellular forms and bind with varying affinities to the IL-1 receptors[81]. However, IL-1ra is the only IL-1 family protein

Table 2.1: Avidity of IL-1 protein binding to the IL-1 receptors

Avidity of IL-1 protein binding to the IL-1 receptors[92][93][313][259][330]	
mIL-1RI	IL-1β = IL-1ra = IL-1α
sIL-1RI	IL-1ra >IL-1α >IL-1β
mIL-1RII	IL-1β >IL-1ra >IL-1α
sIL-1RII	IL-1β >IL-1α >IL-1ra

that binds to the IL-1R without causing any signaling[16][119][300]. IL-1ra fails to recruit the IL-1RAcP to form the active signaling complex. IL-1ra only contacts 2 of the 3 binding sites in the IL-IR binding pocket that are necessary to recruit the IL-1RAcP and to cause activation of the receptor (Fig. 2.4 and Fig. 2.5)[101][209][358]. When the IL-1β domain was added back to IL-1ra, IL-1ra activated the IL-1R[160].

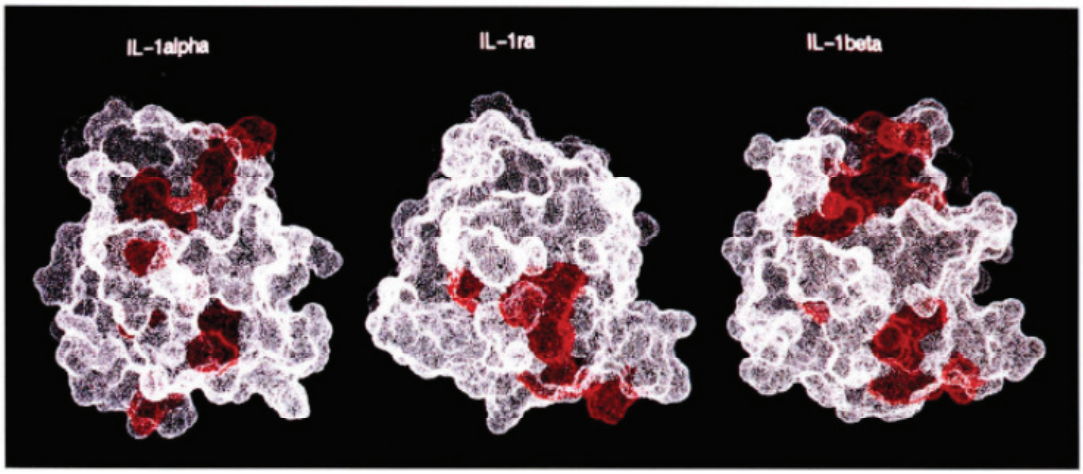

Figure 2.5: The IL-1 receptor binding sites (indicated in red) on IL-1α, IL-1β, and IL-1ra (Evans+ 1995).

The balance between IL-1 and IL-1ra is essential to regulating IL-1-related catabolic pathways and seems to determine the severity of a disease state such as OA[11][17][147]. Therapeutic strategies could be designed to interfere at crucial points within these signaling cascades, such as inhibiting the conversion of pro-IL-1β to mature IL-1β by ICE[82], adding more IL-1ra to influence the cytokine balance in the joint[6], and injecting soluble IL-1Rs to act as IL-1β sinks in the joint space[15][108], among others[4].

2.6 IL-1ra delivery for OA (human, animal models)

Because of IL-1's prominence in arthritis pathogenesis, researchers have used the antagonist molecule IL-1ra to treat both osteoarthritis and rheumatoid arthritis. Clinical trials have explored the safety of soluble IL-1ra[74] and have found that humans can tolerate up to 150 mg of IL-1ra with no adverse symptoms. Patients even showed reduced macrophage infiltration, and improved pain and function scores for up to 3 months after IL-1ra injection, even though the proteins half-life was only 4 h[74][83]. Other clinical trials tested RA patients' tolerance to frequent, high doses of IL-1ra, and found that they tolerated injections up to 7 times a week for 3 weeks, with the only major complaint being injection site irritation[65]. RA patients showed some improvement when they received IL-1ra (anakinra); however, the differences were not significant[78]. Soluble IL-1ra has also been tested in animal models of arthritis. Mice who were given continuous infusion of IL-1ra (1 mg/day) had better inhibition of CIA in both early and late-stage disease, while mice given PEGylated sTNF-RI only showed reduced early disease[191]. Another mouse study investigated the effect of IL-1RAcP versus IL-1ra in inhibiting CIA[315]. While both molecules blocked some of the CIA progression, the IL-1RAcP group did not adversely affect T cell function, while the IL-1ra group showed some negative impact. In the canine ACL transection OA model, soluble doses of IL-1ra reduced the severity and total area of degradation on the tibial plateau over 4 weeks[66]. As diseases, RA and OA behave differently on a molecular level, which might explain why IL-1ra has less success when used in RA versus OA. Most recombinant IL-1ra used in these trials is produced in E. coli[59][41][132], which may affect the proteins potency because E. coli does not glycosylate proteins like mammalian cells do. However, the cost of producing IL-1ra in a mammalian cell system is significantly higher than producing it in bacteria. Alternatively, producing IL-1ra in situ via gene therapy allows IL-1ra to receive proper glycosylation, which in turn may also improve its potency and subsequent patient outcomes[159].

Increasing the retention time of soluble IL-1ra may help make it more effective. By fusing IL-1ra to an antibody to human serum albumin, a ubiquitous protein in the body, researchers showed a significant decrease in the pain/functional impairment in mice with

collagen-induced arthritis compared with soluble IL-1ra[173].

IL-1ra has wide potential to be a powerful therapeutic for treating OA. Currently, large doses of soluble IL-1ra are necessary to achieve therapeutic results because IL-1ra has a slow receptor "on" rate, is rapidly excreted, suffers from poor tissue penetration, and can be thwarted by increased levels of membrane-bound IL-1RI and the decoy soluble IL-1RI[91].

2.7 Drug and Anti-Cytokine Therapies for OA

Steroids are commonly used for OA treatment in the clinic. Drugs such as dexamethasone (Dex) can alleviate swelling and pain in arthritic joints through direct intra-articular injection. However, these drugs are small molecules and are cleared from the joint in a matter of hours[91][146]. To increase the efficacy of steroidal drug treatment and to avoid side effects, researchers have encapsulated Dex into liposomes for controlled delivery. The only marketed liposomal Dex complex, named Lipotalon^{TM}, is available in the EU but is not approved by the FDA[39]. Other liposomal Dex formulations have been evaluated in a mouse model of collagen-induced arthritis. Dex was encapsulated by rehydrating cholesterol-based liposomes in a concentrated solution of Dex-phosphate[283]. Administering these particles in a one-time dose to collagen-induced arthritic (CIA) mice slowed their arthritis progression for 7 days post-administration, while higher daily doses of free Dex were required to achieve the same amount of inflammatory suppression.

Orthokine^{TM}is a commercially available anti-cytokine OA therapy that uses chromium sulfate-modified glass beads to stimulate IL-1ra production from patient-harvested blood and then reinjects the preconditioned serum back into the patients[135][354][295]. The autologous conditioned serum (ACS) groups in the trials had statistically significant reductions in pain and clinical scores that were greater than the control groups' scores and persisted past the treatment window[20][368][242][295].

A novel class of small molecule MMP-13 inhibitors showed moderate chondroprotective effects and improved bone and osteophyte scores in rats with MIA-induced OA as compared to the vehicle controls[22][304]. These MMP-13 inhibiting drugs showed promise for use as a disease-modifying OA drug (DMOAD) because they reduced cartilage destruction and

Table 2.2: Current Drugs for Osteoarthritis Treatment

Osteoarthritis Drug	**Action**	**Side Effects**	**Halts Disease Progression?**
Kinaret^{TM}(Anakinra)	Blocks IL-1 Receptor	None reported	NO
Dexamethasone (Dex)	Steroidal drug	Loss of bone mineralization	NO
Lipotalon^{TM}	Liposomally encapsulated Dex	Loss of bone mineralization	NO
Orthokine^{TM}	Exogenously stimulated autologous serum	None reported	NO
Cytokine Traps	Exogenous sink for IL-1β, IL-1α	None reported	NO
Carticel^{TM}	For treating cartilage defects (non-OA associated)	Arthrofibrosis, delamination of graft	NO
MMP-13 inhibitors	Inhibits MMP-13	None reported (no signs of musculoskeletal side effects that broad MMP inhibitors exhibit)	NO

provided chondroprotection.

Cytokine traps have been created as sinks for disease-inducing cytokines. The cytokine traps work by providing a soluble cytokine receptor, such as IL-1R, complexed with its accessory receptor protein, such as the IL-1RAcP, via recombinant Fc tails. This complex exhibited a 100-fold increase in cytokine affinity over the affinity from the soluble receptor alone[108].

Selectively removing cytokine-inducing cells from the OA joint space could also modify the disease progression. In an explanted OA synovial fibroblast cell culture model, CD14+ OA synovial macrophages were removed from primary OA-derived cell cultures using targeted beads. Cultures that lacked these CD14+ cells showed "significant inhibition" of synovial fibroblast-produced cytokines, leading to the hypothesis that synovial macrophages incite synovial fibroblasts to stay activated[51]. The ability to selectively remove these synovial macrophages in an in vivo setting could be technically complicated, which would limit the effectiveness of this technology. However, targeting CD14+ cells may

provide an alternative strategy for modifying the OA pathology.

Current drug and anti-cytokine strategies have shown moderate success in ameliorating OA inflammation and pain in the short-term. However, these therapies have not shown long-term benefit without chronic injections or oral dosing. OA activates a broad spectrum of cells, cytokines, and metabolites that are not easily or permanently altered by a single protein or drug. Anti-cytokine therapies must embrace multi-valent, controlled delivery approaches, like incorporating multiple cytokines and/or drugs paired with long-release/long-retention delivery vehicles to effectively alter the OA environment to affect disease progression in a permanent manner.

2.8 IL-1ra Gene therapy for OA

Researchers have looked to gene therapy to administer continuous high levels of IL-1ra for arthritis treatment to address the problem of fast protein clearance from the joint. They have explored retroviral[21][46][118][115][355][117], lentiviral[158][159][157] and adenoviral[139][249][350][241] vectors to induce IL-1ra expression in different animal models and human patients.

In a mouse model of IL-1ra gene therapy, mouse HSCs were transduced with an IL-1ra-containing retrovirus and then were transferred into irradiated mice. The primary transduced animals produced IL-1ra within a range of 50-1000 ng/mL. To then prove the stability of the transduction, cells from the primary animals were transferred into secondary lethally irradiated animals, where they produced 40-140 ng/mL IL-1ra for up to 7 months post-transfer[46].

In rats, a lentivirus that expressed IL-1ra efficiently transduced synovial cells in vivo without significant extraneous transduction of other cells. Expression of IL-1ra in immunocompromised rats lasted up to 6 weeks, whereas immunocompetent rats only expressed the protein for 20 days[158].

In rabbits, retroviral expression of IL-1ra ex vivo was evaluated in both allograft and autograft models. The allografted cells expressed protein for 12 days, while autografted cells expressed at least 100 pg IL-1ra/knee for up to 5 weeks[21]. In another study, arthritis

was induced by MCL transection combined with menisectomy, and adenoviral expression vectors containing IL-1ra and/or soluble TNF-RI were directly injected into rabbit knees. The joints were evaluated for protein expression and reduction of synovitis. Rabbits that received IL-1ra showed reduced cartilage degradation, but adding sTNF-RI vector reduced the synovitis as well as some of the degradation[350]. Fernandes et al. used canine cells to deliver IL-1ra to MMT-induced arthritic rabbits using a plasmid-lipid conjugate[124]. The amount of IL-1ra vector injected positively correlated with a decrease in lesion size. Finally, researchers induced arthritis by medial collateral ligament transection together with a medial meniscal transection (MCLT/MMT) and then injected retrovirally transduced allograft cells containing IL-1ra, IL-10, or both IL-1ra and IL-10. Rabbits receiving IL-1ra-transduced cells showed less cartilage breakdown than those receiving IL-10-transduced cells, but animals receiving both genes showed superior chondroprotection over animals who received either single protein[378].

Dogs were given arthritis using the anterior cruciate ligament transection (ACLT) model. Synovial cells were harvested from the left knee, were transfected with IL-1ra, and were then reinjected into the joint space. IL-1ra-transduced cells reduced the appearance of macroscopic lesions on the tibial plateau and femoral condyles, and also decreased the average histologic lesion scores[264].

In horses, synoviocytes were adenovirally transduced with IL-1ra, alone or in tandem with IGF-1, and the effects of these synoviocyte cells were assessed on explanted horse cartilage cultures. Explants cultured with IL-1 or media only were exposed to the transduced synoviocytes. Non-arthritic explants with IL-1ra/IGF had higher PG content than any of the other groups. IL-1-degraded cultures recovered some PG content when exposed to IL-1ra-expressing synoviocytes, but IL-1-degraded cultures fully recovered their PG content when exposed to both IL-1ra and IGF-expressing synoviocytes[249]. The same combination of proteins expressed in Adenoviral-Associated Vectors (AAV) was used to repair chondral defects in horses. There were no significant changes among the groups, however, the IL-1ra/IGF treated group had higher collagen II and PG content[241]. A final equine study showed that an adenoviral vector could express detectable levels of IL-1ra for 28 days and

improved the overall cartilage erosion scores. However, IL-1ra did not affect the joint effusion[139].

A limited number of clinical gene therapy trials have evaluated IL-1ra in humans. Two females with RA in their finger joints had their synovial fibroblasts harvested, retrovirally transduced with IL-1ra, and then reinjected into the affected MCP joints. One patient saw extreme reduction in her joint swelling, while the other showed moderate reduction in her symptoms[355][117]. Evans et al. also delivered transduced autologous synovial fibroblasts to the MCP joints of 9 female RA patients. The joints from patients receiving intermediate or high doses of transduced cells had detectable IL-1ra expression at 1 week post-injection[118]. In a related study, intervertebral disc explants were transduced with a vector expressing IL-1ra. IL-1ra expression reversed matrix degradation in the IVD cultures and also inhibited metal-dependent protease activity[214].

The practical application of gene therapy for OA suffers from concerns about gene vector safety, low transduction efficiency in situ, loss of gene expression over time, cell alterations during ex vivo manipulations, and public perception[264][139][158][355][195][118][116]. Although in the long-term, gene therapy technologies will hopefully overcome these hurdles, the current therapies still lack the combination of efficacy and safety that would override the public and the FDAs reluctance to embrace these therapeutic approaches.

2.9 Animal models for OA

2.9.1 Induced Arthritis

Researchers can induce arthritis in the lab in two main ways: mechanical instability and chemical damage[98][185][279]. The most common mechanical instability OA models involve either transecting the ACL, MCL, or cutting the medial meniscus to destabilize the joint and cause arthritis. These methods have been evaluated in rabbits, dogs, rats, and sheep[9][55][210][349][341]. The canine 'groove' model is a less common OA model that involves inducing mechanical damage to the articular cartilage and then forcing the dogs to load the damaged joint in a transient fashion. This model recapitulates human OA in 10 wks[236].

Monosodium iodoacetate (MIA) is a chemical OA model that causes chondrocyte death, leading to an extreme inflammatory environment[54][76][163][162][364][343]. MIA recapitulates an OA-like phenotype with cartilage lesions visible both macroscopically and histologically. It also induces nociceptors and stimulates pain during OA[255]. The synovial membrane shows signs of hyperplasia and fibrosis. MIA also alters proteoglycan metabolism, reducing the amount of sulfated GAGs present in the cartilage[105][327]. Animals show reduced spontaneous mobility, which indicates pain and joint stiffness (catwalk)[127]. After OA induction by MIA, rats exhibit changes to articular cartilage in tibial plateaus and femoral condyles by 7 days and large-scale bone changes at 28 days. This method does not fully recapitulate osteoarthritis because it causes extreme cartilage damage in a short period of time, but it is used as a model of cartilage degradation and pain during osteoarthritis[114][302][126].

2.9.2 Spontaneous Arthritis

Researchers have created knock-out mice that lack various proteins thought to be critical in osteoarthritis development. Although k.o. models can be powerful research tools, spontaneous arthritis is highly strain-specific. For example, IL-1ra-k.o. mice developed rheumatoid-like arthritis spontaneously when crossed on a Balb/C background, while C57/Bl6 mice showed RA protection[177]. Most of the other IL-1-related gene-knockout mice (IL-1, ICE, iNOS, stromeolysin-1) showed faster cartilage degradation after knock-out[77]. This result was surprising because the literature assumes IL-1 plays a primarily destructive role in OA. The Dunkin-Hartley guinea pig strain shows susceptibility for spontaneous arthritis. At 24 weeks of age, the DH guinea pigs had twice the radiographic score of their age-matched, non-arthritic strain counterparts (Bristol Strain 2) and maintained high IL-1β expression into adulthood, implying a role for IL-1β in spontaneous OA development[281][297][10]. Although spontaneous arthritis animal models can recapitulate the osteoarthritis progression that is seen in humans, disease progression takes time to develop, making drug testing and therapeutic evaluations slow[28][30][31][32][317][251].

2.10 Biomaterials for OA drug/protein delivery

There has been no shortage of biomaterial-based efforts to deliver drugs and protein for OA treatment[211]. The most common approach involves the creation of either solid or liposomal particles that encapsulate a small molecule drug[178][223]. Methotrexate (MTX) (antimetabolite/antifolate agent), dexamethasone (Dex) (glucocorticoid), and indomethacin (Ind) (NSAID) are the current standard drugs for treating OA and show up most frequently as model drugs for encapsulation. These small molecule drugs easily retain their bioactivity when encapsulated. Liposome-encapsulated Dex has been used for IA delivery in healthy and AIA-arthritic rabbits[48]. Dex has also been encapsulated in magnetic PLGA particles[63]. In fact, liposomal Dex is available in Europe for intraarticular delivery for OA[39]. Liposomal Dex reduced arthritis scores and inflammation in a mouse model of arthritis at 8 days post-injection compared with control animals that received daily bolus doses of Dex[283]. Localized or conjugated forms of MTX avoid or minimize its detrimental side effects, such as bone marrow and gastrointestinal toxicities[165]. MTX has been conjugated to hyaluronic acid for controlled delivery in antigen-induced arthritic rats and significantly reduced joint swelling for up to 20 days post-injection[174][175]. Liposomal MTX decreased IL-1 and IL-6 gene expression (as measured by mRNA levels) in AIA-induced rats for 7 days after the initial particle injection[363][362]. MTX was encapsulated in PLA particles for delivery to the rabbit joint. Loading the drug into particles increased the local concentration of MTX while also decreasing the circulating levels of MTX[220][219]. Zhang et al. delivered NIPAAm-ethyl aminobenzoate amphiphilic particles containing Ind to CFA-induced arthritic Sprague-Dawley rats[374]. The Ind-loaded particles reduced paw edema in a more pronounced fashion than a dose of soluble Ind, while also eliminating the gastric ulceration that occurs with free Indomethacin. Clodronate liposomes have been administered intraarticularly to humans with RA[24]. Clodronate eliminates synovial lining macrophages and osteoclasts by inducing apoptosis. Patients receiving clodronate liposomes had reduced CD68 staining, which correlated with reduced cartilage destruction. However, this drug did not affect the FLS, possibly limiting the overall effectiveness of this treatment for OA. The inherent properties of micellar particles make them attractive for targeted drug therapies,

but they have not been investigated for OA applications[196].

Particle systems have been evaluated by themselves for retention and size appropriateness in the intra-articular joint space[179]. Liposomal chelators made of a cholesterol derivative (less than 1 μm) had retention of up to 41% at 21 days[23]. However, these contained no therapeutic payload. Other research investigated albumin microspheres for intraarticular drug delivery to rabbits. The albumin particles were 3.5 μm in size and were loaded with rose bengal dye. They showed 50% retention in the knee for 4 days[282]. Chitosan microparticles have been synthesized for intraarticular delivery of celecoxib to CFA-induced rats. Celecoxib-loaded particles (8 μm diameter) released 50% of their payload by 1 h, and unloaded 80% in 96 h in vitro[334]. Finally, researchers have created hyaluronic acid-coated PLGA particles to increase their adhesiveness and retention in the intra-articular space. The particles were evaluated only for biosafety indicators, but showed no signs of wear and no inflammation[382].

Although small molecule drugs show promise in treating many symptoms of arthritis, the use of biomolecules as therapeutics may have more targeted, biologically-relevant effects on the disease. However, most biomolecules are smaller than the retention threshold of the synovial joint and require a carrier or other mechanism to retain these therapeutics in the target area. One recent approach created a fusion protein from Elastin-Like Peptides and IL-1ra. When injected at physiological temperature, this construct self-assembles into submicron scale "drug depots" that act as reservoirs for the presentation of IL-1ra to macrophages and other inflammatory cells in the arthritic joint space[7][197][305]. Both soluble and aggregated IL-1ra-ELPs reduced IL-1β levels up to 72 h post-stimulation in in vitro cultures[197]. Previous work with just the ELP showed retention in the joint of 4 days, compared with 3.37 h for non-assembling ELPs[36]. However, the fusion protein reduced the native bioactivity of IL-1ra by almost 90% by interfering with its ability to bind to the receptor[305]. In IL-1β-induced arthritic rats, IL-1ra-ELP depots improved the joint phenotype over bolus IL-1ra. The authors noted a less severe pathology in the IL-1ra-ELP-treated femoral condyles and in the histological sections compared with both untreated and bolus IL-1ra-treated tissue[7]. Chondroitin sulfate-coated Gelatin microspheres were

evaluated for retention and delivery of catalase and albumin to mice knee joints[62]. The particles efficiently encapsulated catalase (75% efficient) and released their payload only in the presence of collagenase. A chondroitin sulfate particle coating may help increase the residence time and targeting of particles within the joint space.

Attaching a PEG oligomer or polymer chain to a protein referred to as PEGylation - has been evaluated for increasing the circulation time of various proteins, including IL-1ra[142]. Gaertner et al. took advantage of N-terminal serine/threonines to attach a PEG oligomer to IL-1ra, IL-8, and G-CSF. However, there was only minor improvement to the protein half-life by this strategy[141]. Other groups have also attempted PEGylation using a mono-PEGylated IL-1ra with either a 5k or 10k PEG chain attached to the terminus. PEGylated IL-1ra retained 40% of its original binding activity through thiol-directed conjugation, while randomly conjugated protein only maintained 9.8% activity[371][372].

Microencapsulation techniques have been attempted to deliver therapeutic quantities of protein using particles[360]. A double emulsion process was used for a multi-block copolymer system to encapsulate albumin in vitro[37]. However, this process suffers from low protein encapsulation efficiency (only a few weight % of total formulation) or exposure of the protein to organic solvent. Alternatives include using reverse dialysis of a protein solution against precipitating agents, making protein crystals for encapsulation, and cooling a pre-heated supersaturated solution before dialyzing against pre-formed particles[188][26][326][379].

Other research has attempted to attach proteins to particles (liposomes, micelles, solid particles) for therapeutic delivery or tissue targeting[229][250]. A variety of tethering moieties have been incorporated into biomaterials to allow protein conjugation and delivery. The most common chemical handles are: acetylation[366][253][198][193][106], biotinylation [189][176][71]/Streptavidin[53], maleimide[221][247][270][307][344][171] or thiol-termination [286][252][246][224][205][200][104], hydroxyl termination[201][180], click chemistry (azido functionality)[260][170][86][377], and the ubiquitous EDC-NHS chemistry for carboxylic acid-primary amine linkages[369][277][222][70][56]. The 4-nitrophenol moiety has been used only in a limited fashion and specifically by one research group that employs this functionality for tethering antibodies to liposomal particles[5][97][113][192][217][226][227][244][332]

[338][337][339]. For example, a PEG-PE micelle modified with pNP showed 10-20 antibodies attached to a single particle by fluorescence and SDS-PAGE. The PEG-PE micelles carry a net negative charge that could inhibit non-specific cellular uptake of the micelles[336]. For this thesis research, pNP became a good alternative to EDC-NHS protein tethering, based on the mild reaction conditions for pNP-primary amine displacement and the overall stability of the pNP leaving group. IL-1ra has been encapsulated in PLGA particles for cancer delivery[213]. The particles released significant amounts of IL-1ra for up to 14 days and significantly increased the survival of tumor-bearing mice. Current biomaterial delivery systems exhibit several limitations. First, most drug-delivery particles are hydrophobic, which is not optimal for hydrophilic protein encapsulation. Second, hydrophobic particles, such as PLGA, could cause wear damage to the already-fragile OA cartilage structure. Additionally, these particles usually suffer from non-specific protein adsorption, which causes increased phagocytosis and can lead to increased inflammation. Liposomal particles have limitations as well. Because of their spontaneous, self-assembling structure, they have lower stability in serum than solid polymer particles, and are subject to hydrolysis and oxidation[294][212]. They also tend to leak out encapsulated drugs and can be expensive to manufacture[182][52][353][19][140]. Solid polymer particle systems, such as PLGA, are good at small molecule drug delivery, while liposomes are usually better for protein delivery because they have hydrophilic cores for protein encapsulation. Our amphiphilic system has both drug and protein delivery capabilities in the same particle system. The design of these particles allows for protein immobilization on the surface, as well as hydrophobic drug encapsulation in the particles core. Finally, the literature is short on examples of particles for OA treatment that employ both a targeting moiety and a therapeutic drug in the same particle[27][38][56][71][69][86][112][144][176][256][254][292][346]. Targeted therapies that are delivered intra-articularly will increase the effectiveness of current OA treatments and will serve as the next generation of drug delivery technologies[73][109].

Our IL-1ra-based system has distinct advantages over current particle-based technologies. First, IL-1ra acts as both a targeting ligand and a therapeutic molecule simultaneously,

abrogating the need for multiple ligands. However, our tethering scheme is highly modular because it uses primary amines to conjugate proteins/peptides to the particle surface. For instance, this system could allow the delivery of TGF-β, IL-1ra, and IGF-1 simultaneously. Secondly, the pNP protein tethering moiety has a high conversion efficiency that allows for concentrated protein tethering to the particle surface. RAFT polymerization makes a low polydispersity polymer that will form particles in a narrow size range. The RAFT polymer also allows us to easily form a block copolymer with the monomers of our choice. We incorporate a hydrophilic TEGM segment with a hydrophobic CHM segment, both with predictable size based on stoichiometry, to allow the formation of a "core-shell" or"micellar-like" particle structure when exposed to aqueous solvent (hydrophilic on the outside, hydrophobic on the inside). The polymer chain length can be easily modified by varying the ratio of monomers during polymerization. Finally, although not addressed in the scope of this thesis work, this polymer system can easily incorporate hydrophobic small molecule drugs in its core, allowing us to form dual-action therapeutic particles.

2.10.1 RAFT polymers

Reversible Addition Fragmentation chain Transfer (RAFT) is a recent polymerization strategy whose advantages include a wide range of monomers that can be used and the "non-demanding" reaction conditions. RAFT polymerization uses some of the same principles as classical free radical polymerization, like initiation by UV, thermal activation or gamma initiation, but the chain transfer in RAFT is reversible and leads to simultaneous chain growth without affecting polymerization rates (Fig. 2.6). This growth mechanism creates polymers in a one-step process with a pre-determined MW and low polydispersity index (PDI). The original RAFT paper from Chiefari et al. demonstrated the ability of RAFT transfer agents to build polymers with a narrow MW distribution using styrene and acrylonitrile monomers over 18 h. These polymers had low PDI, especially compared to the same monomers polymerized via standard methods[75].

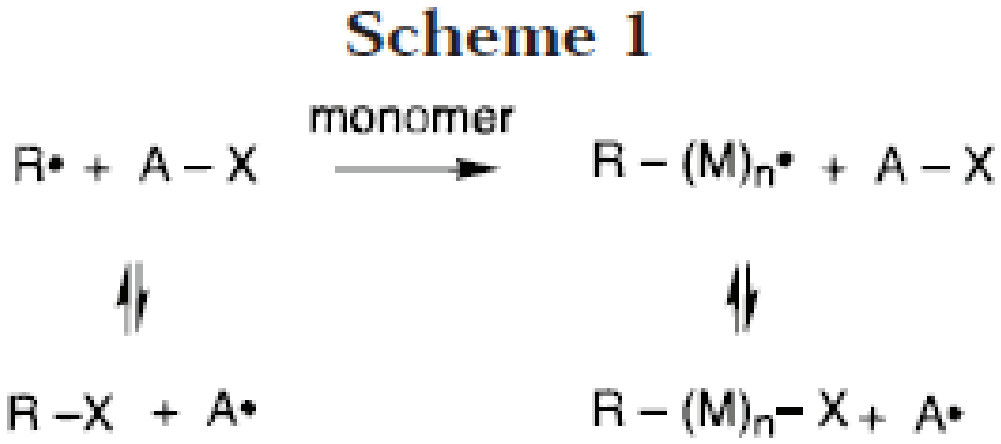

Figure 2.6: Schematic of the general RAFT polymerization strategy (Chiefari+ 1998). A radical initiator (e.g., A radical initiator, such as AIBN (R), reacts with the monomer to make a radical monomer (R-Mn) that then interacts with the dithioester (RAFT agent) (A-X), displacing a radicalized leaving group (A) that further activates monomer units and allows for chain propagation.

RAFT has been broadly used for making monomeric polymer chains as well as block copolymers (di, tri, etc.). Methacrylate polymers were synthesized by RAFT using a 4-nitrophenol (pNP) functional moiety on the chain transfer agent. These polymers had polydispersity indexes of less than 1.3, which is a major improvement over traditional methods that have PDI values closer to 2.0[120]. The polymer chains also showed up to 86% pNP substitution rates when exposed to a modified glycine amino acid in solvent (TEA/DMSO)[183]. RAFT polymerization is able to create a wide range of narrow PDI polymers in a one-step process without protecting/deprotecting steps. It is also compatible with a wide range of monomers and has predictable MW characteristics that make it a modular synthetic process with desirable polymer fidelity[75]. RAFT polymers have great promise for drug and protein delivery applications[240][248][288][324][370].

Other functional handles for protein/peptide tethering have also been employed in

RAFT polymers. A biotin-functionalized RAFT agent was used to form pNIPAAm and pHPMA, as well as a diblock copolymer from NIPAAm/HPMA (PDI<1.3). The diblock polymer formed a "core-shell" structure when exposed to temps above NIPAAms LCST, and left the biotin groups on the surface to allow decoration of the particles with avidin-functionalized molecules[176]. RAFT polymers with protected aldehydes have also been synthesized to allow for post-particle modification with peptides. A p(OEGMA)-block-p(STY-co-TMI) polymer had a PDI of less than 1.2 and formed micelles when exposed to aqueous solvent. Deprotecting the aldehyde functionality allowed for "decoration" of the particles with the RGD peptide. The particles also used the isocyanate groups from the block copolymer to create a cross-linked core to stabilize particles[106].

Diblock RAFT polymers have been formed into micellar particles by dialysis of the polymer solution against water or buffer[375]. Garnier et al. synthesized RAFT copolymers with a poly(butyl acrylate) hydrophobic segment and various hydrophilic segments (poly(dimethyl acrylamide) (pDMA), poly(acryloyloxyethyl methylsulfoxide) (p(M4)), and poly(N-acryloylpyrrolidine) (pAPR). These polymers all formed micelles around 20-100 nm that had rod or worm-like shapes[143].

CHAPTER III

ENGINEERING A RAFT-BASED BLOCK COPOLYMER TO MAKE PROTEIN-DELIVERING PARTICLES

3.1 Summary

Polymer microparticles have been used in a limited fashion to deliver proteins to arthritic joints. Encapsulating proteins within particles can affect their bioactivity due to exposure to solvents and other non-physiologic environments. Solid microparticles are usually hydrophobic in nature, which can cause nonspecific protein adsorption, particle phagocytosis, and can drive inflammation. Developing a particle system that can preserve the protein bioactivity while also exhibiting the stability characteristics of a solid microparticle would increase the effectiveness of a microparticle drug-delivery system. We report here the synthesis and characterization of an amphiphilic RAFT block copolymer that self-assembles into particles in our target size range of 300 nm. The monomer components of the polymer incorporate a "stealth" tetraethylene glycol methacrylate to form a hydrophilic particle corona and a hydrophobic cyclohexyl methacrylate group to form a highly stable particle core. We also report the successful modification of a commercial microRAFT agent with the 4-nitrophenyl moiety, which acts as the protein tethering handle on the particles.

3.2 Introduction

Creating tailored technologies for protein and drug delivery in a disease model is crucial to the ultimate success of that technology. An attractive application is delivery of biological molecules like disease-specific proteins in relevant quantities to the appropriate cells/tissue. Bolus injections of proteins, such as IL-1ra, can be effective therapeutics in the short-term, but require repeat injections and can become quite costly[65]. Current delivery strategies can efficiently encapsulate hydrophobic, non-biological drugs without losing their effectiveness or bioactivity[211][39][178]. However, these polymers have limited application to protein delivery because of their hydrophobicity and solvent use, which both can detrimentally

affect protein bioactivity and encapsulation rate.

PEGylation of the protein itself is one strategy that addresses this limitation. This modification forms pseudo-particles with the protein and increases the effective protein size. However, this addition can affect the protein's bioactivity, even though it may increase body residence time[142][371][372]. Other research has attempted to form "drug depots" with the protein conjugated to a self-assembling recombinant protein[305]. This strategy also severely decreased the bioactivity of the protein by almost 90% in vitro. Therefore, more effective strategies for delivering protein are needed.

Targeted delivery of these therapies is a primary design criterion for current drug/protein delivery technologies. Targeting strategies include RGD (a non-specific integrin binding motif)[383], biotin-streptavidin interactions, which have a strong K_{on}, but can be strongly immunogenic[57], phage-derived peptides[292], folate (ovary, breast, kidney, myeloid cell, and lung cancers), and even antibodies (i.e., breast cancer targeting)[226][112]. Our use of a full protein for synoviocyte targeting has much higher affinity ($IC50_{IL-1ra}$ = 0.4 nM vs. $IC50_{RGD}$ >100 nM) [137][273] and specificity than peptides like RGD. Our targeting protein, IL-1ra, concomitantly acts as an anti-inflammatory therapeutic, giving it strong multi-use potential.

We present a new block copolymer that efficiently and covalently tethers protein by harnessing the power of an aqueous protein tethering chemistry that acts with high efficiency in mild reaction conditions (pH>7.4). This polymer technology can be tailored to make a range of particle sizes while maintaining the same protein tethering chemistry. We harness this technology to create sub-micron-scale particles with a surface-bound anti-inflammatory protein for simultaneous synoviocyte cell targeting and therapeutic functions. This system has wide potential for making modular, multi-functional particles by simply varying the protein mixture during tethering.

3.3 Materials and Methods

3.3.1 μRAFT agent modification

The μRAFT agent was designed and synthesized by Dr. D. Scott Wilson (Murthy Lab, Georgia Institute of Technology) for use in this project and was referenced from [380]. All reagents were obtained from Sigma-Aldrich and used as-is, unless otherwise specified.

3.3.1.1 Synthesis of 17-hydroxy-3,6,9,12,15-pentaoxaheptadecyl 2-((phenylcarbonothioyl)thio)acetate (1)

A solution of N,N'-dicyclohexylcarbodiimide (DCC) (619.0 mg, 3.0 mmol) in 5 mL dichloromethane (DCM) was added drop-wise to a stirred solution of (benzothioylsulfanyl)acetic acid (500 mg, 2.36 mmol), hexaethylene glycol (1.41 g, 5.0 mmol), and a catalytic amount of 4-dimethylaminopyridine (DMAP) in 50 mL DCM at 0°C. After adding the DCC, the solution was allowed to come to room temperature. After 2 additional hours of stirring, the solutions were filtered, and the organic solution was concentrated via rotary evaporation, resuspended in ethyl acetate, and finally evaporated onto silica gel. The desired product was isolated by flash silica gel chromatography on silica gel, using a mixture of ethyl acetate and hexanes (6:4).

3.3.1.2 Synthesis of 1-(4-nitrophenoxy)-1-oxo-2,5,8,11,14,17-hexaoxanonadecan-19-yl 2-((phenylcarbonothioyl)thio)acetate (μRAFT agent)

A solution of 4-nitrophenyl chloroformate (201 mg, 1.0 mmol) in 1 mL of DCM was added drop-wise to a stirred solution of (1) (476 mg) and pyridine (95 mg, 1.5 mmol) maintained at 0°C. After 1 h of stirring, the solutions were filtered, and the organic solution was concentrated via rotary evaporation, was resuspended in ethyl acetate, and finally was evaporated onto silica gel. The desired product was isolated via flash silica gel chromatography on silica gel using a mixture of ethyl acetate and hexanes (4:6).

3.3.2 Tetraethylene Glycol Methacrylate (TEGM) synthesis

Tetraethylene glycol (5.0 g, 25.7 mmol) (#110175, Aldrich, St. Louis, MO, USA), and pyridine (2.0 g, 25.3 mmol) (#PX20202-5, EMD, Gibbstown, NJ, USA) were added to anhydrous dichloromethane (DCM) (100 ml) in a 250 ml flask and stirred for 30 min at

0°C. Methacryloyl chloride (2.6 g, 25 mmol) (#64120, Fluka, Sigma-Aldrich, St. Louis, MO, USA) was added drop-wise to the stirred solution. The reaction was allowed to stir at 0°C for 2 h, and then at room temperature for an additional 2 h. The reaction was then concentrated via rotary evaporation, resuspended in ethyl acetate, and then evaporated onto silica gel. The monomethacrylate product was separated from the di-methacrylate byproduct and any remaining starting materials via flash silica gel chromatography on silica gel, using a mixture of ethyl acetate and hexanes (7:3).

3.3.3 Copolymer synthesis

3.3.3.1 Hydrophilic block synthesis

TEGM (0.9 g, 3.43 mmol), μRAFT agent (22.0 mg, 0.034 mmol), and AIBN (0.5 mg, 0.003 mmol)(#441090, Aldrich, St. Louis, MO) were combined in DMF (1.5 ml). The reaction flask was degassed by five freeze-pump-thaw cycles, and was then immersed in an oil bath and stirred at 65°C. After 20 h, the reaction was terminated by flash freezing in liquid nitrogen. The reaction product was added to DCM (5 ml) and then was precipitated from methanol (25 mL). The supernatant was decanted and the precipitated polymer was subjected to three more rounds of resuspension (DCM) and precipitation (MeOH) before being concentrated under reduced pressure. The purified polymer was analyzed for weight by gel permutation chromatography (THF) and the structure and purity of the resulting polymer were verified by ^{1}H-NMR (DCM).

3.3.3.2 Hydrophobic block synthesis

pTEGM (0.5 g, 1.90 mmol), cyclohexyl methacrylate (213.65 mg, 1.27 mmol) (Tokyo Chemical Industry Co, Ltd., Tokyo, Japan) and AIBN (0.25 mg, 0.0015 mmol) were combined in DMF (1.5 mL). The reaction flask was degassed by five freeze-pump-thaw cycles and was then immersed in an oil bath and was stirred at 65°C. After 20 h, the reaction was terminated by flash freezing in liquid nitrogen. The reaction product was added to DCM (5 mL) and was precipitated using methanol (25 mL). The supernatant was decanted and the precipitated polymer was subjected to three more rounds of resuspension (DCM) and precipitation (MeOH) before being concentrated under reduced pressure. The purified polymer

Table 3.1: Synthesis of hydrophilic polymer chain (Block A): Example Calculations

Block A	μRAFT	TEGM	AIBN	
Molar Ratios	[1]	[100]	[1/10]	60°C, 8 h
Example Calculation	22 mg	900 mg	0.5 mg	
	[0.034 mmols]	[3.43 mmols]	[0.003 mmols]	
	(664.15 mg/mmol)	(263.1 mg/mmol)	(164.21 mg/mmol)	

Table 3.2: Synthesis of block copolymer (Block A+B): Example Calculations

Block A+B	Block A	CHM	AIBN	
Molar Ratios	[3]	[2]	[1/4]	60°C, 20 h
Example Calculation	500 mg	214 mg	0.25 mg	
	[1.90 mmols]	[1.27 mmols]	[0.0015 mmols]	
	263.1 mg/mmol	168.23 mg/mmol	164.21 mg/mmol	

was analyzed for weight by gel permutation chromatography (THF) and the structure and purity were verified by ^{1}H-NMR (DCM).

3.3.4 ^{1}H-NMR and ^{13}C-NMR Analysis

Samples of the modified components (μRAFT, TEGM) and the copolymer were dried under vacuum to remove excess solvent. The samples were resuspended in $CDCl_3$ for NMR analysis. All analyses were run on a 400 MHz low-field NMR (Oxford Instruments, Oxfordshire, England).

3.3.5 MALDI-TOF Mass Spectroscopy

MALDI-TOF mass spectroscopy analysis was done by the Georgia Tech Core Facilities laboratory.

3.3.6 Particle Formation and Protein Tethering

Copolymer was dissolved in THF at a concentration of 40 mg/mL. 50 mL of 0.01 M PBS was added to a 100 mL beaker and was set on a stir plate at 400 rpm. 20 mg polymer, dissolved in 2.5 mL THF/DMF (9:1), was added to the aqueous phase at 20 mL/h using a syringe pump (10 mL syringe, 18 gauge needle). Once the polymer was added, the solution was transferred to a 250 mL round-bottom flask and the solvent was evaporated under reduced pressure for 30 min to remove THF. The particle solution was concentrated by

centrifugation using 100 kDa centrifugal filters (#UFC810096, Amicon Ultra-4 Centrifugal Filters with Ultracel-100 kDa membranes, Millipore, Billerica, MA) (2,750 x rpm, 3 min), and was then sonicated for 30 sec to resuspend any clumped particles.

IL-1ra or heat-denatured Bovine Serum Albumin (HD-BSA) protein was added to the particle solution and the pH was raised to 8.0 using 0.01 M NaOH. The particle+protein solution was allowed to react overnight. Ten mg glycine in PBS was added to quench any remaining reactive groups and was allowed to react for 30 min. The particle solutions were put in 10 kDa dialysis tubing and were dialyzed overnight against PBS with at least 3 buffer changes. The particles were transferred to sterile microcentrifuge tubes and were stored at 4°C until further use.

3.3.7 Cytotoxicity Assay

RAW 264.7 macrophage cells (From the Murthy lab (Georgia Tech); TIB-71, ATCC, Manassas, VA) were cultured using Dulbeccos Minimum Essential Media (DMEM) supplemented with 10% FBS at 37°C, 5% CO_2. At confluency, cells were scraped to remove them from the culture plates. The cell suspension was centrifuged, and the pellet was resuspended in 1 mL media. Cells were counted using a hemacytometer, and diluted to a final concentration of 300,000 cells/mL. One mL was added to each 12-well. Cells were allowed to adhere for 4 h. Supernatant was removed and replaced with pure DMEM overnight to quiesce cells. The next morning, 0.5 mL of phenol-red-free DMEM + particles was added at concentrations of 0.1, 1, and 10 mg/mL. The cells were incubated with the particles in serum-free media for 6 h before analyzing using MTT (Sigma-Aldrich, St. Louis, MO). The MTT assay measures the oxidation of MTT dye by cellular reductase enzymes. It measures cellular metabolic activity and is used as an indirect measure of cell viability and proliferation. MTT substrate (50 μL) was added to each well and was incubated for 2 h at 37°C. 0.5 mL 0.1 M HCl was added to each well to develop the substrate. Each well was pipetted to mix and then transferred to a 96-well plate for colorimetric detection using a plate reader at 570 nm (HTS 7000 Plus, Perkin Elmer, Waltham, MA).

3.3.8 Particle Characterization: Dynamic Light Scattering (DLS)

50 μL of particle solution was resuspended in 3 mL PBS in a cuvette. The DLS instrument (90 Plus Particle Size Analyzer, Brookhaven Instruments Corporation, Holtsville, NY) was allowed to warm up for 10 min and the cuvette was agitated by inverting multiple times quickly before placing in the DLS for analysis. The particles were analyzed 3 times at 1 min each (refractive index: 1.33). The DLS has a scattering angle of 90°, a 35 mW solid state standard laser (660 nm), and a Brookhaven BI-9000AT correlator board. It uses a MAS-OPTION integration system.

3.3.9 Particle Characterization: Fourier Transform Infrared Spectroscopy (FTIR)

Michael Bayless (Soper group, Georgia Tech) helped run the FTIR analysis for the modified components in this work. Infrared (IR) spectra were obtained on a Bruker Alpha-p Fourier transform infrared spectrophotometer.

3.3.10 Particle Characterization: Quantification of 4-nitrophenol (pNP) release

pNP release was quantified by high pressure liquid chromatography (HPLC) using a reverse-phase C18 column (#WAT044375, Nova-Pak C18 column, 4 μm, 4.6 x 150 mm, Waters Corp., Milford, MA) and an isocratic flow profile with 50% methanol in nanopure H_2O, supplemented with 0.01 M tetrabutylammonium bromide (TBAB)[8]. Samples were run at 1 mL/min for 15 min each. A spectrum from 190 nm to 500 nm was collected. The UV-vis spectrum of pNP (λ = 254 nm) has peaks around 405-410 nm, 310-315 nm, and 225 nm (0.1 mM pNP at pH 7.0)[381]. We chose to focus on the peak at 405 nm to avoid any interference at 310 nm that may occur due to proteins in the solution.

3.3.11 Protein Tethering Analysis via Dot Blot

Nitrocellulose membrane was cut to the size of a 96-well plate and placed in a 96-tube PCR tube holder. Ten μL of particles or protein standard was pipetted into each well space and was allowed to dry completely (approx. 1 h). The membrane was blocked in ELISA wash buffer (WB) (25 mL 1% HD-BSA, 200 μL 0.5 M EDTA, 50 μL Tween-20, fill to 100 mL with

PBS) for 1 h at RT on a shaker table. Wash buffer was removed and 1:400 dilution of rabbit anti-IL-1ra antibody (#NB110-4797, Novus Biologicals, Littleton, CO) in ELISA WB was added to the membrane. The membrane was incubated for 1 h at room temperatureon a shaker table. The membrane was washed three times for 5 min each in fresh ELISA WB, then a 1:10,000 dilution of goat anti-rabbit nearIR 800 antibody (IRDye 800CW, Odyssey, LI-COR Biosciences, Lincoln, NE) in ELISA WB was added to the membrane. The blot was covered in foil and was incubated at RT for 1 h on a shaker table. The membrane was washed twice for 5 min in fresh ELISA WB and the blot was imaged using a LICOR nearIR scanner (Odyssey Infrared Imager, LI-COR Biosciences, Lincoln, NE). The intensity of each spot was measured using the LICOR ODYSSEY 2.1 software.

3.4 Results

Our strategy for this aim was to engineer an amphiphilic block copolymer with a stable protein tethering moiety that formed submicron scale particles and allowed protein tethering to the particle surface. Figure 3.1 shows the schematic for the proposed block copolymer. After modifying the commercial RAFT agent and tetraethylene glycol (Fig. 3.2, Fig. 3.3), we performed ^{1}H-NMR, ^{13}C-NMR, MALDI-TOF mass spectrometry, and Fourier Transform Infrared Spectroscopy (FTIR) to verify the synthesized products (μRAFT, Figs. 3.4-3.7, TEGM, Figs. 3.8-3.11). We then used this modified compound, referred herein as the μRAFT agent, as the foundation for our block copolymer. RAFT agents make up a large library of block copolymers [324]. We show that the modified μRAFT agent successfully acts as the base for the polymerization of tetraethylene glycol into our hydrophilic block A polymer (Fig. 3.12). We then added cyclohexyl methacrylate to the block A and reinitiated polymerization to add the hydrophobic block B onto the existing block A' polymer to create our amphiphilic block copolymer. We confirmed this polymerization by ^{1}H-NMR (Figs. 3.13). By GPC analysis, the molecular weight of block A was 2734, and block B was 13029, for a total estimated MW of 15,763 Da (Fig. 3.14).

Example Copolymer Reaction Yields

1134.2 mg monomer –>468.6 mg Block A

468.6 mg Block A + 1,808 mg CHM –>722 mg Copolymer

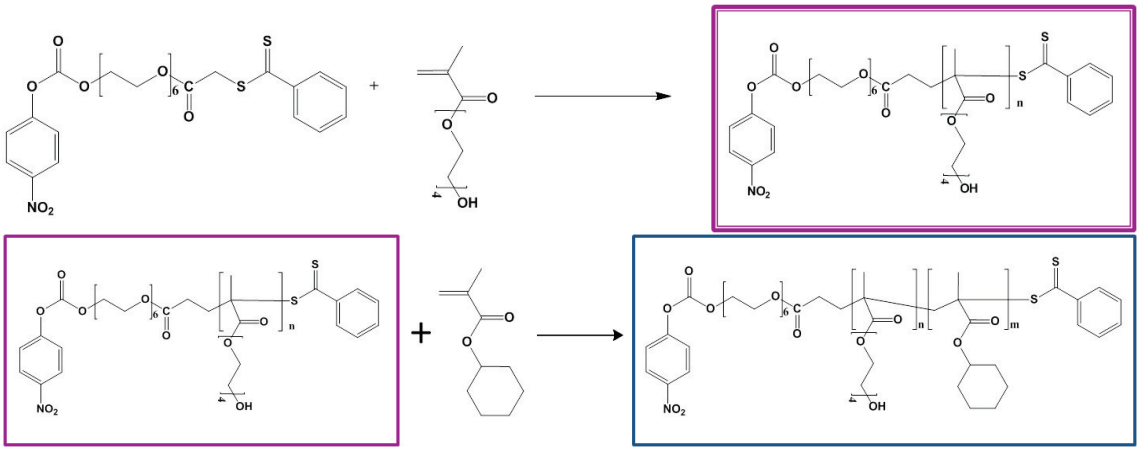

Figure 3.1: Block copolymer synthesis strategy. A modified commercial RAFT agent (μRAFT) was used to facilitate the polymerization. Tetraethylene glycol and μRAFT were mixed and polymerization was initiated using AIBN. Monomeric cyclohexyl methacrylate was added to the product of the first reaction (Block A) and polymerization was re-initiated to form the copolymer (Block A+B).

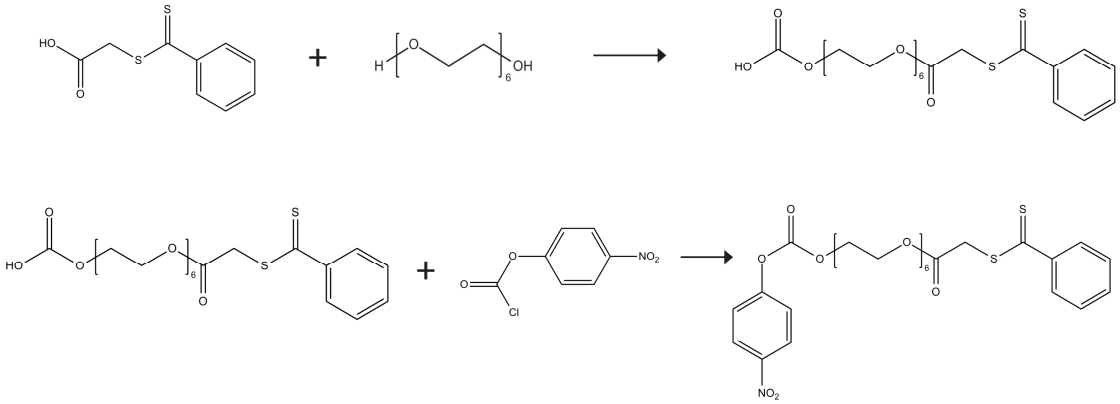

Figure 3.2: Modification Schematic of microRAFT agent. (Benzothioylsulfanyl)acetic acid was first modified with an oligoethylene glycol spacer and then further modified with p-nitrophenyl chloroformate.

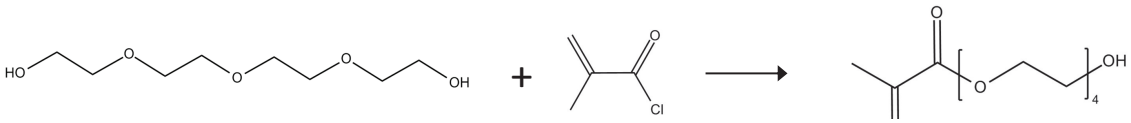

Figure 3.3: Modification Schematic of Tetraethylene Glycol. Tetraethylene glycol was modified in a 1-step reaction to create tetraethylene glycol methacrylate. The resulting product was purified on a silica gel column to remove unmethacrylated and dimethacrylated products.

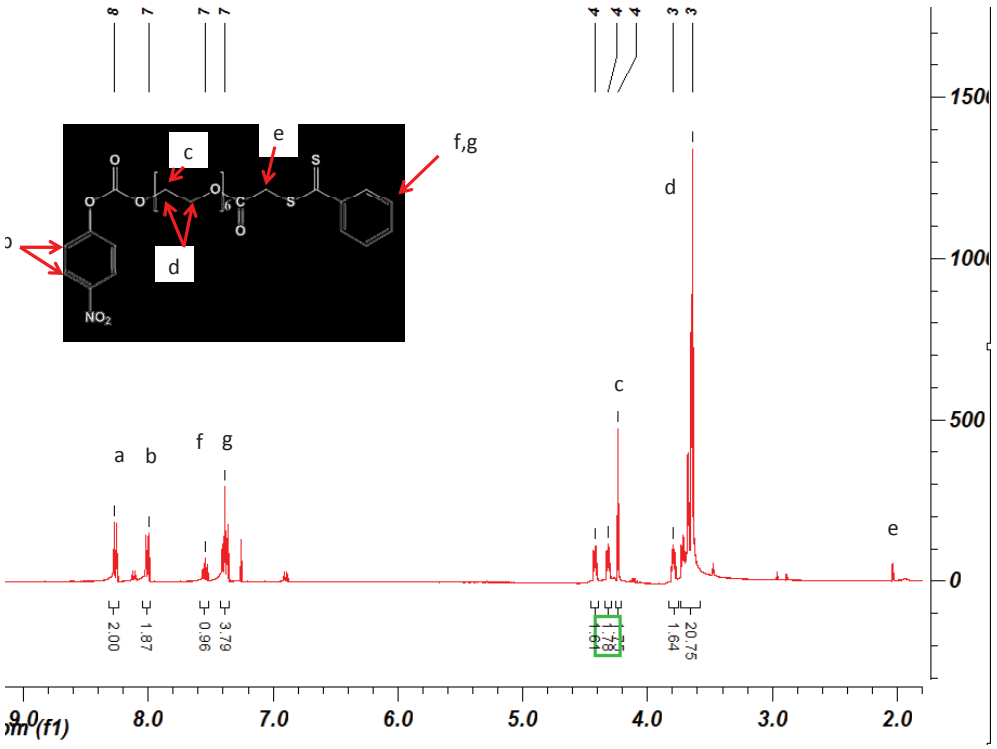

Figure 3.4: Verification of μRAFT modification by ^{1}H-NMR. Peaks were observed at 3.7 ppm (22H, int. value: 20.75+1.64) (c, d), 4.2 (2H, 1.75) (b), and 7.4 (4H, 3.79), 7.5 (1H, 0.96), 8.0 (2H, 1.87), and 8.2 ppm (2H, 2.0) (a, e).

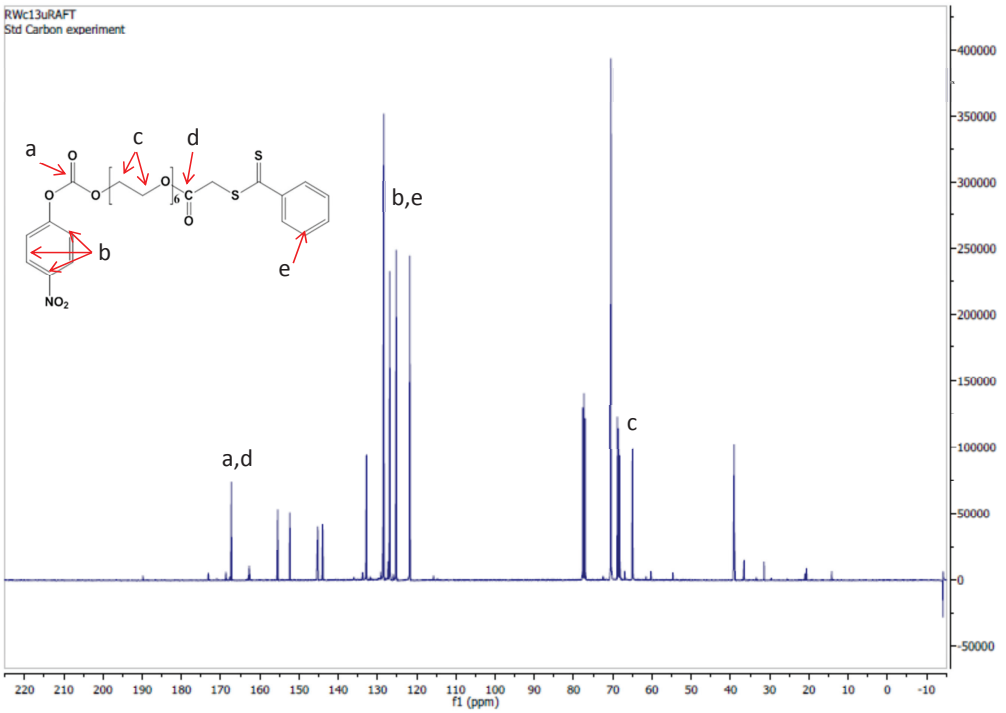

Figure 3.5: Verification of microRAFT modification by ^{13}C-NMR. Peaks were observed at 65-70 ppm (c), 120-150 ppm (b, e), 170 ppm (a, d), and 77 ppm ($CDCl_3$).

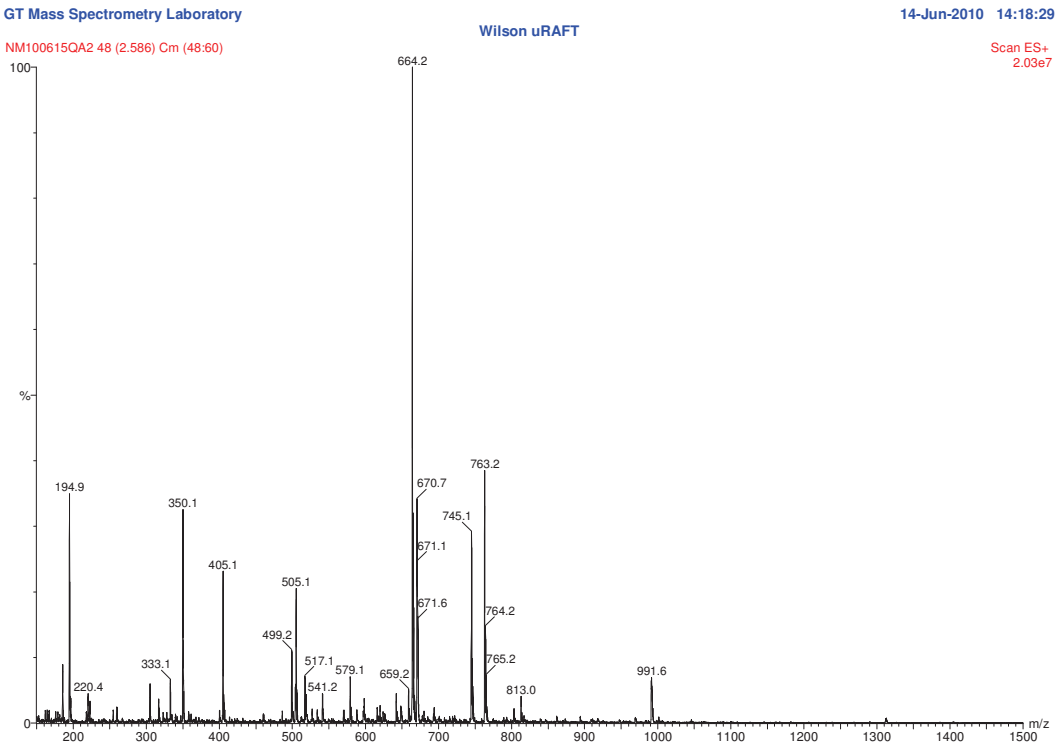

Figure 3.6: Verification of microRAFT modification by mass spectroscopy. MALDI-TOF spectrum of modified μRAFT agent with a theoretical mass-to-charge ratio (M/Z) of 664.15. Experimental value was 664.2.

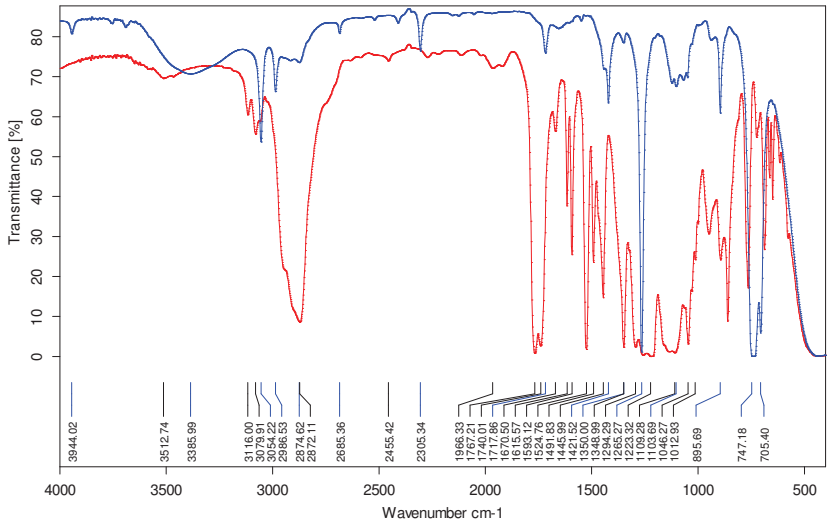

Figure 3.7: Verification of microRAFT modification by FTIR.

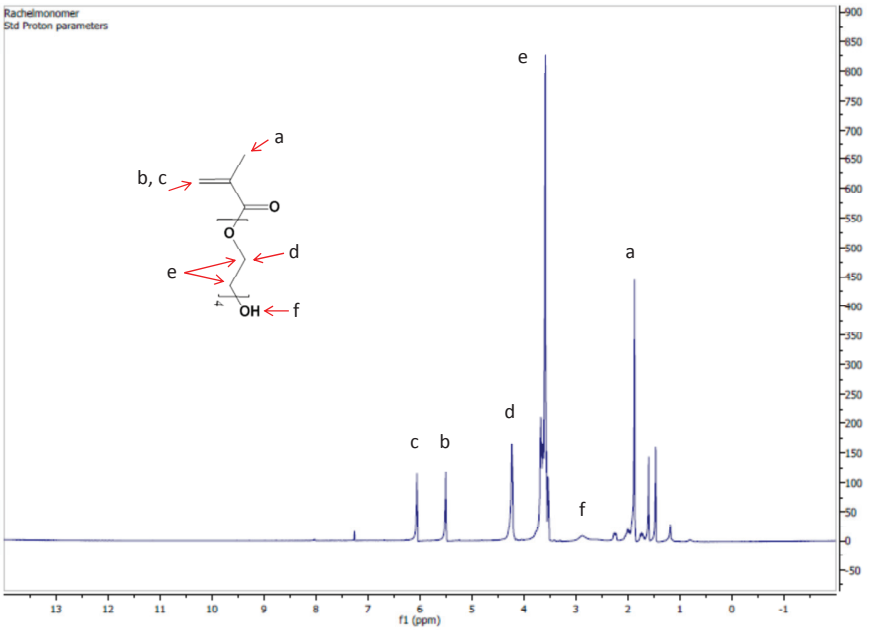

Figure 3.8: Verification of TEGM modification by ^{1}H-NMR. Peaks were observed at 1.9 ppm (3H, 3.55) (a), 3.0 ppm (1H, 1.1) (f), 3.6 ppm (14H, 14.92) (e), 4.2 ppm (2H, 2.94) (d), 5.6 ppm and 6.0 ppm (1H, 1.0; 1H, 1.0) (b,c).

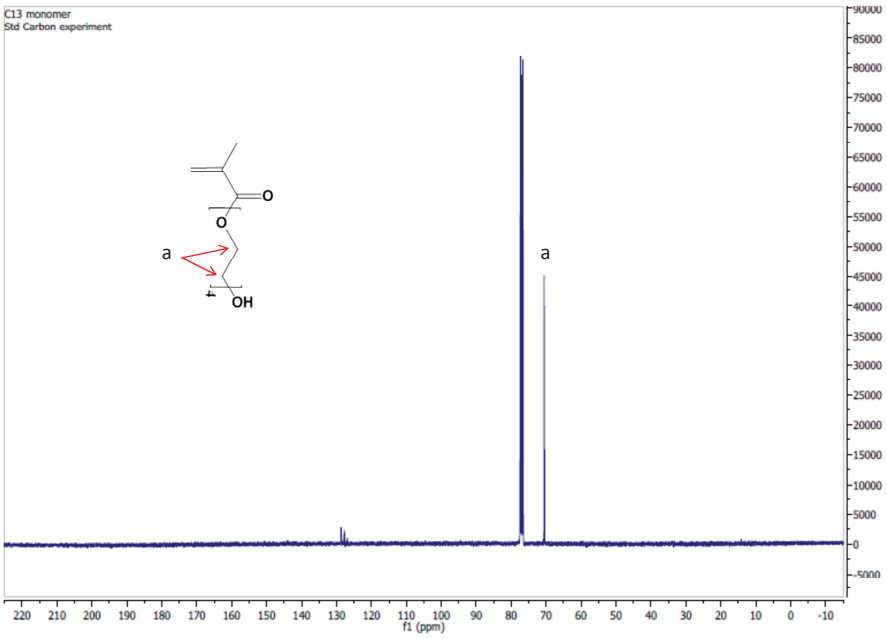

Figure 3.9: Verification of TEGM modification by ^{13}C-NMR. Peaks were observed at 70 ppm (a), and 77 ppm ($CDCl_3$).

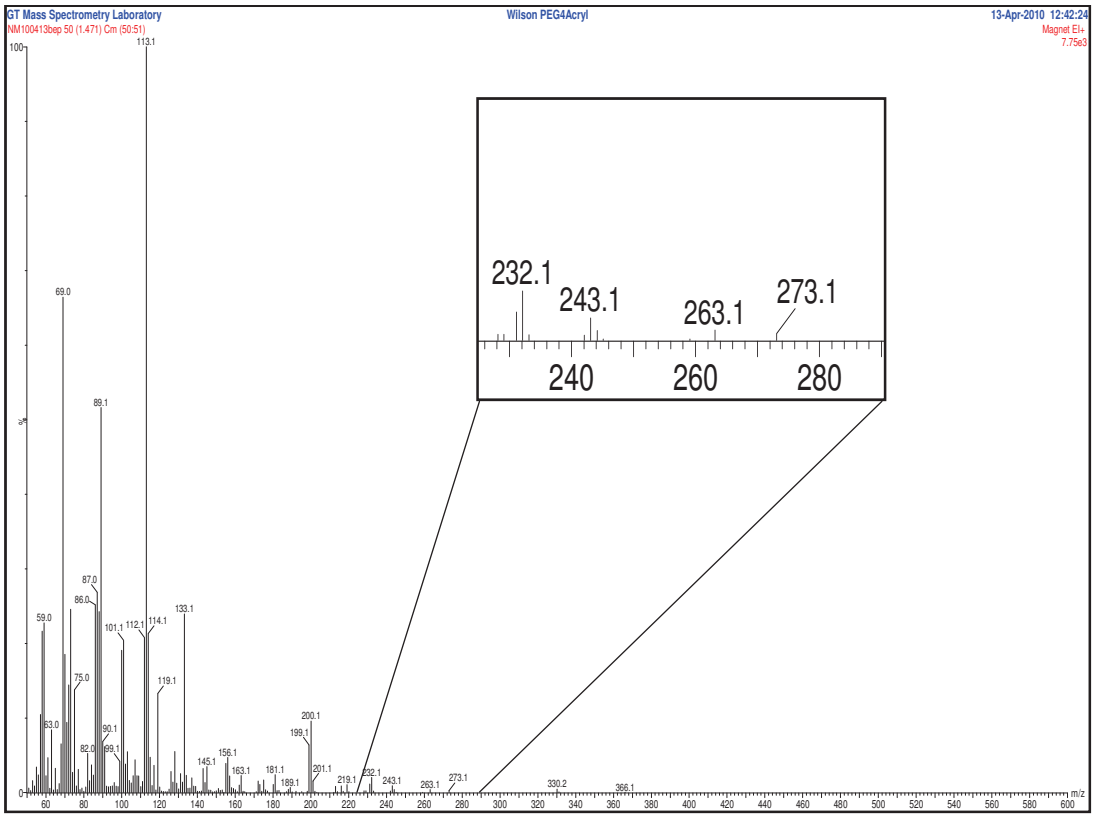

Figure 3.10: Verification of TEGM modification by mass spectroscopy. The theoretical mass-to-charge (M/Z) ratio was calculated to be 263.1. The experimental value of TEGM was 263.4.

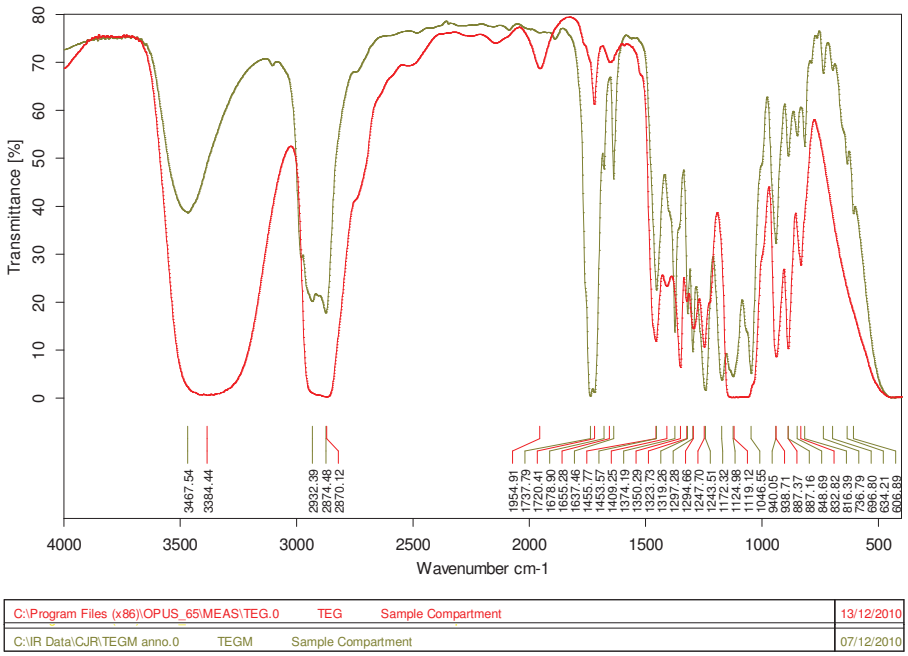

Figure 3.11: Verification of TEGM modification by FTIR.

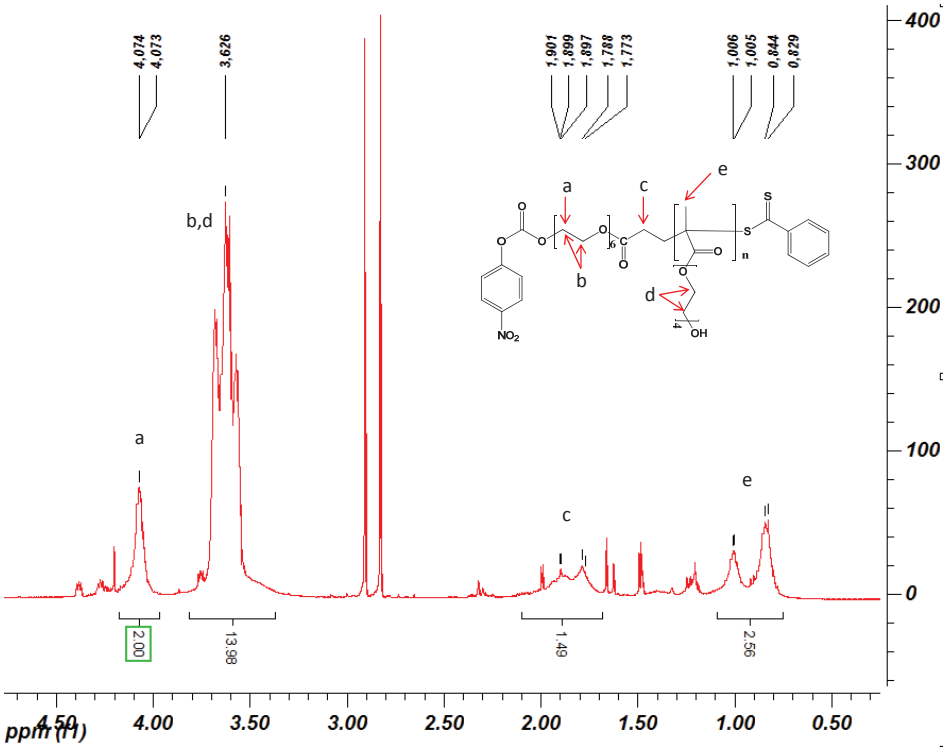

Figure 3.12: Verification of Block A synthesis by ^{1}H-NMR. Peaks were observed at 3.7 ppm (14H, 13.98) (c, f), 4.2 ppm (2H, 2.0) (b, e), 1.9 ppm (2H, 1.49) (g), and 0.9-1.1 ppm (3H, 2.56) (a, h).

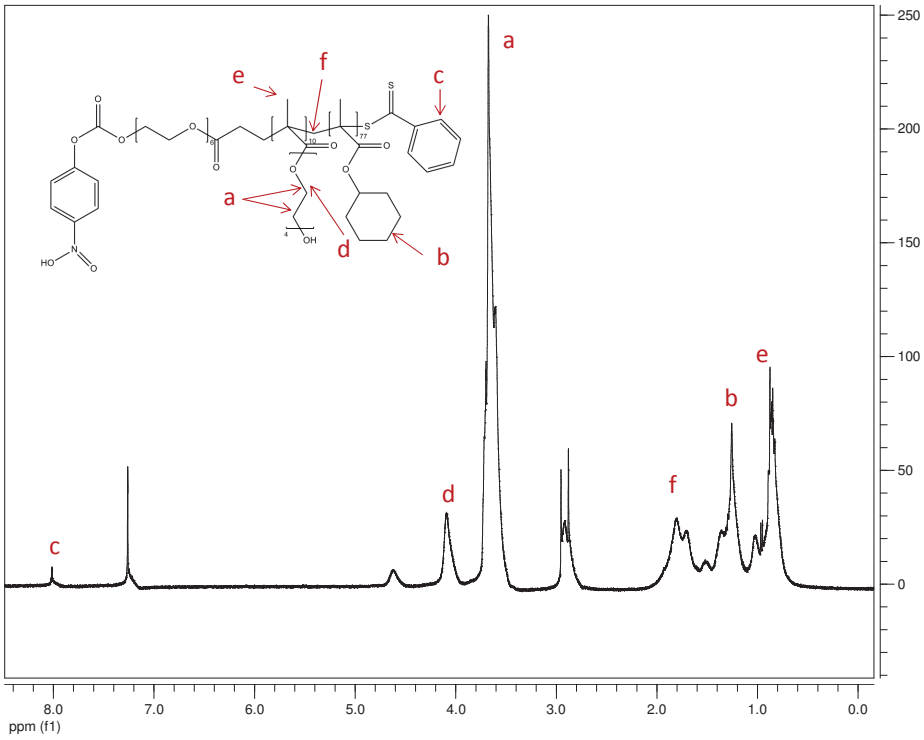

Figure 3.13: Verification of copolymer synthesis by ^{1}H-NMR. Peaks were observed at 3.6 ppm (m*14H) (a), 4.1 ppm (m*2H) (d), 1.3 ppm (n*10H) (b), 0.9 ppm (m*3H, n*3H) (e), 1.9 ppm (6H) (f), and 7.0 ppm (9H)(c). m = number of TEGM monomers; n = number of CHM monomers.

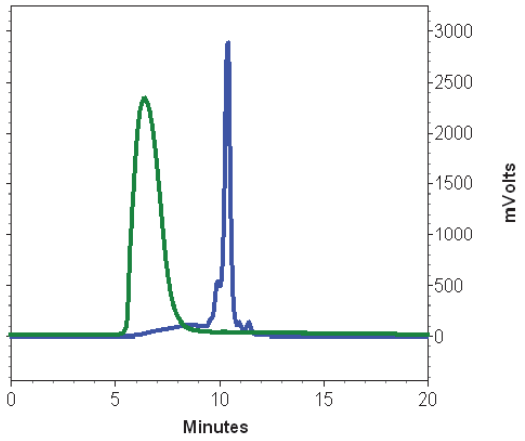

Figure 3.14: Verification of copolymer synthesis by gel permeation chromatography. The molecular weight of the hydrophilic Block A was found to be 2743 Da; The hydrophobic section, Block B, was 13029 Da (15763 Da (Block A+B) - 2734 Da (Block A only) = 13029 Da (Block B)) . Green, Block A+B; Blue, Block A.

To make particles, we added 50 mL 0.01 M PBS, pH 6.0, to a 150 mL beaker with a stir bar. We added 20 mg polymer in a total volume of 2.5 mL THF/DMF (9:1) to the aqueous phase while stirring at 400 rpm (Fig. 3.15). The polymer solubilizes fully in THF, supplemented with up to 10% v/v DMF, but requires at least 48 h to fully resolubilize after vacuum drying. The polymer spontaneously assembled into particles of approximately 280 nm in diameter and maintained their original size over 24 h, even after the addition of protein (Figs. 3.16, 3.17).

The polymer chain is approximately 17 nm long if you assume that the polymer backbone is fully extended. From the GPC data, there are an estimated 10 TEGM monomers per chain (2734 Da/262 g/mol monomer weight) and 77 CHM monomers per chain (13029 Da/168 g/mol monomer weight). Multiplying the number of monomers by their effective volume gives an overall volume of the polymer chain as 15.675 nm^3 (101 cm^3/mol CHM*77 molecules = 12.914 nm^3; 166.25 cm^3/mol TEG*10 molecules = 2.7607 nm^3). The particles' diameter of 280 nm implies that the polymer chains are aggregating in a semi-random manner rather than assembling into a well-defined micellar structure. The volume of a single particle is 11,494,040 nm^3, so there are approximately 733,272 chains per particle.

If there are 1,600,000 particles per mg polymer, that would predict an average molecular weight of each particle to be 0.625 ng/particle. Taking 733,272 chains*15,763 Da/chain = $1.156*10^{10}$ Da per particle, or $1.9196*10^{5}$ ng per particle. These numbers differ by 4 orders of magnitude. Factors that may explain these differences are a loss of polymer in the process between the initial particle formation step and the measurement of the particles by flow, the polymer chain packing may be smaller than the assumed linear conformation and would increase the actual number of polymer chains per particle, and the assumed values for the monomers' volumes may also introduce considerable errors.

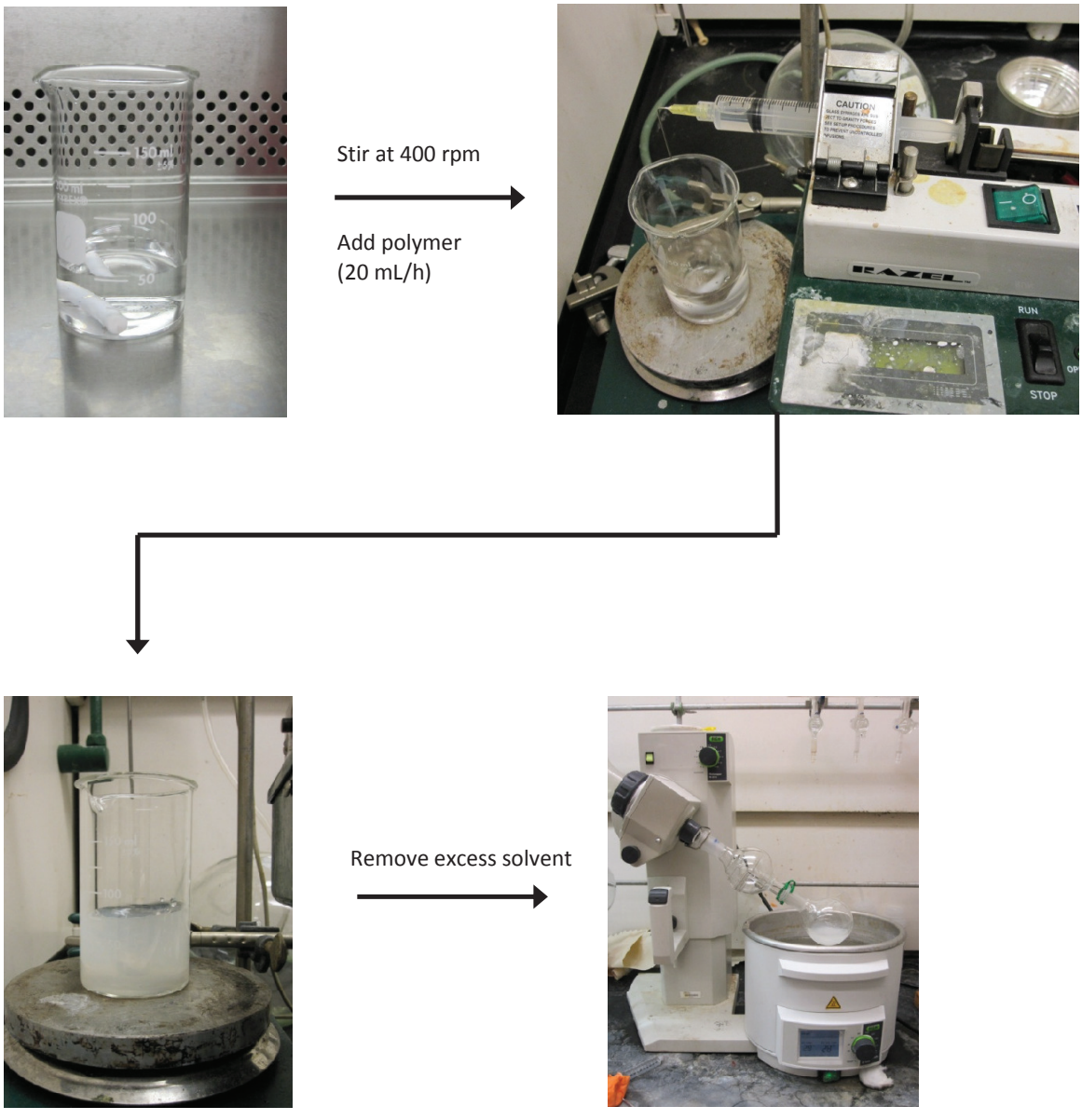

Figure 3.15: Particles were made by dropping polymer into stirring PBS using a syringe pump.

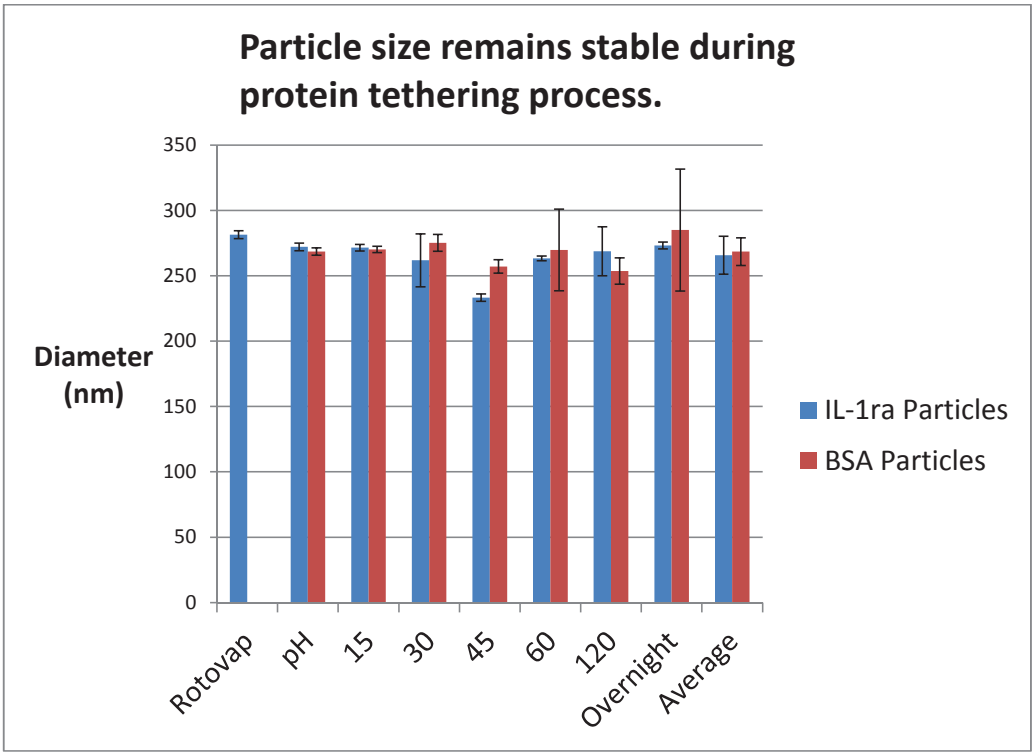

Figure 3.16: DLS sizing of particles. Particles were measured by dynamic light scattering using a refractive index of 1.33 (water). Samples were measured 3 times for 1 min each. Particles were measured after rotoevaporation of solvent (rotovap), after raising the pH to initiate protein tethering (pH), and at 15, 30, 45, 60, 120 min, and overnight after adding protein to the particles. The average of all the measurements was also calculated (Average).

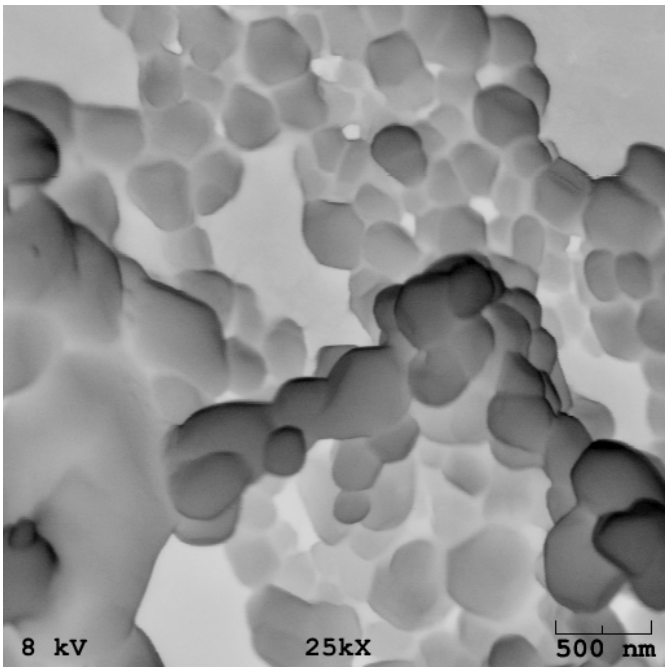

Figure 3.17: SEM images of particles. Particle size was confirmed by scanning electron microscopy.

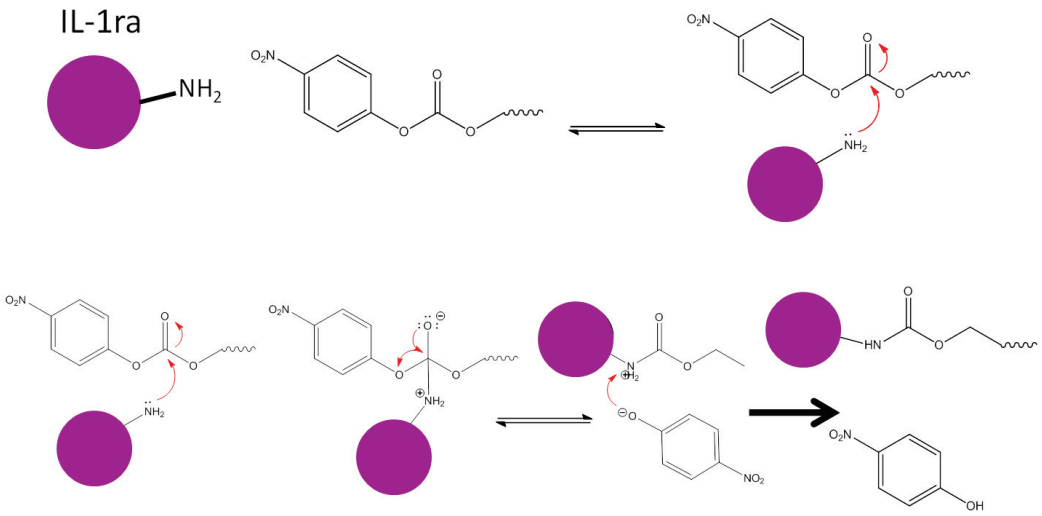

Figure 3.18: Schematic of protein tethering to polymer particle surface. Primary amines on the protein attack the carbonyl group, displacing the pNP and creating a stable peptide bond with the polymer chain.

The schematic of the protein tethering chemistry is shown in Fig. 3.18. To calculate

the theoretical maximum protein tethering on these particles, we determined the quantity of pNP groups per mg of particles (Fig. 3.19). We added ethanolamine to a 1 mg/ml particle solution and stirred for 30 min to fully remove all pNP groups from the particles. Ethanolamine is ideal because it has a free primary amine and dramatically increases the pH of a solution, which helps drive this spontaneous reaction. We then measured UV absorption of the particle solution as compared to known amounts of pNP as well as unreacted polymer solution. 150 μL (1 mg) of particles, with average diameter of 280 nm, released 0.88 nmol pNP. Since each pNP represents a possible site for protein tethering, we can say that the theoretical maximum protein per mg particles is 30,730 g/mol*0.88 nmol pNP, or 27 μg protein/mg particles. The same amount of particles incubated with IL-1ra released only 0.788 nmol pNP, or 89.6% of the maximum (EA) (Fig. 3.19).

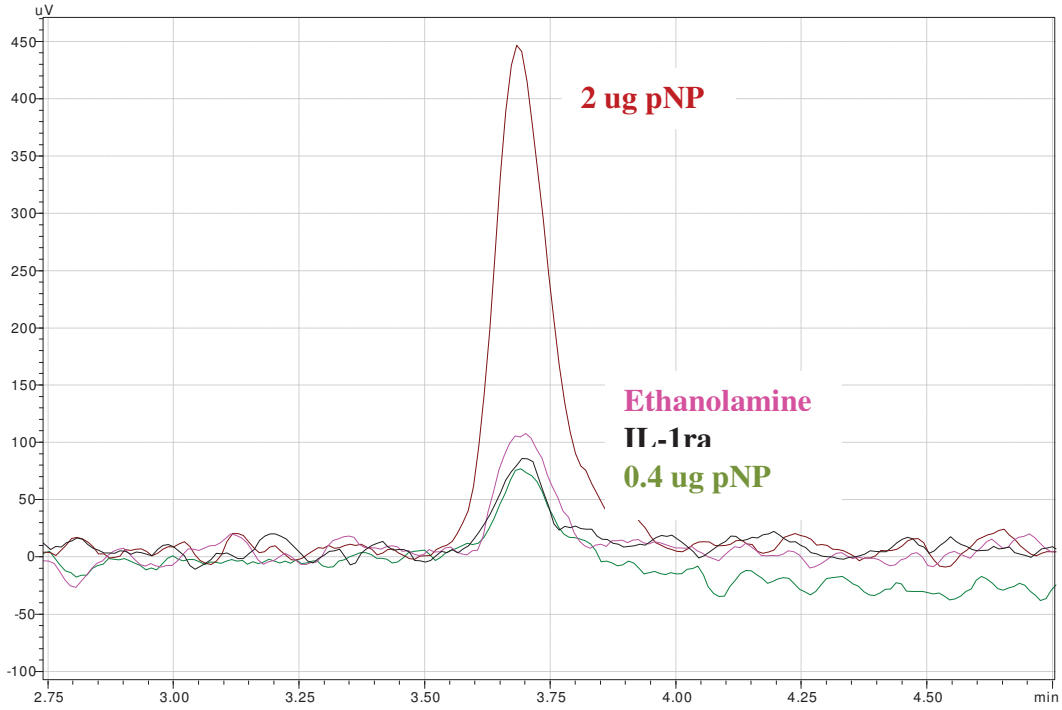

Figure 3.19: HPLC quantification of 4-nitrophenol (pNP) release from particles. Ethanolamine released 0.88 nmol of pNP, while IL-1ra released only 0.788 nmol of pNP. pNP standards were run at the same time for quantification purposes.

A macrophage cell line was incubated with polymer particles at a range of concentrations (0, 0.1, 1, 10 mg/mL) to determine the cytotoxicity of these particles. The metabolic activity of the cells was assayed by the MTT assay. Cells incubated up to 1 mg/mL polymer particles maintained their metabolic activity; however, at 10 mg/mL, the cells had severely reduced activity compared with controls (Fig. 3.20).

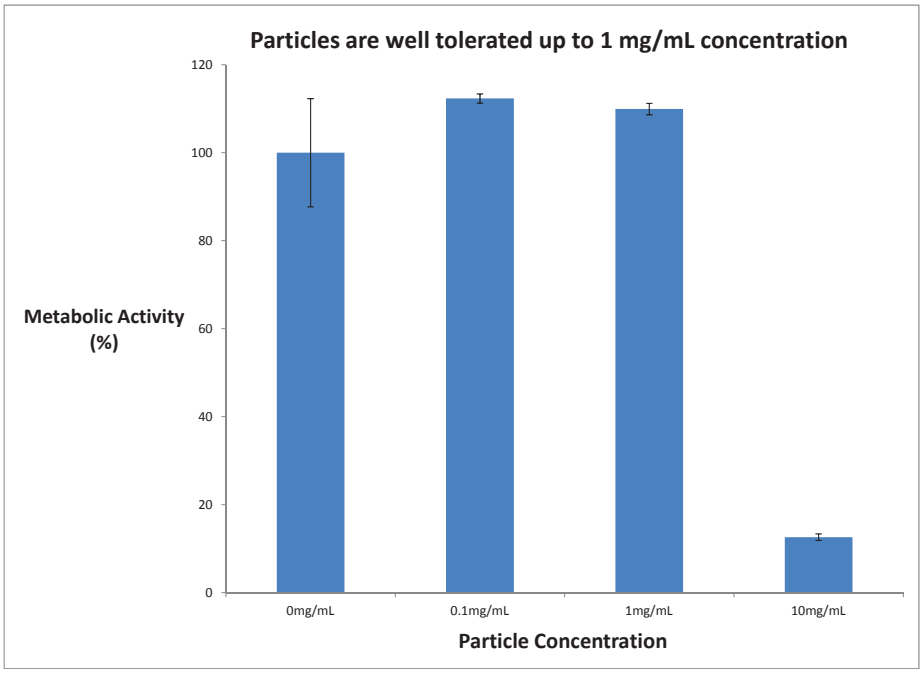

Figure 3.20: Copolymer particles have no significant effect on macrophage metabolic activity at concentrations up to 1 mg/mL in vitro. Particles were incubated with RAW 264.7 macrophage cells at various concentrations to determine their effect on cellular metabolic activity. The cells were serum-starved overnight prior to addition of particles. Cells were incubated with particles for 6 h before assessing the metabolic activity by the colorimetric MTT assay.

We then determined whether the particles could allow protein tethering to their surface. Our polymer design incorporates a 4-nitrophenol group (pNP), which is displaced by primary amines to form a peptide bond at slightly basic pH (>pH 7.4). To demonstrate that protein is tethered to the nanoparticles, we made particles as described above, raised the pH using sterile NaOH and added 1 mg of IL-1ra. The solution reacted for three hours, and any unreacted pNP was quenched by adding 10 mg glycine and reacting for another 30 min. The remaining free protein was dialyzed away using 100 kDa dialysis membranes. We lyophilyzed the particles and analyzed protein attachment by dot blot. Our particles show strong IL-1ra antibody staining, indicating that IL-1ra was successfully tethered to

the particles (Fig. 3.21).

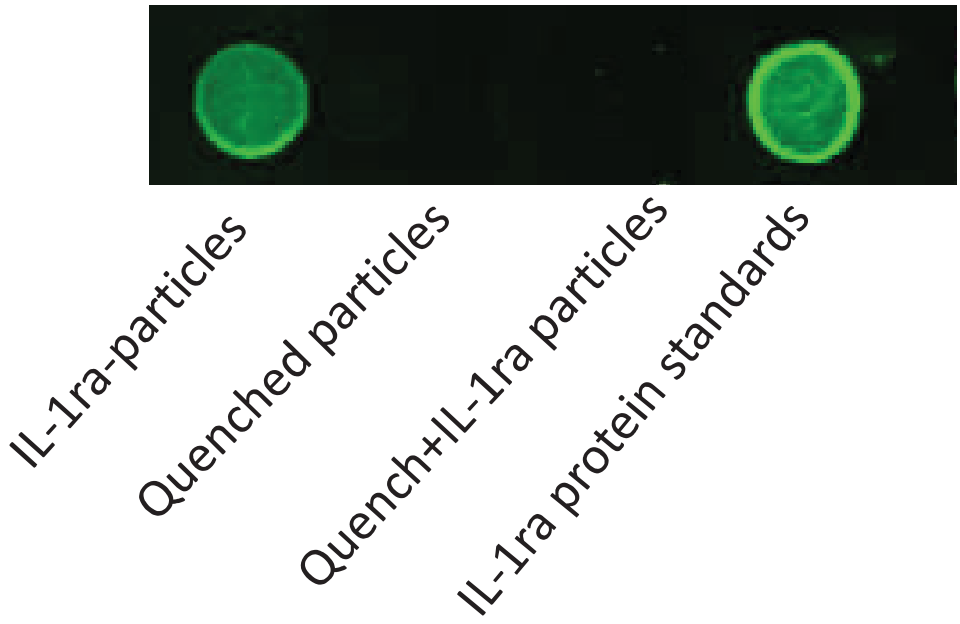

Figure 3.21: Dot Blot for IL-1ra. IL-1ra-tethered particles, glycine-tethered particles, or soluble IL-1ra were dried on nitrocellulose membranes and were probed with anti-IL-1ra antibodies. Blots were imaged using near infrared (800 nm) secondary antibodies and an infrared imager.

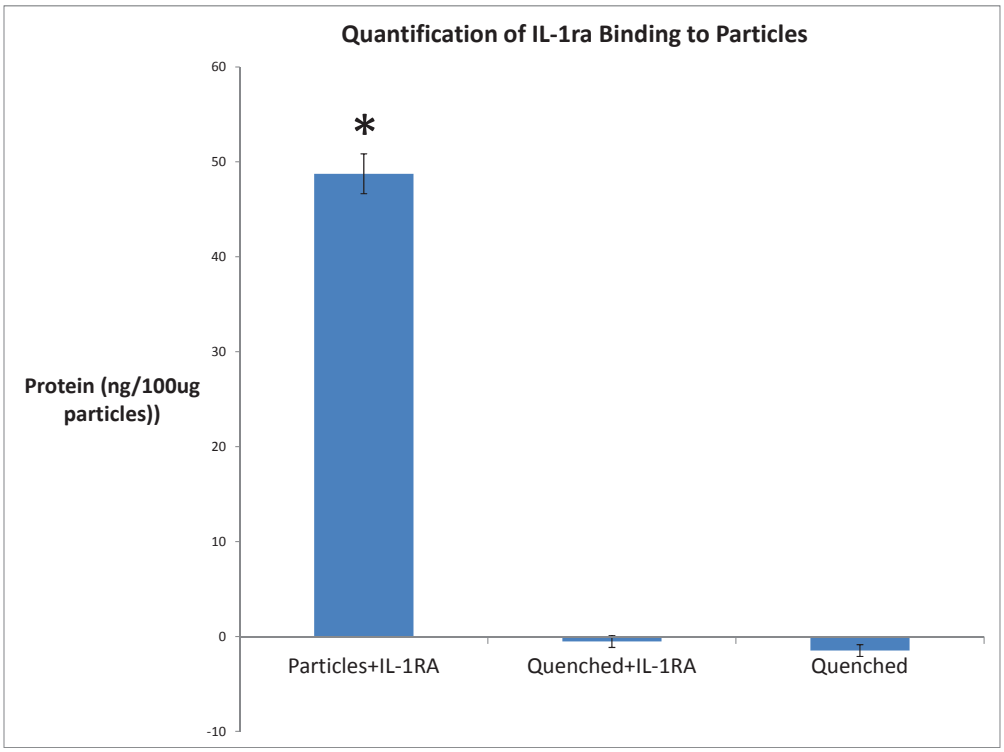

Figure 3.22: Quantification of IL-1ra on particles by dot blot. IL-1ra-tethered particles showed significantly more protein binding than particles quenched with glycine (Quenched) or particles quenched with glycine and exposed to IL-1ra (Quenched+IL-1ra). * = $p<0.0001$.

We found that our BSA-tethered particles showed only background levels of fluorescence (-5.27, s.e.m. = 0.620), while the IL-1ra-tethered particles bound approximately 500 ng IL-1ra per mg of particles (487.46, s.e.m. = 2.098, $p<0.0001$) (Fig. 3.22).

3.5 Discussion

The amphiphilic block copolymer created in this work forms particles and allows protein to be tethered to its surface. Compared to solid polymeric particles, such as PLGA, these

particles provide a hydrophilic, "stealth" environment for the presentation of our anti-inflammatory protein, IL-1ra. Additionally, most current polymer particles do not incorporate a protein tethering handle on the surface and would require reengineering the material to allow for addition of a surface-bound targeting ligand. The release of pNP indicates covalent tethering has occurred between the protein and the particle. This tethering moiety is stable at neutral to slightly acidic pH and has a relatively slow decay rate (around 2 h) compared with that of the highly unstable EDC/NHS intermediate. The increased reaction time is beneficial because it can increase the efficiency of reaction. These particles are non-cytotoxic up to 1 mg/mL concentration in cell culture, which is a generally accepted phenomenon[130][131]. Many polymer systems show significant cytotoxic effects at 10 mg/mL concentrations, as we saw for this system. Our particles showed excellent tethering of IL-1ra (250 ng/mg particles) and had only background levels of signal on albumin-tethered particles. This polymer particle system is easily modified to create larger or smaller particles, based on the molecular weight of the block segments. This system design could incorporate a hydrophobic small molecule drug in the particle's core to create a dual therapeutic strategy. We believe that this copolymer has wide applicability for targeted therapeutic delivery in a wide range of disease states. This particle system could use any protein or peptide of choice because the tethering moiety uses primary amines to anchor the protein to the particle surface. However, our use of IL-1ra in this system has broad application to diseases involving inflammation and/or inflammatory cells, such as cancer and heart disease, because of the ubiquity of IL-1 in these systems.

Additionally, our particle technology has several advantages over the current state-of-the-art polymer particles. First, the stability of the protein tethering moiety on our particles allows for a higher efficiency tethering process compared to standard EDC-NHS tethering chemistry (2 h vs. 10 min. half-life). Secondly, the submicron scale of our particles could allow for better diffusion and retention within the joint space. The size also increased the surface area-to-mass ratio, which increases the potential protein payload per mass of polymer. Finally, our use of an anti-inflammatory protein as the targeting ligand increases the specific targeting of our particles to synoviocytes and other inflammatory cells like

macrophages. Current technologies for intra-articular drug delivery have focused on using sulfate groups to localize particles within the cartilage ECM or phage-panned peptides that bind to collagen II[292]. The ability to tether proteins to a polymer particle and maintain its bioactivity represents a technological advance for protein-polymer therapeutics. Currently, it is possible to encapsulate proteins within polymer particles, but the encapsulation process or the material itself detrimentally affect the protein's bioactivity. Attaching proteins to a polymer particle can be as simple as activating existing carboxylic acid groups on the polymer chain using the EDC-NHS ester reaction; however, this reaction requires there to be carboxylic acids within the polymer chain, which is not always the case. The intermediate ester complex is also highly unstable, resulting in relatively inefficient protein tethering in aqueous solutions. Researchers have also synthesized polymer chains with biotin or streptavidin pendant or terminal groups, but biotin-streptavidin can be immunogenic and is not an ideal tethering solution for therapeutic use. Our technology incorporates a stable pNP group on the end of the polymer chain that is significantly more stable than the EDC-NHS tethering method and does not have the immunogenic concerns of the Biotin-Streptavidin system. Both EDC-NHS and pNP technologies use primary amines located on the protein/peptide as the reactive handle; this reaction scheme is ubiquitous and has a varied effect on the protein's bioactivity. Although we did not measure total protein versus active protein on our particles, we observed a significant amount of binding of our IL-1ra-tethered particles by the IL-1 receptor, as well as the ability of IL-1ra-tethered particles to abrogate IL-1β-induced signaling cascades (see Chapter 4). We expect that some of the protein activity was affected by the tethering process, but we also assert that a significant enough proportion of the activity was maintained to make this a therapeutically relevant technology. Our technology varies from traditional protein-delivering particle systems because it covalently tethers protein to the surface rather than encapsulating it for controlled soluble release. Many therapeutic proteins act by binding to receptors and transducing signal through the receptor's cytoplasmic domains and do not need to be solubly released in order to exert their effect; only proteins that must be internalized to affect their target should be candidates for encapsulation. Finally, using IL-1ra to target these particles to inflammatory

cells in addition to its inherent therapeutic effects should increase the effectiveness of therapeutic drugs that could be encapsulated within the particle core. By localizing particles to the cells that help mediate osteoarthritis, drugs and proteins can be more directly delivered to the appropriate target to increase the benefit of each protein molecule delivered.

3.6 Conclusion

These results establish a new amphiphilic block copolymer made by RAFT polymerization methods that self-assembles into sub-micron scale particles. The polymer particles allow efficient tethering of proteins to their surface via the 4-nitrophenol moiety. This polymer system allows for modular protein attachment, variability in particle size, and potential drug incorporation, all of which give this technology powerful future applications for drug and protein delivery.

CHAPTER IV

IN VITRO BIOLOGICAL CHARACTERIZATION OF IL-1RA-TETHERED POLYMER PARTICLES

4.1 Summary

This work focused on characterizing the bioactivity of the IL-1ra-tethered particles in vitro. We found that the IL-1 receptor binds to IL-1ra on the surface of our particles. Additionally, IL-1ra-tethered particles are bound by synoviocytes in an IL-1-dependent manner. The IL-1ra-tethered particles inhibit NF-κB activation in IL-1-responsive cells after IL-1 stimulation. These experiments establish IL-1ra-tethered particles as a new way to target key OA mediating cells and show that the IL-1ra-tethered particles have added benefit because they also inhibit IL-1β-mediated signaling. This technology is useful because it establishes a new way to target drug-delivering particles to inflammatory cells while simultaneously acting as a therapeutic molecule. It has broader applicability due to its modular protein tethering ability and its potential to deliver proteins to inflammatory cells of interest.

4.2 Introduction

An important goal of drug delivery strategies is to deliver proteins in a controlled manner to the site or cells of interest[146]. Current polymer drug delivery particles have critical disadvantages. The hydrophobicity of many drug-delivering polymers (e.g., PLGA) severely reduces or destroys the bioactivity of encapsulated proteins[148][190][215]. Liposomal particles have a more protein-friendly environment, but are limited by their in vivo instability[294][212]. Methods for delivering and retaining immunomodulatory proteins are critical for improving current OA treatments, as well as other disease pathologies[73][109].

Researchers are actively looking for ways to increase protein retention and control its release in the body. Current in vitro investigations include PEGylating native proteins for systemic injection[142][141][371][372], and creating drug depots[305][7] and encapsulating proteins in polymer particles or liposomes for local protein delivery [62][360][37]. Although

these technologies have shown some progress in increasing protein half-life, all of them reduce the protein bioactivity by at least 50%.

This work characterizes the in vitro behavior of the polymeric particle system created in Aim 1. The protein tethering strategy allows IL-1ra protein to be tethered to the surface of these particles. Once tethered, IL-1ra maintains its bioactivity and actively targets synoviocytes, cells crucial to the OA pathology. This binding happens in an IL-1receptor-dependent manner. Furthermore, IL-1ra-tethered particles are able to inhibit IL-1β-induced NF-κB activation. These studies show that this particle system has the potential to deliver IL-1ra to arthritic joints and that it has potential for localizing/targeting drugs to inflammatory cells of interest as a new way to target OA drug treatments.

4.3 Materials and Methods

4.3.1 Particle Preparation

Briefly, our block copolymer from Aim 1 was resuspended at a concentration of 40 mg/mL in a 9:1 mixture of THF:DMF. 20 mg of polymer was added to a total volume of 2.5 mL THF/DMF and was added to 50 mL of stirring PBS (0.01M, pH 6.0) at a rate of 20 mL/h by syringe pump. Excess solvent was removed by rotary evaporation. The particles were concentrated by centrifugation and were sonicated briefly to resuspend. The pH was raised to 8.0 and protein (AF-488-IL1ra or AF-488-HD-BSA) was added. Particles were sized using dynamic light scattering.

4.3.2 Fluorescent Protein Labeling

We labeled protein with Alexa Fluor 488 to visualize the particles during in vitro experiments. Briefly, particles were made as described above. Protein (IL-1ra or Heat-Denatured Bovine Serum Albumin (HD-BSA)) was reacted with Alexa Fluor 488 maleimide (Alexa Fluor 488 C_5-maleimide, #A10254, Invitrogen Corp., Carlsbad, CA) according to the manufacturers instructions. There are 3 free solvent-accessible cysteines on IL-1ra that can be fluorescently tagged[356], thereby avoiding the more prevalent primary amines (lysine residues), allowing the protein to be fluorescently tagged before tethering it to particles, as well as reducing the chance of altering the protein's bioactivity. The resulting fluorescently

tagged proteins are denoted AF-488-IL-1ra and AF-488-HD-BSA. For the confocal study, AF-594 was used to fluorescently tag the IL-1ra (AF-594-IL-1ra). Protein-tethered particles were stored in PBS solution at 4°C until use.

4.3.3 IL-1ra-tethered Particles Bind To IL-1RI

350 ng of AF-488-IL-1ra (either soluble or tethered to particles) or an equivalent amount of AF488-BSA-tethered particles (control) was incubated with 3 μL (1.5 μg) of recombinant IL-1rI-Fc (#4101I, Symansis Cell Signaling Science, Auckland, NZ) for 2 h at room temperature. Two μL of Protein A-conjugated magnetic beads (#21348, MagnaBind Protein A Beads, Pierce, Rockford, IL) were then added and incubated at room temperature for 30 min. The particle solution was purified by magnetic column (MACS separation columns, #130-042-901, Miltenyi Biotech, Bergisch Gladbach, Germany). The MACS column was set on the magnetic stand and was prepared by washing with 2x 1 mL of MACS buffer (0.5% BSA, 2 mM EDTA in PBS, pH 7.2). The particle solution was added to the column and allowed to flow through. The column was washed with 5x 1 mL MACS buffer. The column was then removed from the magnet and was placed over a flow cytometry tube. Three mL of MACS buffer were used to elute the purified particles from the column. Binding was analyzed by flow cytometry.

4.3.4 Synoviocyte Binding Experiments

The HIG-82 synoviocyte cell line was purchased from ATCC (CRL-1832, ATCC, Manassas, VA). This cell line was originally derived from a female rabbit whose synoviocytes were harvested and immortalized by Georgescu et al.[145][207]. Fibroblast-like synoviocytes play a critical role in the pathology of OA by producing large amounts of inflammatory cytokines. The cells were cultured in Ham's F-12 supplemented with 10% heat-denatured fetal bovine serum at 5% CO_2, with a doubling time around 24 h. Cells were removed from culture using 0.25% trypsin+0.5 mM EDTA. Cells were counted and plated at 2x10^5 cells/6-well. After 6 hours of incubation, the media was replaced with serum-free media overnight. The next day, particles were added to cells and incubated for 2 h at 37°/5% CO_2. Some samples were incubated with 50 μg/mL IL-1β for 2 h to block available IL-1 receptors before adding

particles.

HIG-82 synoviocyte cells were incubated with particles tethered with either AF-488-IL-1ra or AF-488-HD-BSA. At 2 h post-addition of particles, we washed the cells with PBS to remove unbound particles, and stained for cell nuclei with Hoechst dye. Samples were analyzed by flow cytometry and confocal microscopy.

For the confocal samples, we plated HIG-82 cells on glass covers with 8-well divisions (#155411, Lab-Tek^{TM}Chambered Coverglass, Thermo Scientific, Rochester, NY) overnight. The next morning, we added serum-free Ham's F12 containing AF-594-IL-1ra-tethered particles or AF-488-HD-BSA-tethered particles. The cells were then incubated for 2 h at 37°C/5% CO_2. We washed the cells with PBS 3 times to remove unbound particles. We then stained for cell nuclei using 1:10,000 dilution of Hoechst in PBS for 15 min. We imaged the samples using confocal microscopy (particles: IL-1ra: AF594/red; BSA: AF488/green; cell nuclei: Hoechst/blue).

For the flow cytometry samples, we plated HIG-82 cells on 12-well plates and serum starved them overnight. We then blocked some of the cells with 50 μg/mL IL-1β for 2 h prior to adding either IL-1ra or BSA-tethered particles to all wells. The cells were incubated with the particles for an additional 2 h at 37°C/5% CO_2. We washed the cells with PBS 3 times to remove unbound particles and then removed the cells using 0.2 mL trypsin-EDTA (0.25%), quenched with complete media. The cell suspensions were analyzed on an Accuri C6 Flow Cytometer (BD Accuri Cytometers, Inc., Ann Arbor, MI).

4.3.5 Inhibition of IL-1β-Induced Inflammatory Signaling

We obtained NIH 3T3 cells stably transfected with an NF-κB-luciferase reporter construct by Dr. van de Loo (Radboud University, Nijmegen, Netherlands)[315]. These IL-1-responsive cells produce luciferase under control of an NF-κB-responsive promoter. The produced luciferase will oxidize luciferin to produce oxyluciferin, producing luminescence that can be measured by a plate reader.

NIH 3T3 NF-κB-luc cells were plated in 96-well plates at a density of 10^5 cells/mL (100 μL/well). Cells were allowed to adhere for 6 h before replacing the media with serum-free

DMEM+1 mM sodium pyruvate overnight. The next morning, IL-1ra-tethered particles, BSA-tethered particles, or soluble IL-1ra was added to each well (1 μg/mL IL-1ra or equivalent amount of polymer for the BSA particles) and was incubated for 1 h. Then, 10 μL of 1 ng/mL IL-1β was added to each well to stimulate NF-κB activation (final concentration of 0.1 ng/mL IL-1β). Cells were incubated with IL-1β for 6 h before washing 3 times with PBS. Cells were then lysed with 20 μL of Passive Lysis Buffer (PLB, #E1941, Promega, Madison, WI) for 20 min on a gentle vortexer. Lysate (20μL) was added to 100 μL of Luciferase substrate in an opaque white 96-well plate. Luminescence was read using a plate reader (HTS 7000 Plus, Perkin Elmer, Waltham, MA).

4.4 Results

We first tested whether IL-1ra retained its bioactivity when tethered to our particles. To do this, we incubated labeled IL-1ra particles, BSA particles, or soluble IL-1ra with a recombinant IL-1r-Fc. We then captured the IL-1rI using magnetic Protein A-conjugated beads and evaluated the magnetic beads for labeled target protein (IL-1ra or BSA) by flow cytometry. Our IL-1ra particles were bound significantly by the IL-1r, while BSA particles had low levels of binding (Fig. 4.1). Similarly, IL-1ra particles that were not incubated with IL-1rI-Fc showed minimal binding to the Protein A-magnetic beads.

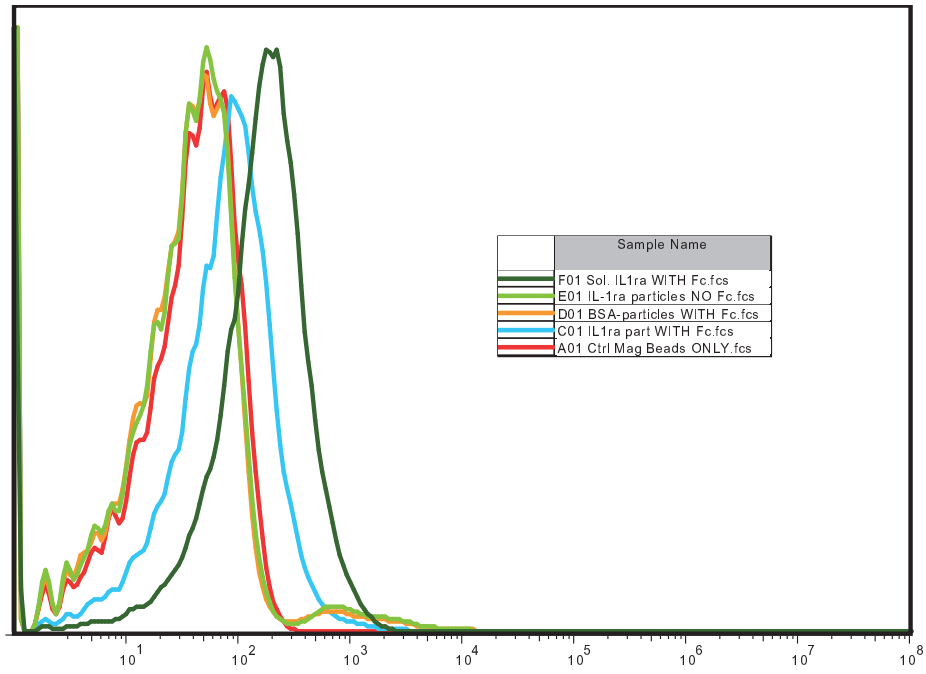

Figure 4.1: IL-1R binds to IL-1ra-tethered particles. Green fluorescent labeled IL-1ra-tethered particles, BSA-tethered particles, or soluble IL-1ra were incubated with rhIL-1 receptor. IL-1 receptors were captured using Protein A-conjugated magnetic beads (n=3). The beads were purified using a magnetic column system and were then analyzed by flow cytometry (n=3). Blue, IL-1rI+IL-1ra-Particles (16.9%); Dark green, sol. IL-1ra (52.8%); Orange, IL-1rI+BSA-particles (2.2%); Lime green, No IL-1rI+IL-1ra-Particles (2.6%); Red, Magnetic Beads Only (0.9%).

We also showed that IL-1ra-tethered particles bind to synoviocytes, our target cell type, by using a synoviocyte cell line (HIG-82). We incubated synoviocytes with IL-1ra particles or BSA particles, and showed that the synoviocytes bound IL-1ra particles better than BSA particles. We also demonstrated that the binding of our IL-1ra particles to synoviocytes was IL-1r-mediated. Pre-incubating synoviocytes with IL-1β for 1 h abrogated the binding of IL-1ra particles to the synoviocytes (Fig. 4.2). The ability to block IL-1ra-particle binding with IL-1β confirms that the interaction between our particles and the synoviocytes is mediated by IL-1 receptors. Furthermore, synoviocyte targeting in vitro shows proof of concept for moving into an in vivo study of particle targeting and retention. Finally, although we

have not tested the ability of our IL-1ra particles to regulate signaling in synoviocytes, this result implies that IL-1ra-tethered particles have the potential to block IL-1β-induced inflammatory signaling cascades.

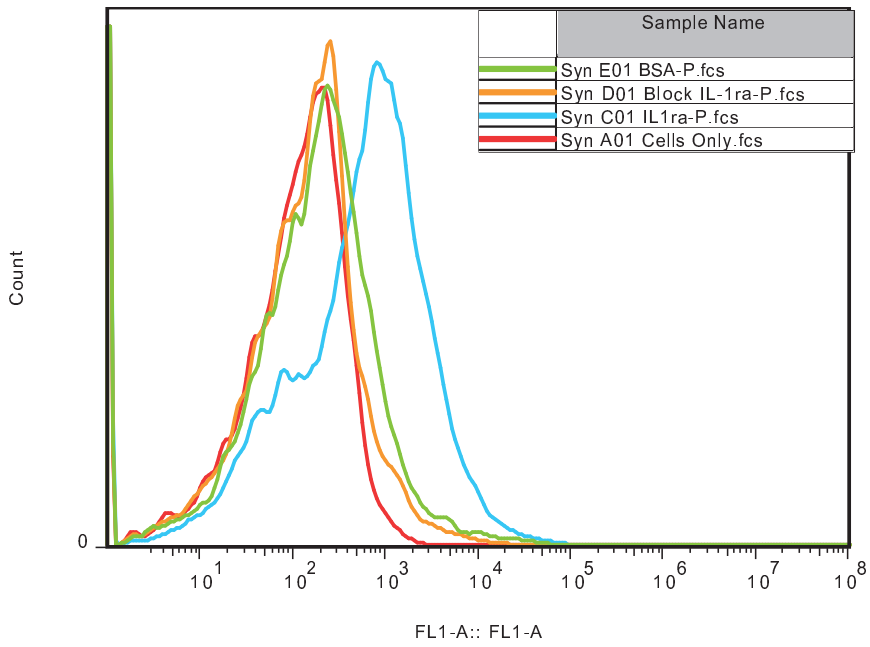

Figure 4.2: IL-1ra-Tethered Particles Are Bound by Synoviocytes: Flow Cytometry Analysis. A synoviocyte cell line (HIG-82) was incubated with fluorescently tagged IL-1ra-tethered particles or fluorescently tagged BSA-tethered particles, with or without an IL-1β pre-blocking step (n=1). Synoviocytes + IL-1ra-Particles (44.0%), Blue; Synoviocytes + BSA-Particles (2.7%), Green; Synoviocytes + Pre-Block + IL-1ra-Particles, (2.8%), Orange; Synoviocytes Only (0.1%), Red.

We also verified that our particles can bind cells of interest by confocal microscopy. HIG-82 cells were incubated with IL-1ra particles or BSA particles for 1 h to allow binding. The cells were then washed and counterstained with Hoechst before imaging them by confocal. Samples incubated with IL-1ra particles had significantly higher colocalization of particles (green) with cell nuclei (blue) than samples that received BSA particles (Fig. 4.3).

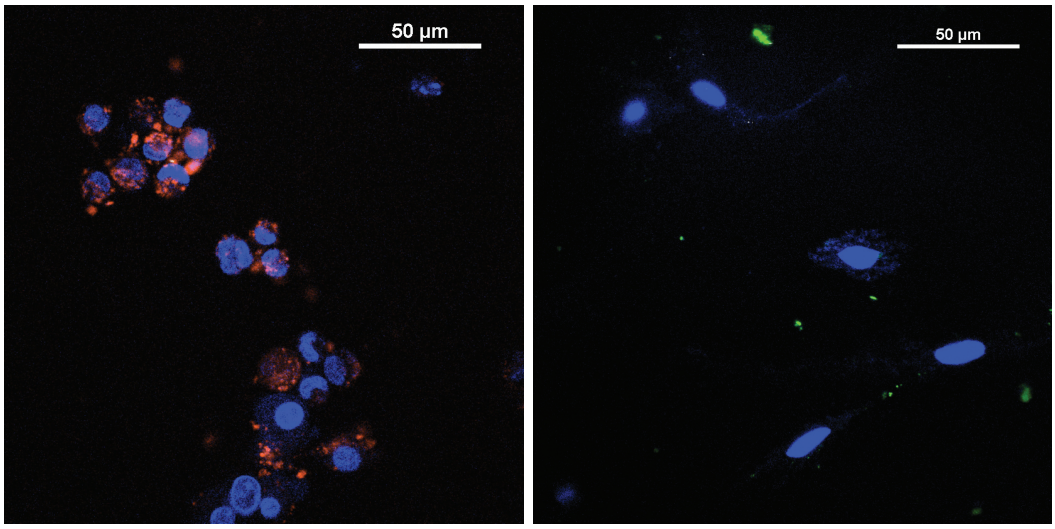

Figure 4.3: IL-1ra-Tethered Particles Are Bound by Synoviocytes: Confocal Microscopy Analysis (10 fields from 4 samples of each group were analyzed). Particles were incubated with a synoviocyte cell line (HIG-82) for 2 h. Samples were rinsed three times with PBS before imaging. IL-1ra-tethered particles, Red; BSA-tethered particles, Green; Nuclei, Blue.

To test whether our IL-1ra particles could inhibit IL-1β-mediated signaling cascades, we used an IL-1-responsive fibroblast cell line, NIH3T3 stably expressing a construct for luciferase driven by a NF-κB-responsive promoter. IL-1β is known to cause NF-κB activation as part of its signaling pathway[204]. We measured our IL-1ra-tethered particles' effectiveness at blocking IL-1β-induced activation of NF-κB by pre-incubating NIH cells for 1 h with either soluble IL-1ra, IL-1ra-tethered particles, or BSA-tethered particles. When these cells were then stimulated with IL-1β, only our IL-1ra-particles and the soluble IL-1ra were able to inhibit NF-κB activation, whereas BSA-particles showed no effect on NF-κB activity (Fig. 4.4). Remarkably, the IL-1ra-particles inhibited NF-κB activation to the same levels as an equal amount of soluble IL-1ra, indicating that the tethered protein retains high bioactivity. Both IL-1ra particles and soluble IL-1ra reduced NF-κB to non-induced levels.

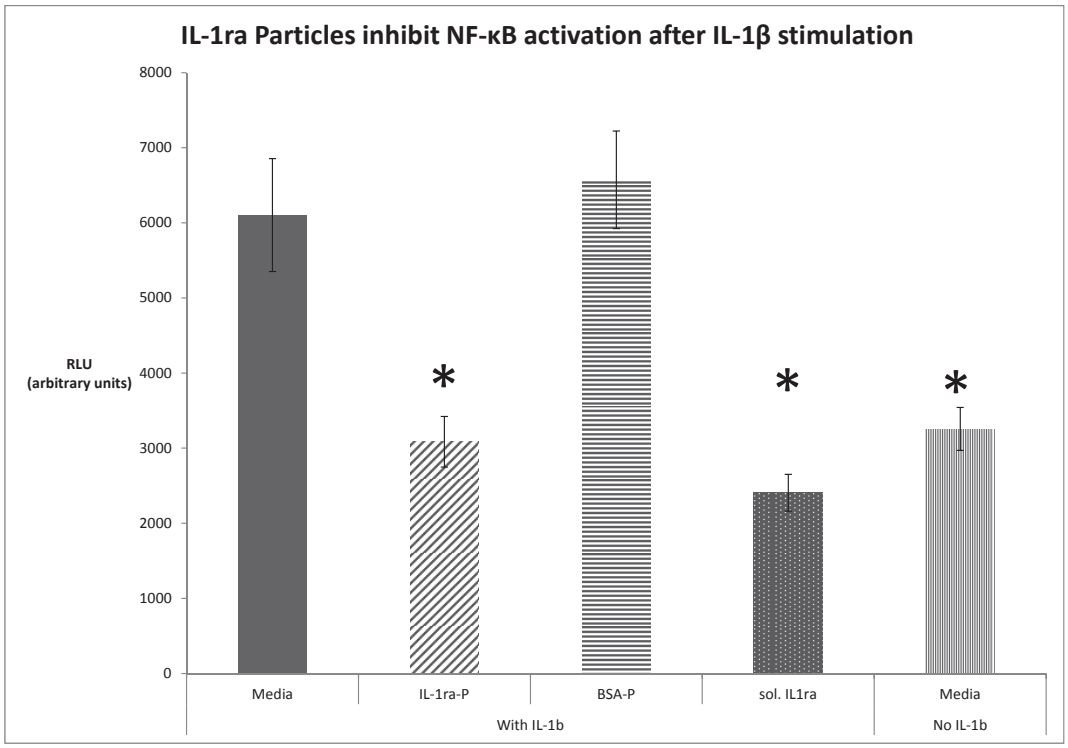

Figure 4.4: IL-1ra-tethered particles reduce IL-1β-induced NF-κB activation as effectively as soluble IL-1ra. NIH 3T3 fibroblasts with an NF-κB-responsive luciferase reporter construct were pre-incubated for 1 h with 1 μg/mL IL-1ra-tethered particles, BSA-tethered particles, or soluble IL-1ra before stimulating with 0.1 ng/mL IL-1β for 6 h. Both IL-1ra particles and soluble IL-1ra inhibited NF-κB activation to comparable levels with unstimulated controls (n=3). * = p<0.004

4.5 Discussion

Our IL-1ra-tethered polymer particles show retention of protein bioactivity and the ability to target synoviocyte cells. The ability of these particles to modulate the activation of NF-κB during IL-1β stimulation indicates that IL-1ra maintains its ability to block the IL-1 signaling pathway. By showing IL-1-mediated binding to synoviocytes, we posit that this cell targeting strategy has potential to improve the effectiveness of drug delivery particles for OA by localizing them via surface-tethered IL-1ra to important inflammatory mediator cells. Although these IL-1ra-tethered particles bind to synoviocytes through IL-1ra, they can also be internalized - either during or after initial interaction with the cells - and may

cause inflammation or toxicity due to their size, although we do not forsee these effects being prevalent at therapeutically relevant dosages. These IL-1ra-tethered particles also have therapeutic benefit on their own, as shown by their ability to reduce NF-κB activation in vitro. The modular nature of the particle's protein tethering moiety suggests that this system could harness the power of other important proteins in addition to IL-1ra for an even more effective therapeutic strategy.

These results are superior to the elastin-like polypeptide-IL-1ra conjugate "depots (ELP-IL1ra) from the Setton lab[305][36]. Although the retention rate of the ELP in vivo was 3.7 days, IL-1ra within the depot showed a 90% reduction in bioactivity in in vitro testing. By presenting IL-1ra on the particle surface, we allow the synoviocytes easy access to the protein and increase the potency of our particle system. Although effective protein delivery from particles is still a challenge, this work adds to promising strategies, such as the phage-panned peptide-targeted nanoparticles from the Hubbell lab[292] and hyaluronic acid-coated PLGA particles[382] or chondroitin sulfate-coated gelatin particles[62]. These particles also have additional benefit because they inhibit IL-1β-induced signaling in addition to their targeting function.

4.6 Conclusions

This work assessed the in vitro bioactivity and targeting behavior of IL-1ra-tethered particles. We found that IL-1ra tethered to our polymer particles was still able to be bound by the IL-1RI. Furthermore, IL-1ra-tethered particles effectively targeted a synoviocyte cell line in vitro in an IL-1β-dependent manner. Finally, these IL-1ra-tethered particles can modulate IL-1β-mediated NF-κB activation in a reporter cell line. These results show that these IL-1ra-tethered particles have the potential to effectively deliver active IL-1ra to key inflammatory cells in vivo and can target synoviocytes, a key mediator cell of osteoarthritis.

CHAPTER V

IN VIVO EVALUATION OF IL-1RA-TETHERED PARTICLE RETENTION IN THE HEALTHY RAT JOINT

5.1 Summary

Current intra-articular drug delivery technologies lack specific targeting strategies and suffer from rapid clearance from the joint space. Specific targeting and localization of drug delivery particles could improve the effectiveness of these drug-delivering particles. Our work used in vivo near-IR imaging to show that IL-1ra-tethered polymeric particles have increased retention in the intra-articular joint space in rats. We demonstrate that this new IL-1ra-targeted particle system has the potential to improve retention of particles in the joint space. Moreover, this new particle system has no adverse effect on the cartilage tissue. We also demonstrate that in vivo imaging can be used for evaluating intra-articular protein delivery. These results provide evidence that these particles prolong the retention time of IL-1ra in the intra-articular space.

5.2 Introduction

Intra-articular drug delivery is the most direct route for administering drugs and proteins for arthritis and other joint disorders and conditions. Localized delivery can avoid problems such as systemic toxicity, biological degradation, and biodistribution issues, and can also reduce the total amount of drug used in each treatment. The synovial membrane surrounding the intra-articular joint space creates a compartment that can retain biomolecules larger than 100 kDa[271]. However, most small molecule drugs and proteins are under this cut-off value and are thus cleared quickly from the joint space. Current technologies for treating OA in vivo show limitations. Bolus injections of protein get cleared from the joint within a few hours of delivery[129][74][83]. Most polymer particles are limited to delivering hydrophobic small molecule drugs. Drug-delivering particles, made of such materials as PLGA, could exacerbate inflammation by producing acidic degradation products. Acidic

environments are known to stimulate inflammatory reactions in the body[96][161][164]. Particles that lack specific targeting moieties have also been cleared relatively quickly from the joint, depending on the size of the particle itself[48][219][220]. Gene therapy-based protein expression is promising for extended therapeutic delivery of proteins to an area; however, protein expression declines over time and can be resistant to reinjection of the same delivery vehicle, essentially negating long-term benefits of this technology[158][21]. Gene therapy also suffers from severe safety concerns, due to side effects, risk vs. benefit trade-offs, and public perception.

Our technology created a non-toxic hydrated particle that retained bioactive protein in vivo in a rat knee joint for up to 14 days. Tethering the protein to the particle carrier increases its retention half-life by three-fold compared to soluble protein, potentially increasing its ability to effect changes in this disease state. The particles do not cause damage to native healthy cartilage tissue. This strategy increases the retention time of IL-1ra in the intra-articular space. By presenting multiple IL-1ra ligands on the particle surface, we can significantly increase the local concentration of IL-1ra at the cell surface and can take advantage of the "multi-valency effect of nanoscale ligand presentation.

5.3 Materials and Methods

5.3.1 Fluorescent Protein Labeling

We labeled IL-1ra with Alexa Fluor 750 prior to tethering it on the particles so we could visualize the retention of IL-1ra-particles and soluble IL-1ra in the joint by IVIS imaging. Briefly, particles were made as previously described (Chapter 3). IL-1ra was reacted with Alexa Fluor 750 maleimide (Alexa Fluor 750 C_5-maleimide, #A30459, Invitrogen Corp., Carlsbad, CA) or DyLight 650 maleimide (#62295, Pierce, Rockford, IL). There are 3 free solvent-accessible cysteines on IL-1ra that can be fluorescently tagged, thereby avoiding the more prevalent primary amines (lysine residues), allowing the protein to be fluorescently tagged before tethering it to particles, as well as reducing the chance of altering the protein's bioactivity[356]. The AF-650-IL-1ra-tethered particles were used to evaluate particle

targeting and localization within the intra-articular joint space. Particles were made as discussed previously and were lyophilized prior to use. Particles were resuspended in distilled water on the day of surgery.

5.3.2 Animal model

Male Lewis rats (10-12 week old) received 50 μL of either particles or soluble IL-1ra protein (5 μg IL-1ra) via intra-articular injection to the right knee joint space, while the left knee received the same volume of saline and served as contralateral controls. Lewis rats were chosen for consistency with established models of OA in the Guldberg lab at Georgia Tech (medial meniscal transection (MMT), medial colateral ligament transection (MCLT)). Transection of the MCL and meniscus causes joint instability and is known to lead to osteoarthritis in animal models.

Rats were deeply anesthetized with isofluorane. The hair was removed from the hind limb surgical sites and the skin was cleaned with alcohol. Rats were positioned on their back, and the leg was flexed to 90° at the knee. Particles were injected into the intra-articular space by palpating the patellar ligament below the patella and injecting the particle solution through the infrapatellar ligament using a sterile 27-gage 0.5" needle. Rats were fully ambulatory following recovery and all injections were well tolerated. At the end point of the study, rats were euthanized using CO_2 asphyxiation.

5.3.3 IVIS Imaging for Particle Retention

Rats were anesthetized using isofluorane. Animals receiving IR-750-IL-1ra-tethered particles or soluble 750-labelled IL-1ra were scanned in an IVIS imaging system (700 Series, Caliper Xenogen IVIS Lumina, Caliper Life Sciences, Hopkinton, MA). The excitation and emission detectors were set at 745 nm and 780 nm. Both hind limbs were scanned to control for background tissue fluorescence. The total photons within a fixed region centered on the knee were measured and were analyzed with non-linear regression models. The data from each animal were normalized to their individual day 0 values. The normalized data were fitted using a one-phase exponential decay with the characteristic equation of:

$Y = (Y_o - NS)*e^{(-K*X)} - NS$

, where Y_o is the intersection of the best-fit line with the Y-axis, NS is the non-specific binding value (i.e., the assymptotic y-value), X is time, and K is inversely proportional to the half-life. The 95% confidence interval for the half-lives are [1.708 - 12.62] (IL-1ra Particles) and [0.7856 - 1.244] (Soluble IL-1ra).

5.3.4 EPIC-μCT

EPIC-μCT has been established as an effective, non-destructive technique for imaging cartilage[261][367][275]. EPIC-μCT uses charged contrast agents to quantify the GAGs in the cartilage. Negatively charged dyes are excluded from healthy cartilage tissue due to the presence of negatively charged GAG chains in the tissue. A lack of dye indicates healthy cartilage tissue. Rat knees were evaluated by μ-CT for cartilage integrity and thickness. Briefly, the explanted rat knee was immersed in 2 mL of 30% Hexabrix in PBS at 37°C for 30 min. The knee was patted dry on a paper towel to remove excess Hexabrix and then was placed in a 16 mm diameter CT tube and was inserted into the CT machine (μCT 40, Scanco Medical, Bassersdorf, Switzerland). Trabecular thickness and bone volume measurement settings in the Scanco software were thresholded to include only cartilage tissue and were used as the primary outcome measures for μ-CT evaluation (cartilage thickness and total cartilage volume, respectively).

The knee tissue was evaluated using the following settings: 45 kVp, 176 μA, 200 ms integration time, a 1024x1024 pixel matrix (Medium resolution), and a 16 μm voxel size. Each knee scan was first re-formatted to vertical slices, contoured by hand and then evaluated for cartilage thickness and attenuation using the following program. Reconstructions were done using sigma = 1, support = 1, lower = 75, upper = 220, and unit = 6. The evaluation script was the uct_evaluation_v6.com; the IPL support script was IPLV6_Trabecular_bone.com, and the user script was uct_evaluation_v6_PRSUCT.com.

5.4 Results

We have previously used near-IR dyes for in vivo imaging to track and quantify protein retention or release[274][45]. These dyes allow for non-invasive, repeated imaging of animals without the expense and hazards of radiolabelling. Rats that received IL-1ra-particles showed significant fluorescent signal for up to 14 days, compared to those receiving soluble protein (Figs. 5.4, 5.5). For instance, IL-1ra-particles had 20% retention at 10 days, whereas over 80% of the soluble IL-1ra had cleared by day 3. IL-1ra-particles had a half-life in the joint of 3 days, while the soluble protein was retained for less than 1 day. The difference between the retention of IL-1ra-particles and soluble IL-1ra was statistically significant ($p<0.0001$). These results show that IL-1ra-tethered particles have better intra-articular retention compared to soluble IL-1ra and are compatible with the cartilage tissue environment.

EPIC-μCT did not detect any adverse effects from our IL-1ra-particle system on the cartilage tissue compared to the contralateral controls; however, this technique may not be sensitive enough to detect initial changes to the tissue (Fig. 5.1). We are processing the tissue samples to confirm this finding by standard histological analysis. There was no difference in the EPIC-μCT-measured cartilage thicknesses or the tissue attenuation among all groups (IL-1ra-Particles, Sol. IL-1ra, Contralateral Controls) (Fig. 5.2, 5.3). The attenuation value is a measure of the sulfated glyocsaminoglycans in the cartilage tissue and provides an indirect assessment of the cartilage extracellular matrix composition.

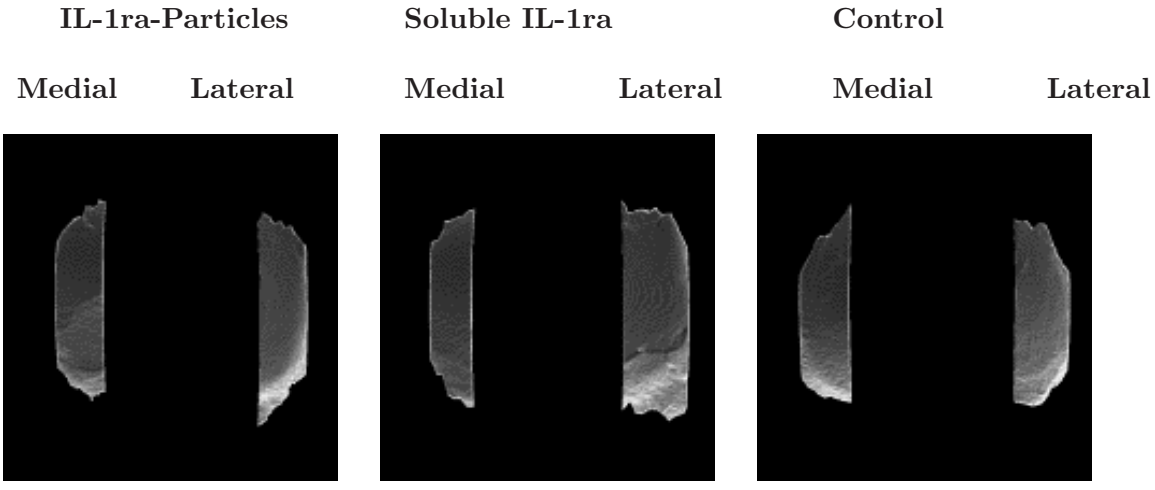

Figure 5.1: Superior View of Tibial Articular Cartilage Surface. Reconstructions of Cartilage from EPIC-μCT Analysis. Visual comparisons confirm that there are no gross differences between cartilage receiving IL-1ra-particles versus soluble IL-1ra or PBS. Medial side, Left; Lateral side, Right.

We are currently processing the tissue for histological analysis to ensure that there are no morphological or phenotypical changes to the cartilage tissue caused by our particles. We also have tissue samples in preparation to look for particle localization within the synovial joint space. However, these results may not be completed by the time of the thesis defense, due to the time necessary to process the tissue after the end of this in vivo study.

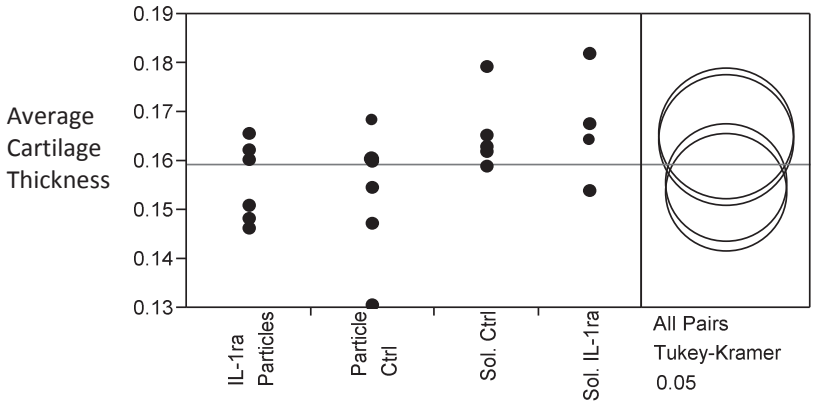

Figure 5.2: No differences in cartilage thickness were detected by EPIC-μCT between IL-1ra-particles and soluble IL-1ra groups. X-axis, animal treatment groups; Y-axis, trabecular thickness, as calculated from EPIC-μCT reconstructions. Sol. Ctrl, contralateral control knees from rats receiving soluble IL-1ra; Sol. IL-1ra, knees receiving soluble IL-1ra; IL-1ra particles, knees receiving IL-1ra-tethered particles; Particle Ctrl, contralateral control knees from rats receiving IL-1ra-tethered particles. Control knees were injected with an equal volume of PBS at the same time as the particles.

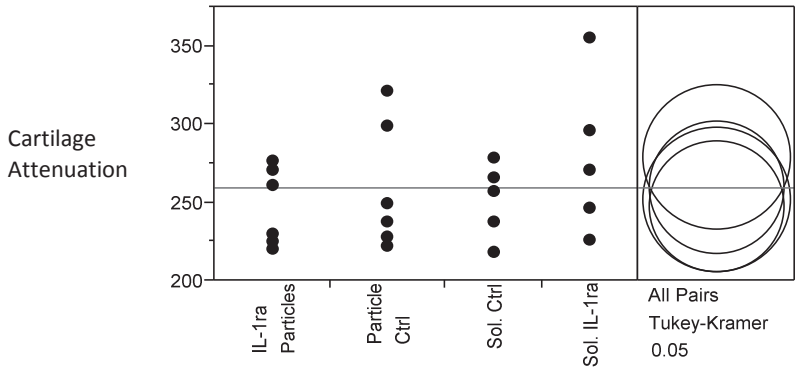

Figure 5.3: EPIC-μCT does not detect any differences in cartilage attenuation between groups receiving IL-1ra particles or soluble IL-1ra. X-axis, animal treatment groups; Y-axis, Bone Volume, as calculated from EPIC-μCT reconstructions. Sol. Ctrl, contralateral control knees from rats receiving soluble IL-1ra; Sol. IL-1ra, knees receiving soluble IL-1ra; IL-1ra particles, knees receiving IL-1ra-tethered particles; Particle Ctrl, contralateral control knees from rats receiving IL-1ra-tethered particles. Control knees were injected with an equal volume of PBS at the same time as the particles.

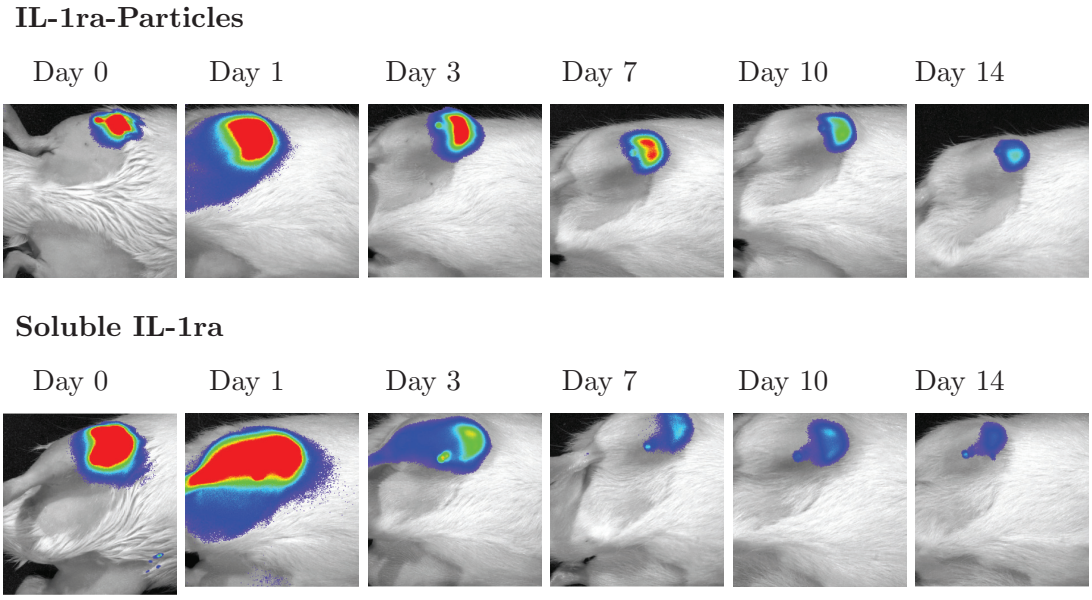

Figure 5.4: IL-1ra-Particles are retained longer than soluble IL-1ra in the intra-articular joint space. IL-1ra was tagged with a near infrared (IR) dye (AF750-maleimide) prior to tethering IL-1ra to particles. IL-1ra-tethered particles or soluble IL-1ra was injected into the right knee of 8-10 wk old rats. Left knees were injected with saline at the same time. Total IR photon counts within a fixed area centered over the rat's knee were measured by IVIS imaging over 14 days.

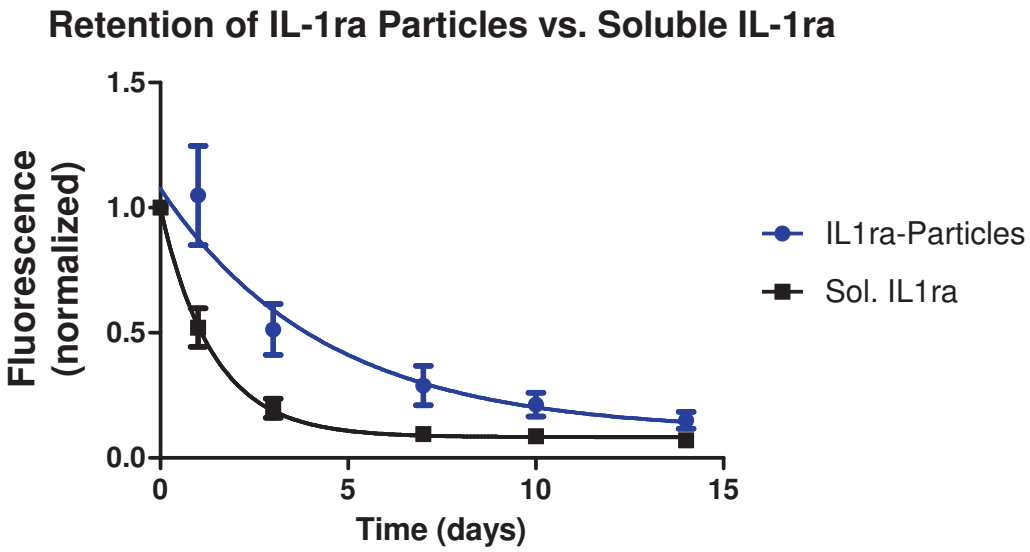

Figure 5.5: IL1ra-particles show attenuated signal compared to soluble IL1ra (IL-1ra-Particles, n = 6; soluble IL-1ra, n = 5). Infrared (IR) photon counts were measured in each rat over 14 days by an IVIS imaging system. All data were normalized by individual rat to its Day 0 photon count. The photon's signal decay was fit using a one-phase exponential decay model. IC_{50} = 3.01 days for IL-1ra-Particles vs. 0.96 days for soluble IL-1ra.

5.5 Discussion

We interrogated whether tethering IL-1ra to particles could increase the residence time in the intra-articular joint space. Healthy rat knee joints retained detectable amounts of IL-1ra-tethered particles for up to 14 days. Previous work suggested that microparticles generally stay longer in the joint than soluble proteins[23][179]. PLGA particles (300-490 nm) with encapsulated betamethasone showed significant anti-inflammatory effect for up to 21 days in Antigen-Induced Arthritic rabbit joints. The goal of this work was to two-fold: one goal was to determine whether this new particle system could increase the retention of IL-1ra compared to a bolus dose of soluble IL-1ra; secondly, we wanted to ensure that this polymer particle system did not cause damage to the cartilage tissue. Part

of the concern with current hydrophobic polymer particles is that their mechanical property mismatch could act as wear particles in the soft cartilage tissue environment. Our material incorporates an oligo(ethylene glycol) chain, which should provide a hydrated corona around the particle. However, we wanted to ensure that this particle system had no adverse effects. The cartilage tissue surface and thickness were the same across groups, regardless of the treatment they received.

This technology is comparable in half-life to the fusion protein system developed by Setton et al.[36][305]. Their elastin-like polypeptide gel had a half-life of 3.7 days in vivo, while ours had a half-life of 3.01 days. However, a fusion protein of IL-1ra and the ELP showed a 90% loss of IL-1ra bioactivity in vitro[305]. Further characterization of this system is necessary to establish the effective bioactivity of tethered IL-1ra for better comparison with the Setton technology; however, since we are not encapsulating IL-1ra within a hydrogel-like system, the bioactivity of our IL-1ra particles should be much higher than the ELP-IL-1ra system. Additionally, although our technology increased IL-1ra half-life in the joint, 3 days may not be long enough to substantially affect OA disease progression. Allen et al. showed that the IL-1ra-ELP technology, which has a 3 day half-life in the joint as well, reduced the severity of cartilage destruction in an IL-1β-induced model of arthritis; however, this model may not be fully representative of a diseased OA joint and may oversell the effectiveness of their ELP-based system. By increasing the particle half-life by optimizing particle size, we can maximize the therapeutic benefit of IL-1ra-tethered particles.

Other attempts to increase protein half-life, such as PEGylation, only moderately increased the systemic residence time of the proteins but also negatively affected the proteins bioactivity[371][141][142]. Other intra-articular drug delivery systems have shown a range of retention times. Radiolabeled liposomes with Dex encapsulated were delivered to healthy rabbit joints and showed 36% retention compared to 2% of free Dex remaining at 24 h[48]. However, other liposomal drug formulations have shown intra-articular half-lives up to 134 h[109]. PLGA microparticles effectively reduced joint swelling for up to 21 days in an antigen-induced arthritic rabbit model[178], although no direct measurement of particle

half-life was assessed. Using a nearIR dye-labeled protein rather than radiolabeled protein to assess the residence time and effectiveness of our therapy has several advantages. First, nearIR dyes require no special handling or processing equipment, while radiolabeling requires careful handling procedures to avoid contamination. Secondly, the nearIR dye is stable over time; the radiolabeled signal decays over time and could affect the accurate detection during the course of an experiment. Finally, biodistribution is easily assessed by merely dissecting and imaging tissue in a nearIR imager. The same assessment is costly and technically involved[107].

5.6 Conclusion

This work tested the in vivo behavior of our IL-1ra-tethered particle system compared with soluble protein. Our particles increased the half-life of IL-1ra in a healthy rat knee joint 3-fold (3.08 days vs. 0.96 days) compared to a bolus injection of soluble IL-1ra. This new polymer particle system showed no adverse effects on the cartilage tissue morphology by EPIC-μCT analysis. This study shows that IL-1ra-tethered particles can increase the retention of therapeutics in the intra-articular joint space. Further analysis is ongoing to assess whether the IL-1ra-tethered particles are localizing to the synovial cells within the joint space and to ensure that the particle-receiving joint tissue morphology is comparable to that of the healthy tissue.

CHAPTER VI

SUMMARY OF CONCLUSIONS

The field of biomaterials had made significant progress toward creating targeted drug delivery particles for a wide array of applications. However, current technologies still lack a robust strategy for controlled delivery of proteins. In this thesis, we created a new way of delivering protein for targeting OA treatment by taking advantage of the signaling mechanism of IL-1ra, a key protein antagonist in OA. IL-1ra acts as an IL-1 antagonist by binding to the IL-1 receptor without inducing receptor-protein internalization or cytoplasmic signaling. We created a new polymer particle system that presents IL-1ra on the particle surface to increase its retention time in the joint space. We characterized this protein-particle system by chemical analysis, and in in vitro and in vivo settings. This work was divided into three specific aims.

Our first goal was to engineer a block copolymer that could form submicron-scale particles to deliver IL-1ra in a controlled manner. We included a stable protein-tethering moiety, 4-nitrophenol, that remained accessible on the surface of the particles after assembly. In chapter 3, we showed that we successfully designed a block copolymer with a hydrophilic monomer (TEGM) segment paired with a hydrophobic monomer (CHM) segment. We were then able to synthesize this copolymer and characterize its ability to form particles and tether IL-1ra to the particle surface. This polymer system has built-in modularity to allow for variation in particle size, choice of protein, and ability to deliver a drug and protein simultaneously. The size of each segment of the block copolymer can be increased or decreased by varying the molar ratio of monomers to μRAFT agent. The overall molecular weight of the polymer can also be increased in the same way. The size of the hydrophobic segment of the block copolymer could be increased to adjust the drug-carrying capacity or to increase the particle stability.

We then characterized the in vitro behavior of our IL-1ra-tethered particles by showing that IL-1ra maintains its bioactivity after tethering it to the particle surface, that it binds to our cells of interest, synoviocytes, in an IL-1-dependent manner, and that IL-1ra-tethered particles can inhibit NF-κB activation after an IL-1β insult. The first study took IL-1ra-tethered particles and incubated them with a recombinant IL-1R-Fc protein. IL-1ra-tethered particles were bound by the IL-1r in significantly higher number compared to BSA-tethered particles (11.9% vs. 1.6% BSA-particles), showing that the IL-1ra maintains its ability to bind the IL-1R and suggesting that its bioactivity is maintained. The second study then looked for IL-1ra-particles to specifically bind to synoviocytes, our target cell of interest in OA. When synoviocytes were incubated with IL-1ra-tethered particles, they showed increased IL-1ra-particle binding (44.0% vs. 2.8%) compared to particles presenting a non-targeting protein. Importantly, this binding was abrogated by pre-blocking the cells with IL-1β (44.0% vs. 2.7%), demonstrating that the IL-1ra-particles target the IL-1 receptor in synoviocytes. When we stimulated IL-1-responsive cells with IL-1β, our IL-1ra-tethered particles reduced IL-1β-initiated NF-κB activation, measured by NF-κB-induced luciferase expression, as much as the same dose of soluble IL-1ra did. Both of these treatments reduced NF-κB activation to the same level as unstimulated controls.

Finally, we examined the retention and effect of IL-1ra-tethered particles in healthy rat knee joints. Our IL-1ra-tethered particles extended the half-life of IR-labeled IL-1ra by three-fold compared to soluble IL-1ra. Additionally, the particles did not cause any detectable wear damage to the cartilage tissue. Full histological analysis of the tissue is ongoing, as is analysis to look at particle targeting within the joint space. We expect that the histology will show no differences between healthy control tissue and tissue that received IL-1ra particles.

In summary, this thesis project engineered and characterized a new polymeric drug delivery particle system for delivering IL-1ra, as outlined in the Specific Aims. The outcomes of this project were as follows: First, we developed a new amphiphilic block copolymer using RAFT polymerization and verified that it formed particles on our desired size scale. We also verified that this polymer particle tethered proteins to its surface under mild reaction

conditions. The modular nature of this material's chemistry allows for it to be used in a range of different applications by varying the tethered surface protein. Secondly, we characterized the behavior of IL-1ra-tethered particles in multiple in vitro tests. We ensured that tethered IL-1ra retained its bioactivity, that IL-1ra-particles targeted a synoviocyte cell line in an IL-1-dependent manner, and that IL-1ra-tethered particles inhibited IL-1β-induced activation of NF-κB. Finally, we examined particle retention in healthy rat knee joints over 14 days. IL-1ra-tethered particles had significantly longer half-life in the intra-articular joint space than soluble IL-1ra protein. These particles did not cause any detectable wear damage to the cartilage tissue, as assessed by EPIC-μCT.

Overall, this project created and characterized a new modular polymer particle system that can deliver IL-1ra in a targeted fashion for treating osteoarthritis. This IL-1ra-based technology shows promise for not only localizing particles to inflammatory cells, but also for modulating the associated inflammatory cascades. This IL-1ra particle system shows promise for treating OA-induced inflammation and should be evaluated in a representative in vivo model of osteoarthritis, such as the ACLT or MMT/MCLT model. Because of the particle size, only 2-3 cells can bind each particle simultaneously, reducing how much of the tethered IL-1ra is actually available for binding to receptors on the cell surface. Optimizing the size of the particle could increase the number of cells that can bind each particle for more effective, long-lasting therapeutic effectiveness. Furthermore, the quantity of IL-1ra that needs to be delivered to counteract chronic IL-1β during OA may require multiple injections or greater quantities of particles than is safe or possible. Due to these limitations, this technology would probably be most effective at slowing or preventing OA progression if it is delivered within the first week after an acute joint injury. The rationale for this timing is to avoid the immediate inflammation that happens after an injury (approximately the first 48 h) but to start inhibiting the onset of chronic inflammation. Additionally, this strategy would be best paired with encapsulated clodronate within the particles to reduce the number of macrophages in the area and thus also reduce the amount of secreted IL-1β in the joint space. Although soluble IL-1ra has been effective in the short term at slowing the onset of OA damage, OA pathology involves more than just IL-1. Pairing this IL-1ra-based

targeting/therapeutic particle strategy with other anti-cytokine proteins and drugs should cooperatively enhance the action of IL-1ra and the other delivered agents.

As mentioned above, the particles should be evaluated for drug encapsulation and release of steroidal or other anti-inflammatory drugs together with surface-tethered IL-1ra. The work here advances the use of block copolymer particles for protein delivery. Our amphiphilic block copolymer particles incorporate the hydrophobic drug-encapsulating properties of PLGA with the "stealth nature of PEG particles to form a hybrid system. Current drug delivery systems generally lack a robust strategy to include targeting peptides or proteins. By incorporating a stable protein-tethering moiety on the particle surface, we provide an easy way to add targeting and/or therapeutic proteins to a basic drug delivery particle to increase its effectiveness.

CHAPTER VII

FUTURE DIRECTIONS

The first step in extending this work is to test the effectiveness of IL-1ra-tethered particles in a relevant OA model. We did preliminary studies using the MIA-induced OA model in rats; however, we saw no improvement in joint phenotype or cartilage degradation in rats receiving our IL-1ra-particles or soluble IL-1ra protein. We expected that at least the soluble protein would show some improvements at 14 days post-treatment, which led us to conclude that the MIA model of osteoarthritis does not create a cytokine environment analogous to that of natural OA. These results are not entirely unexpected because we were unable to find any mention in the literature of using IL-1ra to ameliorate MIA-induced OA in rats. Only two studies used intra-articular injections of IL-1ra in rats, one in an IL-1β-induced model [7] and the other in a collagen-induced arthritis model[29]. Taking these facts and our results as a whole, we believe that using a different model of OA, such as the ACLT or MMT/MCLT model, are more representative of natural OA and will produce a cytokine environment in the joint that is similar to that found in human OA. The ACLT and MMT/MCLT models do take longer to develop an arthritic phenotype, so they are at a disadvantage compared with the near-immediate effects of MIA-induced arthritis. However, when testing cytokine-based treatments, such as our IL-1ra-tethered particles, it is crucial to have the most representative and accurate cytokine environment in the animal model to replicate the disease and evaluate the potential effectiveness of the technology.

Another future strategy would be to test out other proteins, specifically cytokines, that are relevant to OA. Our primary cytokine of interest for OA inflammation was IL-1β. However other cytokines play crucial roles in this complex disease state. One of those, TNF-α, exhibits signs of redundancy with IL-1. Researchers have tested soluble TNF-RI for treating OA[350]. Although administering TNF-RI alone was not sufficient to improve OA symptoms, IL-1ra and TNF-RI together reduced synovitis and decreased the cartilage

damage in a rabbit model of OA. The modularity of our particle technology could allow the delivery of TNF-RI and IL-1ra simultaneously. TGF-β also shows abnormal patterns of receptor expression during OA and the aging process[342]. Adding exogenous TGF-β or a TGF-β receptor antagonist could be an alternate strategy for modulating OA inflammation. However, the exact levels of TGF-β being delivered is crucial to its success because overexpression of TGF-β also leads to negative effects, such as joint fibrosis and osteophyte formation[18][342]. The final protein factor that warrants immediate consideration is IGF-1[249]. Its role in upregulating levels of soluble IL-1RII could provide a natural method of creating an IL-1β sink in the OA joint space.

This thesis work was limited to characterizing the particles' ability to deliver proteins on its surface. However, the polymer was originally conceptualized to include hydrophobic drugs in its core. We believe that adding small hydrophobic drugs, such as dexamethasone or clodronate, to the core of our targeted particles could also improve its efficacy by localizing the drug release to some of the most crucial cells in this disease etiology. Small molecule drugs can inhibit and/or target pathways that may synergize with IL-1ra's anti-inflammatory effect but also can exert their own unique effects as well. Drugs would release either by diffusion and/or by particle disaggregation to release its payload. These particles could also incorporate MMP inhibitors, imaging agents for inflammation, and siRNA to inhibit inflammatory pathways or to influence the macrophage/synoviocyte phenotype in the joint. Combining drugs or small molecule biomolecules could act synergistically with our IL-1ra and other surface-tethered proteins to better address the complex OA pathology.

The protein tethering chemistry could also be altered to address any effects on protein bioactivity that are caused by tethering protein via primary amines. Finding more selective protein tethering chemistries (e.g., maleimides/free cysteines) that interfere less with a protein's bioactivity could be used as an alternative strategy. Proteins could also be attached using enzyme-cleavable sequences rather than covalent linkages to allow protein release and internalization.

Although we chose a sub-micron-scale particle in this work, we could explore a variety of particle sizes for optimal treatment. By increasing the particle size, we reduce the chance

of fast clearance by the synovial fluid; however, increasing the particle size reduces the total surface area available for protein tethering and can affect the particles' diffusion through the cartilage tissue and its mobility in the joint. The best compromise between particle size, clearance rate, and deliverable protein quantity must be found by trial and error.

The block copolymer could also be altered to improve its "stealth" characteristics. Although our polymer used an oligoethylene derivative, the fully carbon backbone of the copolymer is hydrophobic and could cause issues, especially in vivo. We could use a larger pendant poly(ethylene glycol) (PEG) chain to help mask the backbone or we could find a way to use a PEG chain as the main chain of the hydrophilic block copolymer. Both of these could improve the protein-resistant particle shell.

Particle stability in serum and in vivo were not characterized in this work. If the stability of the polymer particles is an issue in its effectiveness, we could increase the particles' stability by adding functionalities to cross-link the core. Previous work has shown that cross-linking increases particle residence time and half-life[376].

In addition to its application in OA, our IL-1ra-tethered particles have possible applications for other diseases, such as cancer and heart disease. IL-1 and macrophages play a crucial role in the neovascularization process in tumors. Targeting macrophages via IL-1ra could interfere with the pro-angiogenic signaling and could also deliver drugs to cause the macrophages to apoptose (clodronate, others), thus eliminating the tumors support network[213]. IL-1ra-tethered particles could also be used to deliver pro-angiogenic or anti-inflammatory drugs to the heart after myocardial infarction (MI) (heart attack). IL-1 is known to play a key role in the overwhelming inflammatory/fibrotic response after MIs. IL-1ra could help push the macrophages toward a more M2-like (wound healing) phenotype and could help improve patient outcomes by reducing inflammation and increasing the hearts contractility. Finally, IL-1ra is known to support islet survival in vitro. These particles could be co-injected during an islet transplant via hepatic portal vein injection or could serve as a support system within an encapsulated islet system, such as the PEG hydrogel system established in the García laboratory.

This particle system has an enormous breadth of possible applications when you consider

varying the targeting/therapeutic proteins on the particle surface. Although IL-1ra is widely applicable and useful, there is a host of applications that would benefit from targeted drug/protein/siRNA/DNA delivery. This polymer particle technology could be developed for cancer therapy and cardiac drug delivery, as well as for in vitro applications, like localized drug delivery and sustained release of drugs to cells within tissue engineered constructs.

APPENDIX A

IL-1RA CLONING PROJECT

A.1 IL-1ra cloning

We obtained the original plasmid containing the human IL-1ra sequence[111] from Dr. Michael Smith (University of Virginia) (Fig. A.1). We grew up the bacteria and sequenced its DNA to verify its fidelity. We then designed PCR primers to amplify the gene sequence (see Table A.1), while adding HindIII restriction enzyme sequences on both ends of the PCR product (Table A.1). After digesting the PCR product and the backbone vector Xa-3 biotinylation vector (PinPoint Xa-3 Vector, #V206A, Promega Corp., Madison, WI) with HindIII and/or CIP treatment (1 h) for 3 h at 37°C, we ran the digested products on a 1.2% agarose gel in TAE buffer, extracted the products using a gel extraction kit (QIAquick, #28704, Qiagen, Valencia, CA), and ligated the reaction mixtures at room temperature overnight. We then transduced chemically competent BL21 E. coli bacteria with the various reaction mixtures and plated the transformed bacteria on Amp-LB agar plates overnight. We selected 6 colonies from each successful reaction and grew them up overnight in 5 mL cultures with ampicillin. We extracted and digested the cultures' DNA with HindIII (or KpnI as a directional control). We found at least 5 clones that had the IL-1ra sequence in the correct orientation (Fig. A.2). We sent those 5 sets of DNA for sequencing and chose one of the confirmed positive clones as our IL-1ra-expressing construct (see subsection: sequencing results). We then transduced chemically competent JM109 E. coli cells with the IL-1ra construct in order to efficiently produce recombinant protein and made a glycerol stock of the JM109/IL-1ra bacteria for future use.

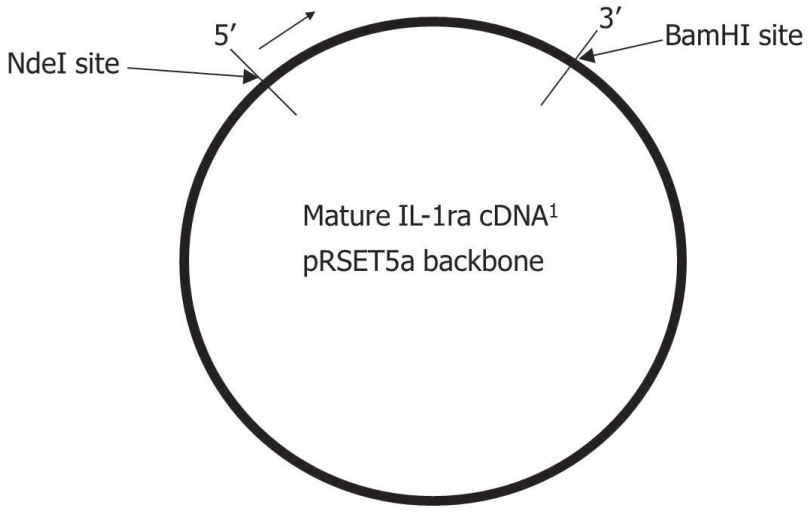

Figure A.1: Original IL-1ra construct from Dr. M. Smith (Eisenberg+ 1990)

A.1.1 Digestion Products

IL-1ra has a KpnI site that cleaves at #149 out of #475 bp in the IL-1ra sequence. There is also a KpnI cleavage site on the Xa-3 backbone, 12 bp past the HindIII terminus of the IL-1ra sequence. Cutting the construct with HindIII should result in the Xa-3 backbone (3284 bp) and the IL-1ra insert (475 bp). Digesting with KpnI in the correct orientation should result in a "backbone" of 3433 bp and an IL-1ra insert of 338 bp. However, if the IL1ra insert is inserted backward, the digest products will be 3610 bp and 149 bp.

HindIII: 475 bp/3284 bp KpnI: Correct Orientation: 338 bp/3433 bp KpnI: Incorrect Orientation: 149 bp/3610 bp

Table A.1: Cloning Primers

Verification Primers*

Primer Name	Primer Location	Primer Sequence
pRSET5a fwd1	#2824 -#14 on pRSET backbone	5-TAA TGC AGG ATC TCG ATC CCG C-3
pRSET5a fwd2	#179-#205	5-CAA CCA ACT AGT TGC TGG ATA CTT GCA 3
pRSET5a fwd3	#281-#302	5-TGG AGG GAA GAT GTG CCT GTC C-3
pRSET5a rev	Reverse complement of #314-#335	5-GCT GGA GTC TGG TCT CAT CAC C-3

Amplification Primers**

Primer Name	Primer Location	Primer Sequence
IL-1ra HindIII fwd 9907	#394-#426	5-CAA GAG **AAG CTT**(Hind) ACC ATG GGA CCC TCT GGG AGA AAA TCC-3
HindIII Reverse Oct	Reverse complement of #849-#879	5-GGA CTA **AAG CTT**(Hind) TTA TCC CTA CTA CTC GTC CTC CTG G-3

Sequencing Primers**

Primer Name	Primer Location	Primer Sequence
XA3 backbone seq fwd	#196-#211	5-GTC TCC AAG ATC CTC GTG AAG G-3
Reverse IL-1ra	Reverse complement of #604-#619	5-CAC CAG ACT TGA CAC AGG ACA G-3
pRSET5a fwd2	IL-1ra #492-#512	5-CAA CCA ACT AGT TGC TGG ATA CTT GCA 3
pRSET5a fwd3	IL-1ra #594-#609	5-TGG AGG GAA GAT GTG CCT GTC C-3
pRSET5A rev	Reverse complement of #622-#637	5-GCT GGA GTC TGG TCT CAT CAC C-3

* numbers refer to original sequence published by Eisenberg+ 1990.

** numbers refer to placement within XaIII+IL-1ra construct, with 1 as the start of the XaIII backbone sequence.

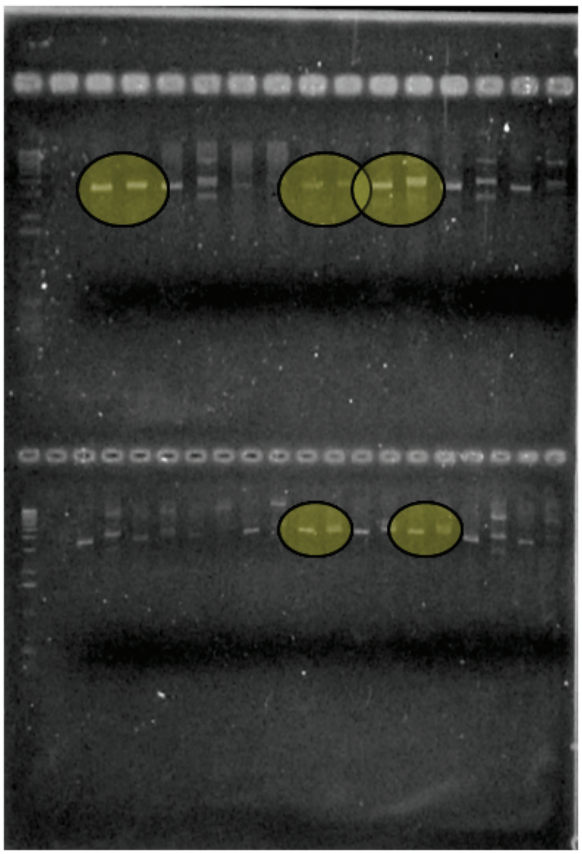

Figure A.2: HindIII and KpnI digest of potential IL-1ra clones

A.1.2 Theoretical Plasmid Map Sequence

DNA sequence: #1 (Beginning of the PinPoint XaIII vector):

5'-ATGAAACTGA AGGTAACAGT CAACGGCACT GCGTATGACG TTGACGTTGA
CGTCGACAAG TCACACGAAA ACCCGATGGG CACCATCCTG TTCGGCGGCG
GCACCGGCGG CGCGCCGGCA CCGGCAGCAG GTGGCGCAGG CGCCGGTAAG
GCCGGAGAGG GCGAGATTCC CGCTCCGCTG GCCGGCACCG TCTCCAAGAT
CTCGTGAAG GAGGGTGACA CGGTCAAGGC TGGTCAGACC GTGCTCGTTC
TCGAGGCCAT G [biotinylated lysine codon][AAG*]ATGGAG ACCGAGATCA
ACGCTCCCAC CGACGGCAAG GTCGAGAAGG TCCTGGTCAA GGAGCGTGAC
GCGGTGCAGG GCGGTCAGGG TCTCATCAAG ATCGGGGATC TCGAGCTCAT
CGAAGGTCGC GAA [start][IL-1ra insert][HindIII][AAG CTT] ACC ATG
GGA CCC TCT GGG AGA AAA TCC AGC AAG ATG CAA GCC TTC AGA

ATC TGG GAT GTT AAC CAG AAG ACC TTC TAT CTG AGG AAC AAC
CAA CTA GTT GCT GGA TAC TTG CAA GGA CCA AAT GTC AAT TTA
GAA GAA AAG ATA GAT GTG GTA CCC ATT GAG CCT CAT GCT CTG
TTC TTG GGA ATC CAT GGA GGG AAG ATG TGc CTG TCC TGT GTC
AAG TCT GGT GAT GAG ACC AGA CTC CAG CTG GAG GCA GTT AAC
ATC ACT GAC CTG AGC GAG AAC AGA AAG CAG GAC AAG CGC TTC
GCC TTC ATC CGC TCA GAC AGT GGC CCC ACC ACC AGT TTT GAG
TCT GCC GCC TGC CCC GGT TGG TTC CTC TGC ACA GCG ATG GAA
GCT GAC CAG CCC GTC AGC CTC ACC AAT ATC CCT GAC GAA GGC
GTC ATG GTC ACC AAA TTC TAC TTC CAG GAG GAC GAG TAG TAG
GGA TAA [HindIII][AAG CTT] CAGCTGGGATC CGGTACCGAT ATCAGATCTC
CCGGGGCGGC CGCGATCTGG TTCTATAGTG TCACCTAAAT CGTATGTGTA
TGATACATAA GGTTATGTAT TAATTGTAGC CGCGTTCTAA CGACAATATG
TCCATATGGT GCACTCTCAG TACAATCTGC TCTGATGCCG CATAGTTAAG
CCAGCCCCGA CACCCGCCAA CACCCGCTGA CGCGCCCTGA CGGGCTTGTC
TGCTCCCGGC ATCCGCTTAC AGACAAGCTG TGACCGTCTC CGGGAGCTGC
ATGTGTCAGA GGTTTTCACC GTCATCACCG AAACGCGCGA GACGAAAGGG
CCTCGTGATA CGCCTATTTT TATAGGTTAA TGTCATGATA ATAATGGTTT
CTTAGACGTC AGGTGGCACT TTTCGGGGAA ATGTGCGCGG AACCCCTATT
TGTTTATTTT TCTAAATACA TTCAAATATG TATCCGCTCA TGAGACAATA
ACCCTGATAA ATGCTTCAAT AATATTGAAA AAGGAAGAGT ATGAGTATTC
AACATTTCCG TGTCGCCCTT ATTCCCTTTT TTGCGGCATT TTGCCTTCCT
GTTTTTGCTC ACCCAGAAAC GCTGGTGAAA GTAAAAGATG CTGAAGATCA
GTTGGGTGCA CGAGTGGGTT ACATCGAACT GGATCTCAAC AGCGGTAAGA
TCCTTGAGAG TTTTCGCCCC GAAGAACGTT TTCCAATGAT GAGCACTTTT
AAAGTTCTGC TATGTGGCGC GGTATTATCC CGTATTGACG CCGGGCAAGA
GCAACTCGGT CGCCGCATAC ACTATTCTCA GAATGACTTG GTTGAGTACT
CACCAGTCAC AGAAAAGCAT CTTACGGATG GCATGACAGT AAGAGAATTA
TGCAGTGCTG CCATAACCAT GAGTGATAAC ACTGCGGCCA ACTTACTTCT

GACAACGATC GGAGGACCGA AGGAGCTAAC CGCTTTTTTG CACAACATGG
GGGATCATGT AACTCGCCTT GATCGTTGGG AACCGGAGCT GAATGAAGCC
ATACCAAACG ACGAGCGTGA CACCACGATG CCTGTAGCAA TGGCAACAAC
GTTGCGCAAA CTATTAACTG GCGAACTACT TACTCTAGCT TCCCGGCAAC
AATTAATAGA CTGGATGGAG GCGGATAAAG TTGCAGGACC ACTTCTGCGC
TCGGCCCTTC CGGCTGGCTG GTTTATTGCT GATAAATCTG GAGCCGGTGA
GCGTGGGTCT CGCGGTATCA TTGCAGCACT GGGGCCAGAT GGTAAGCCCT
CCCGTATCGT AGTTATCTAC ACGACGGGGA GTCAGGCAAC TATGGATGAA
CGAAATAGAC AGATCGCTGA GATAGGTGCC TCACTGATTA AGCATTGGTA
ACTGTCAGAC CAAGTTTACT CATATATACT TTAGATTGAT TTAAAACTTC
ATTTTTAATT TAAAAGGATC TAGGTGAAGA TCCTTTTTGA TAATCTCATG
ACCAAAATCC CTTAACGTGA GTTTTCGTTC CACTGAGCGT CAGACCCCGT
AGAAAAGATC AAAGGATCTT CTTGAGATCC TTTTTTTCTG CGCGTAATCT
GCTGCTTGCA AACAAAAAAA CCACCGCTAC CAGCGGTGGT TTGTTTGCCG
GATCAAGAGC TACCAACTCT TTTTCCGAAG GTAACTGGCT TCAGCAGAGC
GCAGATACCA AATACTGTTC TTCTAGTGTA GCCGTAGTTA GGCCACCACT
TCAAGAACTC TGTAGCACCG CCTACATACC TCGCTCTGCT AATCCTGTTA
CCAGTGGCTG CTGCCAGTGG CGATAAGTCG TGTCTTACCG GGTTGGACTC
AAGACGATAG TTACCGGATA AGGCGCAGCG GTCGGGCTGA ACGGGGGGTT
CGTGCACACA GCCCAGCTTG GAGCGAACGA CCTACACCGA ACTGAGATAC
CTACAGCGTG AGCTATGAGA AAGCGCCACG CTTCCCGAAG GGAGAAAGGC
GGACAGGTAT CCGGTAAGCG GCAGGGTCGG AACAGGAGAG CGCACGAGGG
AGCTTCCAGG GGGAAACGCC TGGTATCTTT ATAGTCCTGT CGGGTTTCGC
CACCTCTGAC TTGAGCGTCG ATTTTTGTGA TGCTCGTCAG GGGGGCGGAG
CCTATGGAAA AACGCCAGCA ACGCGGCCTT TTTACGGTTC CTGGCCTTTT
GCTGGCCTTT TGCTCACATG TTCTTTCCTG CGTTATCCCC TGATTCTGTG
GATAACCGTA TTACCGCCTT TGAGTGAGCT GATACCGCTC GCCGCAGCCG
AACGACCGAG CGCAGCGAGT CAGTGAGCGA GGAAGCGGAA GAGCGCCCAA
TACGCAAACC GCCTCTCCCC GCGCGTTGGC CGATTCATTA ATGCAGGTTA

ACCTGGCTTA TCGAAATTAA TACGACTCAC TATAGGGAGA CCGGCCTCGA GCAGCAAGGA GATGGCGCCC AACAGTCCCC CGGCCACGGG GCCTGCCACC ATACCCACGC CGAAACAAGC GCTCATGAGC CCGAAGTGGC GAGCCCGATC TTCCCCATCG GTGATGTCGG CGATATAGGC GCCAGCAACC GCACCTGTGG CGCCGGTGAT GCCGGCCACG ATGCGTCCGG CGTAGAGGAT CGATCCGGGC TTATCGACTG CACGGTGCAC CAATGCTTCT GGCGTCAGGC AGCCATCGGA AGCTGTGGTA TGGCTGTGCA GGTCGTAAAT CACTGCATAA TTCGTGTCGC TCAAGGCGCA CTCCCGTTCT GGATAATGTT TTTTGCGCCG ACATCATAAC GGTTCTGGCA AATATTCTGA AATGAGCTGT TGACAATTAA TCATCGGCTC GTATAATGTG TGGAATTGTG AGCGGATAAC AATTTCACAC AGGAAACAGA ATTCCCAGCT TGGCTGCAGA ACCATTCCAT TCGTTGATCC GGGAGTAACT CAC - 3'

Amino acid sequence of the whole protein: (Extinction Coeff: 16,980 cm^{-1} M^{-1}) (MW: 30,730 g/mol (287 residues), PI = 5.04)

Calculated from:

`http://www.basic.northwestern.edu/biotools/proteincalc.html`

and

`http://web.expasy.org/cgi-bin/compute_pi/pi_tool`

MKLKVTVNGTAYDVDVDVDKSHENPMGTILFGGGTGGAPA PAAGGAGAGKAGEGEIPAPL AGTVSKILVKEGDTVKAGQTVLVLEAMKMETEINA PTDGKVEKVLVKERDAVQGGQGLIK IGDLELIEGREKLTMGPSGRKSSKMQAFRIW DVNQKTFYLRNNQLVAGYLQGPNVNLEEK IDVVPIEPHALFLGIHGGKMCLSCVKS GDETRLQLEAVNITDLSENRKQDKRFAFIRSDS GPTTSFESAACPGWFLCTAMEAD QPVSLTNIPDEGVMVTKFYFQEDE–G-KL

A.1.3 Sequencing Results

5' - ATGAAACTGA AGGTAACAGT CAACGGCACT GCGTATGACG TTGACGTTGA CGTCGACAAG TCACACGAAA ACCCGATGGG CACCATCCTG TTCGGCGGCG

GCACCGGCGG CGCGCCGGCA CCGGCAGCAG GTGGCGCAGG CGCCGGTAAG GCCGGAGAGG GCGAGATTCC CGCTCCGCTG GCCGGCACCG TCTCCAAGAT CTCGTGAAGTCGAGGCCAT G[AAG*]ATGGAG ACCGAGATCA ACGCTCCCAC CGACG-GCAAG

GTCGAGAAGG TCCTGGTCAA GGAGCGTGAC GCGGTGCAGG GCGGTCAGGG TCTCATCAAG ATCGGGGATC TCGAGCTCAT CGAAGGTCGC GAA AAG CTT ACC ATG GGA CCC TCT GGG AGA AAA TCC AGC AAG ATG CAA GCC TTC AGA ATC TGG GAT GTT AAC CAG AAG ACC TTC TAT CTG AGG AAC AAC CAA CTA GTT GCT GGA TAC TTG CAA GGA CCA AAT GTC AAT TTA GAA GAA AAG ATA GAT GTG GTA CCC ATT GAG CCT CAT GCT CTG TTC TTG GGA ATC CAT GGA GGG AAG ATG TGc CTG TCC TGT GTC AAG TCT GGT GAT GAG ACC AGA CTC CAG CTG GAG GCA GTT AAC ATC ACT GAC CTG AGC GAG AAC AGA AAG CAG GAC AAG CGC TTC GCC TTC ATC CGC TCA GAC AGT GGC CCC ACC ACC AGT TTT GAG TCT GCC GCC TGC CCC GGT TGG TTC CTC TGC ACA GCG ATG GAA GCT GAC CAG CCC GTC AGC CTC ACC AAT ATC CCT GAC GAA GGC GTC ATG GTC ACC AAA TTC TAC TTC CAG GAG GAC GAG TAG TAG GGA TAA AAG CTT CAGCTGGGATC CGGTACCGAT ATCAGATCTC CCGGGGCGGC CGCGATCTGG TTCTATAGTG TCACCTAAAT CGTATGTGTA TGATACATAA GGTTATGTAT TAATTGTAGC CGCGTTCTAA CGACAATATG TCCATATGGT GCACTCTCAG TACAATCTGC TCTGATGCCG CATAGTTAAG CCAGCCCCGA CACCCGCCAA CACCCGCTGA CGCGCCCTGA CGGGCTTGTC TGCTCCCGGC ATCCGCTTAC AGACAAGCTG TGACCGTCTC CGGGAGCTGC ATGTGTCAGA GGTTTTCACC GTCATCACCG AAACGCGCGA GACGAAAGGG CCTCGTGATA CGCCTATTTT TATAGGTTAA TGTCATGATA ATAATGGTTT CTTAGACGTC AGGTGGCACT TTTCGGGGAA ATGTGCGCGG AACCCCTATT TGTTTATTTT TCTAAATACA TTCAAATATG TATCCGCTCA TGAGACAATA ACCCTGATAA ATGCTTCAAT AATATTGAAA AAGGAAGAGT ATGAGTATTC AACATTTCCG TGTCGCCCTT ATTCCCTTTT TTGCGGCATT TTGCCTTCCT GTTTTTGCTC ACCCAGAAAC GCTGGTGAAA GTAAAAGATG CTGAAGATCA GTTGGGTGCA CGAGTGGGTT

ACATCGAACT GGATCTCAAC AGCGGTAAGA TCCTTGAGAG TTTTCGCCCC
GAAGAACGTT TTCCAATGAT GAGCACTTTT AAAGTTCTGC TATGTGGCGC
GGTATTATCC CGTATTGACG CCGGGCAAGA GCAACTCGGT CGCCGCATAC
ACTATTCTCA GAATGACTTG GTTGAGTACT CACCAGTCAC AGAAAAGCAT
CTTACGGATG GCATGACAGT AAGAGAATTA TGCAGTGCTG CCATAACCAT
GAGTGATAAC ACTGCGGCCA ACTTACTTCT GACAACGATC GGAGGACCGA
AGGAGCTAAC CGCTTTTTTG CACAACATGG GGGATCATGT AACTCGCCTT
GATCGTTGGG AACCGGAGCT GAATGAAGCC ATACCAAACG ACGAGCGTGA
CACCACGATG CCTGTAGCAA TGGCAACAAC GTTGCGCAAA CTATTAACTG
GCGAACTACT TACTCTAGCT TCCCGGCAAC AATTAATAGA CTGGATGGAG
GCGGATAAAG TTGCAGGACC ACTTCTGCGC TCGGCCCTTC CGGCTGGCTG
GTTTATTGCT GATAAATCTG GAGCCGGTGA GCGTGGGTCT CGCGGTATCA
TTGCAGCACT GGGGCCAGAT GGTAAGCCCT CCCGTATCGT AGTTATCTAC
ACGACGGGGA GTCAGGCAAC TATGGATGAA CGAAATAGAC AGATCGCTGA
GATAGGTGCC TCACTGATTA AGCATTGGTA ACTGTCAGAC CAAGTTTACT
CATATATACT TTAGATTGAT TTAAAACTTC ATTTTTAATT TAAAAGGATC
TAGGTGAAGA TCCTTTTTGA TAATCTCATG ACCAAAATCC CTTAACGTGA
GTTTTCGTTC CACTGAGCGT CAGACCCCGT AGAAAAGATC AAAGGATCTT
CTTGAGATCC TTTTTTTCTG CGCGTAATCT GCTGCTTGCA AACAAAAAAA
CCACCGCTAC CAGCGGTGGT TTGTTTGCCG GATCAAGAGC TACCAACTCT
TTTTCCGAAG GTAACTGGCT TCAGCAGAGC GCAGATACCA AATACTGTTC
TTCTAGTGTA GCCGTAGTTA GGCCACCACT TCAAGAACTC TGTAGCACCG
CCTACATACC TCGCTCTGCT AATCCTGTTA CCAGTGGCTG CTGCCAGTGG
CGATAAGTCG TGTCTTACCG GGTTGGACTC AAGACGATAG TTACCGGATA
AGGCGCAGCG GTCGGGCTGA ACGGGGGGTT CGTGCACACA GCCCAGCTTG
GAGCGAACGA CCTACACCGA ACTGAGATAC CTACAGCGTG AGCTATGAGA
AAGCGCCACG CTTCCCGAAG GGAGAAAGGC GGACAGGTAT CCGGTAAGCG
GCAGGGTCGG AACAGGAGAG CGCACGAGGG AGCTTCCAGG GGGAAACGCC
TGGTATCTTT ATAGTCCTGT CGGGTTTCGC CACCTCTGAC TTGAGCGTCG

ATTTTTGTGA TGCTCGTCAG GGGGGCGGAG CCTATGGAAA AACGCCAGCA
ACGCGGCCTT TTTACGGTTC CTGGCCTTTT GCTGGCCTTT TGCTCACATG
TTCTTTCCTG CGTTATCCCC TGATTCTGTG GATAACCGTA TTACCGCCTT
TGAGTGAGCT GATACCGCTC GCCGCAGCCG AACGACCGAG CGCAGCGAG
TCAGTGAGCGA GGAAGCGGAA GAGCGCCCAA TACGCAAACC GCCTCTCCCC
GCGCGTTGGC CGATTCATTA ATGCAGGTTA ACCTGGCTTA TCGAAATTAA
TACGACTCAC TATAGGGAGA CCGGCCTCGA GCAGCAAGGA GATGGCGCCC
AACAGTCCCC CGGCCACGGG GCCTGCCACC ATACCCACGC CGAAACAAGC
GCTCATGAGC CCGAAGTGGC GAGCCCGATC TTCCCCATCG GTGATGTCGG
CGATATAGGC GCCAGCAACC GCACCTGTGG CGCCGGTGAT GCCGGCCACG
ATGCGTCCGG CGTAGAGGAT CGATCCGGGC TTATCGACTG CACGGTGCAC
CAATGCTTCT GGCGTCAGGC AGCCATCGGA AGCTGTGGTA TGGCTGTGCA
GGTCGTAAAT CACTGCATAA TTCGTGTCGC TCAAGGCGCA CTCCCGTTCT
GGATAATGTT TTTTGCGCCG ACATCATAAC GGTTCTGGCA AATATTCTGA
AATGAGCTGT TGACAATTAA TCATCGGCTC GTATAATGTG TGGAATTGTG
AGCGGATAAC AATTTCACAC AGGAAACAGA ATTCCCAGCT TGGCTGCAGA
ACCATTCCAT TCGTTGATCC GGGAGTAACT CAC - 3’

A.1.4 Recombinant IL-1ra protein expression

IL-1ra+JM109 E. coli were grown at 37°C and 225 rpm in 500 mL LB broth containing 1 mg biotin (#29129, Thermo Scientific, Rockford, IL) and Ampicillin. The bacteria were considered to be in log growth phase at an OD between 0.03 and 0.05 (1 mm path length, using Nanodrop Cell Cultures setting) and were induced with 50 μL of 1 M IPTG. The cultures then shook overnight at 37°C/225 rpm. The cultures were spun down at 10,000 rpm/4°C for 20 min, and the bacterial pellets were frozen for later use.

The bacterial pellets were thawed in cell lysis buffer (10 mL/1 g bacteria; 50 mM Tris-HCl, pH 7.4, 50 mM NaCl, 5% Glycerol in water) at 4°C while stirring. 1 mL protease inhibitor cocktail (#P8465, Sigma-Aldrich, St. Louis, MO) was added per 4 g bacteria. When the pellet was fully thawed, lysozyme was added to a final concentration of 1 mg/mL

and was stirred for 20 min. Sodium deoxycholate (DOC) was added to the cell lysate at a final concentration of 1 mg/mL and the mixture was stirred for 5 min. 2000 U DNAseI per gram bacteria was added and the lysate was stirred for 30 min at 4°C. The bacterial lysate was centrifuged for 30 min at 10,000 rpm/4°C. The supernatant was then filtered through a 0.45 μm sterile filter, and sodium azide was added at a final concentration of 0.01%. The lysate was stored at 4°C overnight for purification the next day.

Avidin resin (#53146, UltraLink Immobilized Monomeric Avidin Resin, Pierce, Rockford, IL) was packed in a column to purify the biotinylated IL-1ra protein. The pump system (BioRad Econo Gradient Pump, BioRad, Hercules, CA) was prepared by running PBS through for 5 min at 2 mL/min. The column was then attached to the system and more PBS was run through for 10 min at 1.5 mL/min. Elution buffer (50 mg d-biotin (#29129, Thermo Scientific, Rockford, IL) in 100 mL PBS) was run through the column at 1.5 mL/min for 10 min. Regeneration buffer (750 mg glycine in 100 mL dI H2O, pH 2.8) was run through the column for 15 min at 1.5 mL/min. PBS was run through at 2 mL/min for 10 min. Bacterial lysate was applied to the column at 0.5 mL/min for 2 h. PBS wash for 30 min at 2.5 mL/min. Elution buffer applied at 1.2 mL/min for 18 min (equivalent of 9 fractions of 2 min) and eluate was collected. Regeneration buffer was run through the column for 10 min at 1.5 mL/min. PBS+0.01% azide was run through the column for 15 min at 2 mL/min. The column was wrapped on both ends with parafilm and stored at 4°C until further use. For multiple runs in the same day, after the regeneration buffer step, PBS was run through the column for 15 min at 2 mL/min, and protein solution was then applied to the column again.

To remove the excess biotin, the protein eluate was centrifuged in filter conicals (10 kDa MWCO) (Amicon Ultra-15, Millipore, Billerica, MA) at 3,750 x rpm for 20 min. Cold PBS was added to the filtrate and the conicals were spun again. This was repeated twice. The filtrate was removed and run through an endotoxin removal column (EndoTrap Red, Hyglos, Regensburg, Germany) and the eluate was then nanodropped and stored at -80°C until use.

Alternatively, streptavidin resin (#53117, UltraLink Immobilized Streptavidin Plus,

Pierce, Rockford, IL) was packed into the column and used in the following manner: The pump system was prepared by running PBS-/- through for 10 min at 2 mL/min. The column was then attached to the system and flushed for another 10 min at 2 mL/min. Bacterial lysate was then applied to the column at 0.5 mL/min. The column was then rinsed for 30 min with 0.01% Triton-X-100 in PBS at 2.5 mL/min, followed by 30 min of PBS alone at 2.5 mL/min. The attached protein was then eluted using 8 M Guanadine-HCl, pH 1.5 and the eluate was immediately put into a dialysis cassette and immersed in fresh PBS to dialyze the denaturing guanidine out of the solution. Buffer was changed 3 times over 18 h of dialysis (1 h, 2 h, 12 h).

The protein was analyzed by Western blot and Coomassie gel (Fig. A.3).

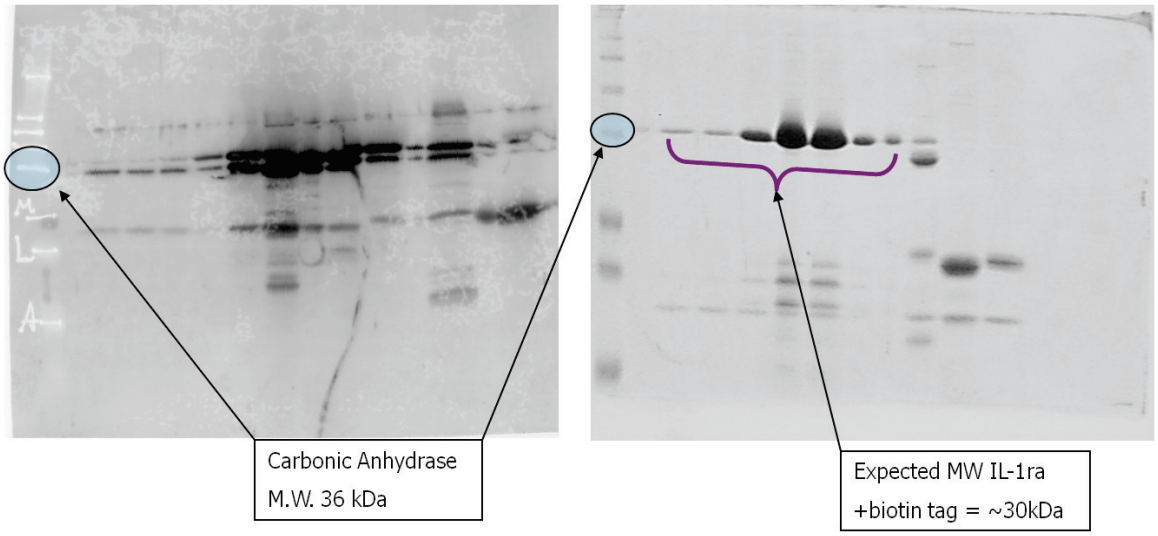

Figure A.3: Western Blot and Coomassie Stain for recombinantly produced IL-1ra

We verified that the biotin tag could be cleaved without affecting the protein by digesting it with factor Xa. The digestion produced the expected size of protein bands without showing signs of further protein cleavage (Figure A.4).

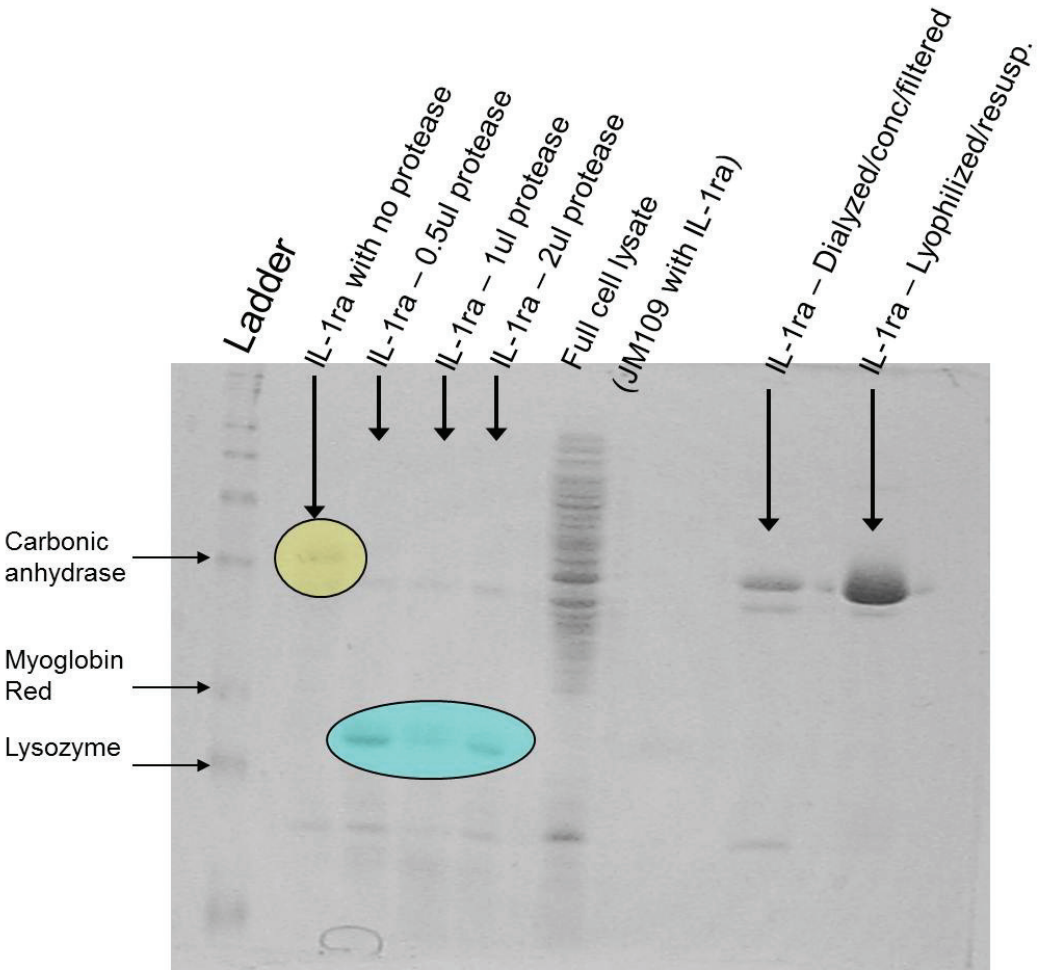

Figure A.4: IL-1ra maintains its expected weight after Xa-mediated cleavage of the biotin tag

The biotinylated IL-1ra was assessed for bioactivity by SPR. A gold-coated coverslip was incubated overnight in hexadecanethiol to set up a hydrophobic self-assembled monolayer. The coverslip was rinsed in 100% ethanol and was equilibrated in PBS before using in the SPR. The SPR run was injected as follows:

1. Protein A (50 μg/mL) at 5 μL/min
2. IL-1RI-Fc (5 μg/mL) at 5 μL/min
3. Lysozyme (25 μg/mL) at 20 μL/min

4. IL-1ra (25 μg/mL) at 20 μL/min

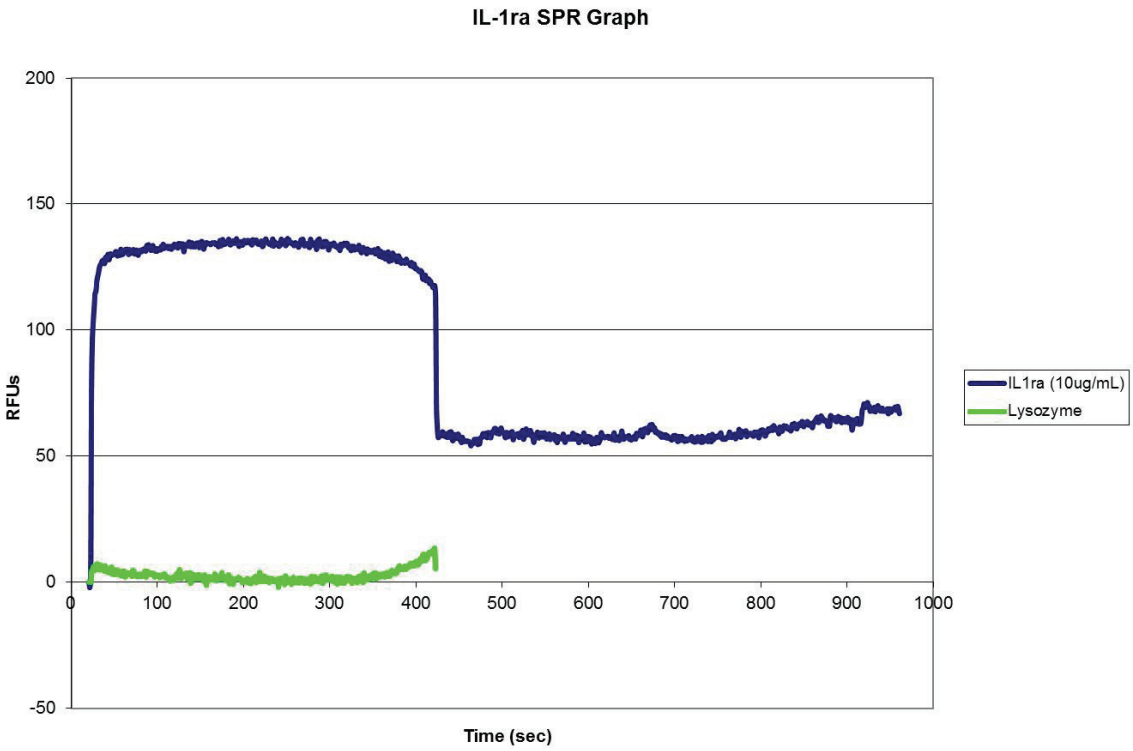

Figure A.5: SPR analysis of bioactivity of recombinant IL-1ra

A.1.5 Endotoxin Removal

The following endotoxin removal protocols were used in attempts to reduce endotoxin contamination of our recombinant IL-1ra:

1. Running protein solution through EndoTrap Red columns (Hyglos)

2. On-column washes with 0.1% Triton-X-100 (50 column volumes, about 250 mL) followed by overnight dialysis against 25 mM Tris-HCl/150 mM NaCl, pH 7.8, followed by Endotoxin Removal Solution (1:10) (Sigma).

3. Denaturation and refolding of protein (8 M guanidine HCl, pH 2.8 or 8 M guanidine HCl, pH 1.5)

4. Washing the protein purification column with Triton-X-114 followed by running the eluted protein throug Endotrap Red columns (p. 62 of Book #4)

5. Running protein solution through Endotoxin Removal columns (Pierce) (p. 87, book #4)

A.2 Results

All endotoxin removal protocols were unsuccessful at reducing endotoxin levels in our recombinant protein without detrimentally affecting the protein itself (Fig. A.#). The only protocol that was able to significantly reduce endotoxin was elution by 8 M guanidine HCl, pH 1.5; however, this elution also denatured the protein irreversibly, thereby eliminating its detection by antibody probing (Fig. A.#). Even using 8 M guanidine HCl at a higher pH (2.8) was unable to significantly affect the levels of endotoxin bound to IL-1ra. The Pierce Endotoxin Removal columns removed both the protein and the endotoxin simultaneously (Fig. A.#).

A.3 Discussion and Conclusions

We successfully cloned the IL-1ra cDNA into a biotinylation vector for expression in E. coli. We sequenced the new construct and verified its accuracy with the predicted sequence. Biotinylated IL-1ra maintained its ability to bind to the IL-1R, as shown by SPR analysis (Fig. A.5). However, we were unable to reduce endotoxin contamination to acceptable levels, preventing us from using this protein in further studies. Endotoxin contamination activates pattern recognition receptors, called TLRs, on inflammatory cells and results in upregulation of inflammatory signaling cascades, which would be counterproductive to our goal of reducing inflammatory signaling in immune cells. The biotinylation tag itself may be causing the endotoxin "stickiness" because of the size of the tag sequence itself (approximately 13 kDa). The biotin tag was initially added to aid in efficienct purification of the protein. Alternative approaches include adding IL-1ra into a His-6 construct or using the original untagged protein and purifying it by affinity purification. These methods would need to be tested for their ability to improve endotoxin removal using the previously attempted methods.

APPENDIX B

CHRONIC INFLAMMATORY RESPONSES TO MICROGEL-BASED IMPLANT COATINGS

Bridges et al. JBMR-A 2010[60]

Amanda W. Bridges,[1,2] Rachel E. Whitmire,[1,2] Neetu Singh,[3] Kellie L. Templeman,[1,4] Julia E. Babensee,[1,2] L. Andrew Lyon,[1,3] and Andrés J. García[1,4]*

[1]Petit Institute for Bioengineering and Bioscience, Georgia Institute of Technology, Atlanta, Georgia 30332-0363, USA

[2]Coulter Department of Biomedical Engineering, Georgia Institute of Technology, Atlanta, Georgia 30332-0363, USA

[3]School of Chemistry and Biochemistry, Georgia Institute of Technology, Atlanta, Georgia 30332-0363, USA

[4]Woodruff School of Mechanical Engineering, Georgia Institute of Technology, Atlanta, Georgia 30332-0363, USA

* Corresponding author: Andrés J. García, Petit Institute for Bioengineering and Bioscience, 315 Ferst Drive, 2314 IBB, Atlanta, GA 30332-0363, USA, Tel.: (404) 894-9384, Fax: (404) 385-1397, Email: andres.garcia@me.gatech.edu

ABSTRACT: Inflammatory responses to implanted biomedical devices elicit a foreign body fibrotic reaction that limits device integration and performance in various biomedical applications. We examined chronic inflammatory responses to microgel conformal coatings consisting of thin films of poly(N-isopropylacrylamide) hydrogel microparticles cross-linked with poly(ethylene glycol) diacrylate deposited on poly(ethylene terephthalate) (PET). Unmodified and microgel-coated PET disks were implanted subcutaneously in rats for 4 weeks and explants were analyzed by histology and immunohistochemistry. Microgel coatings reduced chronic inflammation and resulted in a more mature/organized fibrous capsule. Microgel-coated samples exhibited 22% thinner fibrous capsules that contained 40% fewer

cells compared to unmodified PET disks. Furthermore, microgel-coated samples contained significantly higher levels of macrophages (40%) than unmodified PET controls. These results demonstrate that microgel coatings reduce chronic inflammation to implanted biomaterials.

Keywords: foreign body response, macrophage, hydrogel, polyethylene terephthalate, fibrous capsule

INTRODUCTION: Biomaterials and implantable devices elicit a host foreign body response that often impairs wound healing and tissue remodeling.[1] Implantation of these synthetic materials triggers dynamic, multi-component responses involving protein adsorption, leukocyte recruitment, adhesion and activation, cytokine expression/release, macrophage fusion into multi-nucleated foreign body giant cells (FBGCs), tissue remodeling and fibrous encapsulation of the implant.[2] These inflammatory responses significantly interfere with the biological performance of these devices, often resulting in inadequate performance and failures that may require secondary interventions. Examples of chronic inflammatory responses to biomedical devices include thrombogenic responses on vascular grafts,[3,4] degradation and stress cracking of pacemaker leads,[5,6] tissue fibrosis surrounding mammary prostheses,[7] reactive gliosis around neural probes,[8] degradation in glucose biosensor function,[9] and generation of wear debris around orthopedic joint prostheses.[10]

Fibrous capsule formation around the implant and the presence of macrophages and FBGCs at the tissue-material interface are the hallmarks of a chronic inflammatory response. The $\alpha M\beta 2$ integrin and macrophage mannose receptor have been identified as critical components for FBGC formation.[11] Although the molecular mechanisms leading to macrophage fusion have not been fully elucidated, soluble molecules, signal transducers, and numerous receptors are likely involved.[2] FBGCs have been implicated in biodegradation of polymeric implants through surface oxidation and enzymatic degradation.[12,13] Multinucleated giant cells have been observed in chronically inflamed tissues induced by a foreign stimulus, yet the physiological significance and precise role of FBGCs at the tissue-material interface remains poorly understood. The cell-cell interactions of the foreign body response are quite complex, and the overall biological response to implanted materials is likely a

composite of macrophages, fibroblasts, lymphocytes, and FBGCs. Further elucidation of the molecular events governing inflammation will aid in the development of implantable materials with more appropriate host responses.

Significant research efforts have focused on modifying material properties to generate implants that appropriately integrate with the host tissue while eliciting minimal undesirable effects. A common approach to reduce inflammatory responses is the use of non-fouling (protein adsorption-resistant) polymeric coatings, which have been developed in various forms including polymer brushes and thin or bulk hydrogels. Although many of these methods have been effective when tested in vitro, these coatings usually exhibit high levels of adherent leukocytes, persistent inflammation, and fibrous encapsulation of the implant.[14−16] Long-term tissue fibrosis is particularly limiting for interactive implants such as biosensors, biomedical leads and electrodes, encapsulated cells, and drug delivery systems, because it impedes analyte transport and exchange of nutrients and cellular byproducts with the surrounding medium.[9,17−21] By controlling capsule thickness, implant coatings may have the ability to maintain an open exchange of key biomolecules and extend the in vivo lifetime of these constructs.

We recently engineered a hydrogel-based coating composed of pNIPAm-co-AA microgel particles cross-linked with PEG diacrylate tethered onto a poly(ethylene terephthalate) (PET) substrate.[22] PET was chosen as the base material because this polymer is used in many biomedical devices including sutures, vascular grafts, sewing cuffs for heart valves, and components for percutaneous access devices. PET elicits acute and chronic inflammatory responses, characterized by leukocyte adhesion and fibrous encapsulation.[23,24] We have shown that these microgel coatings modulate events associated with acute inflammation (i.e. protein adsorption and cell adhesion) and significantly reduce leukocyte recruitment and cytokine expression in vivo at early time points.[22] In the present study, we evaluated chronic host responses to these microgel coatings. We demonstrate that these conformal microgel coatings reduce chronic inflammation to implanted materials.

MATERIALS AND METHODS

Sample preparation

Thin sheets of poly(ethylene terephthalate) (AIN Plastics/ThyssenKrupp Materials NA, Madison Heights, MI) were cut into disks (8 mm diameter) using a sterile biopsy punch (Miltex Inc., York, PA) and extensively rinsed in 70% ethanol to remove contaminants introduced during the manufacturing process. Microgel particles were synthesized with 10 mol% acrylic acid as a co-monomer to incorporate functional groups for future modification. pNIPAm-co-AA microgel particles (100 mM total monomer concentration) were synthesized with 2 mol% PEG diacrylate (M.W. 575) by a free radical precipitation polymerization method.[25] Particle composition and size (hydrodynamic radius 334 ± 30 nm) were confirmed by NMR and dynamic light scattering, respectively. Microgel particles were deposited on both sides of PET disks using a spin coating and photo-crosslinking process as previously described.[22,25] AFM and XPS analyses demonstrated uniform conformal microgel coatings, in excellent agreement with previous analyses.[22,25] Unmodified PET disks were used as controls.

After surface functionalization, all samples were rinsed in 70% ethanol on a rocker plate for 4 days, changing the solution daily to remove endotoxin contaminants, and were stored in 70% ethanol until use. Samples contained 10-fold lower levels of endotoxin than the United States Food and Drug Administrations recommended 0.5 EU/mL, as determined by the LAL chromogenic assay (Cambrex, East Rutherford, NJ). Prior to use, samples were rinsed three times in sterile phosphate buffered saline (PBS) and allowed to rehydrate in PBS for at least 1 hour.

Subcutaneous implantation

NIH guidelines for the care and use of laboratory animals (NIH publication #85-23 Rev. 1985) have been observed. Samples (unmodified PET, microgel-coated PET; n = 8 samples/group) were implanted subcutaneously following IACUC-approved procedures to evaluate the chronic phase foreign body response. Male 5 to 6 wk old Wistar rats (Charles River Laboratories, Wilmington, MA) were anesthetized by isofluorane. A single 1-cm incision was made on the dorsum proximal to the spine, and a subcutaneous pocket laterally spanning the dorsum was created. Sterile samples (two per subject, one on either side of the spine) were implanted, and the incision was closed using sterile wound clips. After four

weeks, rats were sacrificed using a CO_2 chamber and samples were explanted, rinsed in sterile PBS, and fixed in formalin. Samples were carefully explanted with the surrounding tissue intact to avoid disrupting the cell-material interface. Explants were bisected in order to avoid edge effects and to standardize the sectioning location for analysis, and they were paraffin-embedded for histological processing.

Histological staining of explants

Histological sections (5 μm thick) were stained for various markers. A Verhoeff-van Gieson kit (Accustain®Elastic Stain kit from Sigma-Aldrich, St. Louis, MO) was used to stain collagen (pink), elastin fibers (black), and nuclei (dark blue). Sixteen total fields per sample (eight fields on both the muscle and skin sides of the implant) were acquired using a high magnification 60X Plan Apo Nikon objective (1.40 NA). ImagePro software (Media Cybernetics, Silver Spring, MD) was used to quantify fibrous capsule thickness.

Sections were also stained using immunohistochemical methods to determine the inflammatory cellular profile at the cell-material interface. Following proteolytic antigen retrieval with pronase (1 mg/mL solution for 10 min), sections were incubated in a mouse monoclonal antibody against the CD68 antigen of macrophages (clone ED1, AbD Serotec, Raleigh, NC), a biotinylated secondary antibody, and an avidin-linked alkaline phosphatase-based developing reagent (Vectastain®ABC-AP Kit, Vector Labs, Burlingame, CA), and counterstained with hematoxylin. Control sections (secondary antibody-only controls and tissue-specific controls) confirmed specificity of the primary antibody for this marker. Sixteen total fields per sample (eight fields on both the muscle and skin sides of the implant) were acquired using a high magnification 60X Plan Apo Nikon objective (1.40 NA). Images were blindly scored for total nuclei, CD68+ cells with one nucleus (macrophages), and CD68+ multi-nucleated cells (foreign body giant cells).

Statistical analysis

Data are presented as mean $\pm$ standard error. Statistical analysis (t-tests, 95% confidence level considered significant) was performed by ANOVA using Systat 11.0 (Systat Software Inc., San Jose, CA).

RESULTS

Fibrous capsule formation surrounding implants

PET disks were functionalized with p(NIPAM-co-AAc-co-PEGDA) microgel particles via a spin coating and photo-crosslinking method to generate uniform, conformal coatings. XPS and AFM analyses confirmed the chemical composition and the uniformity of microgel coating, in excellent agreement with previous studies.[22] Tissue responses to these materials were evaluated using an established subcutaneous rat model to determine the extent of chronic inflammation.[1] Unmodified PET and microgel-coated PET disks were implanted for 4 weeks. Explants were processed histologically, and sections were analyzed for fibrous capsule development using a Verhoeff van Gieson kit to stain collagen and elastin fibers; all nuclei were counterstained for reference (Figure 1). The capsule was defined as the dense tissue adjacent to the implant, and image analysis of high magnification images was used to measure capsule thickness as the perpendicular distance starting at the capsule-implant interface and moving outward. Measurement of fibrous capsule thickness following subcutaneous implantation is a standard measure of chronic inflammation to synthetic materials.[1]

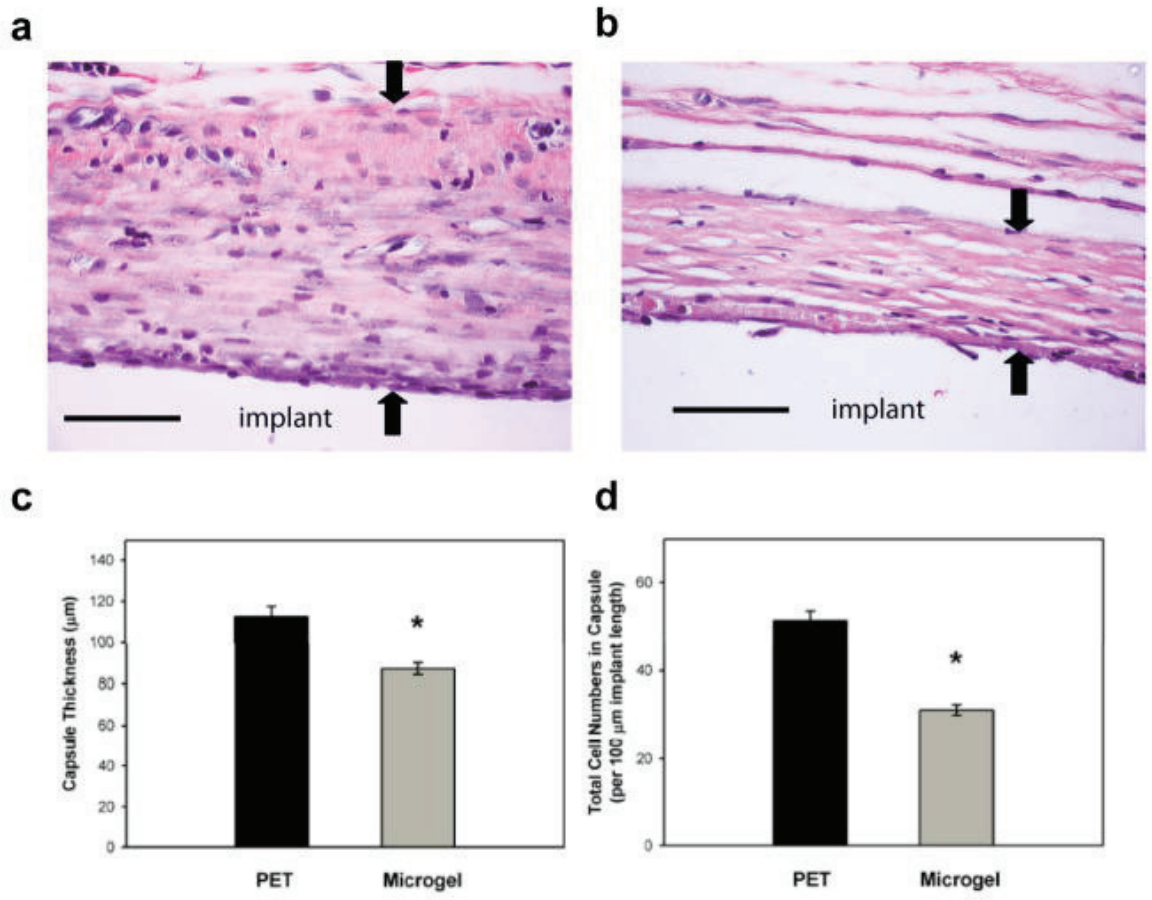

Figure B.1: Figure 1. Microgel coatings reduce chronic inflammation associated with materials implanted subcutaneously in the rat dorsum for 4 wk. Explants were evaluated for fibrous encapsulation by staining collagen (pink), elastin (black), and nuclei (black). Representative images for unmodified PET (a) and microgel-coated PET (b) disks, and the original implant location is designated. Black arrows indicate capsule measurements. Microgel coatings reduced fibrous capsule thickness by 22% compared to unmodified PET controls as quantified in (c), * $p < 0.04$. The density of capsule-associated cells was also significantly reduced in microgel-coated samples (* $p < 5.6 \times 10^{-3}$) compared to unmodified PET controls as quantified in (d). Data is represented as the average value ± standard error of the mean using n = 4-7 samples per treatment group. Scale bar is 50 μm.

Unmodified PET controls exhibited a tissue reaction characteristic of chronic inflammation with a thick collagenous capsule containing high numbers of cells (Figure 1a). Microgel-coated samples exhibited thinner and more compact capsules with more organized collagen fibrils (Figure 1b). Image analysis demonstrated significantly thinner capsules (22%) for microgel-coated PET compared to unmodified PET controls ($p<0.04$, Figure 1c). The average capsule thickness was 112.3 ± 5.1 and 87.3 ± 2.9 μm for PET controls and microgel-coated samples, respectively.

The density of total cells present in the tissue capsules was scored using counterstained nuclei, and sections were quantified in 100 μm increments along the implant interface (Figure 1d). Microgel-coated samples contained approximately 40% fewer capsule-associated cells than their unmodified PET control counterparts ($p<0.01$). The average cell density was 51.2 ± 2.2 and 31.1 ± 1.2 cells per 100 μm length of implant for PET controls and microgel-coated samples, respectively. These results demonstrate that microgel coatings reduce the thickness and cell density of tissue capsules surrounding implanted biomaterials.

Inflammatory cell profile at the implant interface Explant sections were processed to evaluate the composition of cells at the implant-tissue interface (Figure 2). Immunohistochemistry was used stain for the CD68 antigen, a marker of monocytes and tissue macrophages, and all nuclei were counterstained for reference. Images were scored for total CD68+ cells containing one nucleus (macrophages) and CD68+ cells fused to form multinucleated FBGCs.

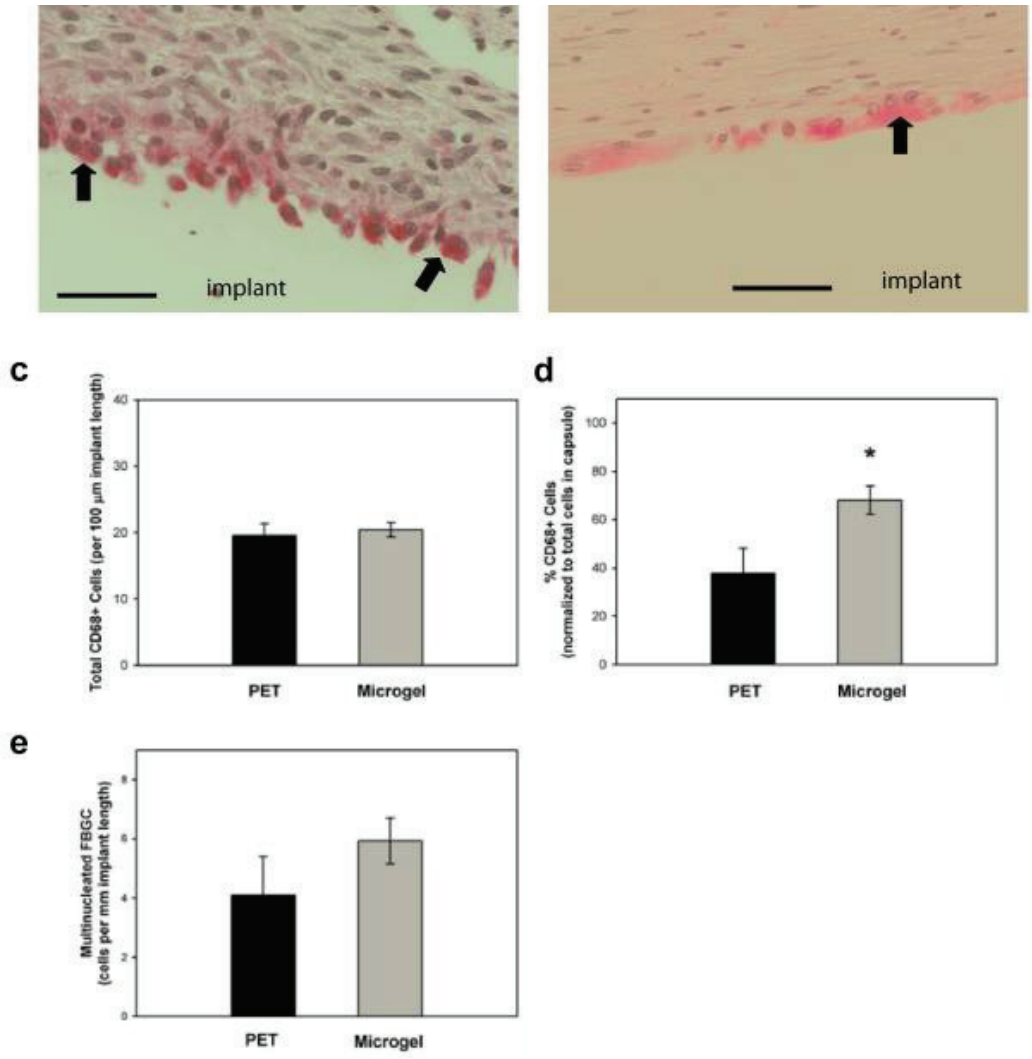

Figure B.2: Figure 2. Inflammatory cell profiles associated with biomaterials implanted subcutaneously in the rat dorsum for 4 wk. Explant sections were stained via immunohistochemical methods for macrophage marker CD68 (pink) and counter-stained with hematoxylin to label nuclei (blue). Representative images for unmodified PET (a) and microgel-coated PET (b) disks, and the original implant location is designated. Total CD68+ cells were quantified in (c), but no statistical differences were found between treatment groups. (d) When normalized to total capsule-associated cells (from Fig. 1d), unmodified PET controls contained proportionately fewer CD68+ cells than microgel-coated PET (* $p < 0.02$). Multinucleated CD68+ cells (FBGCs) at the cell-implant interface were also quantified (e), but no statistical differences were found between treatment groups. FBGCs are designated by black arrows. Data is represented as the average value $\pm$ standard error of the mean using n = 47 samples per treatment group. Scale bar is 50 μm.

High magnification images of unmodified PET controls (Figure 2a) and microgel-coated disks (Figure 2b) revealed that CD68 staining was localized to the capsule, primarily along the capsule-implant interface. All implanted samples, regardless of coating, contained similar levels of CD68+ cells as quantified in Figure 2c (no differences between groups). The average number was 19.5 ± 1.8 and 20.4 ± 1.1 CD68+ cells per 100 μm of implant length for PET controls and microgel-coated samples, respectively. CD68+ cell counts were then normalized to total cells in the fibrous capsule (as quantified in Figure 1d) to determine the relative numbers of macrophages in the capsule. Microgel-coated samples contained significantly higher relative levels of macrophages than unmodified PET controls (Figure 2d, $p<0.02$). The average values were 37.8 ± 10.4 and 68.1 ± 5.8% CD68+ cells for PET controls and microgel-coated samples, respectively. We note that this antibody can potentially stain CD68 antigens in both adipose tissue[26] and fibroblasts,[27] the latter of which are also localized in the fibrous capsule and participate in collagen deposition.

Sections were also scored for multi-nucleated FBGC, designated by black arrows (Figure 2). Few samples contained extensive development of multi-nucleated FBGC. The average values were 4.1 ± 1.3 and 5.9 ± 0.8 FBGCs per mm of implant length for PET controls and microgel-coated samples, respectively. Numbers of FBGC per sample ranged from 1.4-11.1 and 3.0-11.8 cells/mm implant length for PET controls and microgel-coated disks, respectively. No statistical differences were found between groups.

DISCUSSION

We have engineered a hydrogel-based polymeric coating composed of PEG-crosslinked pNIPAm-co-AA microparticles, which are applied to PET substrates using a spin coating and photo-crosslinking method to generate a conformal monolayer.[25] This coating strategy offers many advantages over traditional surface modification methods, including precise control over particle synthesis, the ability to generate complex architectures including mosaic coatings containing variations in particle composition or spatial arrangement, and deposition onto biomedically-relevant materials. We previously demonstrated these coatings reduce protein adsorption and cell adhesion.[25,28] In addition, these microgel coatings reduce leukocyte adhesion and activation, as well as expression of pro-inflammatory cytokines, to

biomedical polymer implants in vivo at acute time points.[22] The results of the present study demonstrate that the microgel coatings also modulate chronic inflammatory events, such as reductions in fibrous capsule thickness and cell density within the capsule.

Microgel coatings reduced chronic inflammation compared to uncoated PET controls as determined by the organization and thickness of the tissue capsule. The more compact and organized structure of the fibrous capsule associated with microgel-coated samples suggests that these coatings lead to faster resolution of the tissue reaction and more mature and thinner capsules. This reduced chronic inflammation is likely related to the reduced monocyte/macrophage adhesion and pro-inflammatory cytokine expression observed at acute time points.[22] Furthermore, tissue associated with microgel-coated samples contained less total cells but proportionately more macrophages than unmodified PET controls. The reduction in total number of cells is consistent with a reduced chronic inflammatory response for microgel-coated samples. The relevance of the relative increase in monocytes/macrophages for the microgel-coated implants compared to the PET controls is not clear at this point. An intriguing possibility is that microgel coatings modulate macrophage profiles towards an "alternatively activated"/anti-inflammatory phenotype[29] that results in reduced chronic inflammation and a faster resolution of the tissue response. Further studies are necessary to characterize macrophage phenotypes and cytokines associated with these biomaterials. Moreover, it will be important to conduct more extensive studies in order to determine inflammatory responses at longer, clinically-relevant implantation times as well as the in vivo stability of these coatings. Previous efforts have focused on hydrogel coatings that exhibit in vitro resistance to protein adsorption and leukocyte adhesion to reduce biomaterial-mediated related inflammation.[14,15,30–35] Although these coatings reduce biofouling in vitro, some of these materials still exhibit high levels of adherent leukocytes and continued inflammation in vivo with significant fibrous encapsulation of the implant. For instance, in vitro protein adsorption was significantly suppressed by photochemically immobilized polymer coatings on silicone rubber substrates and by polyethylene oxide-like tetraglyme coatings, yet neither treatment significantly reduced fibrous capsule thickness when implanted subcutaneously.[14,34] In contrast, other coatings, such as dihydroxypropyl

methacrylate, PEG, and phosphorylcholine-based polymers, have shown reductions in fibrous encapsulation compared to the base substrates.[30−33,35] The reductions in fibrous capsule thickness elicited by these coatings are comparable to those observed in the present study. Taken together, these studies do not reveal a clear correlation between in vitro fouling behavior and in vivo leukocyte adhesion and tissue response. However, it is possible that differences in the surface density, composition, and structure of the non-fouling polymer, material stability, and implantation time point, site and species complicate this relationship. In the present study, microgel coatings reduced fibrous capsule thickness by 22% compared to unmodified control samples. Whether such a reduction in fibrous capsule thickness translates into improved biological performance remains to be determined. Functional testing in specific applications (e.g. glucose sensors, pacing leads, neural electrodes) is required to evaluate the potential of these microgel coatings to ameliorate chronic inflammatory responses to implanted devices. Fibrous capsules on the order of 85 μm thick (as in our current study) may still pose a significant barrier to certain implanted devices or therapeutics by blocking the exchange of nutrients or impeding signal transduction to an external medium. For example, Moussy and colleagues recently demonstrated a correlation between increased collagen deposition surrounding implanted glucose sensors and decreased sensor sensitivity; natural angiogenesis failed to overcome the barrier to glucose diffusion caused by the associated fibrous capsule.[36] The present work provides the foundation for developing a microgel-based coating system incorporating various signaling agents and bioactive therapeutics within a low-fouling background. These biotherapeutic delivery systems offer several advantages over approaches relying on passive non-fouling behavior, including highly controlled presentation/release of immunomodulatory agents, control over reaction kinetics, and versatility through hybrid designs. Biomaterial-associated inflammation/fibrosis and/or implant integration could be further improved by using such complex coatings with mechanisms to deliver immunomodulatory agents, such as IL-1ra, angiostatin, or dexamethasone, which have improved biological responses to implanted materials.[15,37−40]

CONCLUSION

Using a model of chronic biomaterial-mediated inflammation, we demonstrate that surface

coatings comprised of pNIPAm-co-PEG hydrogel microparticles reduce chronic inflammation. Microgel coatings elicited thinner and more compact capsules with more organized collagen fibrils and fewer total cells within the capsule compared to uncoated PET. Our current results demonstrate that microgel particles can be applied as implant coatings to modulate inflammation and achieve more desirable chronic host responses in vivo, with the potential to extend implant performance and lifetime.

ACKNOWLEDGEMENTS

This work was supported by the Georgia Tech/Emory Center (GTEC) for the Engineering of Living Tissues and the Atlanta Clinical and Translational Science Institute (ACTSI) and the National Institutes of Health (R01-EB004496). A.W.B. and R.E.W. were supported by National Science Foundation Graduate Fellowships.

REFERENCES

1. Anderson JM. Biological responses to materials. Annu Rev Mater Res. 2001;31:81110.

2. Anderson JM, Rodriguez A, Chang DT. Foreign body reaction to biomaterials. Semin Immunol. 2008;20(2):86100.

3. Gorbet MB, Sefton MV. Biomaterial-associated thrombosis: roles of coagulation factors, complement, platelets and leukocytes. Biomaterials. 2004;25(26):5681703.

4. Kottke-Marchant K, Anderson JM, Umemura Y, Marchant RE. Effect of albumin coating on the in vitro blood compatibility of Dacron arterial prostheses. Biomaterials. 1989;10(3):14755.

5. Zhao Q, Topham N, Anderson JM, Hiltner A, Lodoen G, Payet CR. Foreign-body giant cells and polyurethane biostability: in vivo correlation of cell adhesion and surface cracking. J Biomed Mater Res. 1991;25(2):17783.

6. Sutherland K, Mahoney JR, 2nd, Coury AJ, Eaton JW. Degradation of biomaterials by phagocyte-derived oxidants. J Clin Invest. 1993;92(5):23607.

7. Destouet JM, Monsees BS, Oser RF, Nemecek JR, Young VL, Pilgram TK. Screening mammography in 350 women with breast implants: prevalence and findings of implant complications. AJR Am J Roentgenol. 1992;159(5):9738. discussion 97981.

8. McGraw J, Hiebert GW, Steeves JD. Modulating astrogliosis after neurotrauma. J Neurosci Res. 2001;63(2):10915.

9. Wisniewski N, Moussy F, Reichert WM. Characterization of implantable biosensor membrane biofouling. Fresenius Journal of Analytical Chemistry. 2000;366(67):611621.

10. Voronov I, Santerre JP, Hinek A, Callahan JW, Sandhu J, Boynton EL. Macrophage phagocytosis of polyethylene particulate in vitro. J Biomed Mater Res. 1998;39(1):4051.

11. McNally AK, Anderson JM. Beta1 and beta2 integrins mediate adhesion during macrophage fusion and multinucleated foreign body giant cell formation. Am J Pathol. 2002;160(2):62130.

12. Henson PM. The immunologic release of constituents from neutrophil leukocytes. I. The role of antibody and complement on nonphagocytosable surfaces or phagocytosable particles. J Immunol. 1971;107(6):153546.

13. Mathur AB, Collier TO, Kao WJ, Wiggins M, Schubert MA, Hiltner A, Anderson JM. In vivo biocompatibility and biostability of modified polyurethanes. J Biomed Mater Res. 1997;36(2):24657.

14. Shen M, Martinson L, Wagner MS, Castner DG, Ratner BD, Horbett TA. PEO-like plasma polymerized tetraglyme surface interactions with leukocytes and proteins: in vitro and in vivo studies. J Biomater Sci Polym Ed. 2002;13(4):36790.

15. Norton LW, Koschwanez HE, Wisniewski NA, Klitzman B, Reichert WM. Vascular endothelial growth factor and dexamethasone release from nonfouling sensor coatings affect the foreign body response. J Biomed Mater Res A. 2007;81(4):85869.

16. van Bilsen PH, Popa ER, Brouwer LA, Vincent J, Taylor CE, de Leij LF, Hendriks M, van Luyn MJ. Ongoing foreign body reaction to subcutaneous implanted (heparin)

modified Dacron in rats. J Biomed Mater Res A. 2004;68(3):4237.

17. Gilligan BJ, Shults MC, Rhodes RK, Updike SJ. Evaluation of a subcutaneous glucose sensor out to 3 months in a dog model. Diabetes Care. 1994;17(8):8827.

18. Biran R, Martin DC, Tresco PA. Neuronal cell loss accompanies the brain tissue response to chronically implanted silicon microelectrode arrays. Exp Neurol. 2005;195(1):11526.

19. Zekorn TD, Horcher A, Mellert J, Siebers U, Altug T, Emre A, Hahn HJ, Federlin K. Biocompatibility and immunology in the encapsulation of islets of Langerhans (bioartificial pancreas) Int J Artif Organs. 1996;19(4):2517.

20. Peek LJ, Middaugh CR, Berkland C. Nanotechnology in vaccine delivery. Adv Drug Deliv Rev. 2008;60(8):91528.

21. Anderson JM. In-vivo biocompatibility of implantable delivery systems and biomaterials. European Journal of Pharmaceutics and Biopharmaceutics. 1994;40(1):18.

22. Bridges AW, Singh N, Burns KL, Babensee JE, Andrew Lyon L, Garcia AJ. Reduced acute inflammatory responses to microgel conformal coatings. Biomaterials. 2008;29(35):460515.

23. Tang L, Eaton JW. Fibrin(ogen) mediates acute inflammatory responses to biomaterials. J Exp Med. 1993;178(6):214756.

24. van der Giessen WJ, Lincoff AM, Schwartz RS, van Beusekom HM, Serruys PW, Holmes DR, Jr, Ellis SG, Topol EJ. Marked inflammatory sequelae to implantation of biodegradable and nonbiodegradable polymers in porcine coronary arteries. Circulation. 1996;94(7):16907.

25. Singh N, Bridges AW, Garcia AJ, Lyon LA. Covalent tethering of functional microgel films onto poly(ethylene terephthalate) surfaces. Biomacromolecules. 2007;8(10):32715.

26. Khazen W, MBika JP, Tomkiewicz C, Benelli C, Chany C, Achour A, Forest C. Expression of macrophage-selective markers in human and rodent adipocytes. FEBS Lett. 2005;579(25):56314.

27. Kunz-Schughart LA, Weber A, Rehli M, Gottfried E, Brockhoff G, Krause SW, Andreesen R, Kreutz M. The classical macrophage marker CD68 is strongly expressed in primary human fibroblasts. Verh Dtsch Ges Pathol. 2003;87:21523.

28. Nolan CM, Reyes CD, Debord JD, Garcia AJ, Lyon LA. Phase transition behavior, protein adsorption, and cell adhesion resistance of poly(ethylene glycol) cross-linked microgel particles. Biomacromolecules. 2005;6(4):20329.

29. Mills CD, Kincaid K, Alt JM, Heilman MJ, Hill AM. M-1/M-2 macrophages and the Th1/Th2 paradigm. J Immunol. 2000;164(12):616673. [PubMed]

30. Moro T, Takatori Y, Ishihara K, Konno T, Takigawa Y, Matsushita T, Chung UI, Nakamura K, Kawaguchi H. Surface grafting of artificial joints with a biocompatible polymer for preventing periprosthetic osteolysis. Nat Mater. 2004;3(11):82936.

31. Wang C, Yu B, Knudsen B, Harmon J, Moussy F, Moussy Y. Synthesis and performance of novel hydrogels coatings for implantable glucose sensors. Biomacromolecules. 2008;9(2):5617.

32. Quinn CP, Pathak CP, Heller A, Hubbell JA. Photo-crosslinked copolymers of 2-hydroxyethyl methacrylate, poly(ethylene glycol) tetra-acrylate and ethylene dimethacrylate for improving biocompatibility of biosensors. Biomaterials. 1995;16(5):38996.

33. Goreish HH, Lewis AL, Rose S, Lloyd AW. The effect of phosphorylcholine-coated materials on the inflammatory response and fibrous capsule formation: in vitro and in vivo observations. J Biomed Mater Res A. 2004;68(1):19.

34. DeFife KM, Shive MS, Hagen KM, Clapper DL, Anderson JM. Effects of photochemically immobilized polymer coatings on protein adsorption, cell adhesion, and the foreign body reaction to silicone rubber. J Biomed Mater Res. 1999;44(3):298307.

35. Hyung Park J, Bae YH. Hydrogels based on poly(ethylene oxide) and poly(tetramethylene oxide) or poly(dimethyl siloxane). III. In vivo biocompatibility and biostability. J Biomed Mater Res A. 2003;64(2):30919.

36. Dungel P, Long N, Yu B, Moussy Y, Moussy F. Study of the effects of tissue reactions on the function of implanted glucose sensors. J Biomed Mater Res A. 2008;85(3):699706.

37. Zhong Y, Bellamkonda RV. Dexamethasone-coated neural probes elicit attenuated inflammatory response and neuronal loss compared to uncoated neural probes. Brain Res. 2007;1148:1527.

38. Kim DH, Smith JT, Chilkoti A, Reichert WM. The effect of covalently immobilized rhIL-1ra-ELP fusion protein on the inflammatory profile of LPS-stimulated human monocytes. Biomaterials. 2007;28(23):336977.

39. Mantovani A, Locati M, Vecchi A, Sozzani S, Allavena P. Decoy receptors: a strategy to regulate inflammatory cytokines and chemokines. Trends Immunol. 2001;22(6):32836.

40. Chavakis T, Athanasopoulos A, Rhee JS, Orlova V, Schmidt-Woll T, Bierhaus A, May AE, Celik I, Nawroth PP, Preissner KT. Angiostatin is a novel anti-inflammatory factor by inhibiting leukocyte recruitment. Blood. 2005;105(3):103643.

APPENDIX C

CENTRIFUGAL DEPOSITION OF MICROGELS FOR RAPID ASSEMBLY OF NON-FOULING THIN FILMS

South et al. ACS Appl Mater Interfaces 2009[319].

Antoinette B. South,[a,b] Rachel E. Whitmire,[c,b] Andrés J. García,[d,b] and L. Andrew Lyon*,[a,b]

School of Chemistry & Biochemistry, Petit Institute for Bioengineering & Bioscience, Wallace H. Coulter Department of Biomedical Engineering, and Woodruff School of Mechanical Engineering, Georgia Institute of Technology, Atlanta, GA 30332

RECEIVED DATE * To whom correspondence should be addressed.

E-mail: lyon@chemistry.gatech.edu

[a]School of Chemistry & Biochemistry

[b]Petit Institute of Bioengineering and Bioscience

[c]Wallace H. Coulter Department of Biomedical Engineering

[d]Woodruff School of Mechanical Engineering

ABSTRACT Thin films assembled from microgel building blocks have been constructed using a simple, high-throughput, and reproducible centrifugation (or "active") deposition technique. When compared to a common passive adsorption method (e.g. dip-coating), microgels that are actively deposited onto a surface have smaller footprints and are more closely packed. Under both active and passive deposition conditions, the microgel footprint areas progressively decrease until a uniform monolayer film is achieved. However, under active deposition, the microgels continue to reduce in size even after a uniform monolayer has been assembled, forming a tightly packed, highly homogenous film. Taking advantage of the rapid and uniform assembly of these films, we demonstrate the use of active deposition towards the fabrication of polyelectrolyte multi-layers containing anionic microgels and a cationic linear polymer. Microgel multi-layers successfully demonstrated effective blocking

of the underlying substrate towards macrophage adhesion, which is a highly sought-after property for modulating the inflammatory response to an implanted biomaterial.

KEYWORDS Hydrogel particles, centrifugation, film interfaces, layer by layer, cellular adhesion

INTRODUCTION The construction of polymeric thin films is a subject of significant industrial importance (e.g. for drug delivery,[1] wettability control,[2] corrosion[3] or cellular adhesion inhibition[4]) and fundamental interest. Over the past few decades, a variety of fabrication techniques have been employed to form films from a variety of building blocks, and their versatility has been demonstrated. Whereas extensive research has been conducted in the use of linear polymers[5−8] and continuous hydrogel networks[9−12] as polymeric film interfaces, recent investigations into the use of solvent-swollen polymer colloids, or microgels, have illustrated the utility of colloidal gels as building blocks.[13−18] When the solvent is water, microgels are composed of a water-soluble polymer cross-linked into a contiguous network, with the diameters of the particles typically ranging from 100 nm to many microns.[19−21] When stimulus-sensitive polymers are used (such as pH sensitive[22] or thermoresponsive[23]) to form microgels, those particles can then exhibit responsive behavior by undergoing a volume phase transition as a function of that stimulus.[13] Given their growing importance in film formation, microgels have been used as building blocks in the construction of films with potential utility in drug release,[24,25] tunable microlenses,[26,27] colloidal crystals,[28−30] and non-fouling films.[31−33] These interfaces have been assembled using a variety of deposition techniques such as dip-coating,[34−40] spin-coating,[24,25,31−33,41,42] or solvent-evaporation.[16,29,30] In addition, different hierarchical structures have been accomplished by layer-by-layer assembly,[24,25,34,41] binary particle mixtures,[39] or phase-separation induced deposition.[16]

One particularly important aspect of film formation is control over the deposited material. For biomedical coatings, for example, the hydrophobicity, morphology, elasticity, and chemistry of a synthetic materials surface can have a dramatic effect on cell phenotype and behavior.[43] Furthermore, complete coverage of the underlying substrate is typically desired

in order to ensure total control of cell adhesion, spreading, and proliferation. Hydrogel-based materials can be fabricated to possess characteristics that make them suitable as a biomaterial because their volume consists mostly of water when in an aqueous environment and they are highly tunable in terms of their mechanical properties and chemical composition. Additionally, in a particulate form, microgels enable further complexity by enabling the assembly of multi-functional interfaces, due to a mixture of various types of microgels that can simultaneously assemble on the same surface, along with additional interesting morphologies. It is this ability to easily tune and adjust an interface that makes microgels an appealing material for controlling and studying how proteins, cells, and tissues interact with a synthetic interface.

In this contribution we report a film fabrication approach that employs centrifugation to assemble a microgel film in a fast, efficient, and reproducible manner. Whereas centrifugation has been used beyond the traditional use of purification, such as in the preparation of liposomes,[44] rapid patterning of cells,[45] or high-speed fabrication of photonic microfluidics,[46] to our knowledge little has been explored in using centrifugation as a polymer film deposition technique. In this work we have demonstrated for the first time the use of centrifugation to fabricate microgel-based films, and explore what effect this additional parameter or force may have on the assembly of microgel monolayers. Our initial hypothesis was that centrifugation would simply decrease the amount of time it would take to create a continuous and uniform monolayercompared to a passive process. However, upon further investigation, it was evident that using centrifugation (referred to herein as "active" deposition) to force soft particles onto a hard substrate resulted in an assembly that had smaller and more closely packed particles than what could be ultimately obtained with simple microgel adsorption ("passive" deposition). To evaluate the generality of this phenomenon, a model system consisting of two microgel particles of different sizes was studied. In addition, possible mechanisms for the observed results were briefly explored in this study. Lastly, we illustrate the techniques ability to construct rapid multi-layered polyelectrolyte layer-by-layer films for fabricating effective uniform non-fouling coatings to prevent macrophage adhesion.

MATERIALS AND METHODS

Materials. All reagents were purchased from Sigma-Aldrich unless otherwise specified. The monomer N-isopropylacrylamide (NIPAm) was recrystallized from hexanes (J.T. Baker) and dried under vacuum prior to use. The cross-linkers N,N-methylenebis(acrylamide) (BIS) and poly(ethylene glycol) diacrylate with average Mw = 575 (PEGDA575), co-monomer acrylic acid (AAc), and initiator ammonium persulfate (APS) were used as received. Buffer chemicals sodium dihydrogen phosphate monohydrate (Fisher Scientific), 2-(N-morpholino)ethanesulfonic acid (MES), sodium chloride (Mallinckrodt), and sodium hydroxide were used as received. The surface modification reagent 3-aminopropyltrimethoxysilane (APTMS, TCI America) was used as received. Covalent attachment chemicals N-hydroxysuccinimide (NHS), N-(3-dimethylaminopropyl)-N-ethylcarbodiimide hydrochloride (EDC), and hydroxylamine hydrochloride were used as received. Poly(diallyldimethylammonium chloride) high molecular weight 400,000-500,000 (PDADMAC) was used as received. Glass disks of 12-mm diameter were purchased from Bellco Glass. Absolute (200 proof) ethanol was used as received from EMD Chemicals Inc. All water used throughout this investigation was house distilled, deionized to a resistance of at least 18 Mω (Barnstead Thermolyne E-Pure system). IC-21 murine macrophage cell line was obtained from ATCC (Manassasa, VA) and cultured as directed. RPMI-1640 media was purchased from Gibco (Invitrogen Corporation, Carlsbad, CA) and/or ATCC (Manassas, VA), supplemented with 10% Fetal Bovine Serum (Invitrogen) and 1% penicillin streptomycin (Gibco) and used to culture the IC-21 cell line. 100 mm and 150 mm tissue culture polystyrene dishes (Corning Inc., Corning, NY) were used to culture cells. PBS (with and without Calcium and Magnesium) were obtained from Gibco. Versene (Gibco) was used to dissociate the cells from the dishes. 12-well plates from Corning (Corning, NY) were bought via Sigma-Aldrich (St. Louis, MO) and used for the cell culture experiments. Calcein and Ethidium homodimer were bought from Invitrogen Corporation (Carlsbad, CA) and used at final concentrations of 4 μM to stain for live and dead cells.

Microgel Synthesis. Microgels were synthesized using aqueous free radical precipitation polymerization. Microgel (1) was synthesized using a total monomer concentration of 70 mM. The molar composition consisted of 85% NIPAm, 5% BIS, and 10% AAc. Surfactant

SDS was used at a concentration of 1 mM. All of these components were dissolved in 49 mL of deionized water and filtered through Whatman #2 filter paper in a vacuum filtration system. The aqueous solution was then transferred to a three-neck round bottom flask and purged with N_2 for approximately 1 hour while the solution was heated to 70°C. The initiator APS (0.0114 g), used in a total final concentration of 1 mM, was dissolved in 1 mL of deionized water and added to initiate the polymerization. The reaction was allowed to proceed for 4 hours at 70°C under a blanket of N_2.

Microgel (2) was synthesized using a total monomer concentration of 100 mM, along with molar compositions of 88% NIPAm, 2% BIS, and 10% AAc. Surfactant SDS and initiator APS were used in concentrations of 0.17 mM and 1 mM, respectively. The remaining conditions of the synthesis were carried out in the same fashion as described for (1).

Non-fouling microgels were synthesized using a total monomer concentration of 100 mM with molar compositions of 88% NIPAm, 2% PEGDA575, and 10% AAc. Surfactant SDS and initiator APS were used in concentrations of 0.17 mM and 1 mM, respectively. The remaining conditions of the synthesis were carried out in the same fashion as described for (1).

Microgel Characterization. Dynamic light scattering (DLS) was used as previously described,[28,47] to measure the hydrodynamic radius and diffusion coefficient of synthesized particles. A Protein Solutions DynaPro equipped with a temperature controlled microsampler was used. Light scattering data was collected at an interval of 10 seconds per reading with a photodiode detector fixed at 90° relative to the incident the laser light (783.9 nm). Dynamics Software was used to calculate the autocorrelation decay from the random fluctuations in scattered light intensity. This information was then used to determine the diffusion coefficient of the sample in solution, which correlates with the hydrodynamic radius of the particles using the Stokes-Einstein equation. Electrophoretic measurements were performed with a Malvern Instruments Zetasizer. All measurements were conducted using a dilute solution of microgels in pH 7.4 phosphate buffer containing 100 mM ionic strength (PBS).

Film Preparation. The 12-mm diameter glass coverslip disks were placed in a ceramic

glass slide holder and cleaned using a sequential solvent sonication method. A sequential solvent sonication method proceeded with the following solvent sequence using a Bransonic 2510 Ultrasonicator (42 kHz +/- 6% output): 30 minutes in dilute soapy (Alconox) water, 15 minutes in deionized water, 15 minutes in acetone, 15 minutes in absolute ethanol, and 15 minutes in isopropyl alcohol. Afterwards, the glass was immediately equilibrated for 30 minutes in absolute ethanol and 1% by volume APTMS was added. The glass was incubated with the APTMS-ethanol solution for 2 hours under gentle agitation. The glass was then rinsed with a 70% aqueous ethanol solution and deionized water, and then dried under a gentle stream of N_2.

Cleaned and dried glass disks were individually placed at the bottom of 24-well plates and PBS was immediately added. The glass was allowed to equilibrate for 30 minutes, and the buffer was then replaced with a 0.1 mg/mL solution of microgels in pH 7.4 phosphate buffer containing 100 mM ionic strength (PBS). For centrifuged films, the well plates were placed immediately across a counter-weighted well plate in an Eppendorf 5804R centrifuge equipped with a plate-holding rotor. Films were centrifugally deposited at a maximum rotor speed of 2,250 x g for a specific amount of time. Passively adsorbed microgel films were made by simply controlling the exposure time of the functionalized glass to the microgel solution. After deposition, the films were rinsed with deionized water and dried under a gentle stream of N_2. All films were deposited at room temperature.

Samples prepared using non-fouling microgels were deposited using a 0.8 mg/mL microgel solution in PBS. Centrifugation was carried out at 2,250 x g for 5 minutes at room temperature. Afterwards, the monolayers were covalently attached to the amine-functionalized glass by activating the acids on the particles. To accomplish this, EDC/NHS bioconjugation chemistry was employed. A solution containing 2 mM EDC and 5 mM NHS was prepared in 10 mM MES buffer (pH 6) and allowed to react with the non-fouling microgel film for 2 hours at room temperature. After rinsing the films with water, they were exposed to a 10 mM solution of hydroxylamine in MES buffer for 10 minutes to quench the EDC/NHS reaction. The films were then rinsed with water to remove excess reagents.

Multilayer formation. In the past, our group has amply demonstrated the use of microgels in the fabrication of multi-layered thin films.[24,25,34,41] In this study, microgel monolayer films were constructed using active deposition in the same fashion as described above. To add an additional layer, a 0.14 monoM (molar concentration of monomer) solution of PDADMAC was added to the film and allowed to adsorb to the microgel film for 30 minutes. The films were then washed five times with deionized water. Another layer of microgels was then added to the well and centrifuged onto the surface, as described above. This process was repeated until four microgel layers were deposited. The thickness of the microgel multilayer film was determined by using a razor blade to scratch the surface of the film to expose the underlying substrate, and AFM was used to determine the height of the film compared to the substrate.

Atomic Force Microscopy Imaging and Analysis. Microgel films were imaged using an Asylum Research MFP-3D Instrument (Santa Barbara, CA). Imaging was performed and processed using the MFP-3D software under the IgorPro (WaveMetrics Inc., Lake Oswego, OR) environment. Non-contact mode aluminum-coated silicon nitride cantilevers were purchased from NanoWorld (force constant = 42 N/m, resonance frequency = 320 kHz). All images were taken in air under ambient conditions.

Quantitative image analysis was performed to calculate the average particle footprint area on the glass surface. Briefly, an iterative inverse mask was created to highlight the particles and the image was flattened to the 2nd order. A histogram was then generated to evaluate the bimodal distribution of surface height and particle height. Three times the standard deviation of the surface height was added to the average height of the surface to account for variations in the surface around the particles. A new inverted mask was generated based on this calculation, and the percentage of the image that was masked was calculated. This percentage was divided by the number of particles (counted manually) to give an average particle footprint area. The radial distribution function for the images was calculated using code written in-house in the IDL v. 6.1 programming environment.

In Vitro Cellular Adhesion Studies. Microgel multi-layer films were sterilized after assembly in 70% ethanol aqueous solution. Before use with cells, films were washed three times

in sterile PBS, and then equilibrated in fresh PBS for at least 1 hour before use. A murine peritoneal macrophage cell line, IC-21, was employed to test for adhesion to the multi-layer films in vitro. Macrophages are one of the primary mediators of the inflammatory response, and can fuse to form the foreign body giant cells that make up a significant portion of the fibrous capsule around an implanted biomaterial. The use of a macrophage cell line is standard for examining non-fouling behavior in vitro due to this cell type's extremely adhesive nature and role in the body's response to a biomaterial. The IC-21 cell line is a virally transformed murine peritoneal macrophage line that expresses many of the standard macrophage surface proteins and maintains the phagocytic and cytolytic behaviors characteristic of untransformed macrophages. IC-21 cells were cultured in RPMI-1640 media supplemented with 10% fetal bovine serum (FBS) and 1% penicillin streptomycin (PS). The cultures were grown at 37°C with 5% CO_2. The cells were removed using Versene, counted by hemacytometer, then diluted to a concentration of 200,000 cells/1.5 mL media. The microgel films were placed in a sterile 12-well culture dish, and 1.5 mL of cells/media were added. The films were incubated at 37°C for 4 hours, after which the excess media/cells were aspirated and samples were transferred to new wells and fresh media. Samples were incubated overnight and stained the next day with 4 μM calcein and ethidium homodimer in PBS. Samples were imaged at 20x magnification with a Nikon Eclipse E400 upright microscope (Nikon Instruments, Inc., Melville, NY). Images were taken with Spot Advanced software (Diagnostic Instruments, Sterling Heights, MI). Eight representative images were taken per sample, with three samples per group. Cells were counted using the public domain NIH ImageJ program (developed at the U.S. National Institutes of Health and available on the Internet at

`http://rsb.info.nih.gov/nih-image/`

). The cell count was averaged over all representative images of the same sample type, and the error bars shown represent the standard error for the group of three samples.

RESULTS AND DISCUSSION To study assembled microgel monolayers using the active

centrifugation deposition technique, two different anionic microgel particles composed of N-isopropylacrylamide (NIPAm), acrylic acid (AAc), and the cross-linker N,N-methylenebis(acrylamide) (BIS) were synthesized; these particles were used in the Coulombically-driven assembly of microgel films onto cationic silane-modified glass substrates. The particles were characterized using dynamic and static light scattering, and atomic force microscopy; the results of these characterizations are summarized in Table 1. The hydrodynamic radius of particle (1) is roughly half the size of particle (2), due to differences in cross-linker density, total monomer concentration in the reaction, and amount of surfactant used in the synthesis. Accordingly, the diffusion coefficient for (1) is twice as large as (2). Additionally, (2) has an approximately 6 times larger footprint area when passively adsorbed onto a surface, and is slightly softer than (1), as evidenced by the higher Rs/Rh (radius on the surface/radius in solution) ratio. However, both particles types have similar electrophoretic mobilities. Therefore, any differences seen under centrifugal deposition will be due to differences in sedimentation velocity, not the surface accessibility of anionic charges on the particle for attachment to the cationic substrate.

Microgel	Hydrodynamic Radius, R_h (nm) at room temperature [a]	Hydrodynamic Radius, R_h (nm) at 40ºC [a]	Particle Footprint Area (nm^2) [b]	Particle Footprint Area (nm^2) [c]	R_s/R_h	Diffusion Coefficient (cm^2/s) [a]	Electrophoretic Mobility ($m^2/ s \bullet V$) [d]
1	171 ± 0.6 (15 ± 5% PD)	164 ± 1 (14 ± 2% PD)	$9.4 \times 10^4 \pm 2 \times 10^3$	$5.5 \times 10^4 \pm 2 \times 10^3$	1.01	$13.4 \pm 0.4 \times 10^{-9}$	-1.0×10^{-2}
2	365 ± 4 (14 ± 0.3% PD)	277 ± 4 (10 ± 2% PD)	$5.7 \times 10^5 \pm 1 \times 10^4$	$2.9 \times 10^5 \pm 2 \times 10^4$	1.17	$6.4 \pm 0.1 \times 10^{-9}$	-1.06×10^{-2}

Figure C.1: Table 1. Microgel Characteristics. [a] Determined by dynamic light scattering in pH 7.4 phosphate buffer containing 100 mM ionic strength (PBS) at room temperature. [b] Determined by atomic force microscopy on 30 minute passively deposited samples. [c] Determined by atomic force microscopy at time point of active deposition where the particle footprint area was smallest. [d] Determined by electrophoretic light scattering in PBS at room temperature.

Centrifugal, or active, deposition is performed by placing the substrates of interest at the bottom of each well in a multiwell-plate (e.g. a cell culture plate), followed by the

addition of a microgel dispersion into the well above the substrate. The plates are then placed in a swinging bucket, well-plate rotor. When the rotor spins, the well-plates swing out so as to align the centrifugal force (g), perpendicular to the plane of each substrate, thereby forcing the colloidal particles onto the substrate. For all experiments described in this study, the maximum centrifugal force of the rotor (2,250x g) was used. Because of its utility in the deposition of films on multiple samples simultaneously, centrifugal film deposition is fast, reproducible, and many samples can be made in parallel with a high degree of quality control.

Microgels (1) and (2) were both subject to active film deposition, with passive deposition being used as a comparison throughout this entire study. Atomic force microscopy has been used previously to study passively adsorbed microgel particle monolayers.[40] It is important to point out that the microgels were dispersed and deposited in a phosphate buffered saline solution of high ionic strength (100 mM); these conditions have previously been shown to be appropriate for reducing anionic repulsion between microgels during film formation.[39] Microgels that are actively deposited form films that are fundamentally different than those deposited passively. As can be seen in Figure 1, when active deposition is used (Figure 1b and 1d), the microgels appear to be smaller and more closely packed than those deposited passively (Figure 1a and 1c). This difference in particle size is perhaps more clearly seen when smaller scan sizes are used (Figure 1 insets). It is also worth noting that regardless of the deposition method, the particles all have heights of only 10-15 nm in the dehydrated state, illustrating the extremely low polymer density of the particles, as we have described previously.[39,41] The calculated radial distribution functions for these images, also shown in Figure 1, quantitatively illustrate the differences in particle spacing and nearest neighbor probability. Both particle (1) and particle (2) show nearest neighbor distances that are closer under active deposition, thus confirming that these films are more tightly packed when actively deposited as compared to passive adsorption. One might expect that microgels would flatten under centrifugal force and therefore result in particles with larger footprint areas and a film that has decreased particle density. However, the opposite is apparent in these experiments, which must mean the particles have some mobility to slide along the

substrates surface (most likely from the contribution of buffer salts reducing the Coulombic attraction between particle and surface).

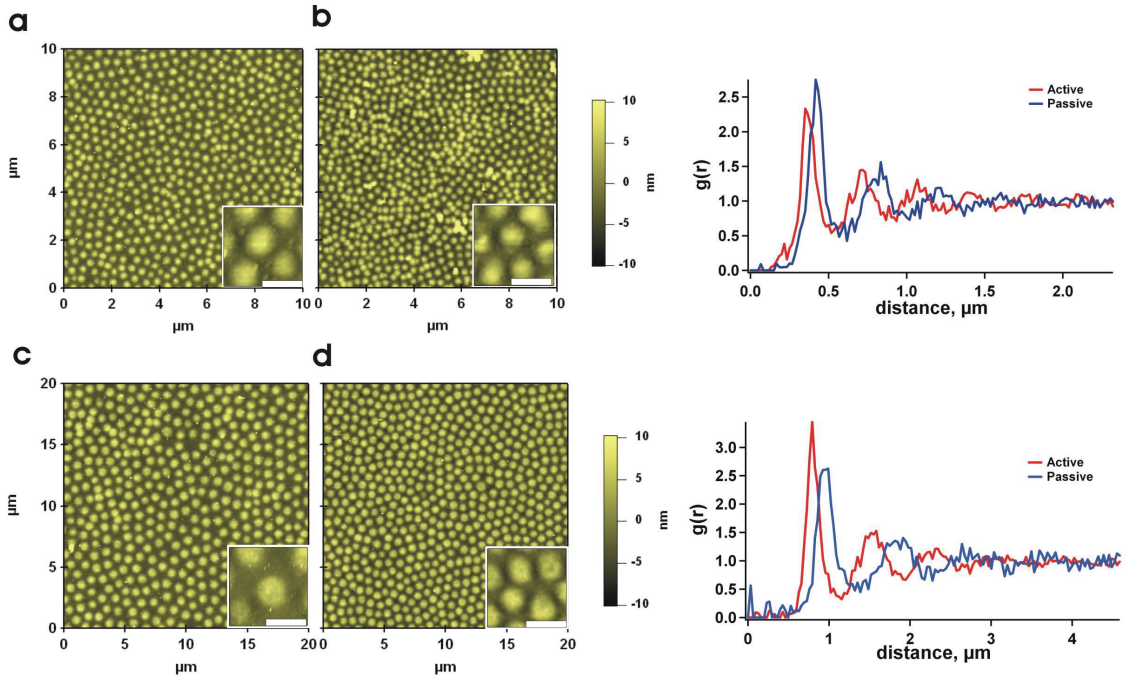

Figure C.2: Figure 1. Height traces, using atomic force microscopy, of microgels (1) (a and b) and (2) (c and d) under passive deposition (a and c) and active centrifugal deposition (b and d). Microgels (1) and (2) were passively deposited for 16 hours. Microgels (1) and (2) were actively deposited for 10 min and 5 min respectively. Inset scale bars are 0.5 μm (a and b) and 1 μm (c and d). On the right, radial distribution functions are shown for each particle type and deposition condition, illustrating the quantitative differences in particle spacing between active and passive deposition.

The evolution of the microgel films was monitored as a function of deposition time under both active and passive conditions (Figure 2). The larger microgels (2) obtained uniform coverage faster than the smaller microgels (1) when centrifuged onto a surface. This is expected due to larger or more massive particles having a higher sedimentation velocity. The opposite was true for the passively adsorbed microgels, as the smaller particles have a higher diffusion coefficient and therefore reach the surface faster, assuming an equivalent

sticking probability. In addition, the particle footprint area was monitored as a function of time. Under both deposition conditions and for both microgel types, the microgel footprints appeared to decrease until the film reached a uniform monolayer. However, under active deposition, the microgels continued to shrink even after apparently forming a uniform monolayer. The deswelling ratio of these particles in solution is approximately 0.96 and 0.76 for microgels (1) and (2) respectively. The ratio of particle radius on a film of active to passive deposition is approximately 0.76 and 0.71 for microgels (1) and (2) respectively. Therefore it appears that active deposition shrinks microgels to a greater or at least similar extent as deswelling the microgels in solution. There are a few possible mechanisms by which active deposition might result in smaller microgels that pack more tightly. For example, centrifugation could cause the microgels to concentrate in the solution above the substrate, and thus deswell due to an increase in the local osmotic pressure.[48−50] Alternatively, the use of a high ionic strength buffer (100 mM) during deposition could permit the particles to desorb or rearrange on the surface, thereby dynamically reconfiguring the interface as microgels continue to strike the interface at a high velocity. Finally, it may be the case that actively deposited microgels have somewhat different adsorption/adhesion characteristics than those of passively deposited microgels.

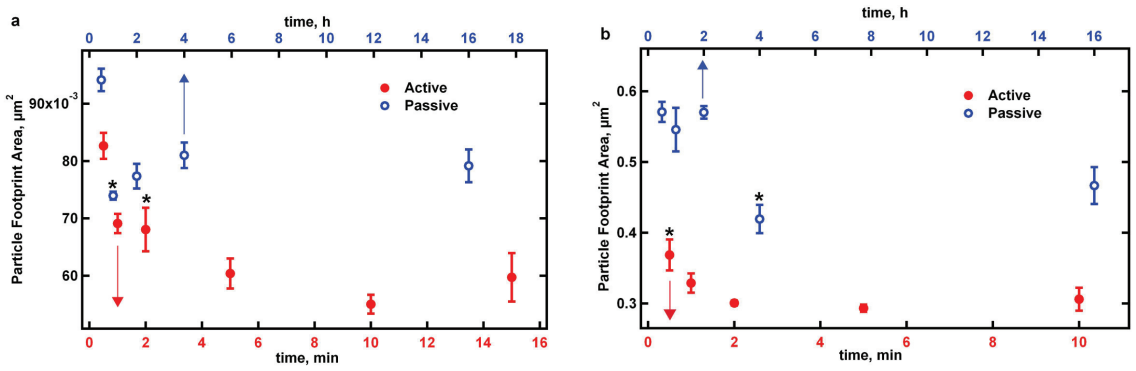

Figure C.3: Figure 2. Microgel footprint area as a function of deposition time for centrifugation (active) and passive deposition techniques. (a) Microgel (1) and (b) microgel (2). *Denotes formation of a uniform monolayer without patchy particle coverage. Error bars represent the standard error of the mean particle footprint area taken from three 10 μm x 10 μm (a) or 20 μm x 20 μm for (b) atomic force microscopy images.

Considering these possibilities, it is unlikely that microgel pre-concentration during centrifugation is exclusively responsible for these observations, as small particle footprints might be expected early in the deposition, as well. However, Figure 2 clearly shows the microgels are initially larger and grow smaller over time during film assembly. Therefore, a dynamic rearrangement at the interface must be occurring during the formation of the film, both under active and passive deposition conditions, with the effect persisting even after formation of a uniform monolayer under active conditions. To further explore this phenomenon, we used a two-step deposition method, the results of which are shown in Figure 3. In this experiment, microgels were first adsorbed passively to obtain partial coverage, and then without replacing microgels or removing the film from solution, samples were subjected to active microgel deposition conditions. The results illustrate that under these conditions, the average particle footprint area does still decrease upon active deposition, but not to the same extent as that observed during active deposition alone. Additionally, if particles are first passively adsorbed until a uniform monolayer is generated, additional centrifugation does not induce a statistically meaningful change in the adsorbed microgel size. These data

suggest that the passively adsorbed microgels do not rearrange dramatically or desorb from the surface during further active deposition. When space is available for microgels to deposit (Figure 3a), it appears that lateral repulsion between microgels might result in some decrease in microgel footprint. However, when microgels centrifuged on top of the passively deposited particles are unable to make their way onto the substrate (Figure 3b), significant restructuring of the interface is not observed. These results are in agreement with a previous study using similar pNIPAm-co-AAc microgels adsorbed on an amine-modified surface, where the authors illustrated that even with increasing NaCl concentrations there was no evidence of particle desorption from the surface.[35]

Considering these results, it is therefore likely that particle adsorption is fundamentally different between the two cases. Passive adsorption likely results in a polymer chain conformation that is closer to the thermodynamic minimum, whereas the active approach results in a polymer conformation that is higher in energy (kinetically determined) and is therefore more likely to evolve and age during centrifugation. This theory is further reiterated by observing the impact of ionic strength of the dispersion buffer on film assembly. When microgels are dispersed in a lower ionic strength buffer (2 mM), there is also a noticeable difference in microgel size and spacing (see Supporting Information). Though the particles are not as small and highly packed as under high ionic strength (100 mM) conditions, due to reduced shielding of repulsive side chains, active deposition once again results in a smaller size and spacing of microgels on the surface compared to passive deposition. This observation suggests that even when shielding of the anionic side chains is significantly reduced, centrifugation can still overcome particle-particle repulsion to a greater extent than a dip-coating method, presumably due to the higher energy used in deposition.

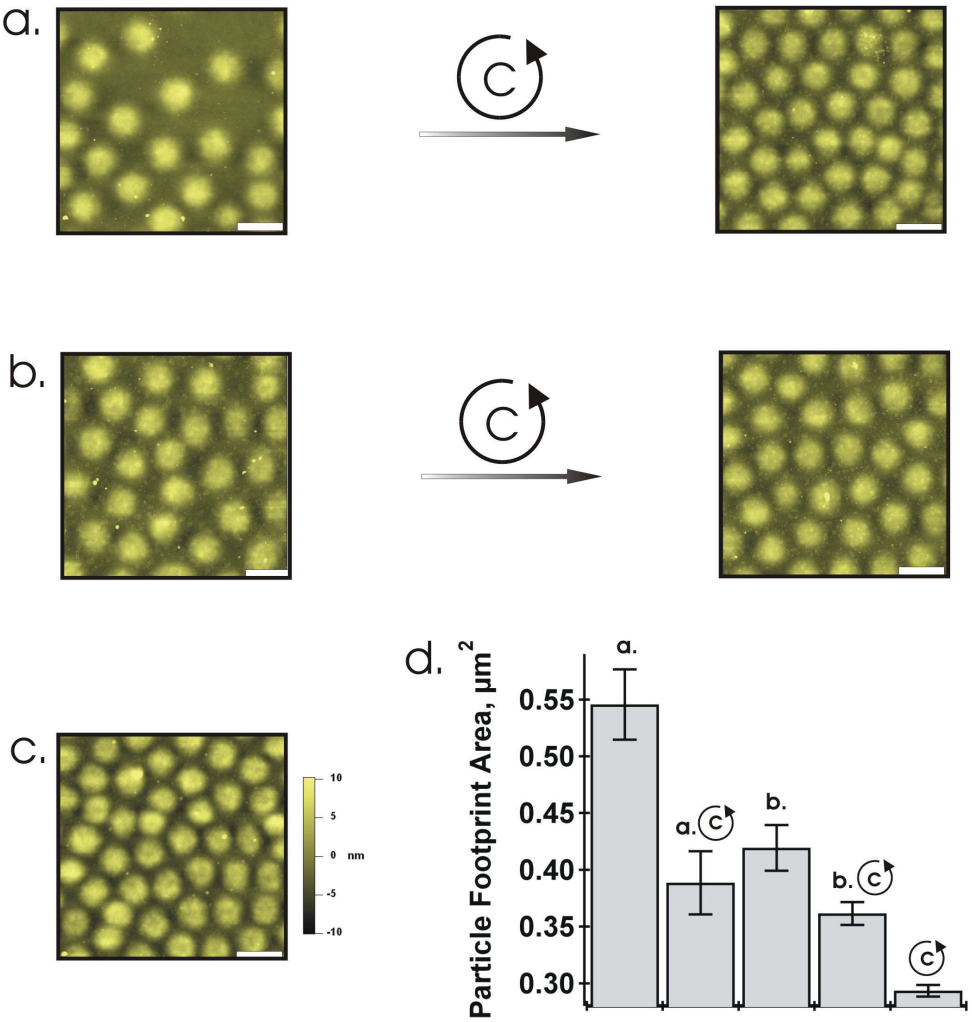

Figure C.4: Figure 3. Height traces, using atomic force microscopy characterization, of the two-step deposition process for microgel (2). (a) A sub-monolayer, exhibiting patchy coverage, was passively deposited first and then subjected to centrifugal deposition. (b) A uniform monolayer was first deposited passively and then subjected to centrifugal deposition. (c) Shows a uniform monolayer deposited actively for comparison. Scale bar is 1 μm. (d) Bar graph showing the average particle footprint area for all samples. Error bars represent the standard error of the mean particle footprint area taken from three 20 μm x 20 μm AFM images.

The recent work of FitzGerald et al. (40) seems to support the hypothesis that particles

can reorganize laterally because of interparticle repulsion. These investigators studied the passive adsorption of pH-sensitive microgel particles using liquid AFM imaging. Their results demonstrate the dynamic nature of such particles at the particlesurface interface. When these particles are in their nondeformable latex form at higher pH, they observe a significant deviation from what is expected from the random sequential adsorption model of hard spheres, where the diameter of the particles at the interface is almost twice the size of that in solution. Furthermore, when the pH was adjusted to more acidic conditions, thus inducing a latex-to-swollen microgel transition, this swelling pressure caused neighboring particles to desorb from the surface. Even though coulombic interactions exist between the particle and substrate, the particleparticle interactions dominate in their example. These results illustrate an extreme case of dynamic microgel adsorption where lateral particle interactions can dictate particle coverage. Similarly, our results illustrate that polymeric particles can undergo size changes and film rearrangement as a function of coverage, albeit in the limit of strong microgelsurface interactions.

Multi-layered polyelectrolyte microgel interfaces, which we have demonstrated previously,[24,25,34,41] were fabricated using rapid centrifugal film deposition to illustrate the utility of the technique. The progression of layers of a multi-layered microgel film is shown in Figure 4. Atop a glass substrate that was rendered cationic by amine functionalization, anionic microgels (microgel 2) were alternatively layered with poly(diallyldimethylammonium chloride), or PDADMAC, as a cationic polymer. As more layers are added, up to four layers of microgels (with a resulting height of approximately 60 nm, thus illustrating the deposition of additional layers), less of the underlying glass substrate appears to be exposed and the resulting film is quite uniform. In light of this observation, we constructed multilayers of non-fouling microgels to aid in preventing cellular adhesion to a surface. In the past we have used spin-coating to fabricate a monolayer of non-fouling microgels containing the cross-linker poly(ethylene glycol) diacrylate or PEG-DA.[31−33] PEG is a polymer widely known to resist protein and cellular adhesion due to its high degree of hydration and comformational flexibility,[4,51−53] Previously we have shown that spin-coating of non-fouling microgels onto

a substrate provided the high coverage needed to block the background substrate from protein and cellular adhesion. However, spin coating is an intrinsically serial process that can be quite wasteful of material. However, as shown below, centrifugation-based assembly can be parallelized and also provides the required high coverages using a rapid multi-layering approach in a non-wasteful manner.

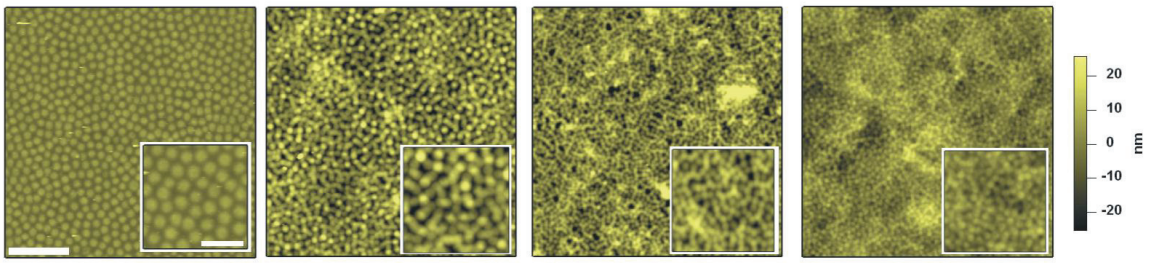

Figure C.5: Figure 4. AFM images of microgel thin films constructed in a multi-layered fashion (using microgel 2). Each image has a 20 μm x 20 μm scan size (5 μm scale bar) with a 5 μm x 5μm (2 μm scale bar) inset. Images were obtained from 1, 2, 3, and 4 layer films (left to right) formed by active deposition.

The results in Figure 5 demonstrate the effectiveness of actively deposited non-fouling microgel multi-layers towards blocking macrophage adhesion. Macrophages adhere and spread well on the positive control tissue culture polystyrene (TCPS). Glass that was extensively cleaned also shows cellular adhesion and spreading with an approximately five-fold reduction in number of cells adhering compared to TCPS. However, four-layer microgel films, which were generated quickly using centrifugation deposition, showed significant blockage of macrophage adhesion with an over 200-fold and over 30-fold reduction in number of adherent cells compared to TCPS and cleaned glass respectively. Furthermore, the few cells that adhere to the surface of the microgel multi-layer films do not appear to be able to spread, and therefore it is speculated that these cells have found small defects in the film, which presumably could be blocked with additional layers. Optimization of the film properties in the context of non-fouling biomaterial coatings will be the subject of later studies.

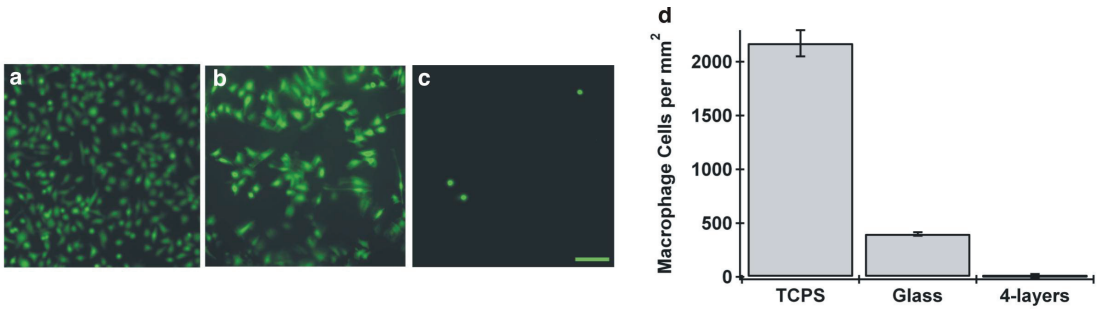

Figure C.6: Figure 5. Fluorescence microscopy of fluorescently stained macrophages adhering on (a) tissue culture polystyrene (TCPS), (b) cleaned glass, and (c) 4 actively deposited layers of PEG cross-linked pNIPAm microgels. Scale bar represents 100 μm. (d) Quantitative cellular adhesion from fluorescence microscopy images with error bars representing the standard error.

CONCLUSION Centrifugation has been demonstrated to be a rapid and robust method for generating colloidal films. When using soft anionic microgel particles to construct an interface, centrifugation deposition results in particles that are smaller and more closely packed compared to a more common dip-coating, or passive adsorption, technique. The footprint area of centrifuged particles actively shrinks during assembly, even after they have formed a uniform monolayer. Passively deposited microgels stop decreasing in footprint size once they have reached a uniform film, and when these films are subjected to centrifugally forced microgels afterwards, the centrifugation approach does not force significant morphological changes in the deposited particles. The impact of this phenomenon on particle adhesion, modulus, and film stability is currently being explored in our labs. In addition, it has been demonstrated that the centrifugal deposition approach enables a functional multi-layered microgel interface with a high degree of uniformity and substrate coverage. These interfaces can be used in the development of microstructured hydrogel coatings for controlling biological and cellular adhesions, and exploited for various other applications in which complexity, tunability, and uniformity is desired.

Acknowledgment. We thank the Nils Kröger group for the use of their Zetasizer instrument. We also like to think Prof. K.C. Chan (Albany State University, Physics) for discussions about radial distribution functions, and Mr. Jae Kyu Cho (Georgia Institute of Technology, ChBE) for help using the IDL program for calculating radial distribution functions. Furthermore, we thank the Georgia Institute of Technology for providing GTEC II funding for this research.

Supporting Information Available: Atomic Force Microscopy comparing active and passive deposition techniques under low and high ionic strength buffers is available in supporting information. This materials is available free of charge via the internet at

`http://pubs.acs.org`

.

REFERENCES AND NOTES

1. Yoshida M, Langer R, Lendlein A, Lahann J. Polym Rev. 2006;46(4):347375.
2. Motornov M, Sheparovych R, Tokarev I, Roiter Y, Minko S. Langmuir. 2007;23(1):1319.
3. Cho SH, White SR, Braun PV. Adv Mater. 2009;21(6):645.
4. Lopez GP, Ratner BD, Tidwell CD, Haycox CL, Rapoza RJ, Horbett TA. J Biomed Mater Res. 1992;26(4):415439.
5. De Gennes PG. Adv Colloid Interface Sci. 1987;27(34):189209.
6. Douglas JF, Johnson HE, Granick S. Science. 1993;262(5142):20102012.
7. van de Ven TGM. Adv Colloid Interface Sci. 1994;48:121140.
8. Kaellrot N, Linse P. Macromolecules. 2007;40(13):46694679.
9. Kim SW, Bae YH, Okano T. Pharm Res. 1992;9(3):283290.
10. Kirker KR, Luo Y, Nielson JH, Shelby J, Prestwich GD. Biomaterials. 2002;23(17):36613671.
11. Schmaljohann D, Oswald J, Jorgensen B, Nitschke M, Beyerlein D, Werner C. Biomacromolecules. 2003;4(6):17331739.

12. Shu XZ, Liu Y, Palumbo F, Prestwich GD. Biomaterials. 2003;24(21):38253834.

13. Nayak S, Lyon LA. Angew Chem, Int Ed. 2005;44(47):76867708.

14. Lyon LA, Meng Z, Singh N, Sorrell CD, John AS. Chem Soc Rev. 2009;38(4):865874.

15. Hendrickson GR, Lyon LA. Soft Matter. 2009;5(1):2935.

16. Lynch I, Miller I, Gallagher WM, Dawson KA. J Phys Chem B. 2006;110(30):1458114589.

17. Wei YY, Luo YW, Li BF, Li BG. Colloid Polym Sci. 2006;284(10):11711178.

18. Ugur S, Elaissari A, Yargi O, Pekcan O. Colloid Polym Sci. 2007;285(4):423430.

19. Pelton R. Adv Colloid Interface Sci. 2000;85(1):133.

20. Jones CD, Lyon LA. Macromolecules. 2000;33(22):83018306.

21. Gan DJ, Lyon LA. J Am Chem Soc. 2001;123(31):75117517.

22. Saunders BR, Crowther HM, Vincent B. Macromolecules. 1997;30(3):482487.

23. Wu X, Pelton RH, Hamielec AE, Woods DR, McPhee W. Colloid Polym Sci. 1994;272(4):467477.

24. Nolan CM, Serpe MJ, Lyon LA. Biomacromolecules. 2004;5(5):19401946.

25. Serpe MJ, Yarmey KA, Nolan CM, Lyon LA. Biomacromolecules. 2005;6(1):408413.

26. Kim J, Serpe Michael J, Lyon LA. J Am Chem Soc. 2004;126(31):95129513.

27. Serpe MJ, Kim J, Lyon LA. Adv Mater. 2004;16(2):184187.

28. Debord JD, Lyon LA. J Phys Chem B. 2000;104(27):63276331.

29. Hellweg T, Dewhurst CD, Eimer W, Kratz K. Langmuir. 2004;20(11):43304335.

30. McGrath JG, Bock RD, Cathcart JM, Lyon LA. Chem Mater. 2007;19(7):15841591.

31. Nolan CM, Reyes CD, Debord JD, Garcia AJ, Lyon LA. Biomacromolecules. 2005;6(4):20322039.

32. Singh N, Bridges AW, Garcia AJ, Lyon LA. Biomacromolecules. 2007;8(10):32713275.

33. Bridges AW, Singh N, Burns KL, Babensee JE, Lyon LA, Garcia AJ. Biomaterials. 2008;29(35):46054615.

34. Serpe MJ, Jones CD, Lyon LA. Langmuir. 2003;19(21):87598764.

35. Nerapusri V, Keddie JL, Vincent B, Bushnak IA. Langmuir. 2006;22(11):50365041.

36. Nerapusri V, Keddie JL, Vincent B, Bushnak IA. Langmuir. 2007;23(19):95729577.

37. Hoefl S, Zitzler L, Hellweg T, Herminghaus S, Mugele F. Polymer. 2007;48(1):245254.

38. Schmidt S, Hellweg T, von Klitzing R. Langmuir. 2008;24(21):1259512602.

39. Sorrell CD, Lyon LA. Langmuir. 2008;24(14):72167222.

40. FitzGerald PA, Dupin D, Armes SP, Wanless EJ. Soft Matter. 2007;3(5):580586.

41. Sorrell CD, Lyon LA. J Phys Chem B. 2007;111(16):40604066.

42. Schmidt S, Motschmann H, Hellweg T, von Klitzing R. Polymer. 2008;49(3):749756.

43. Anderson JM. Annu Rev Mater Res. 2001;31:81110.

44. Zhang L, Hu J, Lu Z. J Colloid Interface Sci. 1997;190(1):7680.

45. Barrett DG, Yousaf MN. Angew Chem, Int Ed. 2007;46(39):74377439.

46. Lee SK, Yi GR, Yang SM. Lab Chip. 2006;6(9):11711177.

47. Yi YD, Bae YC. J Appl Polym Sci. 1998;67(12):20872092.

48. St John AN, Breedveld V, Lyon LA. J Phys Chem B. 2007;111(27):77967801.

49. St John AN, Lyon LA. J Phys Chem B. 2008;112(36):1125811263.

50. Meng Z, Cho JK, Breedveld V, Lyon LA. J Phys Chem B. 2009;113(14):45904599.

51. Gombotz WR, Wang GH, Horbett TA, Hoffman AS. J Biomed Mater Res. 1991;25(12):15471562.

52. Jeon SI, Andrade JD. J Colloid Interface Sci. 1991;142(1):159166.

53. Pale-Grosdemange C, Simon ES, Prime KL, Whitesides GM. J Am Chem Soc. 1991;113(1):1220.

APPENDIX D

APPLICATION OF IL-1RA-TETHERED PARTICLES IN AN OSTEOARTHRITIC RAT MODEL

The technology developed in this thesis work was tested in two different experiments using an MIA model of osteoarthritis in rats. In both experiments, rats were injected in the right knee with MIA and were allowed to ambulate freely for 7 days prior to beginning any treatment. The first experiment used a low dose of MIA (0.3 mg/knee) and allowed OA to progress up to 3 weeks after MIA injection. The second experiment used a high dose of MIA (1 mg/knee) and the rats were allowed to progress for 3 weeks.

In the low-dose experiment, we saw no significant cartilage damage in any group, including the group that received MIA and no further treatment (Fig. D.1). We concluded that the MIA dose was too low to allow noticeable macroscopic changes at 3 weeks. For the following experiment, we increased the dose and kept the evaluation period the same. However, in this case, we saw severe cartilage damage in all groups, including those that received a bolus dose of soluble IL-1ra. Although there is no published evidence that soluble IL-1ra can attenuate OA damage in MIA models, other models of OA have shown improvements after bolus IL-1ra injections[][]. We expected that rats that were treated with soluble IL-1ra would show improvement in phenotype and would act as our positive controls. However, even the bolus IL-1ra group showed severe cartilage damage (Fig. D.2). We conclude from this set of experiments that the MIA model of OA most likely does not create a representative inflammatory environment in the joint. Other models of OA, specifically those that are induced by mechanical changes (ACL transection, MCL transection, medial meniscal transection) better represent the clinical, physiological changes seen during OA. Testing out this IL-1ra particle system in these models should allow us to better assess the effectiveness of our technology for treating OA in both acute and chronic disease models.

[Low Dose MIA Animal Experiment]

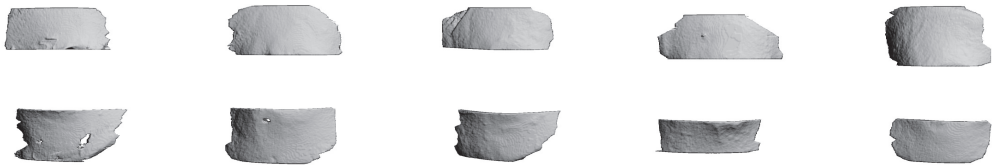

Figure D.1: Tibial cartilage reconstructions of rats receiving 0.3 mg MIA. Left to Right: small particles, low dose; large particles, high dose; large particles, low dose; MIA only; saline only.

[High Dose MIA Animal Experiment]

Figure D.2: EPIC-μCT reconstructions of the tibial plateau cartilage in rats with MIA-induced osteoarthritis (1 mg MIA/40 μL). Only right knees were injected with MIA. Left knees were injected with an equal volume of saline and served as healthy contralateral controls. 7 days post-MIA injection, the right knees were re-injected with IL-1ra-tethered particles, soluble IL-1ra, or saline; left knees were again injected with equal volume of saline. Left to right: MIA-only left knee; MIA-only right knee; IL-1ra bolus left knee; IL-1ra bolus right knee; IL-1ra particles left knee; IL-1ra particles right knee.

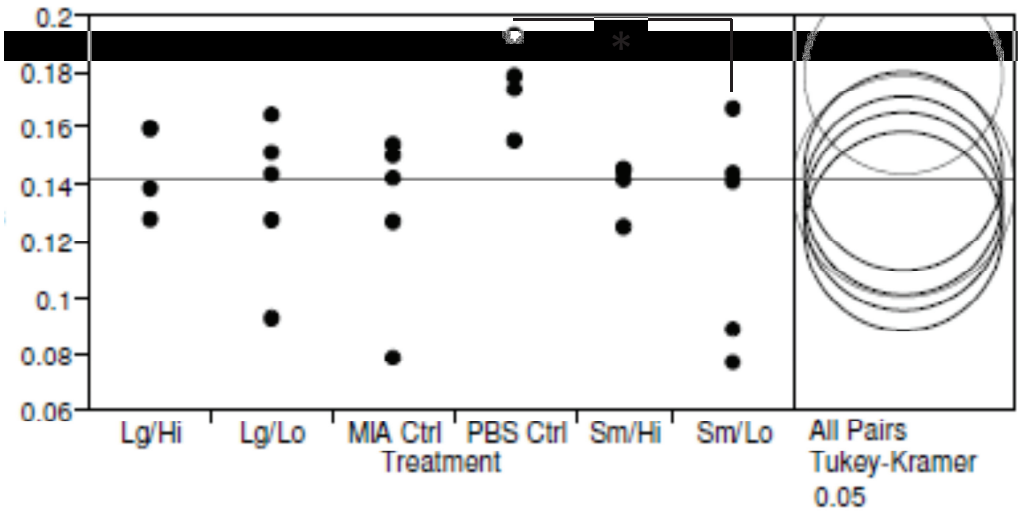

Figure D.3: Comparison of tibial cartilage thicknesses among groups from the low-dose MIA study. All animals received 0.3 mg MIA in the right knee only. Left knees received equal amounts of injected saline. No significant differences were detected among contralateral knees or among MIA-treated knees, regardless of treatment group. Differences in cartilage thickness were not statistically significant among groups except for between the contralateral control knees and the small particle/low dose group ($p = 0.0243$). All other comparisons, including between the MIA-treated knees and the contralateral controls, were not statistically significant ($p > 0.05$). Lg/lo = large particles, low dose; Lg/hi = large particles, high dose; Sm/lo = small particles, low dose; Sm/hi = small particles, high dose; MIA Ctrl = saline only; PBS ctrl = contralateral knees that only received saline injections.

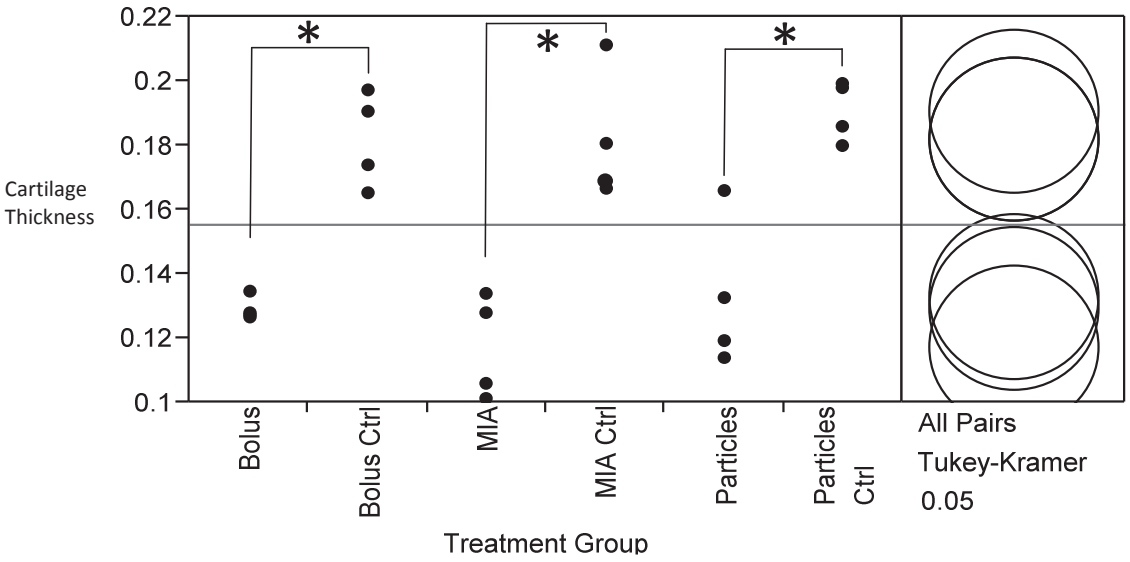

Figure D.4: Comparison of cartilage thicknesses among groups from the high-dose MIA study. All animals received 1 mg MIA in the right knee only. Left knees received equal amounts of injected saline. No significant differences were detected among contralateral knees or among MIA-treated knees, regardless of treatment group. Differences in cartilage thickness were statistically significant between the contralateral controls and MIA-treated knees for each group (Bolus vs. Bolus Ctrl; MIA vs. MIA Ctrl; Particles vs. Particles Ctrl) (* $p < 0.038$).

REFERENCES

[1] Abramson, S. B. and Amin, A., "Blocking the effects of il-1 in rheumatoid arthritis protects bone and cartilage," *Rheumatology*, vol. 41, no. 9, pp. 972–980, 2002.

[2] Adamopoulos, I. E., Sabokbar, A., Wordsworth, B. P., Carr, A., Ferguson, D. J., and Athanasou, N. A., "Synovial fluid macrophages are capable of osteoclast formation and resorption," *J Pathol*, vol. 208, no. 1, pp. 35–43, 2006.

[3] Ahmad, R., Sylvester, J., Ahmad, M., and Zafarullah, M., "Adaptor proteins and ras synergistically regulate il-1-induced adamts-4 expression in human chondrocytes," *J Immunol*, vol. 182, no. 8, pp. 5081–7, 2009.

[4] Alcaraz, M. J., Megias, J., Garcia-Arnandis, I., Clerigues, V., and Guillen, M. I., "New molecular targets for the treatment of osteoarthritis," *Biochem Pharmacol*, vol. 80, no. 1, pp. 13–21, 2010.

[5] Alexander, J., Cargill, R., Michelson, S. R., and Schwam, H., "(acyloxy)alkyl carbamates as novel bioreversible prodrugs for amines: increased permeation through biological membranes," *J Med Chem*, vol. 31, no. 2, pp. 318–22, 1988.

[6] Allen, K. D., Adams, S. B., J., Mata, B. A., Shamji, M. F., Gouze, E., Jing, L., Nettles, D. L., Latt, L. D., and Setton, L. A., "Gait and behavior in an il1beta-mediated model of rat knee arthritis and effects of an il1 antagonist," *J Orthop Res*, vol. 29, no. 5, pp. 694–703, 2011.

[7] Allen, K. D., Adams, S. B., and Setton, L. A., "Evaluating intra-articular drug delivery for the treatment of osteoarthritis in a rat model," *Tissue Eng Part B Rev*, vol. 16, no. 1, pp. 81–92, 2010.

[8] Almasi, A., Fischer, E., and Perjesi, P., "A simple and rapid ion-pair hplc method for simultaneous quantitation of 4-nitrophenol and its glucuronide and sulfate conjugates," *J Biochem Biophys Methods*, vol. 69, pp. 43–50, 2006.

[9] Ameye, L. G. and Young, M. F., "Animal models of osteoarthritis: lessons learned while seeking the "holy grail"," *Curr Opin Rheumatol*, vol. 18, no. 5, pp. 537–47, 2006.

[10] Anderson-MacKenzie, J. M., Quasnichka, H. L., Starr, R. L., Lewis, E. J., Billingham, M. E., and Bailey, A. J., "Fundamental subchondral bone changes in spontaneous knee osteoarthritis," *Int J Biochem Cell Biol*, vol. 37, no. 1, pp. 224–36, 2005.

[11] Arend, W. P. and Guthridge, C. J., "Biological role of interleukin 1 receptor antagonist isoforms," *Ann Rheum Dis*, vol. 59 Suppl 1, pp. i60–4, 2000.

[12] Arend, W. P., Malyak, M., Smith, M. F., J., Whisenand, T. D., Slack, J. L., Sims, J. E., Giri, J. G., and Dower, S. K., "Binding of il-1 alpha, il-1 beta, and il-1 receptor antagonist by soluble il-1 receptors and levels of soluble il-1 receptors in synovial fluids," *J Immunol*, vol. 153, no. 10, pp. 4766–74, 1994.

[13] Arner, E. C. and Tortorella, M. D., "Signal transduction through chondrocyte integrin receptors induces matrix metalloproteinase synthesis and synergizes with interleukin-1," *Arthritis Rheum*, vol. 38, no. 9, pp. 1304–14, 1995.

[14] Attur, M. G., Dave, M., Cipolletta, C., Kang, P., Goldring, M. B., Patel, I. R., Abramson, S. B., and Amin, A. R., "Reversal of autocrine and paracrine effects of interleukin 1 (il-1) in human arthritis by type ii il-1 decoy receptor. potential for pharmacological intervention," *J Biol Chem*, vol. 275, no. 51, pp. 40307–15, 2000.

[15] Attur, M. G., Dave, M. N., Leung, M. Y., Cipolletta, C., Meseck, M., Woo, S. L., and Amin, A. R., "Functional genomic analysis of type ii il-1beta decoy receptor: potential for gene therapy in human arthritis and inflammation," *J Immunol*, vol. 168, no. 4, pp. 2001–10, 2002.

[16] Auron, P. E., "The interleukin 1 receptor: ligand interactions and signal transduction," *Cytokine Growth Factor Rev*, vol. 9, no. 3-4, pp. 221–37, 1998.

[17] Bajayo, A., Goshen, I., Feldman, S., Csernus, V., Iverfeldt, K., Shohami, E., Yirmiya, R., and Bab, I., "Central il-1 receptor signaling regulates bone growth and mass," *Proc Natl Acad Sci U S A*, vol. 102, no. 36, pp. 12956–61, 2005.

[18] Bakker, A. C., van de Loo, F. A., van Beuningen, H. M., Sime, P., van Lent, P. L., van der Kraan, P. M., Richards, C. D., and van den Berg, W. B., "Overexpression of active tgf-beta-1 in the murine knee joint: evidence for synovial-layer-dependent chondro-osteophyte formation," *Osteoarthritis Cartilage*, vol. 9, no. 2, pp. 128–36, 2001.

[19] Bakker-Woudenberg, I. A., ten Kate, M. T., Guo, L., Working, P., and Mouton, J. W., "Improved efficacy of ciprofloxacin administered in polyethylene glycol-coated liposomes for treatment of klebsiella pneumoniae pneumonia in rats," *Antimicrob Agents Chemother*, vol. 45, no. 5, pp. 1487–92, 2001.

[20] Baltzer, A. W., Moser, C., Jansen, S. A., and Krauspe, R., "Autologous conditioned serum (orthokine) is an effective treatment for knee osteoarthritis," *Osteoarthritis Cartilage*, vol. 17, no. 2, pp. 152–60, 2009.

[21] Bandara, G., Mueller, G. M., Galea-Lauri, J., Tindal, M. H., Georgescu, H. I., Suchanek, M. K., Hung, G. L., Glorioso, J. C., Robbins, P. D., and Evans, C. H., "Intraarticular expression of biologically active interleukin 1-receptor-antagonist protein by ex vivo gene transfer," *Proc Natl Acad Sci U S A*, vol. 90, no. 22, pp. 10764–8, 1993.

[22] Baragi, V. M., Becher, G., Bendele, A. M., Biesinger, R., Bluhm, H., Boer, J., Deng, H., Dodd, R., Essers, M., Feuerstein, T., Gallagher, B. M., J., Gege, C., Hochgurtel, M., Hofmann, M., Jaworski, A., Jin, L., Kiely, A., Korniski, B., Kroth, H., Nix, D., Nolte, B., Piecha, D., Powers, T. S., Richter, F., Schneider, M., Steeneck, C., Sucholeiki, I., Taveras, A., Timmermann, A., Van Veldhuizen, J., Weik, J., Wu, X., and Xia, B., "A new class of potent matrix metalloproteinase 13 inhibitors for potential treatment of osteoarthritis: Evidence of histologic and clinical efficacy without musculoskeletal toxicity in rat models," *Arthritis Rheum*, vol. 60, no. 7, pp. 2008–18, 2009.

[23] Bard, D. R., Knight, C. G., and Page Thomas, D. P., "The retention and distribution in the rabbit knee of a radionuclide complexed with a lipophilic chelator in liposomes," *Clin Exp Rheumatol*, vol. 1, no. 2, pp. 113–7, 1983.

[24] Barrera, P., Blom, A., van Lent, P. L., van Bloois, L., Beijnen, J. H., van Rooijen, N., de Waal Malefijt, M. C., van de Putte, L. B., Storm, G., and van den Berg, W. B., "Synovial macrophage depletion with clodronate-containing liposomes in rheumatoid arthritis," *Arthritis Rheum*, vol. 43, no. 9, pp. 1951–9, 2000.

[25] Barton, N. J., Stevens, D. A., Hughes, J. P., Rossi, A. G., Chessell, I. P., Reeve, A. J., and McQueen, D. S., "Demonstration of a novel technique to quantitatively assess inflammatory mediators and cells in rat knee joints," *J Inflamm (Lond)*, vol. 4, p. 13, 2007.

[26] Basu, S. K., Govardhan, C. P., Jung, C. W., and Margolin, A. L., "Protein crystals for the delivery of biopharmaceuticals," *Expert Opin Biol Ther*, vol. 4, no. 3, pp. 301–17, 2004.

[27] Beduneau, A., Saulnier, P., Hindre, F., Clavreul, A., Leroux, J. C., and Benoit, J. P., "Design of targeted lipid nanocapsules by conjugation of whole antibodies and antibody fab' fragments," *Biomaterials*, vol. 28, no. 33, pp. 4978–90, 2007.

[28] Bendele, A., McComb, J., Gould, T., McAbee, T., Sennello, G., Chlipala, E., and Guy, M., "Animal models of arthritis: relevance to human disease," *Toxicol Pathol*, vol. 27, no. 1, pp. 134–42, 1999.

[29] Bendele, A. M., Chlipala, E. S., Scherrer, J., Frazier, J., Sennello, G., Rich, W. J., and Edwards, C. K., r., "Combination benefit of treatment with the cytokine inhibitors interleukin-1 receptor antagonist and pegylated soluble tumor necrosis factor receptor type i in animal models of rheumatoid arthritis," *Arthritis Rheum*, vol. 43, no. 12, pp. 2648–59, 2000.

[30] Bendele, A. M. and Hulman, J. F., "Spontaneous cartilage degeneration in guinea-pigs," *Arthritis and Rheumatism*, vol. 31, no. 4, pp. 561–565, 1988.

[31] Bendele, A. M., White, S. L., and Hulman, J. F., "Osteoarthrosis in guinea-pigs - histopathologic and scanning electron-microscopic features," *Laboratory Animal Science*, vol. 39, no. 2, pp. 115–121, 1989.

[32] Bendele, A. M., White, S. L., and Hulman, J. F., *Osteoarthritis in guinea pigs: Histopathologic and scanning electron microscopic features*. Washington D.C.: Registry of Comparative Pathology, 1991.

[33] Benito, M. J., Veale, D. J., FitzGerald, O., van den Berg, W. B., and Bresnihan, B., "Synovial tissue inflammation in early and late osteoarthritis," *Ann Rheum Dis*, vol. 64, no. 9, pp. 1263–7, 2005.

[34] Berenbaum, F., "Targeted therapies in osteoarthritis: a systematic review of the trials on www.clinicaltrials.gov," *Best Pract Res Clin Rheumatol*, vol. 24, no. 1, pp. 107–19, 2010.

[35] Bertrand, J., Cromme, C., Umlauf, D., Frank, S., and Pap, T., "Molecular mechanisms of cartilage remodelling in osteoarthritis," *Int J Biochem Cell Biol*, vol. 42, no. 10, pp. 1594–601, 2010.

[36] Betre, H., Liu, W., Zalutsky, M. R., Chilkoti, A., Kraus, V. B., and Setton, L. A., "A thermally responsive biopolymer for intra-articular drug delivery," *J Control Release*, vol. 115, no. 2, pp. 175–82, 2006.

[37] Bezemer, J. M., Radersma, R., Grijpma, D. W., Dijkstra, P. J., van Blitterswijk, C. A., and Feijen, J., "Microspheres for protein delivery prepared from amphiphilic multiblock copolymers. 2. modulation of release rate," *J Control Release*, vol. 67, no. 2-3, pp. 249–60, 2000.

[38] Bhattacharya, S., Franz, A., Li, X., and Jasti, B., "Synthesis of folate-conjugated amphiphiles for tumor-targeted drug delivery," *J Drug Target*, vol. 16, no. 10, pp. 780–9, 2008.

[39] Bias, P., Labrenz, R., and Rose, P., "Sustained-release dexamethasone palmitate - pharmacokinetics and efficacy in patients with activated inflammatory osteoarthritis of the knee," *Clinical Drug Investigation*, vol. 21, no. 6, pp. 429–436, 2001.

[40] Billinghurst, R. C., Dahlberg, L., Ionescu, M., Reiner, A., Bourne, R., Rorabeck, C., Mitchell, P., Hambor, J., Diekmann, O., Tschesche, H., Chen, J., Van Wart, H., and Poole, A. R., "Enhanced cleavage of type ii collagen by collagenases in osteoarthritic articular cartilage," *J Clin Invest*, vol. 99, no. 7, pp. 1534–45, 1997.

[41] Biovitrum(Amgen), "Kineret: Important product safety information," 2008.

[42] Bitton, R., "The economic burden of osteoarthritis," *Am J Manag Care*, vol. 15, no. 8 Suppl, pp. S230–5, 2009.

[43] Blom, A. B., van Lent, P. L., Holthuysen, A. E., van der Kraan, P. M., Roth, J., van Rooijen, N., and van den Berg, W. B., "Synovial lining macrophages mediate osteophyte formation during experimental osteoarthritis," *Osteoarthritis Cartilage*, vol. 12, no. 8, pp. 627–35, 2004.

[44] Blom, A. B., van Lent, P. L., Libregts, S., Holthuysen, A. E., van der Kraan, P. M., van Rooijen, N., and van den Berg, W. B., "Crucial role of macrophages in matrix metalloproteinase-mediated cartilage destruction during experimental osteoarthritis: involvement of matrix metalloproteinase 3," *Arthritis Rheum*, vol. 56, no. 1, pp. 147–57, 2007.

[45] Boerckel, J., Kolambkar, Y., Dupont, K., Uhring, B., Phelps, E., Stevens, H., Garcia, A. J., and Guldberg, R., "Effects of protein dose and delivery system on bmp-mediated bone regeneration," *Biomaterials*, vol. 32, pp. 5241–5251, 2011.

[46] Boggs, S. S., Patrene, K. D., Mueller, G. M., Evans, C. H., Doughty, L. A., and Robbins, P. D., "Prolonged systemic expression of human il-1 receptor antagonist (hil-1ra) in mice reconstituted with hematopoietic cells transduced with a retrovirus carrying the hil-1ra cdna," *Gene Ther*, vol. 2, no. 9, pp. 632–8, 1995.

[47] Bomsztyk, K., Sims, J. E., Stanton, T. H., Slack, J., McMahan, C. J., Valentine, M. A., and Dower, S. K., "Evidence for different interleukin 1 receptors in murine b- and t-cell lines," *Proc Natl Acad Sci U S A*, vol. 86, no. 20, pp. 8034–8, 1989.

[48] Bonanomi, M. H., Velvart, M., Stimpel, M., Roos, K. M., Fehr, K., and Weder, H. G., "Studies of pharmacokinetics and therapeutic effects of glucocorticoids entrapped in liposomes after intraarticular application in healthy rabbits and in rabbits with antigen-induced arthritis," *Rheumatol Int*, vol. 7, no. 5, pp. 203–12, 1987.

[49] Bondeson, J., "Activated synovial macrophages as targets for osteoarthritis drug therapy," *Curr Drug Targets*, vol. 11, no. 5, pp. 576–85, 2010.

[50] Bondeson, J., Blom, A. B., Wainwright, S., Hughes, C., Caterson, B., and van den Berg, W. B., "The role of synovial macrophages and macrophage-produced mediators in driving inflammatory and destructive responses in osteoarthritis," *Arthritis Rheum*, vol. 62, no. 3, pp. 647–57, 2010.

[51] Bondeson, J., Wainwright, S. D., Lauder, S., Amos, N., and Hughes, C. E., "The role of synovial macrophages and macrophage-produced cytokines in driving aggrecanases, matrix metalloproteinases, and other destructive and inflammatory responses in osteoarthritis," *Arthritis Res Ther*, vol. 8, no. 6, p. R187, 2006.

[52] Bonte, F. and Juliano, R. L., "Interactions of liposomes with serum proteins," *Chem Phys Lipids*, vol. 40, no. 2-4, pp. 359–72, 1986.

[53] Bontempo, D. and Maynard, H. D., "Streptavidin as a macroinitiator for polymerization: In situ protein-polymer conjugate formation," *Journal of the American Chemical Society*, vol. 127, no. 18, pp. 6508–6509, 2005.

[54] Bove, S., "Weight bearing as a measure of disease progression and efficacy of anti-inflammatory compounds in a model of monosodium iodoacetate-induced osteoarthritis," *Osteoarthritis and Cartilage*, vol. 11, no. 11, pp. 821–830, 2003.

[55] Bove, S. E., Laemont, K. D., Brooker, R. M., Osborn, M. N., Sanchez, B. M., Guzman, R. E., Hook, K. E., Juneau, P. L., Connor, J. R., and Kilgore, K. S., "Surgically induced osteoarthritis in the rat results in the development of both osteoarthritis-like joint pain and secondary hyperalgesia," *Osteoarthritis Cartilage*, vol. 14, no. 10, pp. 1041–8, 2006.

[56] Brandhonneur, N., Chevanne, F., Vie, V., Frisch, B., Primault, R., Le Potier, M. F., and Le Corre, P., "Specific and non-specific phagocytosis of ligand-grafted plga microspheres by macrophages," *Eur J Pharm Sci*, vol. 36, no. 4-5, pp. 474–85, 2009.

[57] Breitz, H. B., Weiden, P. L., Beaumier, P. L., Axworthy, D. B., Seiler, C., Su, F. M., Graves, S., Bryan, K., and Reno, J. M., "Clinical optimization of pretargeted radioimmunotherapy with antibody-streptavidin conjugate and 90y-dota-biotin," *J Nucl Med*, vol. 41, no. 1, pp. 131–40, 2000.

[58] Brennan, F. M., Chantry, D., Jackson, A. M., Maini, R. N., and Feldmann, M., "Cytokine production in culture by cells isolated from the synovial membrane," *J Autoimmun*, vol. 2 Suppl, pp. 177–86, 1989.

[59] Bresnihan, B., Alvaro-Gracia, J. M., Cobby, M., Doherty, M., Domljan, Z., Emery, P., Nuki, G., Pavelka, K., Rau, R., Rozman, B., Watt, I., Williams, B., Aitchison, R., McCabe, D., and Musikic, P., "Treatment of rheumatoid arthritis with recombinant human interleukin-1 receptor antagonist," *Arthritis Rheum*, vol. 41, no. 12, pp. 2196–204, 1998.

[60] Bridges, A. W., Whitmire, R. E., Singh, N., Templeman, K. L., Babensee, J. E., Lyon, L. A., and Garcia, A. J., "Chronic inflammatory responses to microgel-based implant coatings," *J Biomed Mater Res A*, vol. 94, no. 1, pp. 252–8, 2010.

[61] Brooks, P. M., "The burden of musculoskeletal disease–a global perspective," *Clin Rheumatol*, vol. 25, no. 6, pp. 778–81, 2006.

[62] Brown, K. E., Leong, K., Huang, C. H., Dalal, R., Green, G. D., Haimes, H. B., Jimenez, P. A., and Bathon, J., "Gelatin/chondroitin 6-sulfate microspheres for the delivery of therapeutic proteins to the joint," *Arthritis Rheum*, vol. 41, no. 12, pp. 2185–95, 1998.

[63] Butoescu, N., Seemayer, C. A., Foti, M., Jordan, O., and Doelker, E., "Dexamethasone-containing plga superparamagnetic microparticles as carriers for the local treatment of arthritis," *Biomaterials*, vol. 30, no. 9, pp. 1772–80, 2009.

[64] Calich, A. L., Domiciano, D. S., and Fuller, R., "Osteoarthritis: can anti-cytokine therapy play a role in treatment?," *Clin Rheumatol*, vol. 29, no. 5, pp. 451–5, 2010.

[65] Campion, G. V., Lebsack, M. E., Lookabaugh, J., Gordon, G., and Catalano, M., "Dose-range and dose-frequency study of recombinant human interleukin-1 receptor antagonist in patients with rheumatoid arthritis. the il-1ra arthritis study group," *Arthritis Rheum*, vol. 39, no. 7, pp. 1092–101, 1996.

[66] Caron, J. P., Fernandes, J. C., Martel-Pelletier, J., Tardif, G., Mineau, F., Geng, C., and Pelletier, J. P., "Chondroprotective effect of intraarticular injections of interleukin-1 receptor antagonist in experimental osteoarthritis. suppression of collagenase-1 expression," *Arthritis Rheum*, vol. 39, no. 9, pp. 1535–44, 1996.

[67] Carter, D. B., Deibel, M. R., J., Dunn, C. J., Tomich, C. S., Laborde, A. L., Slightom, J. L., Berger, A. E., Bienkowski, M. J., Sun, F. F., McEwan, R. N., and et al., "Purification, cloning, expression and biological characterization of an interleukin-1 receptor antagonist protein," *Nature*, vol. 344, no. 6267, pp. 633–8, 1990.

[68] CDC, "Osteoarthritis," 2011.

[69] Ceponis, A., Waris, E., Monkkonen, J., Laasonen, L., Hyttinen, M., Solovieva, S. A., Hanemaaijer, R., Bitsch, A., and Konttinen, Y. T., "Effects of low-dose, noncytotoxic, intraarticular liposomal clodronate on development

of erosions and proteoglycan loss in established antigen-induced arthritis in rabbits," *Arthritis Rheum*, vol. 44, no. 8, pp. 1908–16, 2001.

[70] Chen, G. and Hoffman, A. S., "Preparation and properties of thermoreversible, phase-separating enzyme-oligo(n-isopropylacrylamide) conjugates," *Bioconjug Chem*, vol. 4, no. 6, pp. 509–14, 1993.

[71] Cheng, C., Wei, H., Zhu, J. L., Chang, C., Cheng, H., Li, C., Cheng, S. X., Zhang, X. Z., and Zhuo, R. X., "Functionalized thermoresponsive micelles self-assembled from biotin-peg-b-p(nipaam-co-hmaam)-b-pmma for tumor cell target," *Bioconjug Chem*, vol. 19, no. 6, pp. 1194–201, 2008.

[72] Chevalier, X., "Upregulation of enzymatic activity by interleukin-1 in osteoarthritis," *Biomed Pharmacother*, vol. 51, no. 2, pp. 58–62, 1997.

[73] Chevalier, X., "Intraarticular treatments for osteoarthritis: new perspectives," *Curr Drug Targets*, vol. 11, no. 5, pp. 546–60, 2010.

[74] Chevalier, X., Goupille, P., Beaulieu, A. D., Burch, F. X., Bensen, W. G., Conrozier, T., Loeuille, D., Kivitz, A. J., Silver, D., and Appleton, B. E., "Intraarticular injection of anakinra in osteoarthritis of the knee: a multicenter, randomized, double-blind, placebo-controlled study," *Arthritis Rheum*, vol. 61, no. 3, pp. 344–52, 2009.

[75] Chiefari, J., Chong, Y. K., Ercole, F., Krstina, J., Jeffery, J., Le, T. P. T., Mayadunne, R. T. A., Meijs, G. F., Moad, C. L., Moad, G., Rizzardo, E., and Thang, S. H., "Living free-radical polymerization by reversible addition-fragmentation chain transfer: The raft process," *Macromolecules*, vol. 31, no. 16, pp. 5559–5562, 1998.

[76] Cialdai, C., Giuliani, S., Valenti, C., Tramontana, M., and Maggi, C. A., "Effect of intra-articular 4-(s)-amino-5-(4-4-[2,4-dichloro-3-(2,4-dimethyl-8-quinolyloxymethyl)phen ylsulfonamido]-tetrahydro-2H-4-pyranylcarbonyl piperazino)-5-oxopentyl](trimethyl)ammonium chloride hydrochloride (men16132), a kinin b2 receptor antagonist, on nociceptive response in monosodium iodoacetate-induced experimental osteoarthritis in rats," *J Pharmacol Exp Ther*, vol. 331, no. 3, pp. 1025–32, 2009.

[77] Clements, K. M., Price, J. S., Chambers, M. G., Visco, D. M., Poole, A. R., and Mason, R. M., "Gene deletion of either interleukin-1beta, interleukin-1beta-converting enzyme, inducible nitric oxide synthase, or stromelysin 1 accelerates the development of knee osteoarthritis in mice after surgical transection of the medial collateral ligament and partial medial meniscectomy," *Arthritis Rheum*, vol. 48, no. 12, pp. 3452–63, 2003.

[78] Cohen, S., Hurd, E., Cush, J., Schiff, M., Weinblatt, M. E., Moreland, L. W., Kremer, J., Bear, M. B., Rich, W. J., and McCabe, D., "Treatment of rheumatoid arthritis with anakinra, a recombinant human interleukin-1 receptor antagonist, in combination with methotrexate: results of a twenty-four-week, multicenter, randomized, double-blind, placebo-controlled trial," *Arthritis Rheum*, vol. 46, no. 3, pp. 614–24, 2002.

[79] Colotta, F., Dower, S. K., Sims, J. E., and Mantovani, A., "The type ii 'decoy' receptor: a novel regulatory pathway for interleukin 1," *Immunol Today*, vol. 15, no. 12, pp. 562–6, 1994.

[80] Colotta, F., Re, F., Muzio, M., Polentarutti, N., Minty, A., Caput, D., Ferrara, P., and Mantovani, A., "Interleukin-13 induces expression and release of interleukin-1 decoy receptor in human polymorphonuclear cells," *J Biol Chem*, vol. 269, no. 17, pp. 12403–6, 1994.

[81] Colotta, F., Saccani, S., Giri, J. G., Dower, S. K., Sims, J. E., Introna, M., and Mantovani, A., "Regulated expression and release of the il-1 decoy receptor in human mononuclear phagocytes," *J Immunol*, vol. 156, no. 7, pp. 2534–41, 1996.

[82] Cornelis, S., Kersse, K., Festjens, N., Lamkanfi, M., and Vandenabeele, P., "Inflammatory caspases: targets for novel therapies," *Curr Pharm Des*, vol. 13, no. 4, pp. 367–85, 2007.

[83] Cunnane, G., Madigan, A., Murphy, E., FitzGerald, O., and Bresnihan, B., "The effects of treatment with interleukin-1 receptor antagonist on the inflamed synovial membrane in rheumatoid arthritis," *Rheumatology (Oxford)*, vol. 40, no. 1, pp. 62–9, 2001.

[84] Curtis, B. M., Widmer, M. B., deRoos, P., and Qwarnstrom, E. E., "Il-1 and its receptor are translocated to the nucleus," *J Immunol*, vol. 144, no. 4, pp. 1295–303, 1990.

[85] Dawson, J., Engelhardt, P., Kastelic, T., Cheneval, D., MacKenzie, A., and Ramage, P., "Effects of soluble interleukin-1 type ii receptor on rabbit antigen-induced arthritis: clinical, biochemical and histological assessment," *Rheumatology (Oxford)*, vol. 38, no. 5, pp. 401–6, 1999.

[86] De, P., Gondi, S. R., and Sumerlin, B. S., "Folate-conjugated thermoresponsive block copolymers: highly efficient conjugation and solution self-assembly," *Biomacromolecules*, vol. 9, no. 3, pp. 1064–70, 2008.

[87] Deleuran, B. W., Chu, C. Q., Field, M., Brennan, F. M., Katsikis, P., Feldmann, M., and Maini, R. N., "Localization of interleukin-1 alpha, type 1 interleukin-1 receptor and interleukin-1 receptor antagonist in the synovial membrane and cartilage/pannus junction in rheumatoid arthritis," *Br J Rheumatol*, vol. 31, no. 12, pp. 801–9, 1992.

[88] Deleuran, B. W., Chu, C. Q., Field, M., Brennan, F. M., Mitchell, T., Feldmann, M., and Maini, R. N., "Localization of tumor necrosis factor receptors in the synovial tissue and cartilage-pannus junction in patients with rheumatoid arthritis. implications for local actions of tumor necrosis factor alpha," *Arthritis Rheum*, vol. 35, no. 10, pp. 1170–8, 1992.

[89] Deyerle, K. L., Sims, J. E., Dower, S. K., and Bothwell, M. A., "Pattern of il-1 receptor gene expression suggests role in noninflammatory processes," *J Immunol*, vol. 149, no. 5, pp. 1657–65, 1992.

[90] Dickensheets, H. L. and Donnelly, R. P., "Ifn-gamma and il-10 inhibit induction of il-1 receptor type i and type ii gene expression by il-4 and il-13 in human monocytes," *J Immunol*, vol. 159, no. 12, pp. 6226–33, 1997.

[91] Dinarello, C. A., "Biologic basis for interleukin-1 in disease," *Blood*, vol. 87, no. 6, pp. 2095–147, 1996.

[92] Dinarello, C. A., "Interleukin-1, interleukin-1 receptors and interleukin-1 receptor antagonist," *Int Rev Immunol*, vol. 16, no. 5-6, pp. 457–99, 1998.

[93] Dinarello, C. A., "The il-1 family and inflammatory diseases," *Clin Exp Rheumatol*, vol. 20, no. 5 Suppl 27, pp. S1–13, 2002.

[94] Dinarello, C. A., "Immunological and inflammatory functions of the interleukin-1 family," *Annu Rev Immunol*, vol. 27, pp. 519–50, 2009.

[95] Dinarello, C. A. and Savage, N., "Interleukin-1 and its receptor," *Crit Rev Immunol*, vol. 9, no. 1, pp. 1–20, 1989.

[96] Ding, A. and Schwendeman, S., "Acidic microclimate ph distribution in plga microspheres monitored by confocal laser scanning microscopy.," *Pharm Res*, vol. 25, pp. 2041–2052, 2008.

[97] Ding, N., "Polymeric micelle-based local delivery methods and devices," 2007.

[98] Dinser, R., "Animal models for arthritis," *Best Pract Res Clin Rheumatol*, vol. 22, no. 2, pp. 253–67, 2008.

[99] Dower, S. K., Kronheim, S. R., Hopp, T. P., Cantrell, M., Deeley, M., Gillis, S., Henney, C. S., and Urdal, D. L., "The cell surface receptors for interleukin-1 alpha and interleukin-1 beta are identical," *Nature*, vol. 324, no. 6094, pp. 266–8, 1986.

[100] Dower, S. K., Kronheim, S. R., March, C. J., Conlon, P. J., Hopp, T. P., Gillis, S., and Urdal, D. L., "Detection and characterization of high affinity plasma membrane receptors for human interleukin 1," *J Exp Med*, vol. 162, no. 2, pp. 501–15, 1985.

[101] Dripps, D. J., Brandhuber, B. J., Thompson, R. C., and Eisenberg, S. P., "Interleukin-1 (il-1) receptor antagonist binds to the 80-kda il-1 receptor but does not initiate il-1 signal transduction," *J Biol Chem*, vol. 266, no. 16, pp. 10331–6, 1991.

[102] Dripps, D. J., Verderber, E., Ng, R. K., Thompson, R. C., and Eisenberg, S. P., "Interleukin-1 receptor antagonist binds to the type ii interleukin-1 receptor on b cells and neutrophils," *J Biol Chem*, vol. 266, no. 30, pp. 20311–5, 1991.

[103] Dubois, C. M., Ruscetti, F. W., Palaszynski, E. W., Falk, L. A., Oppenheim, J. J., and Keller, J. R., "Transforming growth factor beta is a potent inhibitor of interleukin 1 (il-1) receptor expression: proposed mechanism of inhibition of il-1 action," *J Exp Med*, vol. 172, no. 3, pp. 737–44, 1990.

[104] Dufresne, M. H., Gauthier, M. A., and Leroux, J. C., "Thiol-functionalized polymeric micelles: from molecular recognition to improved mucoadhesion," *Bioconjug Chem*, vol. 16, no. 4, pp. 1027–33, 2005.

[105] Dumond, H., Presle, N., Pottie, P., Pacquelet, S., Terlain, B., Netter, P., Gepstein, A., Livne, E., and Jouzeau, J. Y., "Site specific changes in gene expression and cartilage metabolism during early experimental osteoarthritis," *Osteoarthritis Cartilage*, vol. 12, no. 4, pp. 284–95, 2004.

[106] Duong, H. T. T., Nguyen, T. L. U., and Stenzel, M. H., "Micelles with surface conjugated rgd peptide and crosslinked polyurea core via raft polymerization," *Polymer Chemistry*, vol. 1, no. 2, pp. 171–182, 2010.

[107] Düzgüneş, N., *Liposomes*. No. v. 465 in Methods in enzymology, Elsevier Academic Press, 2009.

[108] Economides, A. N., Carpenter, L. R., Rudge, J. S., Wong, V., Koehler-Stec, E. M., Hartnett, C., Pyles, E. A., Xu, X., Daly, T. J., Young, M. R., Fandl, J. P., Lee, F., Carver, S., McNay, J., Bailey, K., Ramakanth, S., Hutabarat, R., Huang, T. T., Radziejewski, C., Yancopoulos, G. D., and Stahl, N., "Cytokine traps: multi-component, high-affinity blockers of cytokine action," *Nat Med*, vol. 9, no. 1, pp. 47–52, 2003.

[109] Edwards, S. H., "Intra-articular drug delivery: The challenge to extend drug residence time within the joint," *Vet J*, vol. 190, no. 1, pp. 15–21, 2011.

[110] Eisenberg, S. P., Brewer, M. T., Verderber, E., Heimdal, P., Brandhuber, B. J., and Thompson, R. C., "Interleukin 1 receptor antagonist is a member of the interleukin 1 gene family: evolution of a cytokine control mechanism," *Proc Natl Acad Sci U S A*, vol. 88, no. 12, pp. 5232–6, 1991.

[111] Eisenberg, S. P., Evans, R. J., Arend, W. P., Verderber, E., Brewer, M. T., Hannum, C. H., and Thompson, R. C., "Primary structure and functional expression from complementary dna of a human interleukin-1 receptor antagonist," *Nature*, vol. 343, no. 6256, pp. 341–6, 1990.

[112] ElBayoumi, T. A. and Torchilin, V. P., "Tumor-targeted nanomedicines: enhanced antitumor efficacy in vivo of doxorubicin-loaded, long-circulating liposomes modified with cancer-specific monoclonal antibody," *Clin Cancer Res*, vol. 15, no. 6, pp. 1973–80, 2009.

[113] Elbayoumi, T. A. and Torchilin, V. P., "Current trends in liposome research," *Methods Mol Biol*, vol. 605, pp. 1–27, 2010.

[114] Elron-Gross, I., Glucksam, Y., and Margalit, R., "Liposomal dexamethasone-diclofenac combinations for local osteoarthritis treatment," *Int J Pharm*, vol. 376, no. 1-2, pp. 84–91, 2009.

[115] Evans, C. H., Ghivizzani, S. C., and Robbins, P. D., "Orthopedic gene therapy in 2008," *Mol Ther*, vol. 17, no. 2, pp. 231–44, 2009.

[116] Evans, C. H., Gouze, J. N., Gouze, E., Robbins, P. D., and Ghivizzani, S. C., "Osteoarthritis gene therapy," *Gene Ther*, vol. 11, no. 4, pp. 379–89, 2004.

[117] Evans, C. H., Robbins, P. D., Ghivizzani, S. C., Herndon, J. H., Kang, R., Bahnson, A. B., Barranger, J. A., Elders, E. M., Gay, S., Tomaino,

M. M., Wasko, M. C., Watkins, S. C., Whiteside, T. L., Glorioso, J. C., Lotze, M. T., and Wright, T. M., "Clinical trial to assess the safety, feasibility, and efficacy of transferring a potentially anti-arthritic cytokine gene to human joints with rheumatoid arthritis," *Hum Gene Ther*, vol. 7, no. 10, pp. 1261–80, 1996.

[118] Evans, C. H., Robbins, P. D., Ghivizzani, S. C., Wasko, M. C., Tomaino, M. M., Kang, R., Muzzonigro, T. A., Vogt, M., Elder, E. M., Whiteside, T. L., Watkins, S. C., and Herndon, J. H., "Gene transfer to human joints: progress toward a gene therapy of arthritis," *Proc Natl Acad Sci U S A*, vol. 102, no. 24, pp. 8698–703, 2005.

[119] Evans, R. J., Bray, J., Childs, J. D., Vigers, G. P., Brandhuber, B. J., Skalicky, J. J., Thompson, R. C., and Eisenberg, S. P., "Mapping receptor binding sites in interleukin (il)-1 receptor antagonist and il-1 beta by site-directed mutagenesis. identification of a single site in il-1ra and two sites in il-1 beta," *J Biol Chem*, vol. 270, no. 19, pp. 11477–83, 1995.

[120] Fahlman, B. D., *Materials Chemistry*. Springer London, Limited, 2011.

[121] Fan, Z., Soder, S., Oehler, S., Fundel, K., and Aigner, T., "Activation of interleukin-1 signaling cascades in normal and osteoarthritic articular cartilage," *Am J Pathol*, vol. 171, no. 3, pp. 938–46, 2007. Fan, Zhiyong Soder, Stephan Oehler, Stephan Fundel, Katrin Aigner, Thomas Research Support, Non-U.S. Gov't United States The American journal of pathology Am J Pathol. 2007 Sep;171(3):938-46. Epub 2007 Jul 19.

[122] Farahat, M. N., Yanni, G., Poston, R., and Panayi, G. S., "Cytokine expression in synovial membranes of patients with rheumatoid arthritis and osteoarthritis," *Ann Rheum Dis*, vol. 52, no. 12, pp. 870–5, 1993.

[123] FDA, "Summary minutes: Arthritis advisory committee of the fda," May 7, 1999 1996.

[124] Fernandes, J., Tardif, G., Martel-Pelletier, J., Lascau-Coman, V., Dupuis, M., Moldovan, F., Sheppard, M., Krishnan, B. R., and Pelletier, J. P., "In vivo transfer of interleukin-1 receptor antagonist gene in osteoarthritic rabbit knee joints: prevention of osteoarthritis progression," *Am J Pathol*, vol. 154, no. 4, pp. 1159–69, 1999.

[125] Fernandes, J. C., Martel-Pelletier, J., and Pelletier, J. P., "The role of cytokines in osteoarthritis pathophysiology," *Biorheology*, vol. 39, no. 1-2, pp. 237–46, 2002.

[126] Fernihough, J., Gentry, C., Malcangio, M., Fox, A., Rediske, J., Pellas, T., Kidd, B., Bevan, S., and Winter, J., "Pain related behaviour in two models of osteoarthritis in the rat knee," *Pain*, vol. 112, no. 1-2, pp. 83–93, 2004.

[127] Ferreira-Gomes, J., Adaes, S., and Castro-Lopes, J. M., "Assessment of movement-evoked pain in osteoarthritis by the knee-bend and catwalk tests: a clinically relevant study," *J Pain*, vol. 9, no. 10, pp. 945–54, 2008.

[128] Firestein, G. S., Boyle, D. L., Yu, C., Paine, M. M., Whisenand, T. D., Zvaifler, N. J., and Arend, W. P., "Synovial interleukin-1 receptor antagonist and interleukin-1 balance in rheumatoid arthritis," *Arthritis Rheum*, vol. 37, no. 5, pp. 644–52, 1994.

[129] Firestein, G. S., Budd, R. C., Harris, E. D. J., McInnes, I. B., Ruddy, S., and Sergent, J. S., *Kelley's Textbook of Rheumatology, 8th Edition*, vol. 1. W. B. Saunders Company, 8th ed., 2009.

[130] Fischer, D., Bieber, T., Li, Y., Elsasser, H.-P., and Kissel, T., "A novel non-viral vector for dna delivery based on low molecular weight, branched polyethyleneimine: Effect of molecular weight on transfection efficiency and cytotoxicity," *Pharm Res*, vol. 16, pp. 1273–1279, 1999.

[131] Fischer, D., Li, Y., Ahlemeyer, B., Krieglstein, J., and Kissel, T., "In vitro cytotoxicity testing of polycations: influence of polymer structure on cell viability and hemolysis," *Biomaterials*, vol. 24, pp. 1121–1131, 2003.

[132] Flexyx, "Kineret (amgen inc.) (generic name - anakinra) online information," 2008.

[133] Fosang, A. J. and Little, C. B., "Drug insight: aggrecanases as therapeutic targets for osteoarthritis," *Nat Clin Pract Rheumatol*, vol. 4, no. 8, pp. 420–7, 2008.

[134] Fosang, A. J., Rogerson, F. M., East, C. J., and Stanton, H., "Adamts-5: the story so far," *Eur Cell Mater*, vol. 15, pp. 11–26, 2008.

[135] Fox, B. A. and Stephens, M. M., "Treatment of knee osteoarthritis with orthokine-derived autologous conditioned serum," *Expert Rev Clin Immunol*, vol. 6, no. 3, pp. 335–45, 2010.

[136] Foxwell, B. M., Barrett, K., and Feldmann, M., "Cytokine receptors: structure and signal transduction," *Clin Exp Immunol*, vol. 90, no. 2, pp. 161–9, 1992.

[137] Fredericks, L. Z., Forte, C., Capuano, I. V., Zhou, H., Vanden Bos, T., and Carter, P., "Identification of potent human anti-il-1ri antagonist antibodies," *Protein Eng Des Sel*, vol. 17, pp. 95–106, 2004.

[138] Freemont, A. J., Byers, R. J., Taiwo, Y. O., and Hoyland, J. A., "In situ zymographic localisation of type ii collagen degrading activity in osteoarthritic human articular cartilage," *Ann Rheum Dis*, vol. 58, no. 6, pp. 357–65, 1999.

[139] Frisbie, D. D., Ghivizzani, S. C., Robbins, P. D., Evans, C. H., and McIlwraith, C. W., "Treatment of experimental equine osteoarthritis by in vivo delivery of the equine interleukin-1 receptor antagonist gene," *Gene Ther*, vol. 9, no. 1, pp. 12–20, 2002.

[140] Gabizon, A. and Martin, F., "Polyethylene glycol-coated (pegylated) liposomal doxorubicin. rationale for use in solid tumours," *Drugs*, vol. 54 Suppl 4, pp. 15–21, 1997.

[141] Gaertner, H. F. and Offord, R. E., "Site-specific attachment of functionalized poly(ethylene glycol) to the amino terminus of proteins," *Bioconjug Chem*, vol. 7, no. 1, pp. 38–44, 1996.

[142] Gao, W., Liu, W., Christensen, T., Zalutsky, M. R., and Chilkoti, A., "In situ growth of a peg-like polymer from the c terminus of an intein fusion protein improves pharmacokinetics and tumor accumulation," *Proc Natl Acad Sci U S A*, vol. 107, no. 38, pp. 16432–7, 2010.

[143] Garnier, S. and Laschewsky, A., "Non-ionic amphiphilic block copolymers by raft-polymerization and their self-organization," *Colloid and Polymer Science*, vol. 284, no. 11, pp. 1243–1254, 2006.

[144] Gaucher, G., Dufresne, M. H., Sant, V. P., Kang, N., Maysinger, D., and Leroux, J. C., "Block copolymer micelles: preparation, characterization and application in drug delivery," *J Control Release*, vol. 109, no. 1-3, pp. 169–88, 2005.

[145] Georgescu, H. I., Mendelow, D., and Evans, C. H., "Hig-82: an established cell line from rabbit periarticular soft tissue, which retains the "activatable" phenotype," *In Vitro Cell Dev Biol*, vol. 24, no. 10, pp. 1015–22, 1988.

[146] Gerwin, N., Hops, C., and Lucke, A., "Intraarticular drug delivery in osteoarthritis," *Adv Drug Deliv Rev*, vol. 58, no. 2, pp. 226–42, 2006.

[147] Girard, S., Kadhim, H., Larouche, A., Roy, M., Gobeil, F., and Sebire, G., "Pro-inflammatory disequilibrium of the il-1 beta/il-1ra ratio in an experimental model of perinatal brain damages induced by lipopolysaccharide and hypoxia-ischemia," *Cytokine*, vol. 43, no. 1, pp. 54–62, 2008.

[148] Giteau, A., Venier-Julienne, M., Aubert-Pouessel, A., and Benoit, J. P., "How to achieve sustained and complete protein release from plga-based microparticles," *Int J Pharm*, vol. 350, pp. 14–26, 2008.

[149] Glasson, S. S., Askew, R., Sheppard, B., Carito, B., Blanchet, T., Ma, H. L., Flannery, C. R., Peluso, D., Kanki, K., Yang, Z., Majumdar, M. K., and Morris, E. A., "Deletion of active adamts5 prevents cartilage degradation in a murine model of osteoarthritis," *Nature*, vol. 434, no. 7033, pp. 644–8, 2005.

[150] Glasson, S. S., Askew, R., Sheppard, B., Carito, B. A., Blanchet, T., Ma, H. L., Flannery, C. R., Kanki, K., Wang, E., Peluso, D., Yang, Z., Majumdar, M. K., and Morris, E. A., "Characterization of and osteoarthritis susceptibility in adamts-4-knockout mice," *Arthritis Rheum*, vol. 50, no. 8, pp. 2547–58, 2004.

[151] Goldring, M. B., "The role of cytokines as inflammatory mediators in osteoarthritis: lessons from animal models," *Connect Tissue Res*, vol. 40, no. 1, pp. 1–11, 1999.

[152] Goldring, M. B., "Update on the biology of the chondrocyte and new approaches to treating cartilage diseases," *Best Pract Res Clin Rheumatol*, vol. 20, no. 5, pp. 1003–25, 2006.

[153] Goldring, M. B. and Goldring, S. R., "Osteoarthritis," *J Cell Physiol*, vol. 213, no. 3, pp. 626–34, 2007.

[154] Goldring, S. R. and Goldring, M. B., "Clinical aspects, pathology and pathophysiology of osteoarthritis," *J Musculoskelet Neuronal Interact*, vol. 6, no. 4, pp. 376–8, 2006.

[155] Goldring, S. R., "Osteoporosis and rheumatic diseases," *Primer on the metabolic bone diseases and disorders of mineral metabolism, Third edition*, pp. 299–301, 1996.

[156] Goupille, P., Mulleman, D., and Chevalier, X., "Is interleukin-1 a good target for therapeutic intervention in intervertebral disc degeneration: lessons from the osteoarthritic experience," *Arthritis Res Ther*, vol. 9, no. 6, p. 110, 2007.

[157] Gouze, E., Pawliuk, R., Gouze, J. N., Pilapil, C., Fleet, C., Palmer, G. D., Evans, C. H., Leboulch, P., and Ghivizzani, S. C., "Lentiviral-mediated gene delivery to synovium: potent intra-articular expression with amplification by inflammation," *Mol Ther*, vol. 7, no. 4, pp. 460–6, 2003.

[158] Gouze, E., Pawliuk, R., Pilapil, C., Gouze, J. N., Fleet, C., Palmer, G. D., Evans, C. H., Leboulch, P., and Ghivizzani, S. C., "In vivo gene delivery to synovium by lentiviral vectors," *Mol Ther*, vol. 5, no. 4, pp. 397–404, 2002.

[159] Gouze, J. N., Gouze, E., Palmer, G. D., Liew, V. S., Pascher, A., Betz, O. B., Thornhill, T. S., Evans, C. H., Grodzinsky, A. J., and Ghivizzani, S. C., "A comparative study of the inhibitory effects of interleukin-1 receptor antagonist following administration as a recombinant protein or by gene transfer," *Arthritis Res Ther*, vol. 5, no. 5, pp. R301–9, 2003.

[160] Greenfeder, S. A., Varnell, T., Powers, G., Lombard-Gillooly, K., Shuster, D., McIntyre, K. W., Ryan, D. E., Levin, W., Madison, V., and Ju, G., "Insertion of a structural domain of interleukin (il)-1 beta confers agonist activity to the il-1 receptor antagonist. implications for il-1 bioactivity," *J Biol Chem*, vol. 270, no. 38, pp. 22460–6, 1995.

[161] Griffith, L., "Polymeric biomaterials," *Acta Materialia*, vol. 48, pp. 263–277, 2007.

[162] Guingamp, C., Gegout-Pottie, P., Philippe, L., Terlain, B., Netter, P., and Gillet, P., "Mono-iodoacetate-induced experimental osteoarthritis: a dose-response study of loss of mobility, morphology, and biochemistry," *Arthritis Rheum*, vol. 40, no. 9, pp. 1670–9, 1997.

[163] Guzman, R. E., Evans, M. G., Bove, S., Morenko, B., and Kilgore, K., "Mono-iodoacetate-induced histologic changes in subchondral bone and articular cartilage of rat femorotibial joints: an animal model of osteoarthritis," *Toxicol Pathol*, vol. 31, no. 6, pp. 619–24, 2003.

[164] Hakkarainen, M., Hoglund, A., Odelius, K., and Albertsson, A.-C., "Tuning the release rate of acidic degradation products through macromolecular design of caprolactone-based copolymers," *Journal of the American Chemical Society*, vol. 129, pp. 6308–6312, 2007.

[165] Hamstra, D. A., Page, M., Maybaum, J., and Rehemtulla, A., "Expression of endogenously activated secreted or cell surface carboxypeptidase a sensitizes tumor cells to methotrexate-alpha-peptide prodrugs," *Cancer Res*, vol. 60, no. 3, pp. 657–65, 2000.

[166] Hannum, C. H., Wilcox, C. J., Arend, W. P., Joslin, F. G., Dripps, D. J., Heimdal, P. L., Armes, L. G., Sommer, A., Eisenberg, S. P., and Thompson,

R. C., "Interleukin-1 receptor antagonist activity of a human interleukin-1 inhibitor," *Nature*, vol. 343, no. 6256, pp. 336–40, 1990.

[167] Haskill, S., Martin, G., Van Le, L., Morris, J., Peace, A., Bigler, C. F., Jaffe, G. J., Hammerberg, C., Sporn, S. A., Fong, S., and et al., "cdna cloning of an intracellular form of the human interleukin 1 receptor antagonist associated with epithelium," *Proc Natl Acad Sci U S A*, vol. 88, no. 9, pp. 3681–5, 1991.

[168] Haupt, J. L., Frisbie, D. D., McIlwraith, C. W., Robbins, P. D., Ghivizzani, S., Evans, C. H., and Nixon, A. J., "Dual transduction of insulin-like growth factor-i and interleukin-1 receptor antagonist protein controls cartilage degradation in an osteoarthritic culture model," *J Orthop Res*, vol. 23, no. 1, pp. 118–26, 2005.

[169] Haynes, M. K., Hume, E. L., and Smith, J. B., "Phenotypic characterization of inflammatory cells from osteoarthritic synovium and synovial fluids," *Clin Immunol*, vol. 105, no. 3, pp. 315–25, 2002.

[170] Hein, C. D., Liu, X. M., and Wang, D., "Click chemistry, a powerful tool for pharmaceutical sciences," *Pharm Res*, vol. 25, no. 10, pp. 2216–30, 2008.

[171] Heredia, K. L., Bontempo, D., Ly, T., Byers, J. T., Halstenberg, S., and Maynard, H. D., "In situ preparation of protein - "smart" polymer conjugates with retention of bioactivity," *Journal of the American Chemical Society*, vol. 127, no. 48, pp. 16955–16960, 2005.

[172] Hochberg, M. C., "Epidemiologic considerations in the primary prevention of osteoarthritis," *J Rheumatol*, vol. 18, no. 10, pp. 1438–40, 1991.

[173] Holt, L. J., Basran, A., Jones, K., Chorlton, J., Jespers, L. S., Brewis, N. D., and Tomlinson, I. M., "Anti-serum albumin domain antibodies for extending the half-lives of short lived drugs," *Protein Eng Des Sel*, vol. 21, no. 5, pp. 283–8, 2008.

[174] Homma, A., Sato, H., Okamachi, A., Emura, T., Ishizawa, T., Kato, T., Matsuura, T., Sato, S., Tamura, T., Higuchi, Y., Watanabe, T., Kitamura, H., Asanuma, K., Yamazaki, T., Ikemi, M., Kitagawa, H., Morikawa, T., Ikeya, H., Maeda, K., Takahashi, K., Nohmi, K., Izutani, N., Kanda, M., and Suzuki, R., "Novel hyaluronic acid-methotrexate conjugates for osteoarthritis treatment," *Bioorg Med Chem*, vol. 17, no. 13, pp. 4647–56, 2009.

[175] Homma, A., Sato, H., Tamura, T., Okamachi, A., Emura, T., Ishizawa, T., Kato, T., Matsuura, T., Sato, S., Higuchi, Y., Watanabe, T., Kitamura, H., Asanuma, K., Yamazaki, T., Ikemi, M., Kitagawa, H., Morikawa, T., Ikeya, H., Maeda, K., Takahashi, K., Nohmi, K., Izutani, N., Kanda, M., and Suzuki, R., "Synthesis and optimization of hyaluronic acid-methotrexate conjugates to maximize benefit in the treatment of osteoarthritis," *Bioorg Med Chem*, vol. 18, no. 3, pp. 1062–75, 2010.

[176] Hong, C. Y. and Pan, C. Y., "Direct synthesis of biotinylated stimuli-responsive polymer and diblock copolymer by raft polymerization using biotinylated trithiocarbonate as raft agent," *Macromolecules*, vol. 39, no. 10, pp. 3517–3524, 2006.

[177] Horai, R., Saijo, S., Tanioka, H., Nakae, S., Sudo, K., Okahara, A., Ikuse, T., Asano, M., and Iwakura, Y., "Development of chronic inflammatory arthropathy resembling rheumatoid arthritis in interleukin 1 receptor antagonist-deficient mice," *J Exp Med*, vol. 191, no. 2, pp. 313–20, 2000.

[178] Horisawa, E., Hirota, T., Kawazoe, S., Yamada, J., Yamamoto, H., Takeuchi, H., and Kawashima, Y., "Prolonged anti-inflammatory action of dl-lactide/glycolide copolymer nanospheres containing betamethasone sodium phosphate for an intra-articular delivery system in antigen-induced arthritic rabbit," *Pharm Res*, vol. 19, no. 4, pp. 403–10, 2002.

[179] Horisawa, E., Kubota, K., Tuboi, I., Sato, K., Yamamoto, H., Takeuchi, H., and Kawashima, Y., "Size-dependency of dl-lactide/glycolide copolymer particulates for intra-articular delivery system on phagocytosis in rat synovium," *Pharm Res*, vol. 19, no. 2, pp. 132–9, 2002.

[180] Hu, X. L., Liu, S., Chen, X. S., Mo, G. J., Xie, Z. G., and Jing, X. B., "Biodegradable amphiphilic block copolymers bearing protected hydroxyl groups: Synthesis and characterization," *Biomacromolecules*, vol. 9, no. 2, pp. 553–560, 2008.

[181] Huang, K. and Wu, L. D., "Aggrecanase and aggrecan degradation in osteoarthritis: a review," *J Int Med Res*, vol. 36, no. 6, pp. 1149–60, 2008.

[182] Hunt, C. A., "Liposomes disposition in vivo. v. liposome stability in plasma and implications for drug carrier function," *Biochim Biophys Acta*, vol. 719, no. 3, pp. 450–63, 1982.

[183] Hwang, J., Li, R. C., and Maynard, H. D., "Well-defined polymers with activated ester and protected aldehyde side chains for bio-functionalization," *J Control Release*, vol. 122, no. 3, pp. 279–86, 2007.

[184] Iliopoulos, D., Malizos, K. N., Oikonomou, P., and Tsezou, A., "Integrative microrna and proteomic approaches identify novel osteoarthritis genes and their collaborative metabolic and inflammatory networks," *PLoS One*, vol. 3, no. 11, p. e3740, 2008.

[185] Inglis, J. J., Schutze, M. U., and McNamee, K. E., "What we have learned about pain from rodent models of arthritis," *Curr Rheumatol Rev*, vol. 6, no. 3, 2010.

[186] Ishii, H., Tanaka, H., Katoh, K., Nakamura, H., Nagashima, M., and Yoshino, S., "Characterization of infiltrating t cells and th1/th2-type cytokines in the synovium of patients with osteoarthritis," *Osteoarthritis Cartilage*, vol. 10, no. 4, pp. 277–81, 2002. Ishii, H Tanaka, H Katoh, K Nakamura, H Nagashima, M Yoshino, S England Osteoarthritis and cartilage / OARS, Osteoarthritis Research Society Osteoarthritis Cartilage. 2002 Apr;10(4):277-81.

[187] Jacques, C., Gosset, M., Berenbaum, F., and Gabay, C., "The role of il-1 and il-1ra in joint inflammation and cartilage degradation," *Vitam Horm*, vol. 74, pp. 371–403, 2006.

[188] Jen, A. and Merkle, H. P., "Diamonds in the rough: protein crystals from a formulation perspective," *Pharm Res*, vol. 18, no. 11, pp. 1483–8, 2001.

[189] Jochum, F. D., Roth, P. J., Kessler, D., and Theato, P., "Double thermoresponsive block copolymers featuring a biotin end group," *Biomacromolecules*, vol. 11, no. 9, pp. 2432–2439, 2010.

[190] Johnson, P., Skornia, S., Stabenfelt, S., and Willits, R., "Maintaining bioactivity of ngf for controlled release from plga using peg," *J Biomed Mater Res A*, vol. 86A, pp. 420–427, 2008.

[191] Joosten, L. A., Helsen, M. M., van de Loo, F. A., and van den Berg, W. B., "Anticytokine treatment of established type ii collagen-induced arthritis in dba/1 mice. a comparative study using anti-tnf alpha, anti-il-1 alpha/beta, and il-1ra," *Arthritis Rheum*, vol. 39, no. 5, pp. 797–809, 1996.

[192] Joralemon, M. J., Smith, N. L., Holowka, D., Baird, B., and Wooley, K. L., "Antigen-decorated shell cross-linked nanoparticles: synthesis, characterization, and antibody interactions," *Bioconjug Chem*, vol. 16, no. 5, pp. 1246–56, 2005.

[193] Jule, E., Nagasaki, Y., and Kataoka, K., "Lactose-installed poly(ethylene glycol)-poly(d,l-lactide) block copolymer micelles exhibit fast-rate binding and high affinity toward a protein bed simulating a cell surface. a surface plasmon resonance study," *Bioconjugate Chemistry*, vol. 14, no. 1, pp. 177–186, 2003. Times Cited: 50.

[194] Karna, E., Miltyk, W., Palka, J. A., Jarzabek, K., and Wolczynski, S., "Hyaluronic acid counteracts interleukin-1-induced inhibition of collagen biosynthesis in cultured human chondrocytes," *Pharmacol Res*, vol. 54, no. 4, pp. 275–81, 2006.

[195] Kay, J. D., Gouze, E., Oligino, T. J., Gouze, J. N., Watson, R. S., Levings, P. P., Bush, M. L., Dacanay, A., Nickerson, D. M., Robbins, P. D., Evans, C. H., and Ghivizzani, S. C., "Intra-articular gene delivery and expression of interleukin-1ra mediated by self-complementary adeno-associated virus," *J Gene Med*, vol. 11, no. 7, pp. 605–14, 2009.

[196] Kedar, U., Phutane, P., Shidhaye, S., and Kadam, V., "Advances in polymeric micelles for drug delivery and tumor targeting," *Nanomedicine*, vol. 6, no. 6, pp. 714–29, 2010.

[197] Kim, D. H., Smith, J. T., Chilkoti, A., and Reichert, W. M., "The effect of covalently immobilized rhil-1ra-elp fusion protein on the inflammatory profile of lps-stimulated human monocytes," *Biomaterials*, vol. 28, no. 23, pp. 3369–77, 2007.

[198] Kim, Y., Hechler, B., Gao, Z.-G., Gachet, C., and Jacobson, K. A., "Pegylated dendritic unimolecular micelles as versatile carriers for ligands of g protein-coupled receptors," *Bioconjugate Chemistry*, vol. 20, no. 10, 2009.

[199] Kobayashi, M., Squires, G. R., Mousa, A., Tanzer, M., Zukor, D. J., Antoniou, J., Feige, U., and Poole, A. R., "Role of interleukin-1 and tumor necrosis factor alpha in matrix degradation of human osteoarthritic cartilage," *Arthritis Rheum*, vol. 52, no. 1, pp. 128–35, 2005.

[200] Koning, G. A., Schiffelers, R. M., Wauben, M. H., Kok, R. J., Mastrobattista, E., Molema, G., ten Hagen, T. L., and Storm, G., "Targeting of

angiogenic endothelial cells at sites of inflammation by dexamethasone phosphate-containing rgd peptide liposomes inhibits experimental arthritis," *Arthritis Rheum*, vol. 54, no. 4, pp. 1198–208, 2006.

[201] Korytkowska-Walach, A., Porwol, A., and Gibas, M., "Temperature-responsive hydrogels containing new lcst methacrylate macromonomers," *E-Polymers*, 2007.

[202] Kotlarz, H., Gunnarsson, C. L., Fang, H., and Rizzo, J. A., "Insurer and out-of-pocket costs of osteoarthritis in the us: evidence from national survey data," *Arthritis Rheum*, vol. 60, no. 12, pp. 3546–53, 2009.

[203] Kotlarz, H., Gunnarsson, C. L., Fang, H., and Rizzo, J. A., "Osteoarthritis and absenteeism costs: evidence from us national survey data," *J Occup Environ Med*, vol. 52, no. 3, pp. 263–8, 2010.

[204] Kracht, M., Weber, A., and Wasiliew, P., "Interleukin 1 (il-1) pathway," 18 January 2010 2010.

[205] Kulkarni, S., Schilli, C., Grin, B., Muller, A. H., Hoffman, A. S., and Stayton, P. S., "Controlling the aggregation of conjugates of streptavidin with smart block copolymers prepared via the raft copolymerization technique," *Biomacromolecules*, vol. 7, no. 10, pp. 2736–41, 2006.

[206] Kuno, K. and Matsushima, K., "The il-1 receptor signaling pathway," *J Leukoc Biol*, vol. 56, no. 5, pp. 542–7, 1994.

[207] Kurz, B., Steinhagen, J., and Schunke, M., "Articular chondrocytes and synoviocytes in a co-culture system: influence on reactive oxygen species-induced cytotoxicity and lipid peroxidation," *Cell Tissue Res*, vol. 296, no. 3, pp. 555–63, 1999.

[208] Lane, N. E., Brandt, K., Hawker, G., Peeva, E., Schreyer, E., Tsuji, W., and Hochberg, M. C., "Oarsi-fda initiative: defining the disease state of osteoarthritis," *Osteoarthritis Cartilage*, vol. 19, no. 5, pp. 478–82, 2011.

[209] Lang, D., Knop, J., Wesche, H., Raffetseder, U., Kurrle, R., Boraschi, D., and Martin, M. U., "The type ii il-1 receptor interacts with the il-1 receptor accessory protein: a novel mechanism of regulation of il-1 responsiveness," *J Immunol*, vol. 161, no. 12, pp. 6871–7, 1998.

[210] Laprade, R. F., Wentorf, F. A., Olson, E. J., and Carlson, C. S., "An in vivo injury model of posterolateral knee instability," *Am J Sports Med*, vol. 34, no. 8, pp. 1313–21, 2006.

[211] Larsen, C., Ostergaard, J., Larsen, S. W., Jensen, H., Jacobsen, S., Lindegaard, C., and Andersen, P. H., "Intra-articular depot formulation principles: role in the management of postoperative pain and arthritic disorders," *J Pharm Sci*, vol. 97, no. 11, pp. 4622–54, 2008.

[212] Lasic, D. D. and Papahadjopoulos, D., *Medical applications of liposomes*. Elsevier, 1998.

[213] Lavi, G., Voronov, E., Dinarello, C. A., Apte, R. N., and Cohen, S., "Sustained delivery of il-1 ra from biodegradable microspheres reduces the number of murine b16 melanoma lung metastases," *J Control Release*, vol. 123, no. 2, pp. 123–30, 2007.

[214] Le Maitre, C. L., Hoyland, J. A., and Freemont, A. J., "Interleukin-1 receptor antagonist delivered directly and by gene therapy inhibits matrix degradation in the intact degenerate human intervertebral disc: an in situ zymographic and gene therapy study," *Arthritis Res Ther*, vol. 9, no. 4, p. R83, 2007.

[215] Lee, E., Park, K.-H., Kang, D., Park, I., Min, H., Lee, D., Kim, S., Kim, J., and Na, K., "Protein complexed with chondroitin sulfate in poly(lactide-co-glycolide) microspheres," *Biomaterials*, vol. 28, pp. 2754–2762, 2007.

[216] Lennard, A., Gorman, P., Carrier, M., Griffiths, S., Scotney, H., Sheer, D., and Solari, R., "Cloning and chromosome mapping of the human interleukin-1 receptor antagonist gene," *Cytokine*, vol. 4, no. 2, pp. 83–9, 1992.

[217] Levchenko, T. S., Hartner, W. C., Verma, D. D., Bernstein, E. A., and Torchilin, V. P., "Atp-loaded liposomes for targeted treatment in models of myocardial ischemia," *Methods Mol Biol*, vol. 605, pp. 361–75, 2010.

[218] L'Hermette, M. F., Tourny-Chollet, C., Polle, G., and Dujardin, F. H., "Articular cartilage, degenerative process, and repair: current progress," *Int J Sports Med*, vol. 27, no. 9, pp. 738–44, 2006.

[219] Liang, L. S., Jackson, J., Min, W., Risovic, V., Wasan, K. M., and Burt, H. M., "Methotrexate loaded poly(l-lactic acid) microspheres for intra-articular delivery of methotrexate to the joint," *J Pharm Sci*, vol. 93, no. 4, pp. 943–56, 2004.

[220] Liang, L. S., Wong, W., and Burt, H. M., "Pharmacokinetic study of methotrexate following intra-articular injection of methotrexate loaded poly(l-lactic acid) microspheres in rabbits," *J Pharm Sci*, vol. 94, no. 6, pp. 1204–15, 2005.

[221] Liao, C., Sun, Q., Liang, B., Shen, J., and Shuai, X., "Targeting egfr-overexpressing tumor cells using cetuximab-immunomicelles loaded with doxorubicin and superparamagnetic iron oxide," *Eur J Radiol*, 2010.

[222] Licciardi, M., Craparo, E. F., Giammona, G., Armes, S. P., Tang, Y., and Lewis, A. L., "in vitro biological evaluation of folate-functionalized block copolymer micelles for selective anti-cancer drug delivery," *Macromol Biosci*, vol. 8, no. 7, pp. 615–26, 2008.

[223] Liggins, R. T., Cruz, T., Min, W., Liang, L., Hunter, W. L., and Burt, H. M., "Intra-articular treatment of arthritis with microsphere formulations of paclitaxel: biocompatibility and efficacy determinations in rabbits," *Inflamm Res*, vol. 53, no. 8, pp. 363–72, 2004.

[224] Liu, J., Liu, H., Boyer, C., Bulmus, V., and Davis, T. P., "Approach to peptide decorated micelles via raft polymerization," *Journal of Polymer Science Part a-Polymer Chemistry*, vol. 47, no. 3, pp. 899–912, 2009.

[225] Lories, R. J., "Joint homeostasis, restoration, and remodeling in osteoarthritis," *Best Pract Res Clin Rheumatol*, vol. 22, no. 2, pp. 209–20, 2008.

[226] Lukyanov, A. N., Elbayoumi, T. A., Chakilam, A. R., and Torchilin, V. P., "Tumor-targeted liposomes: doxorubicin-loaded long-circulating liposomes modified with anti-cancer antibody," *J Control Release*, vol. 100, no. 1, pp. 135–44, 2004.

[227] Lukyanov, A. N., Gao, Z., and Torchilin, V. P., "Micelles from polyethylene glycol/phosphatidylethanolamine conjugates for tumor drug delivery," *J Control Release*, vol. 91, no. 1-2, pp. 97–102, 2003.

[228] Madhavan, S., Anghelina, M., Rath-Deschner, B., Wypasek, E., John, A., Deschner, J., Piesco, N., and Agarwal, S., "Biomechanical signals exert sustained attenuation of proinflammatory gene induction in articular chondrocytes," *Osteoarthritis Cartilage*, vol. 14, no. 10, pp. 1023–32, 2006.

[229] Mahmud, A., Xiong, X. B., Aliabadi, H. M., and Lavasanifar, A., "Polymeric micelles for drug targeting," *J Drug Target*, vol. 15, no. 9, pp. 553–84, 2007.

[230] Majumdar, M. K., Askew, R., Schelling, S., Stedman, N., Blanchet, T., Hopkins, B., Morris, E. A., and Glasson, S. S., "Double-knockout of adamts-4 and adamts-5 in mice results in physiologically normal animals and prevents the progression of osteoarthritis," *Arthritis Rheum*, vol. 56, no. 11, pp. 3670–4, 2007.

[231] Malemud, C. J., "Cytokines as therapeutic targets for osteoarthritis," *BioDrugs*, vol. 18, no. 1, pp. 23–35, 2004.

[232] Martel-Pelletier, J., "Pathophysiology of osteoarthritis," *Osteoarthritis Cartilage*, vol. 7, no. 4, pp. 371–3, 1999.

[233] Martel-Pelletier, J., "Proinflammatory mediators and osteoarthritis," *Osteoarthritis Cartilage*, vol. 7, no. 3, pp. 315–6, 1999.

[234] Martel-Pelletier, J., Alaaeddine, N., and Pelletier, J. P., "Cytokines and their role in the pathophysiology of osteoarthritis," *Front Biosci*, vol. 4, pp. D694–703, 1999.

[235] Martel-Pelletier, J., McCollum, R., DiBattista, J., Faure, M. P., Chin, J. A., Fournier, S., Sarfati, M., and Pelletier, J. P., "The interleukin-1 receptor in normal and osteoarthritic human articular chondrocytes. identification as the type i receptor and analysis of binding kinetics and biologic function," *Arthritis Rheum*, vol. 35, no. 5, pp. 530–40, 1992.

[236] Mastbergen, S. C., Marijnissen, A. C., Vianen, M. E., van Roermund, P. M., Bijlsma, J. W., and Lafeber, F. P., "The canine 'groove' model of osteoarthritis is more than simply the expression of surgically applied damage," *Osteoarthritis Cartilage*, vol. 14, no. 1, pp. 39–46, 2006.

[237] McMahan, C. J., Slack, J. L., Mosley, B., Cosman, D., Lupton, S. D., Brunton, L. L., Grubin, C. E., Wignall, J. M., Jenkins, N. A., Brannan, C. I., and et al., "A novel il-1 receptor, cloned from b cells by mammalian expression, is expressed in many cell types," *EMBO J*, vol. 10, no. 10, pp. 2821–32, 1991.

[238] Melchiorri, C., Meliconi, R., Frizziero, L., Silvestri, T., Pulsatelli, L., Mazzetti, I., Borzi, R. M., Uguccioni, M., and Facchini, A., "Enhanced and coordinated in vivo expression of inflammatory cytokines and nitric oxide synthase by chondrocytes from patients with osteoarthritis," *Arthritis Rheum*, vol. 41, no. 12, pp. 2165–74, 1998.

[239] Mitchell, P. G., Magna, H. A., Reeves, L. M., Lopresti-Morrow, L. L., Yocum, S. A., Rosner, P. J., Geoghegan, K. F., and Hambor, J. E., "Cloning, expression, and type ii collagenolytic activity of matrix metalloproteinase-13 from human osteoarthritic cartilage," *J Clin Invest*, vol. 97, no. 3, pp. 761–8, 1996.

[240] Moad, G., Rizzardo, E., and Thang, S. H., "Living radical polymerization by the raft process - a second update," *Australian Journal of Chemistry*, vol. 62, no. 11, pp. 1402–1472, 2009.

[241] Morisset, S., Frisbie, D. D., Robbins, P. D., Nixon, A. J., and McIlwraith, C. W., "Il-1ra/igf-1 gene therapy modulates repair of microfractured chondral defects," *Clin Orthop Relat Res*, vol. 462, pp. 221–8, 2007.

[242] Moser, C., Baltzer, A. W., Krauspe, R., Reinecke, J., and Wehling, P., "Autologous conditioned serum (acs) compared to hyaluronan- and saline-injections for the treatment of knee osteoarthritis," *Bone*, vol. 40, no. 6, pp. S233–S234, 2007.

[243] Murata, K., Yoshitomi, H., Tanida, S., Ishikawa, M., Nishitani, K., Ito, H., and Nakamura, T., "Plasma and synovial fluid micrornas as potential biomarkers of rheumatoid arthritis and osteoarthritis," *Arthritis Res Ther*, vol. 12, no. 3, p. R86, 2010.

[244] Musacchio, T., Laquintana, V., Latrofa, A., Trapani, G., and Torchilin, V. P., "Peg-pe micelles loaded with paclitaxel and surface-modified by a pbr-ligand: Synergistic anticancer effect," *Molecular Pharmaceutics*, vol. 6, no. 2, pp. 468–479, 2009.

[245] Muzio, M., Polentarutti, N., Sironi, M., Poli, G., De Gioia, L., Introna, M., Mantovani, A., and Colotta, F., "Cloning and characterization of a new isoform of the interleukin 1 receptor antagonist," *J Exp Med*, vol. 182, no. 2, pp. 623–8, 1995.

[246] Narain, R., Gonzales, M., Hoffman, A. S., Stayton, P. S., and Krishnan, K. M., "Synthesis of monodisperse biotinylated p(nipaam)-coated iron oxide magnetic nanoparticles and their bioconjugation to streptavidin," *Langmuir*, vol. 23, no. 11, pp. 6299–6304, 2007.

[247] Nasongkla, N., Shuai, X., Ai, H., Weinberg, B. D., Pink, J., Boothman, D. A., and Gao, J., "crgd-functionalized polymer micelles for targeted doxorubicin delivery," *Angew Chem Int Ed Engl*, vol. 43, no. 46, pp. 6323–7, 2004.

[248] Nicolas, J., Mantovani, G., and Haddleton, D. M., "Living radical polymerization as a tool for the synthesis of polymer-protein/peptide bioconjugates," *Macromolecular Rapid Communications*, vol. 28, no. 10, pp. 1083–1111, 2007.

[249] Nixon, A. J., Haupt, J. L., Frisbie, D. D., Morisset, S. S., McIlwraith, C. W., Robbins, P. D., Evans, C. H., and Ghivizzani, S., "Gene-mediated restoration of cartilage matrix by combination insulin-like growth factor-i/interleukin-1 receptor antagonist therapy," *Gene Ther*, vol. 12, no. 2, pp. 177–86, 2005.

[250] Nobs, L., Buchegger, F., Gurny, R., and Allemann, E., "Current methods for attaching targeting ligands to liposomes and nanoparticles," *J Pharm Sci*, vol. 93, no. 8, pp. 1980–92, 2004.

[251] Nordling, C., Karlsson-Parra, A., Jansson, L., Holmdahl, R., and Klareskog, L., "Characterization of a spontaneously occurring arthritis in male dba/1 mice," *Arthritis Rheum*, vol. 35, no. 6, pp. 717–22, 1992.

[252] Nystrom, A. M. and Wooley, K. L., "Thiol-functionalized shell crosslinked knedel-like (sck) nanoparticles: a versatile entry for their conjugation with biomacromolecules," *Tetrahedron*, vol. 64, no. 36, pp. 8543–8552, 2008.

[253] Oba, M., Aoyagi, K., Miyata, K., Matsumoto, Y., Itaka, K., Nishiyama, N., Yamasaki, Y., Koyama, H., and Kataoka, K., "Polyplex micelles with cyclic rgd peptide ligands and disulfide cross-links directing to the enhanced transfection via controlled intracellular trafficking," *Mol Pharm*, vol. 5, no. 6, pp. 1080–92, 2008.

[254] Oerlemans, C., Bult, W., Bos, M., Storm, G., Nijsen, J. F., and Hennink, W. E., "Polymeric micelles in anticancer therapy: targeting, imaging and triggered release," *Pharm Res*, vol. 27, no. 12, pp. 2569–89, 2010.

[255] Okamoto, M. and Atsuta, Y., "Cartilage degeneration is associated with augmented chemically-induced joint pain in rats: a pilot study," *Clin Orthop Relat Res*, vol. 468, no. 5, pp. 1423–7, 2010.

[256] O'Neil, C. P., van der Vlies, A. J., Velluto, D., Wandrey, C., Demurtas, D., Dubochet, J., and Hubbell, J. A., "Extracellular matrix binding mixed micelles for drug delivery applications," *J Control Release*, vol. 137, no. 2, pp. 146–51, 2009.

[257] O'Neill, L. A., "The interleukin-1 receptor/toll-like receptor superfamily: 10 years of progress," *Immunol Rev*, vol. 226, pp. 10–8, 2008.

[258] O'Neill, L. A. and Dinarello, C. A., "The il-1 receptor/toll-like receptor superfamily: crucial receptors for inflammation and host defense," *Immunol Today*, vol. 21, no. 5, pp. 206–9, 2000.

[259] O'Neill, L. A. and Greene, C., "Signal transduction pathways activated by the il-1 receptor family: ancient signaling machinery in mammals, insects, and plants," *J Leukoc Biol*, vol. 63, no. 6, pp. 650–7, 1998.

[260] O'Reilly, R. K., Joralemon, M. J., Hawker, C. J., and Wooley, K. L., "Facile syntheses of surface-functionalized micelles and shell cross-linked nanoparticles," *Journal of Polymer Science Part a-Polymer Chemistry*, vol. 44, no. 17, pp. 5203–5217, 2006.

[261] Palmer, A. W., Guldberg, R. E., , and Levenston, M. E., "Analysis of cartilage matrix fixed charge density and three-dimensional morphology via contrast-enhanced microcomputed tomography.," *Proc Natl Acad Sci U S A*, vol. 103, pp. 19255–19260, 2006.

[262] Palmer, A. W., Wilson, C. G., Baum, E. J., and Levenston, M. E., "Composition-function relationships during il-1-induced cartilage degradation and recovery," *Osteoarthritis Cartilage*, vol. 17, no. 8, pp. 1029–39, 2009.

[263] Palmer, G., "Interferon stimulates interleukin 1 receptor antagonist production in human articular chondrocytes and synovial fibroblasts," *Annals of the Rheumatic Diseases*, vol. 63, no. 1, pp. 43–49, 2004.

[264] Pelletier, J. P., Caron, J. P., Evans, C., Robbins, P. D., Georgescu, H. I., Jovanovic, D., Fernandes, J. C., and Martel-Pelletier, J., "In vivo suppression of early experimental osteoarthritis by interleukin-1 receptor antagonist using gene therapy," *Arthritis Rheum*, vol. 40, no. 6, pp. 1012–9, 1997.

[265] Pelletier, J. P., DiBattista, J. A., Roughley, P., McCollum, R., and Martel-Pelletier, J., "Cytokines and inflammation in cartilage degradation," *Rheum Dis Clin North Am*, vol. 19, no. 3, pp. 545–68, 1993.

[266] Pelletier, J. P., Faure, M. P., DiBattista, J. A., Wilhelm, S., Visco, D., and Martel-Pelletier, J., "Coordinate synthesis of stromelysin, interleukin-1, and oncogene proteins in experimental osteoarthritis. an immunohistochemical study," *Am J Pathol*, vol. 142, no. 1, pp. 95–105, 1993.

[267] Pelletier, J. P., Martel-Pelletier, J., and Abramson, S. B., "Osteoarthritis, an inflammatory disease: potential implication for the selection of new therapeutic targets," *Arthritis Rheum*, vol. 44, no. 6, pp. 1237–47, 2001.

[268] Pelletier, J. P., McCollum, R., DiBattista, J., Loose, L. D., Cloutier, J. M., and Martel-Pelletier, J., "Regulation of human normal and osteoarthritic chondrocyte interleukin-1 receptor by antirheumatic drugs," *Arthritis Rheum*, vol. 36, no. 11, pp. 1517–27, 1993.

[269] Pelletier, J. P., Mineau, F., Ranger, P., Tardif, G., and Martel-Pelletier, J., "The increased synthesis of inducible nitric oxide inhibits il-1ra synthesis by human articular chondrocytes: possible role in osteoarthritic cartilage degradation," *Osteoarthritis Cartilage*, vol. 4, no. 1, pp. 77–84, 1996.

[270] Pennadam, S. S., Lavigne, M. D., Dutta, C. F., Firman, K., Mernagh, D., Gorecki, D. C., and Alexander, C., "Control of a multisubunit dna motor by a thermoresponsive polymer switch," *J Am Chem Soc*, vol. 126, no. 41, pp. 13208–9, 2004.

[271] Perman, V., *Clinical biochemistry of Domestic Animals, 3rd Ed.* Academic Press, 1980.

[272] Pettipher, E. R., Higgs, G. A., and Henderson, B., "Interleukin 1 induces leukocyte infiltration and cartilage proteoglycan degradation in the synovial joint," *Proc Natl Acad Sci U S A*, vol. 83, no. 22, pp. 8749–53, 1986.

[273] Pfaff, M., Tangemann, K., Mueller, B., Gurrath, M., Mueller, G., Kessler, H., Timpl, R., and Engel, J., "Selective recognition of cyclic rgd peptides of nmr defined conformation by alphaiib beta3, alpha v beta 3, and alpha 5 beta 1 integrins.," *J Biol Chem*, vol. 269, pp. 20233–20238, 1994.

[274] Phelps, E., Landazuri, N., Thule, P., Taylor, W., and Garcia, A. J., "Bioartificial matrices for therapeutic vascularization," *Proc Natl Acad Sci U S A*, vol. 107, pp. 3323–3328, 2010.

[275] Piscaer, T. M., van Osch, G. J., Verhaar, J. A., and Weinans, H., "Imaging of experimental osteoarthritis in small animal models," *Biorheology*, vol. 45, no. 3-4, pp. 355–64, 2008.

[276] Poole, A. R., "An introduction to the pathophysiology of osteoarthritis," *Front Biosci*, vol. 4, pp. D662–70, 1999.

[277] Pourcelle, V., Freichels, H., Stoffelbach, F., Auzely-Velty, R., Jerome, C., and Marchand-Brynaert, J., "Light induced functionalization of pcl-peg block copolymers for the covalent immobilization of biomolecules," *Biomacromolecules*, vol. 10, no. 4, pp. 966–974, 2009.

[278] Pratta, M. A., Scherle, P. A., Yang, G., Liu, R. Q., and Newton, R. C., "Induction of aggrecanase 1 (adam-ts4) by interleukin-1 occurs through activation of constitutively produced protein," *Arthritis Rheum*, vol. 48, no. 1, pp. 119–33, 2003.

[279] Pritzker, K. P., "Animal models for osteoarthritis: processes, problems and prospects," *Ann Rheum Dis*, vol. 53, no. 6, pp. 406–20, 1994.

[280] Pujol, J. P., Chadjichristos, C., Legendre, F., Bauge, C., Beauchef, G., Andriamanalijaona, R., Galera, P., and Boumediene, K., "Interleukin-1 and transforming growth factor-beta 1 as crucial factors in osteoarthritic cartilage metabolism," *Connect Tissue Res*, vol. 49, no. 3, pp. 293–7, 2008.

[281] Quasnichka, H. L., Anderson-MacKenzie, J. M., and Bailey, A. J., "Subchondral bone and ligament changes precede cartilage degradation in guinea pig osteoarthritis," *Biorheology*, vol. 43, no. 3-4, pp. 389–97, 2006.

[282] Ratcliffe, J. H., Hunneyball, I. M., Wilson, C. G., Smith, A., and Davis, S. S., "Albumin microspheres for intra-articular drug delivery: investigation of their retention in normal and arthritic knee joints of rabbits," *J Pharm Pharmacol*, vol. 39, no. 4, pp. 290–5, 1987.

[283] Rauchhaus, U., Schwaiger, F. W., and Panzner, S., "Separating therapeutic efficacy from glucocorticoid side-effects in rodent arthritis using novel, liposomal delivery of dexamethasone phosphate: long-term suppression of arthritis facilitates interval treatment," *Arthritis Res Ther*, vol. 11, no. 6, p. R190, 2009.

[284] Re, F., Muzio, M., De Rossi, M., Polentarutti, N., Giri, J. G., Mantovani, A., and Colotta, F., "The type ii "receptor" as a decoy target for interleukin 1 in polymorphonuclear leukocytes: characterization of induction by dexamethasone and ligand binding properties of the released decoy receptor," *J Exp Med*, vol. 179, no. 2, pp. 739–43, 1994.

[285] Reboul, P., Pelletier, J. P., Tardif, G., Cloutier, J. M., and Martel-Pelletier, J., "The new collagenase, collagenase-3, is expressed and synthesized by human chondrocytes but not by synoviocytes. a role in osteoarthritis," *J Clin Invest*, vol. 97, no. 9, pp. 2011–9, 1996.

[286] Reulen, S. W. A., Dankers, P. Y. W., Bomans, P. H. H., Meijer, E. W., and Merkx, M., "Collagen targeting using protein-functionalized micelles: The strength of multiple weak interactions," *Journal of the American Chemical Society*, vol. 131, no. 21, pp. 7304–7312, 2009.

[287] Revell, P. A., Mayston, V., Lalor, P., and Mapp, P., "The synovial membrane in osteoarthritis: a histological study including the characterisation of the cellular infiltrate present in inflammatory osteoarthritis using monoclonal antibodies," *Ann Rheum Dis*, vol. 47, no. 4, pp. 300–7, 1988.

[288] Rieger, J., Grazon, C., Charleux, B., Alaimo, D., and Jrme, C., "Pegylated thermally responsive block copolymer micelles and nanogels viain situraft aqueous dispersion polymerization," *Journal of Polymer Science Part A: Polymer Chemistry*, vol. 47, no. 9, pp. 2373–2390, 2009.

[289] Roach, H. I., Aigner, T., Soder, S., Haag, J., and Welkerling, H., "Pathobiology of osteoarthritis: pathomechanisms and potential therapeutic targets," *Curr Drug Targets*, vol. 8, no. 2, pp. 271–82, 2007.

[290] Rollin, R., Marco, F., Jover, J. A., Garcia-Asenjo, J. A., Rodriguez, L., Lopez-Duran, L., and Fernandez-Gutierrez, B., "Early lymphocyte activation in the synovial microenvironment in patients with osteoarthritis: comparison with rheumatoid arthritis patients and healthy controls," *Rheumatol Int*, vol. 28, no. 8, pp. 757–64, 2008.

[291] Rosoff, P. M., "Il-1 receptors: structure and signals," *Semin Immunol*, vol. 2, no. 2, pp. 129–37, 1990.

[292] Rothenfluh, D. A., Bermudez, H., O'Neil, C. P., and Hubbell, J. A., "Biofunctional polymer nanoparticles for intra-articular targeting and retention in cartilage," *Nat Mater*, vol. 7, no. 3, pp. 248–54, 2008.

[293] Rudolphi, K., Gerwin, N., Verzijl, N., van der Kraan, P., and van den Berg, W., "Pralnacasan, an inhibitor of interleukin-1beta converting enzyme, reduces joint damage in two murine models of osteoarthritis," *Osteoarthritis Cartilage*, vol. 11, no. 10, pp. 738–46, 2003.

[294] Samad, A., Sultana, Y., and Aqil, M., "Liposomal drug delivery systems: an update review," *Curr Drug Deliv*, vol. 4, no. 4, pp. 297–305, 2007.

[295] Sampson, S., Reed, M., Silvers, H., Meng, M., and Mandelbaum, B., "Injection of platelet-rich plasma in patients with primary and secondary knee osteoarthritis: a pilot study," *Am J Phys Med Rehabil*, vol. 89, no. 12, pp. 961–9, 2010.

[296] Samuels, J., Krasnokutsky, S., and Abramson, S. B., "Osteoarthritis: a tale of three tissues," *Bull NYU Hosp Jt Dis*, vol. 66, no. 3, pp. 244–50, 2008.

[297] Santangelo, K. S., Pieczarka, E. M., Nuovo, G. J., Weisbrode, S. E., and Bertone, A. L., "Temporal expression and tissue distribution of interleukin-1beta in two strains of guinea pigs with varying propensity for spontaneous knee osteoarthritis," *Osteoarthritis Cartilage*, vol. 19, no. 4, pp. 439–48, 2011.

[298] Scheinecker, C., Redlich, K., and Smolen, J. S., "Cytokines as therapeutic targets: advances and limitations," *Immunity*, vol. 28, no. 4, pp. 440–4, 2008.

[299] Schlaak, J. F., Pfers, I., Meyer Zum Buschenfelde, K. H., and Marker-Hermann, E., "Different cytokine profiles in the synovial fluid of patients with osteoarthritis, rheumatoid arthritis and seronegative spondylarthropathies," *Clin Exp Rheumatol*, vol. 14, no. 2, pp. 155–62, 1996.

[300] Schreuder, H., Tardif, C., Trump-Kallmeyer, S., Soffientini, A., Sarubbi, E., Akeson, A., Bowlin, T., Yanofsky, S., and Barrett, R. W., "A new cytokine-receptor binding mode revealed by the crystal structure of the il-1 receptor with an antagonist," *Nature*, vol. 386, no. 6621, pp. 194–200, 1997.

[301] Schreuder, H. A., Rondeau, J. M., Tardif, C., Soffientini, A., Sarubbi, E., Akeson, A., Bowlin, T. L., Yanofsky, S., and Barrett, R. W., "Refined crystal structure of the interleukin-1 receptor antagonist. presence of a disulfide link and a cis-proline," *Eur J Biochem*, vol. 227, no. 3, pp. 838–47, 1995.

[302] Schuelert, N. and McDougall, J. J., "Grading of monosodium iodoacetate-induced osteoarthritis reveals a concentration-dependent sensitization of nociceptors in the knee joint of the rat," *Neurosci Lett*, vol. 465, no. 2, pp. 184–8, 2009.

[303] Serra, R., Johnson, M., Filvaroff, E. H., LaBorde, J., Sheehan, D. M., Derynck, R., and Moses, H. L., "Expression of a truncated, kinase-defective tgf-beta type ii receptor in mouse skeletal tissue promotes terminal chondrocyte differentiation and osteoarthritis," *J Cell Biol*, vol. 139, no. 2, pp. 541–52, 1997.

[304] Settle, S., Vickery, L., Nemirovskiy, O., Vidmar, T., Bendele, A., Messing, D., Ruminski, P., Schnute, M., and Sunyer, T., "Cartilage degradation biomarkers predict efficacy of a novel, highly selective matrix metalloproteinase 13 inhibitor in a dog model of osteoarthritis: confirmation by multivariate analysis that modulation of type ii collagen and aggrecan degradation peptides parallels pathologic changes," *Arthritis Rheum*, vol. 62, no. 10, pp. 3006–15, 2010.

[305] Shamji, M. F., Betre, H., Kraus, V. B., Chen, J., Chilkoti, A., Pichika, R., Masuda, K., and Setton, L. A., "Development and characterization of a fusion protein between thermally responsive elastin-like polypeptide and interleukin-1 receptor antagonist: sustained release of a local antiinflammatory therapeutic," *Arthritis Rheum*, vol. 56, no. 11, pp. 3650–61, 2007.

[306] Shen, P. C., Wu, C. L., Jou, I. M., Lee, C. H., Juan, H. Y., Lee, P. J., Chen, S. H., and Hsieh, J. L., "T helper cells promote disease progression of osteoarthritis by inducing macrophage inflammatory protein-1gamma," *Osteoarthritis Cartilage*, vol. 19, no. 6, pp. 728–36, 2011.

[307] Shi, M., Wosnick, J. H., Ho, K., Keating, A., and Shoichet, M. S., "Immuno-polymeric nanoparticles by diels-alder chemistry," *Angew Chem Int Ed Engl*, vol. 46, no. 32, pp. 6126–31, 2007.

[308] Shirakawa, F., Tanaka, Y., Ota, T., Suzuki, H., Eto, S., and Yamashita, U., "Expression of interleukin 1 receptors on human peripheral t cells," *J Immunol*, vol. 138, no. 12, pp. 4243–8, 1987.

[309] Silvestri, T., Pulsatelli, L., Dolzani, P., Frizziero, L., Facchini, A., and Meliconi, R., "In vivo expression of inflammatory cytokine receptors in the joint compartments of patients with arthritis," *Rheumatol Int*, vol. 26, no. 4, pp. 360–8, 2006.

[310] Sims, J. E., "Il-1 and il-18 receptors, and their extended family," *Curr Opin Immunol*, vol. 14, no. 1, pp. 117–22, 2002.

[311] Sims, J. E., Gayle, M. A., Slack, J. L., Alderson, M. R., Bird, T. A., Giri, J. G., Colotta, F., Re, F., Mantovani, A., Shanebeck, K., and et al., "Interleukin 1 signaling occurs exclusively via the type i receptor," *Proc Natl Acad Sci U S A*, vol. 90, no. 13, pp. 6155–9, 1993.

[312] Sims, J. E., March, C. J., Cosman, D., Widmer, M. B., MacDonald, H. R., McMahan, C. J., Grubin, C. E., Wignall, J. M., Jackson, J. L., Call, S. M., and et al., "cdna expression cloning of the il-1 receptor, a member of the immunoglobulin superfamily," *Science*, vol. 241, no. 4865, pp. 585–9, 1988.

[313] Slack, J., McMahan, C. J., Waugh, S., Schooley, K., Spriggs, M. K., Sims, J. E., and Dower, S. K., "Independent binding of interleukin-1 alpha and interleukin-1 beta to type i and type ii interleukin-1 receptors," *J Biol Chem*, vol. 268, no. 4, pp. 2513–24, 1993.

[314] Slack, J. L., Schooley, K., Bonnert, T. P., Mitcham, J. L., Qwarnstrom, E. E., Sims, J. E., and Dower, S. K., "Identification of two major sites in the type i interleukin-1 receptor cytoplasmic region responsible for coupling to pro-inflammatory signaling pathways," *J Biol Chem*, vol. 275, no. 7, pp. 4670–8, 2000.

[315] Smeets, R. L., Joosten, L. A., Arntz, O. J., Bennink, M. B., Takahashi, N., Carlsen, H., Martin, M. U., van den Berg, W. B., and van de Loo, F. A., "Soluble interleukin-1 receptor accessory protein ameliorates collagen-induced arthritis by a different mode of action from that of interleukin-1 receptor antagonist," *Arthritis Rheum*, vol. 52, no. 7, pp. 2202–11, 2005.

[316] Smith, M. D., Triantafillou, S., Parker, A., Youssef, P. P., and Coleman, M., "Synovial membrane inflammation and cytokine production in patients with early osteoarthritis," *J Rheumatol*, vol. 24, no. 2, pp. 365–71, 1997.

[317] Sokoloff, L., Crittenden, L. B., Yamamoto, R. S., and Jay, G. E., J., "The genetics of degenerative joint disease in mice," *Arthritis Rheum*, vol. 5, pp. 531–46, 1962.

[318] Song, R. H., Tortorella, M. D., Malfait, A. M., Alston, J. T., Yang, Z., Arner, E. C., and Griggs, D. W., "Aggrecan degradation in human articular

cartilage explants is mediated by both adamts-4 and adamts-5," *Arthritis Rheum*, vol. 56, no. 2, pp. 575–85, 2007.

[319] South, A. B., Whitmire, R. E., Garcia, A. J., and Lyon, L. A., "Centrifugal deposition of microgels for the rapid assembly of nonfouling thin films," *ACS Appl Mater Interfaces*, vol. 1, no. 12, pp. 2747–54, 2009.

[320] Spriggs, M. K., Lioubin, P. J., Slack, J., Dower, S. K., Jonas, U., Cosman, D., Sims, J. E., and Bauer, J., "Induction of an interleukin-1 receptor (il-1r) on monocytic cells. evidence that the receptor is not encoded by a t cell-type il-1r mrna," *J Biol Chem*, vol. 265, no. 36, pp. 22499–505, 1990.

[321] Spriggs, M. K., Nevens, P. J., Grabstein, K., Dower, S. K., Cosman, D., Armitage, R. J., McMahan, C. J., and Sims, J. E., "Molecular characterization of the interleukin-1 receptor (il-1r) on monocytes and polymorphonuclear cells," *Cytokine*, vol. 4, no. 2, pp. 90–5, 1992.

[322] Stannus, O., Jones, G., Cicuttini, F., Parameswaran, V., Quinn, S., Burgess, J., and Ding, C., "Circulating levels of il-6 and tnf-alpha are associated with knee radiographic osteoarthritis and knee cartilage loss in older adults," *Osteoarthritis and Cartilage*, vol. 18, no. 11, pp. 1441–1447, 2010. Times Cited: 5.

[323] Stanton, H., Rogerson, F. M., East, C. J., Golub, S. B., Lawlor, K. E., Meeker, C. T., Little, C. B., Last, K., Farmer, P. J., Campbell, I. K., Fourie, A. M., and Fosang, A. J., "Adamts5 is the major aggrecanase in mouse cartilage in vivo and in vitro," *Nature*, vol. 434, no. 7033, pp. 648–52, 2005.

[324] Stenzel, M. H., "Raft polymerization: an avenue to functional polymeric micelles for drug delivery," *Chem Commun (Camb)*, no. 30, pp. 3486–503, 2008.

[325] Stockman, B. J., Scahill, T. A., Strakalaitis, N. A., Brunner, D. P., Yem, A. W., and Deibel, M. R., J., "Solution structure of human interleukin-1 receptor antagonist protein," *FEBS Lett*, vol. 349, no. 1, pp. 79–83, 1994.

[326] Stolnik, S. and Shakesheff, K., "Formulations for delivery of therapeutic proteins," *Biotechnol Lett*, vol. 31, no. 1, pp. 1–11, 2009.

[327] Strassle, B. W., Mark, L., Leventhal, L., Piesla, M. J., Jian Li, X., Kennedy, J. D., Glasson, S. S., and Whiteside, G. T., "Inhibition of osteoclasts prevents cartilage loss and pain in a rat model of degenerative joint disease," *Osteoarthritis Cartilage*, vol. 18, no. 10, pp. 1319–28, 2010.

[328] Struglics, A., Larsson, S., Pratta, M. A., Kumar, S., Lark, M. W., and Lohmander, L. S., "Human osteoarthritis synovial fluid and joint cartilage contain both aggrecanase- and matrix metalloproteinase-generated aggrecan fragments," *Osteoarthritis Cartilage*, vol. 14, no. 2, pp. 101–13, 2006.

[329] Stylianou, E., O'Neill, L. A., Rawlinson, L., Edbrooke, M. R., Woo, P., and Saklatvala, J., "Interleukin 1 induces nf-kappa b through its type i but not its type ii receptor in lymphocytes," *J Biol Chem*, vol. 267, no. 22, pp. 15836–41, 1992.

[330] Svenson, M., Hansen, M. B., Heegaard, P., Abell, K., and Bendtzen, K., "Specific binding of interleukin 1 (il-1) beta and il-1 receptor antagonist (il-1ra) to human serum. high-affinity binding of il-1ra to soluble il-1 receptor type i," *Cytokine*, vol. 5, no. 5, pp. 427–35, 1993.

[331] Symons, J. A., Young, P. R., and Duff, G. W., "Soluble type ii interleukin 1 (il-1) receptor binds and blocks processing of il-1 beta precursor and loses affinity for il-1 receptor antagonist," *Proc Natl Acad Sci U S A*, vol. 92, no. 5, pp. 1714–8, 1995.

[332] Szostak, J. and Roberts, R., "Rna-antibody fusions and their selection," 2003.

[333] Tetlow, L. C., Adlam, D. J., and Woolley, D. E., "Matrix metalloproteinase and proinflammatory cytokine production by chondrocytes of human osteoarthritic cartilage: associations with degenerative changes," *Arthritis Rheum*, vol. 44, no. 3, pp. 585–94, 2001.

[334] Thakkar, H., Sharma, R. K., Mishra, A. K., Chuttani, K., and Murthy, R. S., "Celecoxib incorporated chitosan microspheres: in vitro and in vivo evaluation," *J Drug Target*, vol. 12, no. 9-10, pp. 549–57, 2004.

[335] ThePharmaLetter, "Fda panel rejects pfizer's tenidap application," 1996.

[336] Torchilin, V. P., "Lipid-core micelles for targeted drug delivery," *Curr Drug Deliv*, vol. 2, no. 4, pp. 319–27, 2005.

[337] Torchilin, V. P., Levchenko, T. S., Lukyanov, A. N., Khaw, B. A., Klibanov, A. L., Rammohan, R., Samokhin, G. P., and Whiteman, K. R., "p-nitrophenylcarbonyl-peg-pe-liposomes: fast and simple attachment of specific ligands, including monoclonal antibodies, to distal ends of peg chains via p-nitrophenylcarbonyl groups," *Biochim Biophys Acta*, vol. 1511, no. 2, pp. 397–411, 2001.

[338] Torchilin, V. P., Lukyanov, A. N., and Gao, Z., "Micelle delivery system loaded with a pharmaceutical agent," 2006 2003.

[339] Torchilin, V. P., Sawant, R., and Kale, A., "Condition-dependent, multiple target delivery system," 2008.

[340] Umlauf, D., Frank, S., Pap, T., and Bertrand, J., "Cartilage biology, pathology, and repair," *Cell Mol Life Sci*, vol. 67, no. 24, pp. 4197–211, 2010.

[341] van den Berg, W. B., "Lessons from animal models of osteoarthritis," *Curr Rheumatol Rep*, vol. 10, no. 1, pp. 26–9, 2008.

[342] van den Berg, W. B., "Osteoarthritis year 2010 in review: pathomechanisms," *Osteoarthritis Cartilage*, vol. 19, no. 4, pp. 338–41, 2011.

[343] van der Kraan, P. M., Vitters, E. L., van de Putte, L. B., and van den Berg, W. B., "Development of osteoarthritic lesions in mice by "metabolic" and "mechanical" alterations in the knee joints," *Am J Pathol*, vol. 135, no. 6, pp. 1001–14, 1989.

[344] van Tilborg, G. A., Vucic, E., Strijkers, G. J., Cormode, D. P., Mani, V., Skajaa, T., Reutelingsperger, C. P., Fayad, Z. A., Mulder, W. J., and Nicolay, K., "Annexin a5-functionalized bimodal nanoparticles for mri and fluorescence imaging of atherosclerotic plaques," *Bioconjug Chem*, vol. 21, no. 10, pp. 1794–803, 2010.

[345] Vankemmelbeke, M. N., Holen, I., Wilson, A. G., Ilic, M. Z., Handley, C. J., Kelner, G. S., Clark, M., Liu, C., Maki, R. A., Burnett, D., and Buttle, D. J., "Expression and activity of adamts-5 in synovium," *Eur J Biochem*, vol. 268, no. 5, pp. 1259–68, 2001.

[346] Vanniasinghe, A. S., Bender, V., and Manolios, N., "The potential of liposomal drug delivery for the treatment of inflammatory arthritis," *Semin Arthritis Rheum*, vol. 39, no. 3, pp. 182–96, 2009.

[347] Verbruggen, G., "Chondroprotective drugs in degenerative joint diseases," *Rheumatology (Oxford)*, vol. 45, no. 2, pp. 129–38, 2006.

[348] Vigers, G. P., Caffes, P., Evans, R. J., Thompson, R. C., Eisenberg, S. P., and Brandhuber, B. J., "X-ray structure of interleukin-1 receptor antagonist at 2.0-a resolution," *J Biol Chem*, vol. 269, no. 17, pp. 12874–9, 1994.

[349] Wancket, L. M., Baragi, V., Bove, S., Kilgore, K., Korytko, P. J., and Guzman, R. E., "Anatomical localization of cartilage degradation markers in a surgically induced rat osteoarthritis model," *Toxicol Pathol*, vol. 33, no. 4, pp. 484–9, 2005.

[350] Wang, H. J., Yu, C. L., Kishi, H., Motoki, K., Mao, Z. B., and Muraguchi, A., "Suppression of experimental osteoarthritis by adenovirus-mediated double gene transfer," *Chin Med J (Engl)*, vol. 119, no. 16, pp. 1365–73, 2006.

[351] Wang, J., Elewaut, D., Veys, E. M., and Verbruggen, G., "Insulin-like growth factor 1-induced interleukin-1 receptor ii overrides the activity of interleukin-1 and controls the homeostasis of the extracellular matrix of cartilage," *Arthritis Rheum*, vol. 48, no. 5, pp. 1281–91, 2003.

[352] Webb, G. R., Westacott, C. I., and Elson, C. J., "Osteoarthritic synovial fluid and synovium supernatants up-regulate tumor necrosis factor receptors on human articular chondrocytes," *Osteoarthritis Cartilage*, vol. 6, no. 3, pp. 167–76, 1998.

[353] Webb, M. S., Logan, P., Kanter, P. M., St-Onge, G., Gelmon, K., Harasym, T., Mayer, L. D., and Bally, M. B., "Preclinical pharmacology, toxicology and efficacy of sphingomyelin/cholesterol liposomal vincristine for therapeutic treatment of cancer," *Cancer Chemother Pharmacol*, vol. 42, no. 6, pp. 461–70, 1998.

[354] Wehling, P., Moser, C., Frisbie, D., McIlwraith, C. W., Kawcak, C. E., Krauspe, R., and Reinecke, J. A., "Autologous conditioned serum in the treatment of orthopedic diseases: the orthokine therapy," *BioDrugs*, vol. 21, no. 5, pp. 323–32, 2007.

[355] Wehling, P., Reinecke, J., Baltzer, A. W., Granrath, M., Schulitz, K. P., Schultz, C., Krauspe, R., Whiteside, T. W., Elder, E., Ghivizzani, S. C.,

Robbins, P. D., and Evans, C. H., "Clinical responses to gene therapy in joints of two subjects with rheumatoid arthritis," *Hum Gene Ther*, vol. 20, no. 2, pp. 97–101, 2009.

[356] Wen, Z.-Q., Cao, X., and Vance, A., "Conformation and side chains environments of recombinant human interleukin-1 receptor antagonist (rh-il-1ra) probed by raman, raman optical activity, and uv-resonance raman spectroscopy," *J Pharm Sci*, vol. 97, pp. 2228–2241, 2008.

[357] Wernicke, D., Seyfert, C., Hinzmann, B., and Gromnica-Ihle, E., "Cloning of collagenase 3 from the synovial membrane and its expression in rheumatoid arthritis and osteoarthritis," *J Rheumatol*, vol. 23, no. 4, pp. 590–5, 1996.

[358] Wesche, H., Neumann, D., Resch, K., and Martin, M. U., "Co-expression of mrna for type i and type ii interleukin-1 receptors and the il-1 receptor accessory protein correlates to il-1 responsiveness," *FEBS Lett*, vol. 391, no. 1-2, pp. 104–8, 1996.

[359] Westacott, C. I. and Sharif, M., "Cytokines in osteoarthritis: mediators or markers of joint destruction?," *Semin Arthritis Rheum*, vol. 25, no. 4, pp. 254–72, 1996.

[360] Whitaker, M. J., Hao, J., Davies, O. R., Serhatkulu, G., Stolnik-Trenkic, S., Howdle, S. M., and Shakesheff, K. M., "The production of protein-loaded microparticles by supercritical fluid enhanced mixing and spraying," *J Control Release*, vol. 101, no. 1-3, pp. 85–92, 2005.

[361] Wieland, H. A., Michaelis, M., Kirschbaum, B. J., and Rudolphi, K. A., "Osteoarthritis - an untreatable disease?," *Nat Rev Drug Discov*, vol. 4, no. 4, pp. 331–44, 2005.

[362] Williams, A. S., Camilleri, J. P., and Williams, B. D., "Suppression of adjuvant-induced arthritis by liposomally conjugated methotrexate in the rat," *Br J Rheumatol*, vol. 33, no. 6, pp. 530–3, 1994.

[363] Williams, A. S., Topley, N., Dojcinov, S., Richards, P. J., and Williams, B. D., "Amelioration of rat antigen-induced arthritis by liposomally conjugated methotrexate is accompanied by down-regulation of cytokine mrna expression," *Rheumatology (Oxford)*, vol. 40, no. 4, pp. 375–83, 2001.

[364] Williams, J. M. and Brandt, K. D., "Exercise increases osteophyte formation and diminishes fibrillation following chemically induced articular cartilage injury," *J Anat*, vol. 139 (Pt 4), pp. 599–611, 1984.

[365] Wilson, C. G., Palmer, A. W., Zuo, F., Eugui, E., Wilson, S., Mackenzie, R., Sandy, J. D., and Levenston, M. E., "Selective and non-selective metalloproteinase inhibitors reduce il-1-induced cartilage degradation and loss of mechanical properties," *Matrix Biol*, vol. 26, no. 4, pp. 259–68, 2007.

[366] Xiao, N.-Y., Li, A.-L., Liang, H., and Lu, J., "A well-defined novel aldehyde-functionalized glycopolymer: Synthesis, micelle formation, and its protein immobilization," *Macromolecules*, vol. 41, no. 7, pp. 2374–2380, 2008. Times Cited: 29.

[367] Xie, L., Lin, A., Guldberg, R., , and Levenston, M. E., "Nondestructive assessment of sgag content and distribution in normal and degraded rat articular cartilage via epic-mct," *Osteoarthritis Cartilage*, vol. 18, pp. 65–72, 2010.

[368] Yang, K. G., Raijmakers, N. J., van Arkel, E. R., Caron, J. J., Rijk, P. C., Willems, W. J., Zijl, J. A., Verbout, A. J., Dhert, W. J., and Saris, D. B., "Autologous interleukin-1 receptor antagonist improves function and symptoms in osteoarthritis when compared to placebo in a prospective randomized controlled trial," *Osteoarthritis Cartilage*, vol. 16, no. 4, pp. 498–505, 2008.

[369] Yang, X., Grailer, J. J., Pilla, S., Steeber, D. A., and Gong, S., "Tumor-targeting, ph-responsive, and stable unimolecular micelles as drug nanocarriers for targeted cancer therapy," *Bioconjug Chem*, 2010. Bioconjug Chem. 2010 Feb 17.

[370] York, A. W., Kirkland, S. E., and McCormick, C. L., "Advances in the synthesis of amphiphilic block copolymers via raft polymerization: stimuli-responsive drug and gene delivery," *Adv Drug Deliv Rev*, vol. 60, no. 9, pp. 1018–36, 2008.

[371] Yu, P., Zheng, C., Chen, J., Zhang, G., Liu, Y., Suo, X., and Su, Z., "Investigation on pegylation strategy of recombinant human interleukin-1 receptor antagonist," *Bioorg Med Chem*, vol. 15, no. 16, pp. 5396–405, 2007.

[372] Yu, P., Zhang, G., Bi, J., Lu, X., Wang, Y., and Su, Z., "Facile purification of mono-pegylated interleukin-1 receptor antagonist and its characterization with multi-angle laser light scattering," *Process Biochemistry*, vol. 42, no. 6, pp. 971–977, 2007.

[373] Zayed, N., Afif, H., Chabane, N., Mfuna-Endam, L., Benderdour, M., Martel-Pelletier, J., Pelletier, J. P., Motiani, R. K., Trebak, M., Duval, N., and Fahmi, H., "Inhibition of interleukin-1beta-induced matrix metalloproteinases 1 and 13 production in human osteoarthritic chondrocytes by prostaglandin d2," *Arthritis Rheum*, vol. 58, no. 11, pp. 3530–40, 2008.

[374] Zhang, J. X., Yan, M. Q., Li, X. H., Qiu, L. Y., Li, X. D., Li, X. J., Jin, Y., and Zhu, K. J., "Local delivery of indomethacin to arthritis-bearing rats through polymeric micelles based on amphiphilic polyphosphazenes," *Pharm Res*, vol. 24, no. 10, pp. 1944–53, 2007.

[375] Zhang, L., Liu, W., Lin, L., Chen, D., and Stenzel, M. H., "Degradable disulfide core-cross-linked micelles as a drug delivery system prepared from vinyl functionalized nucleosides via the raft process," *Biomacromolecules*, vol. 9, no. 11, pp. 3321–31, 2008.

[376] Zhang, L., Nguyen, T. L., Bernard, J., Davis, T. P., Barner-Kowollik, C., and Stenzel, M. H., "Shell-cross-linked micelles containing cationic polymers synthesized via the raft process: toward a more biocompatible gene delivery system," *Biomacromolecules*, vol. 8, no. 9, pp. 2890–901, 2007.

[377] Zhang, S. and Zhao, Y., "Rapid release of entrapped contents from multi-functionalizable, surface cross-linked micelles upon different stimulation," *Journal of the American Chemical Society*, vol. 132, no. 31, pp. 10642–10644, 2010.

[378] Zhang, X., Mao, Z., and Yu, C., "Suppression of early experimental osteoarthritis by gene transfer of interleukin-1 receptor antagonist and interleukin-10," *J Orthop Res*, vol. 22, no. 4, pp. 742–50, 2004.

[379] Zhang, Y., Zhu, W., Wang, B., and Ding, J., "A novel microgel and associated post-fabrication encapsulation technique of proteins," *J Control Release*, vol. 105, no. 3, pp. 260–8, 2005.

[380] Zhang, Y., Gu, W., Xu, H., and Liu, S., "Facile fabrication of hybrid nanoparticles surface grafted with multi-responsive polymer brushes via block copolymer micellization and self-catalyzed core gelation," *Journal of Polymer Science Part A: Polymer Chemistry*, vol. 46, no. 7, pp. 2379–2389, 2008.

[381] Zhao, S., Ma, H., Wang, M., Cao, C., Xiong, J., Xu, Y., and Yao, S., "Study on the mechanism of photo-degradation of p-nitrophenol exposed to 254 nm uv light," *J Hazardous Materials*, vol. 180, pp. 86–90, 2010.

[382] Zille, H., Paquet, J., Henrionnet, C., Scala-Bertola, J., Leonard, M., Six, J. L., Deschamp, F., Netter, P., Verges, J., Gillet, P., and Grossin, L., "Evaluation of intra-articular delivery of hyaluronic acid functionalized biopolymeric nanoparticles in healthy rat knees," *Biomed Mater Eng*, vol. 20, no. 3, pp. 235–42, 2010.

[383] Zupancich, J. A., Bates, F. S., and Hillmyer, M. A., "Synthesis and self-assembly of rgd-functionalized peo-pb amphiphiles," *Biomacromolecules*, vol. 10, no. 6, pp. 1554–63, 2009.

VITA

Rachel Elisabeth Whitmire was born in Houston, TX. She attended a wide range of schools growing up, from public school to a German school (1^{st} grade) to being homeschooled by her mother. She attended Bellaire High School in Bellaire, TX before starting college at Rice University in 2001. She completed a bachelor's of science in Civil Engineering and a bachelor's of arts in French Studies in 2006. After changing direction in 2005, she stayed a 5th year at Rice doing research with Dr. Jennifer West and taking bio-related courses. She joined the Bioengineering program at Georgia Tech in August 2006. When she is not in lab, she enjoys cooking and baking, knitting, pretending she's an interior decorator, and spending time with her boyfriend, Jay, and their furry canine daughter, Emma.